Supporting Information

Metal and Organic Templates Together Control the Size of Covalent Macrocycles and Cages

Roy Lavendomme, Tanya K. Ronson, Jonathan R. Nitschke

Department of Chemistry, University of Cambridge, Lensfield Road, Cambridge CB2 1EW, United Kingdom.

Table of Contents

1. Experimental Section S2
   1.1 Synthesis and characterization of square macrocycle Pd_4[4+4] **3·(MeCN)$_4$** S3
   1.2 Synthesis and characterization of 1,3,5-tris(3-pyridyl)benzene **T1** S8
   1.3 Synthesis and characterization of templated macrocycle Pd_3[3+3] **5·T1** S9
   1.4 Synthesis and characterization of templated macrocycle Pd_4[4+4] **6·T2** S17
   1.5 Synthesis and characterization of reduced macrocycle Pd_3[3+3] **7·T1** S25
   1.6 Synthesis and characterization of reduced macrocycle Pd_4[4+4] **8·T2** S30
   1.7 Synthesis and characterization of demetallated macrocycle [3+3] **9** S35
   1.8 Synthesis and characterization of demetallated macrocycle [4+4] **10** S39
   1.9 Synthesis and characterization of bridged macrocycles **5$_2$·T3$_3$** S43
   1.10 Synthesis and characterization of cages Pd_6[4+6] **12·(MeCN)$_6$** and Pd_9[6+9] **13·(MeCN)$_9$** S51
   1.11 Enrichment of cages Pd_6[4+6] **12·Cl$_6$** and Pd_9[6+9] **13·Cl$_9$** S57
   1.12 Synthesis and characterization of templated cage **13·T3$_3$·Cl$_3$** S59
   1.13 Reduction and demetallation of cages Pd_6[4+6] **12·Cl$_6$** and Pd_9[6+9] **13·Cl$_9$** S62
2. Anion binding by macrocycles **5** and **6** S65
3. Anion binding by cages **12** and **13** S67
4. Cage assembly attempts with tris-anilines other than **11** S68
5. Aniline exchange S69
6. Potential cage formation from tetrakis-aniline building blocks S75
7. X-ray Crystallography S77
   7.1 [**3**]·8AsF_6·8MeCN·2H_2O S77
   7.2 [**5$_2$·T3$_3$**]·11SbF_6·BF_4·7.75(C_6H_6)·5.25MeCN·H_2O [+ solvent] S78
   7.3 [**12·Cl$_6$**]·6(AsF_6)·4C_6H_6 [+ solvent] S79
   7.4 Calculation of angle α S80
8. Modelling S81
9. References S100

1. Experimental Section

The reactions were not performed under inert atmosphere or anhydrous conditions unless otherwise stated. Commercial HPLC grade MeOH and MeCN and reagent grade dioxane were used as solvents. CH_2Cl_2 was distilled prior to use. Silica gel 60 (0.040–0.063 mm) was used for flash chromatography. Preparative layer chromatography (PLC) were performed with Silica gel 60 F_{254}, 1 mm thick plates from Merck. The starting compounds **1, 2**, **4**, **11**, **14a-g**, **T2**, $[Pd(MeCN)_4](BF_4)_2$, BH_3·THF and ethylenediamine were commercial. **S1**[1] and **T3**[2] were prepared according to reported procedures. Complexes **15a-f** were not isolated but directly used from crude solution. $[Pd(MeCN)_4](BF_4)_2$ was stored under inert atmosphere. ***Caution***: benzidine **2** is a known carcinogen and should be handled with extra care.

Useful information regarding syntheses:

- Concentration and order of addition of subcomponents was observed to have a significant effect on the outcome of the self-assemblies (*e.g.* attempts to synthesize cages **12** and **13** with $[Pd^{2+}]$ = 60 mM led to polymeric precipitate; mixing polyanilines with Pd(II) without aldehyde can lead to precipitate). Therefore, most self-assemblies were performed at $[Pd^{2+}]$ = 2–4 mM and adding either Pd(II) or the polyaniline last.
- The reducing agent BH_3·THF is volatile and small scale reactions may require higher amounts to account for the volatility of the reagent: typically, on the scale of 0.4 mmol of imine, BH_3·THF was added stepwise in 100 µL steps (1 M, 0.1 mmol, 0.25 equiv. expected) but, on NMR scale (0.006 mmol of imine), BH_3·THF was added stepwise in 6 µL steps (1 M, 0.006 mmol, 1 equiv. expected) leading to similar results.

NMR spectra were recorded at either 9.4 Tesla (Bruker Avance III HD 400 equipped with a Smart Probe) or 11.7 Tesla (Bruker Avance III HD 500 equipped with a Smart Probe or Bruker Avance 500 equipped with a TCI CryoProbe or Bruker Avance 500 equipped with a DCH CryoProbe). Solvent signals were used for chemical shift referencing: ^1H signal at 1.94 ppm for CHD_2CN, 7.26 ppm for $CHCl_3$, 2.50 ppm for DMSO-d_5; ^{13}C signal at 1.32 ppm for CD_3CN, 77.16 ppm for $CDCl_3$. Abbreviations: s: singlet, d: doublet, dd: doublet of doublet, ddd: doublet of doublet of doublet, dt: doublet of triplet, t: triplet, br: broad signal, m: multiplet. Edited HSQC refers to multiplicity-edited sequence showing CH_2 correlation spots in negative phase (blue) and CH/CH_3 correlation spots in positive phase (red).

DOSY NMR experiments were performed on a Bruker Avance 500 NMR spectrometer equipped with a TCI CryoProbe or a Smart Probe. Maximum gradient strength was 5.35 G/mm at 10 A. DOSY measurements were performed using the standard Bruker pulse program, ledbpgp2s, employing a stimulated echo and longitudinal eddy-current delay (LED) using a gradient ramp from 5% to 95%. Relaxation delay was set to 10 s. Diffusion delay Δ (d20) and diffusion gradient length δ (2 × p30) were optimized for individual experiments. Individual rows of the quasi-2D diffusion databases were phased and baseline corrected. Raw DOSY data were processed using the Bayesian DOSY transform program in MestReNova 9.0.1-13254 or the peak height fit in MestReNova 11.0.5-18998.

Electrospray ionization low resolution mass spectrometry (ESI-LRMS) was undertaken on a Micromass Quattro LC mass spectrometer (capillary voltage 2.0-3.8 kV; cone voltage 5-30 eV; source block temp. 313-333 K; desolvation temp. 313-333 K) infused from a Harvard syringe pump at a rate of 10 µL min^{-1}. Electrospray ionization high resolution mass spectrometry (ESI-HRMS) was performed on a Thermofisher LTQ Orbitrap XL hybrid ion trap mass spectrometer (for compounds containing imines which are more sensitive, the following parameters were used: spray voltage 4.5 kV; capillary voltage 40-50 V; tube lens 100-160 V; capillary temp. 333 K).

Reactions under microwave irradiation were performed on a CEM Discover SP microwave synthesizer.

1.1 Synthesis and characterization of square macrocycle Pd_4[4+4] **3·(MeCN)$_4$**

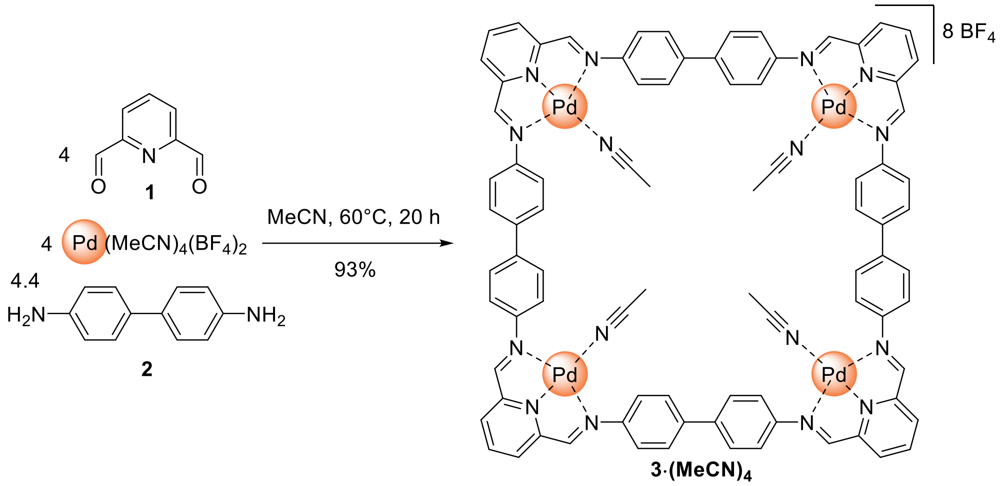

To a stirred solution of 2,6-diformylpyridine **1** (27.4 mg, 0.203 mmol) and benzidine **2** (40.7 mg, 0.221 mmol) in 50 mL MeCN was added a solution of $[Pd(MeCN)_4](BF_4)_2$ (92.7 mg, 0.208 mmol) in 1 mL MeCN. The orange solution was stirred at 60°C for 20 h. The solution was cooled down to *r.t.*, concentrated to a volume of *ca.* 10 mL with a rotary evaporator, filtered and slowly poured into 30 mL of Et_2O. The precipitate was collected by centrifugation, washed with 5 mL Et_2O and dried under vacuum affording **3·(MeCN)$_4$(BF$_4$)$_8$** as an orange/brown solid (114 mg, 0.0471 mmol, FW = 2417.66 g/mol). Yield: 93%.

^{1}H NMR (500 MHz, CD_3CN, 298 K) δ (ppm) = 8.58 (t, *J* = 8.0 Hz, 4H, H^a), 8.40 (s, 8H, H^c), 8.25 (d, *J* = 8.1 Hz, 8H, H^b), 7.93 (d, *J* = 8.6 Hz, 16H, H^e), 7.67 (d, *J* = 8.7 Hz, 16H, H^d).

^{13}C NMR (126 MHz, CD_3CN, 298 K) δ (ppm) = 174.01, 156.93, 146.90, 146.78, 142.83, 131.85, 129.67, 124.59.

ESI-LRMS for **3·S1$_4$** $[(C_{136}H_{136}N_{16}Pd_4Si_8)^{8+} + n\ BF_4^-]$ m/z (charge, calculated, found) = [**3·S1$_4$** + 2 BF_4]$^{6+}$, calcd: 469.77, found: 469.62; [**3·S1$_4$** + 3 BF_4]$^{5+}$, calcd: 581.08, found: 581.02; [**3·S1$_4$** + 4 BF_4]$^{4+}$, calcd: 748.05, found: 748.12; [**3·S1$_4$** + 5 BF_4]$^{3+}$, calcd: 1026.34, found: 1026.11.

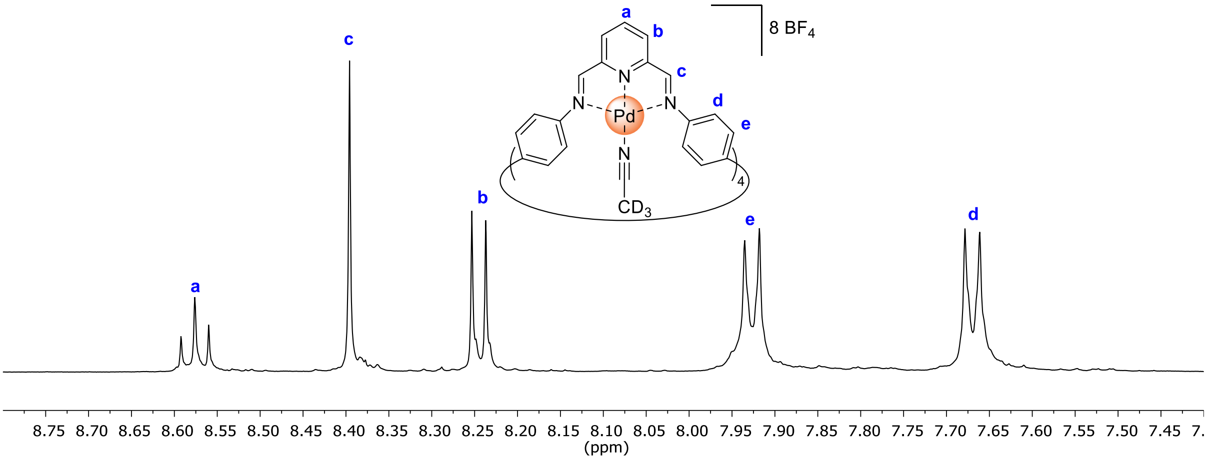

Figure S1. ^{1}H NMR spectrum of **3·(CD$_3$CN)$_4$** (500 MHz, CD_3CN, 298 K).

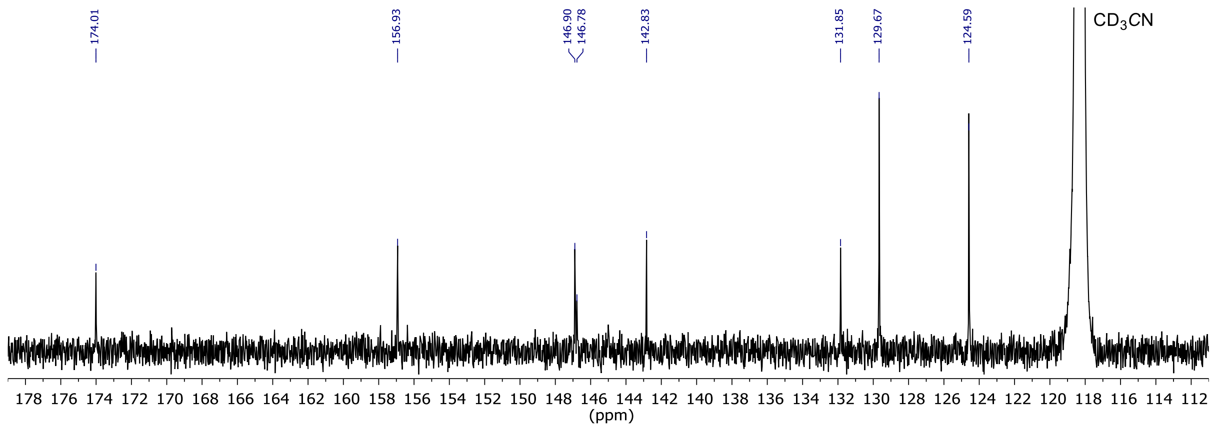

Figure S2. ^{13}C NMR spectrum of **3·(CD$_3$CN)$_4$** (126 MHz, CD$_3$CN, 298 K).

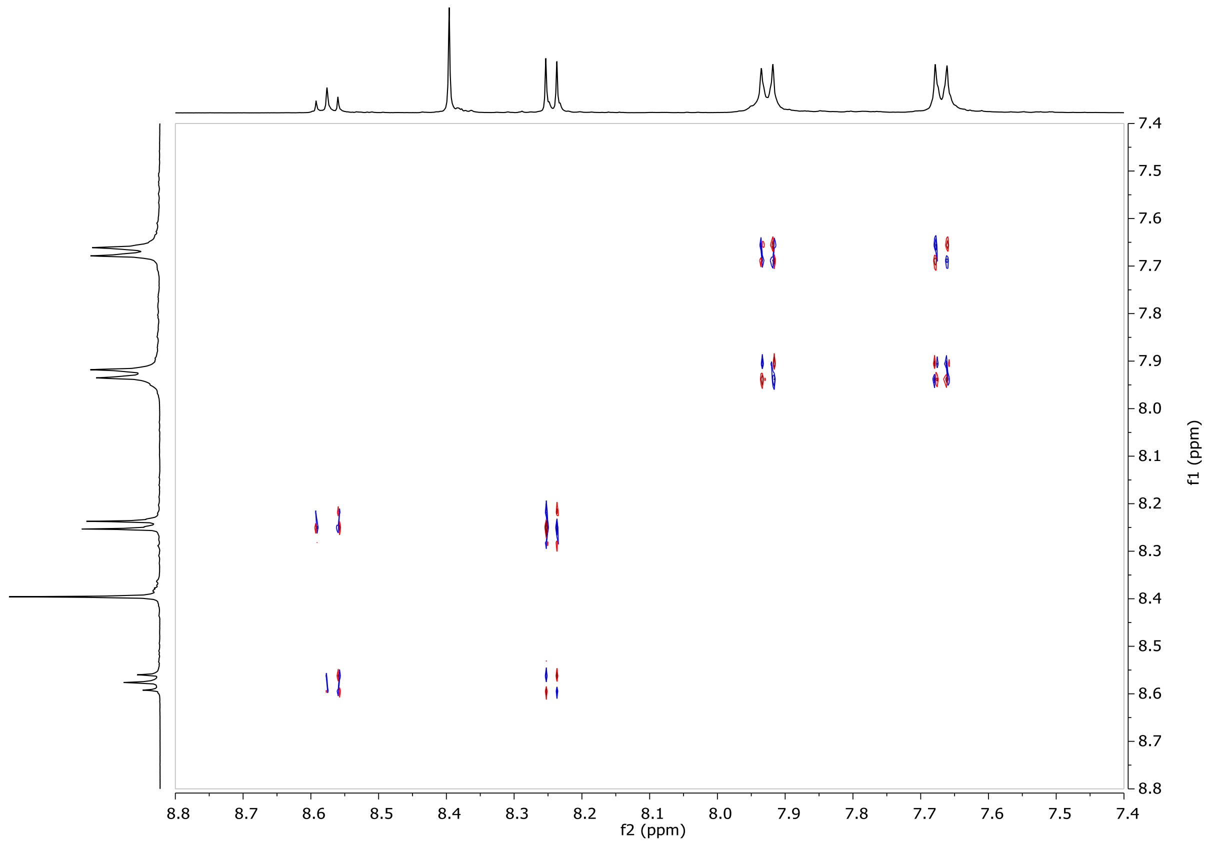

Figure S3. dqfCOSY spectrum of **3·(CD$_3$CN)$_4$** (500 MHz, CD$_3$CN, 298 K).

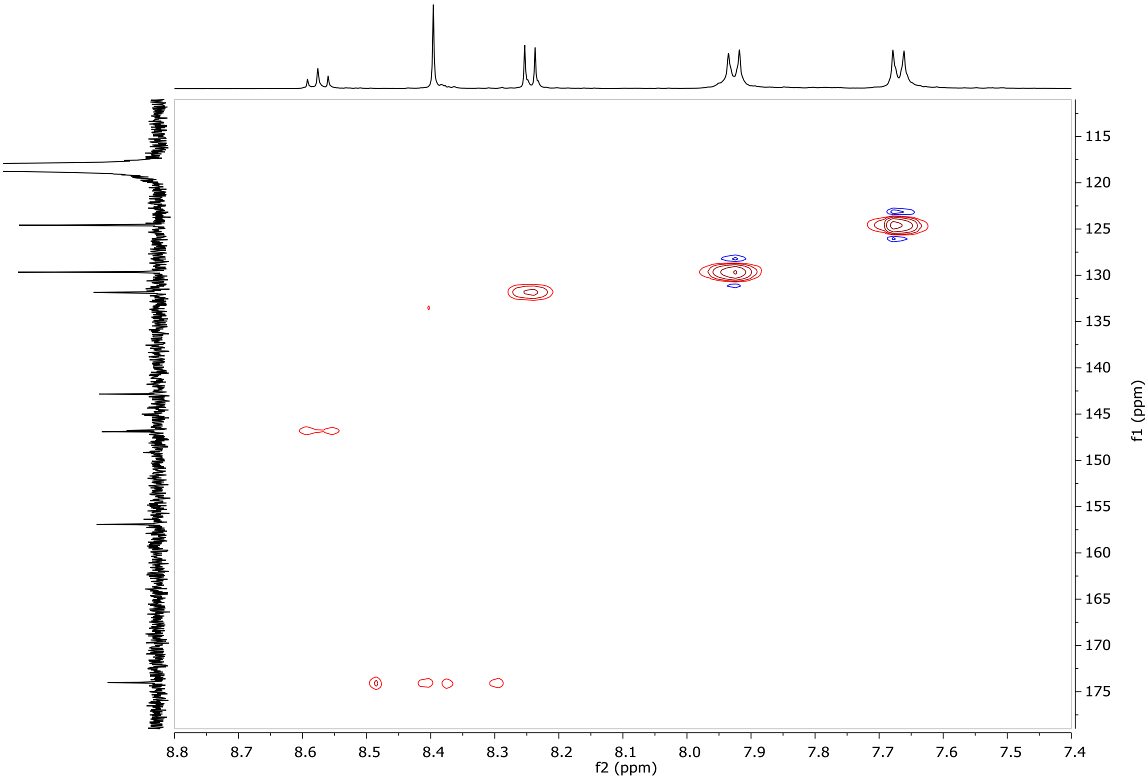

Figure S4. Edited ^{1}H-^{13}C HSQC spectrum of **3·(CD$_3$CN)$_4$** (11.7 Tesla, CD$_3$CN, 298 K). The unusual shape of the correlation spot for the N=CH is most likely caused by a ^{1}J coupling constant value out of the usual range covered by standard HSQC parameters.

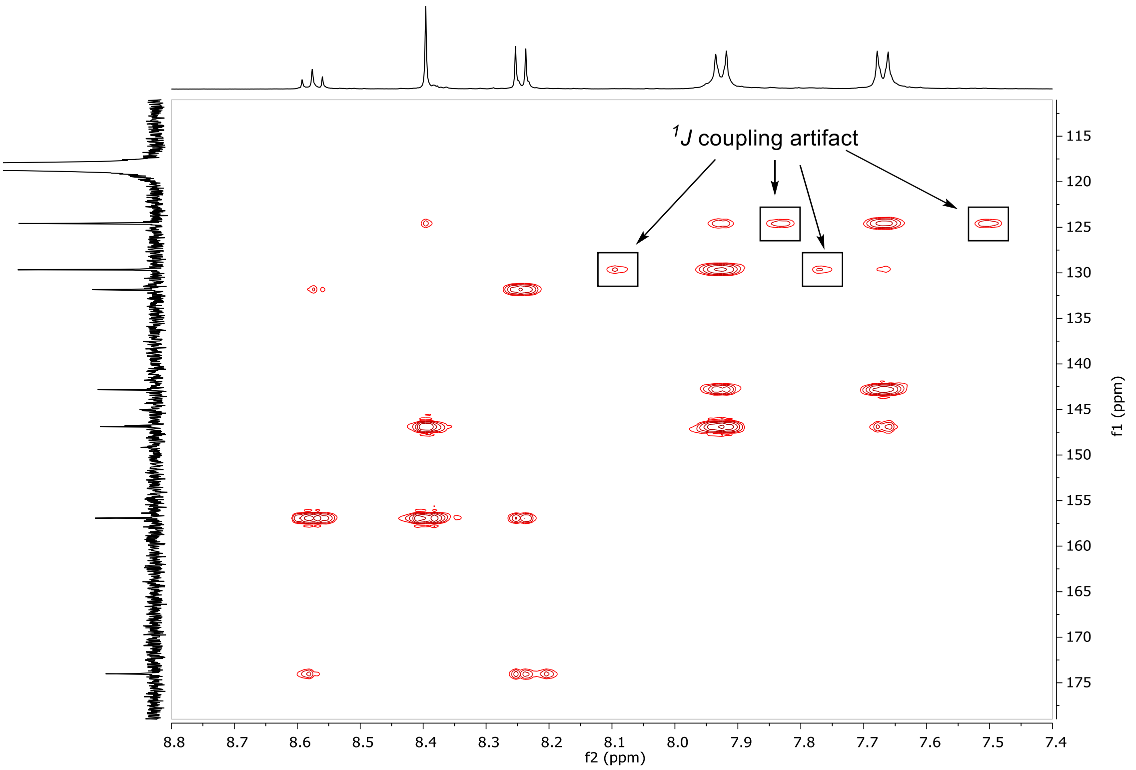

Figure S5. ^{1}H-^{13}C HMBC spectrum of **3·(CD$_3$CN)$_4$** (11.7 Tesla, CD$_3$CN, 298 K). The ^{1}J coupling artifacts are caused by ^{1}J coupling constant values out of the range filtered by standard HMBC parameters.

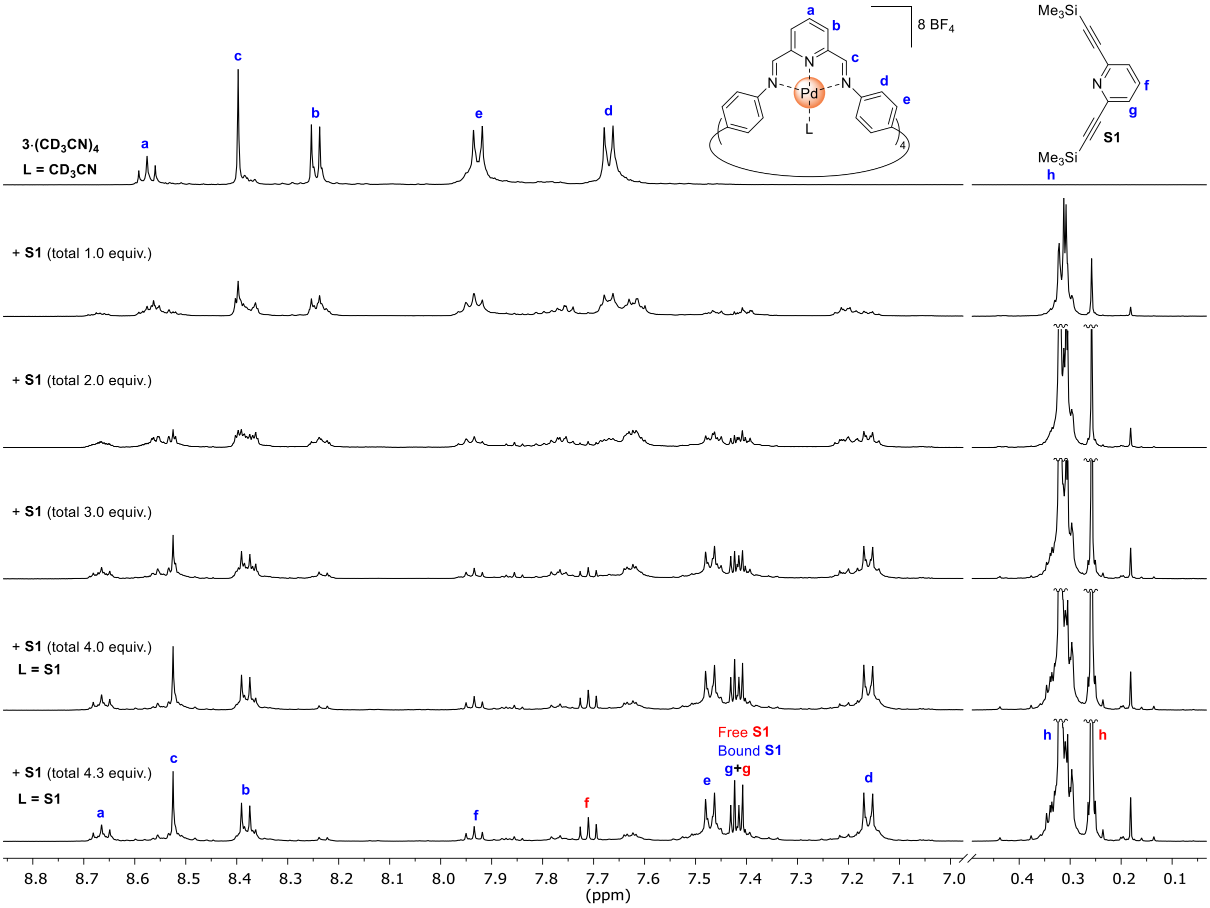

Figure S6A. Gradual formation of **3·S1**$_4$ upon addition of **S1** in a solution of **3·(CD**$_3$**CN)**$_4$ in CD_3CN monitored by ^{1}H NMR spectroscopy (500 MHz, CD_3CN, 298 K). The minor species in the bottom spectrum correspond to partial degradation of **3**. Further additions of **4** did not increase the amount of **3·S1**$_4$ as shown by the bottom spectrum. **3·S1**$_4$ remained stable over days in solution at *r.t.* Note that addition of pyridine, *n*$Bu_4N^+Cl^-$ or *n*$Bu_4N^+Br^-$ in place of **S1** led to complete degradation of **3**.

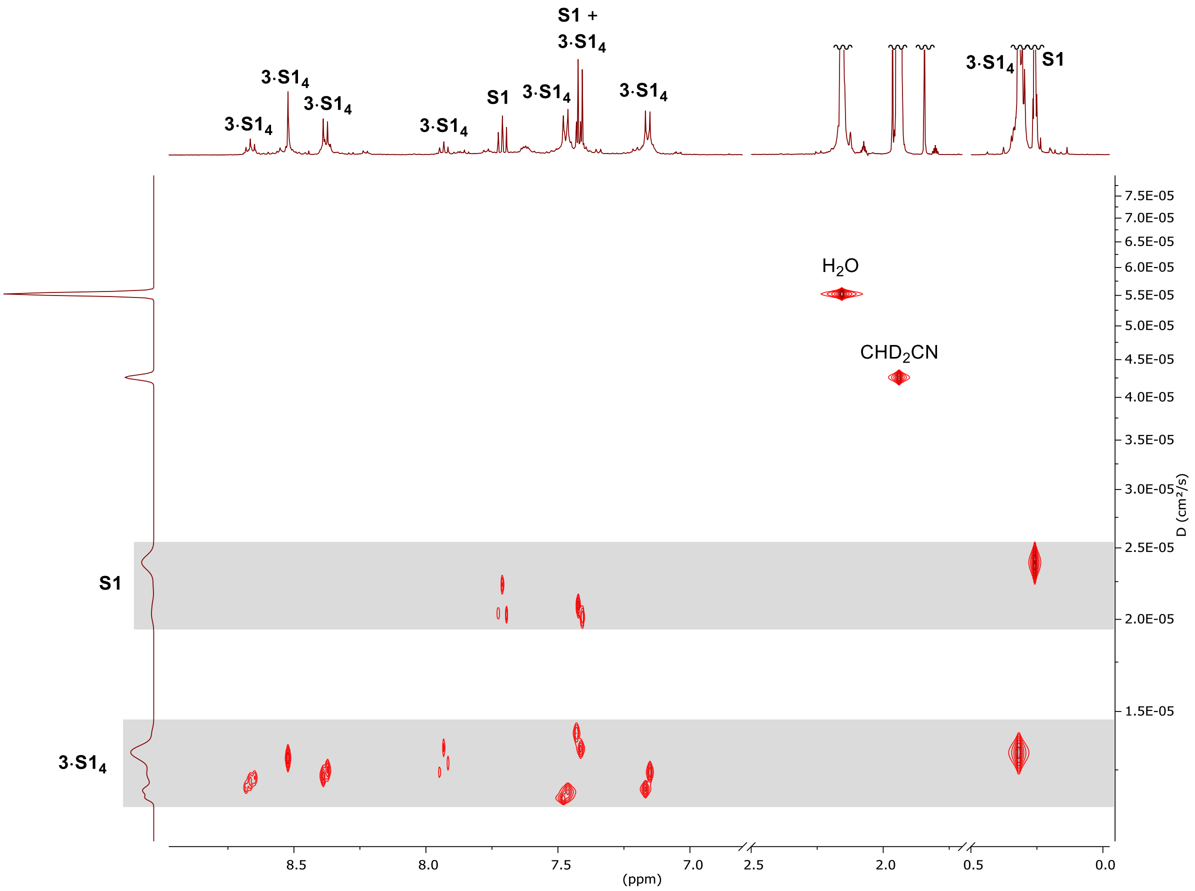

Figure S6B. [1]H DOSY spectrum of **3·S1**$_4$ (500 MHz, CD_3CN, 298 K, diffusion delay Δ = 100 ms, diffusion gradient length δ = 2200 μs). The DOSY was processed by peak height fit on selected peaks (**3·S1**$_4$**, S1**, H_2O and CHD_2CN).

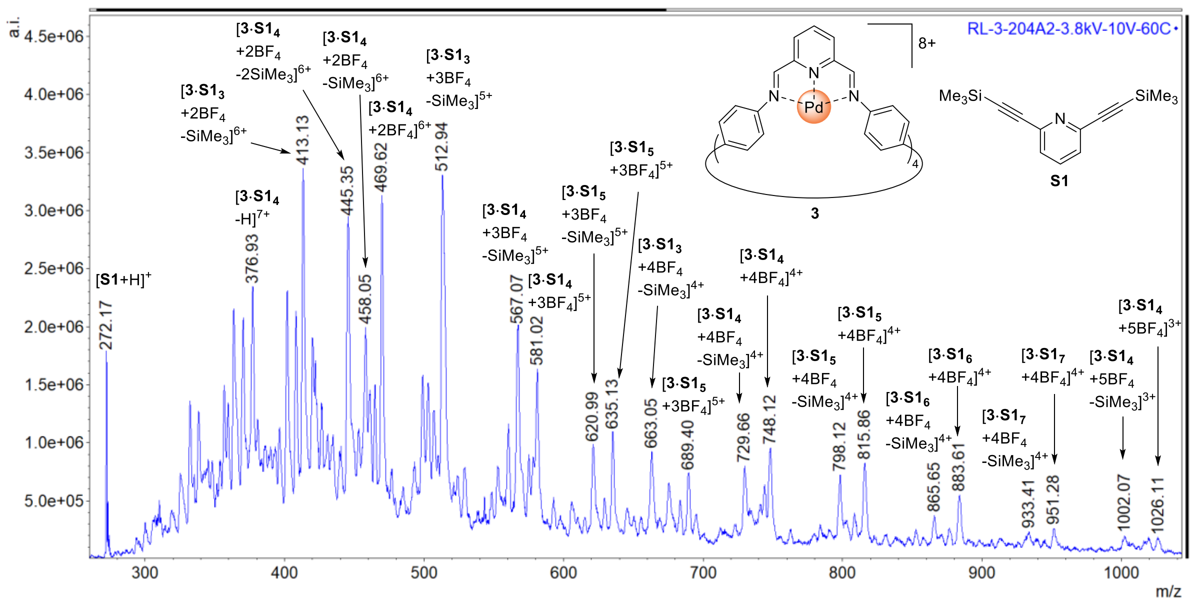

Figure S7. ESI-LRMS of **3·S1**$_4$. The loss of $SiMe_3$ is suspected to originate from ESI-MS conditions. Weaker peaks corresponding to adducts with additional **S1** are also observed.

1.2 Synthesis and characterization of 1,3,5-tris(3-pyridyl)benzene **T1**

Procedure adapted from the literature.[3]

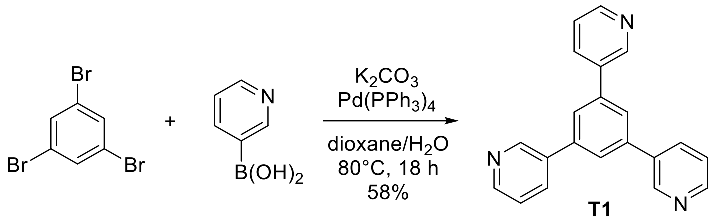

A solution of K_2CO_3 (2.8 g, 20 mmol) in 10 mL H_2O and 20 mL dioxane was degassed by bubbling nitrogen for 20 minutes under stirring. To this solution were added $Pd(PPh_3)_4$ (175 mg, 0.151 mmol), 1,3,5-tribromobenzene (315 mg, 1.00 mmol) and pyridine-3-boronic acid (492 mg, 4.00 mmol). The biphasic mixture was strongly stirred at 80°C under N_2 for 18 h. The mixture was cooled down to *r.t.* and slowly poured into 100 mL H_2O. The precipitate was collected by filtration, washed with 5 mL H_2O and dried under vacuum. The solid was triturated in 15 mL CH_2Cl_2 and the suspension was subjected to column chromatography (SiO_2, CH_2Cl_2/MeOH, from 1:0 to 85:15, v/v) affording **T1** as an off-white solid (179 mg, 0.578 mmol, FW = 309.37 g/mol). Yield: 58%.

Spectral data are in accordance with the literature.[3] R_f (SiO_2, CH_2Cl_2/MeOH, 85:15, v/v) = 0.50. **^{1}H NMR** (500 MHz, $CDCl_3$, 298 K) δ (ppm) = 8.96 (d, J = 2.3 Hz, 3H, H^e), 8.68 (dd, J = 4.8, 1.6 Hz, 3H, H^d), 7.99 (ddd, *J* = 7.9, 2.3, 1.7 Hz, 3H, H^b), 7.80 (s, 3H, H^a), 7.44 (dd, *J* = 7.9, 4.8 Hz, 3H, H^c).

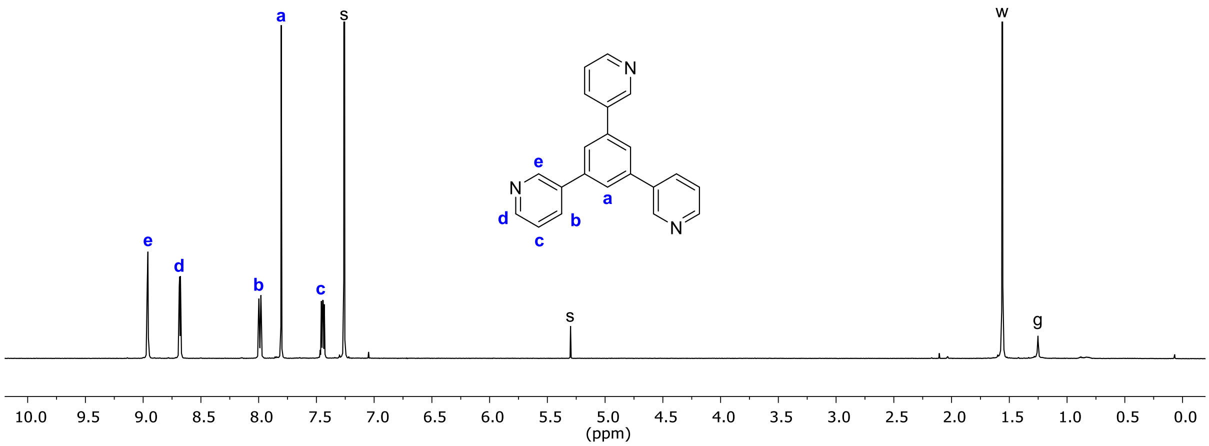

Figure S8. ^{1}H NMR spectrum of **T1** (500 MHz, $CDCl_3$, 298 K). s: residual solvents; w: water; g: grease.

1.3 Synthesis and characterization of templated macrocycle Pd_3[3+3] **5·T1**

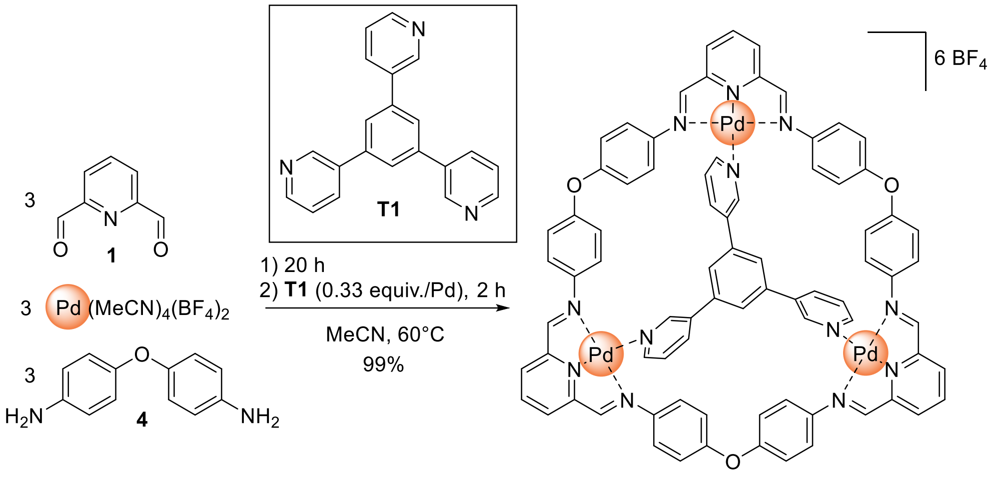

To a stirred suspension of 2,6-diformylpyridine **1** (27.1 mg, 0.201 mmol) and 4,4'-oxydianiline **4** (40.1 mg, 0.200 mmol) in 50 mL MeCN was added a solution of $[Pd(MeCN)_4](BF_4)_2$ (89.3 mg, 0.201 mmol) in 1 mL MeCN. The orange mixture was stirred at 60°C for 20 h. 1,3,5-tris(3-pyridyl)benzene **T1** (20.4 mg, 0.0659 mmol) was added and the mixture was stirred at 60°C for 2 h. The solution was cooled down to *r.t.*, concentrated to a volume of *ca.* 5 mL with a rotary evaporator, filtered and slowly poured into 30 mL of Et_2O. The mixture was shaken and left to rest 10 minutes for complete precipitation then the precipitate was collected by centrifugation, washed with 5 mL Et_2O and dried under vacuum affording **5·T1(BF$_4$)$_6$** as an orange solid (136 mg, 0.0664 mmol, FW = 2047.45 g/mol). Yield: 99%.

^{1}H NMR (500 MHz, CD_3CN, 298 K, major conformer) δ (ppm) = 8.79 (dd, *J* = 5.8, 1.4 Hz, 2H), 8.78 (d, *J* = 2.0 Hz, 1H), 8.68 (d, *J* = 5.4 Hz, 1H), 8.61 (d, *J* = 1.9 Hz, 2H), 8.59 – 8.52 (m, 3H), 8.44 (s, 2H), 8.33 (s, 2H), 8.30 (s, 2H), 8.29 – 8.23 (m, 6H), 8.21 (dt, *J* = 7.9, 1.6 Hz, 1H), 8.05 (dt, *J* = 7.9, 1.7 Hz, 2H), 7.49 (dd, *J* = 7.9, 5.7 Hz, 1H), 7.45 (d, *J* = 8.8 Hz, 4H), 7.41 (dd, *J* = 7.9, 5.8 Hz, 2H), 7.37 (d, *J* = 8.8 Hz, 4H), 7.20 (d, *J* = 9.0 Hz, 4H), 7.06 – 7.01 (m, 11H), 6.94 (d, *J* = 8.9 Hz, 4H).

^{13}C NMR (126 MHz, CD_3CN, 298 K) δ (ppm) = 175.75, 175.29, 173.50, 158.99, 158.24, 157.82, 155.99, 155.79, 155.65, 152.00, 151.52, 150.49, 150.03, 146.29, 146.23, 143.65, 143.48, 142.51, 141.74, 141.25, 141.08, 140.52, 138.66, 138.30, 131.63, 131.59, 129.95, 128.10, 128.01, 127.60, 125.99, 124.92, 124.86, 120.58, 120.54, 120.02.

ESI-HRMS for **5·T1** [$(C_{78}H_{54}N_{12}O_3Pd_3)^{6+}$] m/z = [**5·T1**]$^{6+}$, calcd: 254.3593, found: 254.3595; [**5·T1** - H]$^{5+}$, calcd: 305.0297, found: 305.0302; [**5·T1** + F]$^{5+}$, calcd: 309.0310, found: 309.0313; [**5·T1** + BF_4]$^{5+}$, calcd: 322.6320, found: 322.6324; [**5·T1** + 2 F]$^{4+}$, calcd: 391.0384, found: 391.0391; [**5·T1** + F + BF_4]$^{4+}$, calcd: 408.0398, found: 408.0404; [**5·T1** + F + 2 BF_4]$^{3+}$, calcd: 573.0544, found: 573.0557.

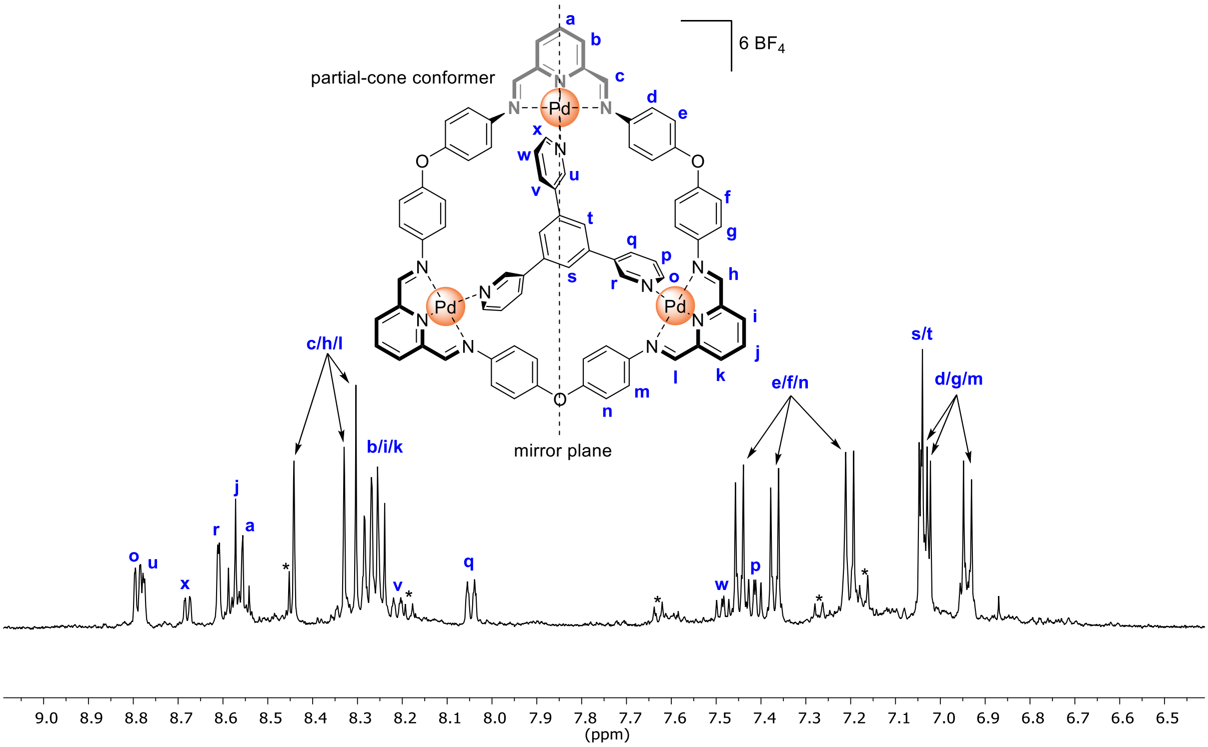

Figure S9. ^{1}H NMR spectrum of **5·T1** (500 MHz, CD_3CN, 298 K). * Signals inferred to correspond to the minor C_{3v}-symmetric cone conformer (see DOSY in Figure S14).

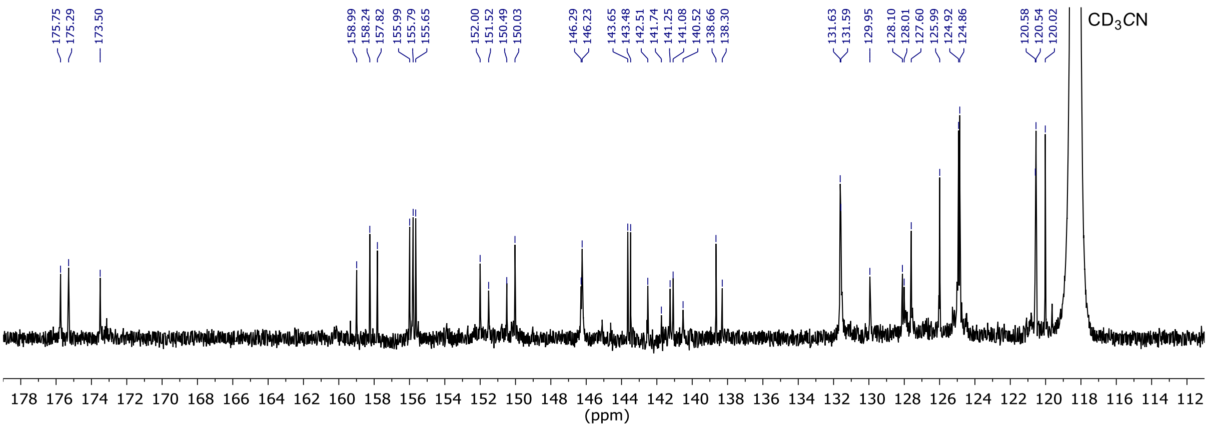

Figure S10. ^{13}C NMR spectrum of **5·T1** (126 MHz, CD_3CN, 298 K).

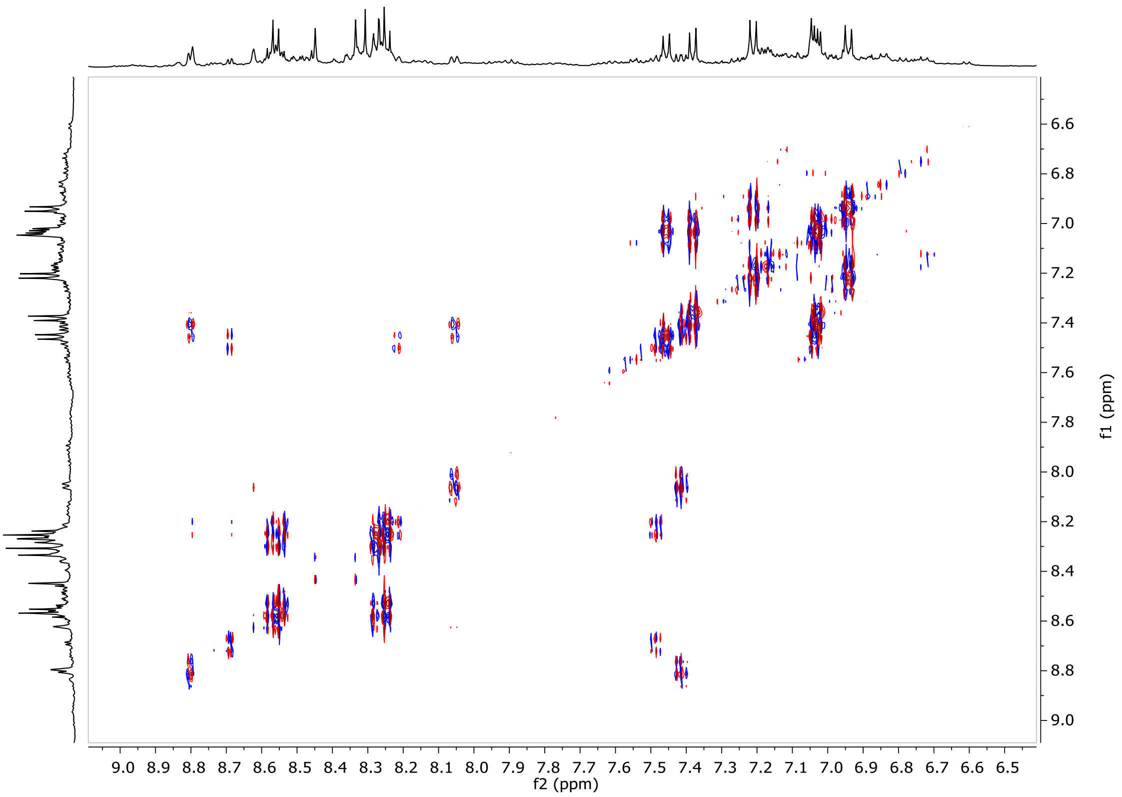

Figure S11. dqfCOSY spectrum of **5·T1** (500 MHz, CD_3CN, 298 K).

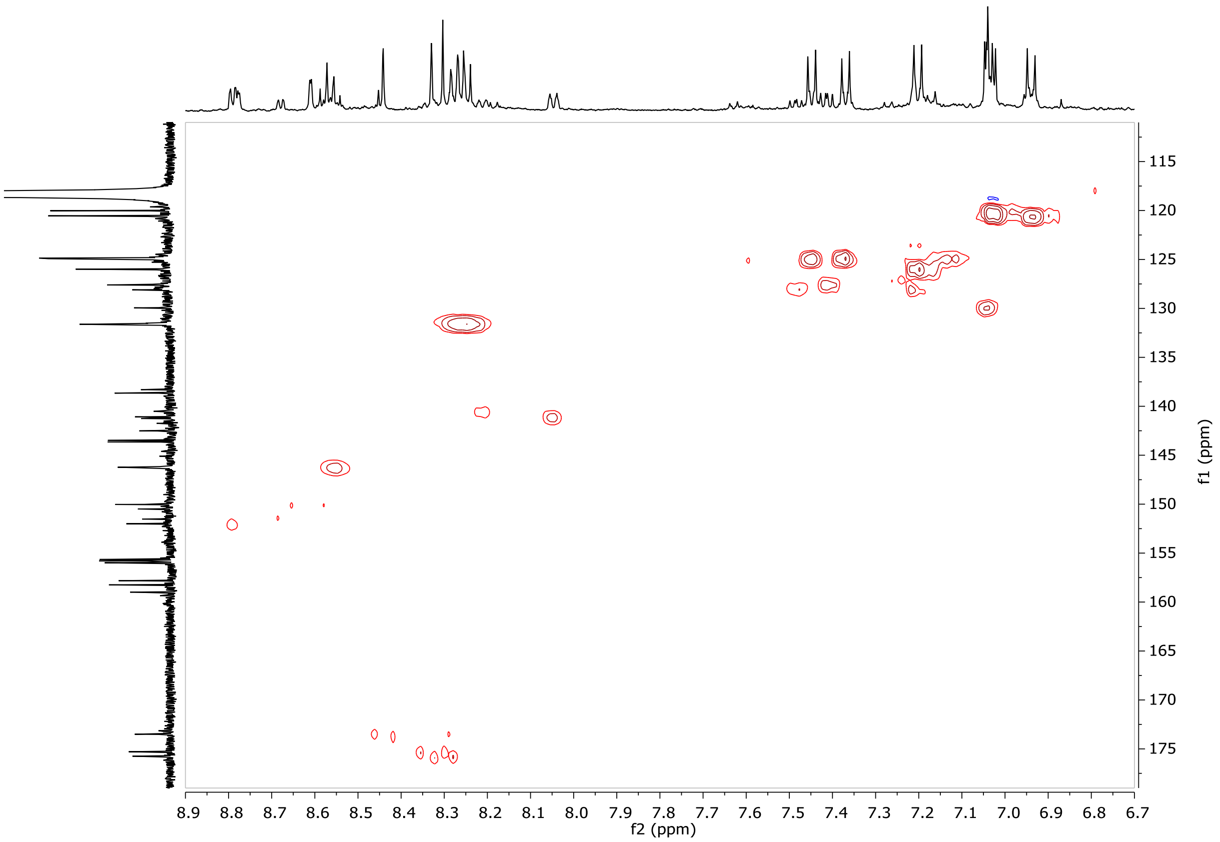

Figure S12. Edited ^1H-^{13}C HSQC spectrum of **5·T1** (11.7 Tesla, CD_3CN, 298 K). The unusual shape of the correlation spot for the N=CH is most likely caused by a ^1J coupling constant value out of the usual range covered by standard HSQC parameters.

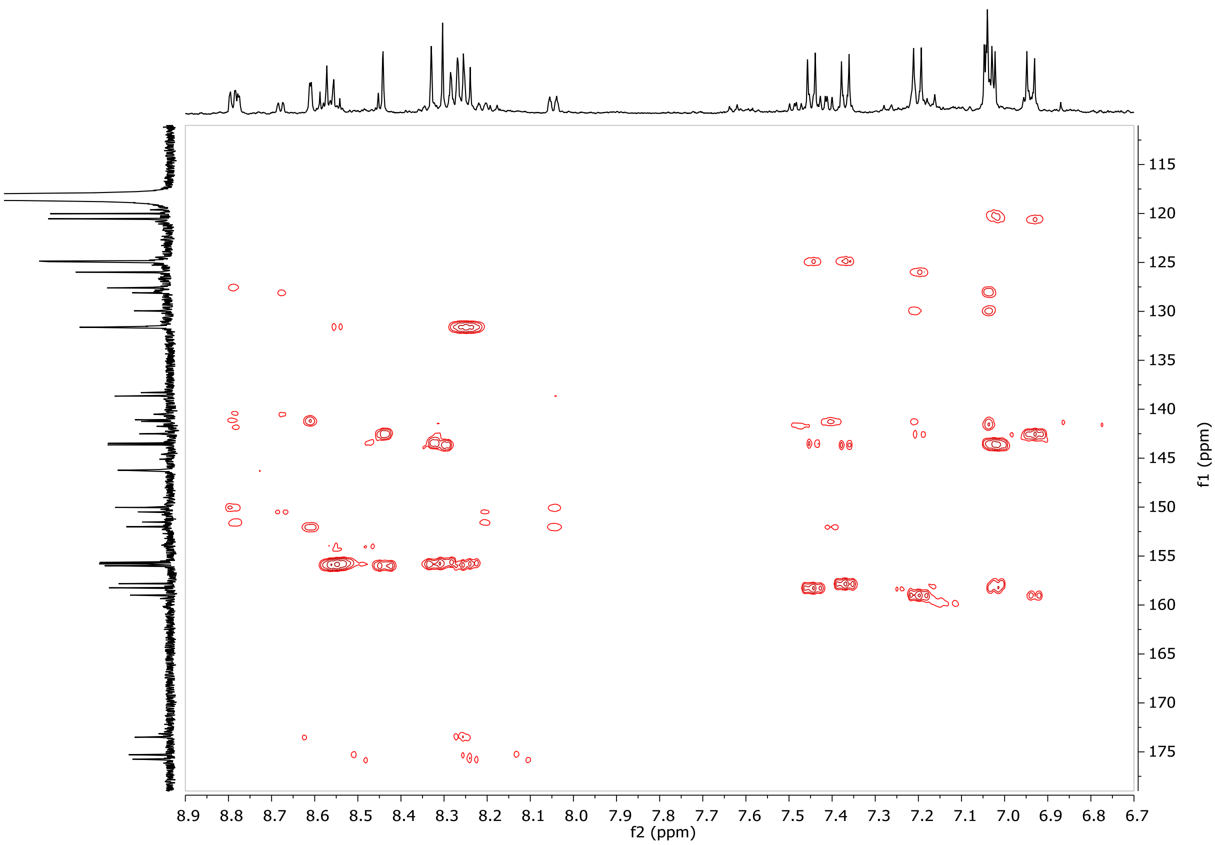

Figure S13. ^{1}H-^{13}C HMBC spectrum of **5·T1** (11.7 Tesla, CD_3CN, 298 K).

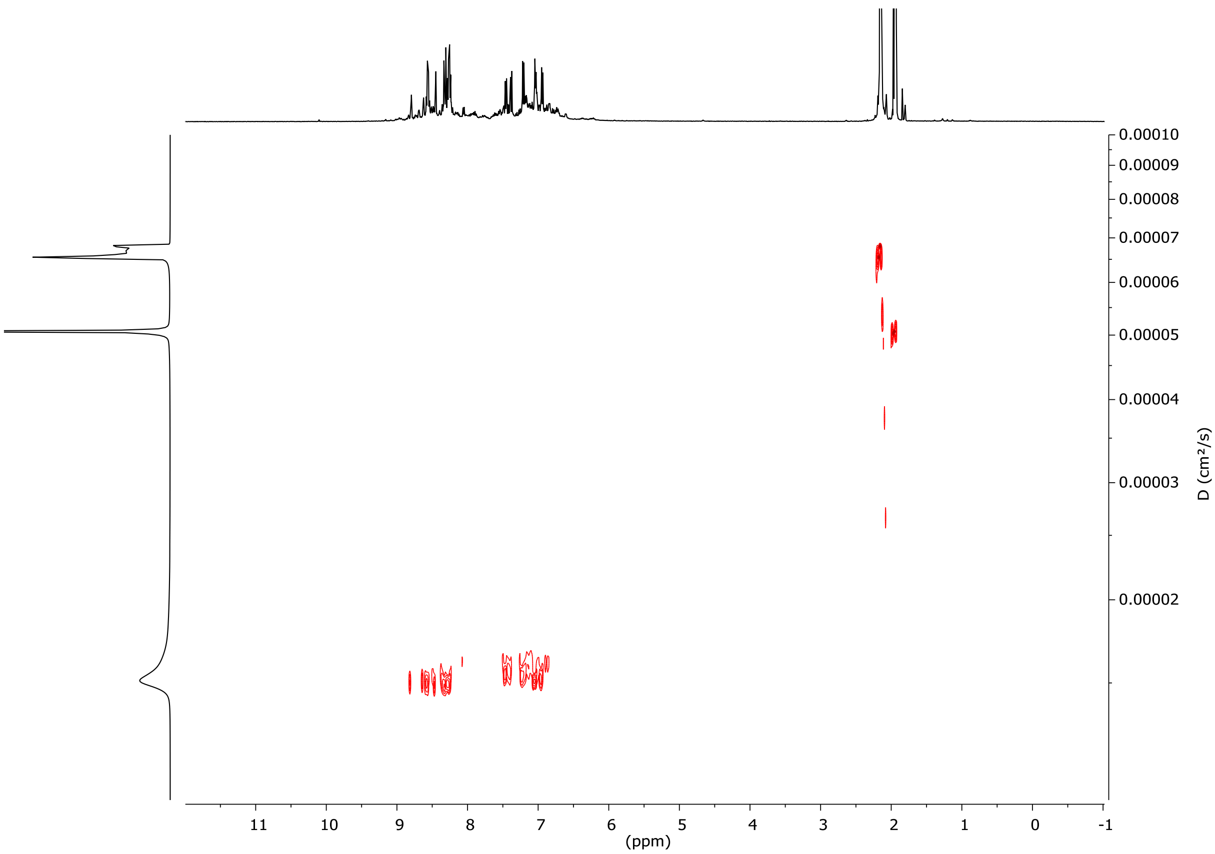

Figure S14. ^{1}H DOSY spectrum of **5·T1** (500 MHz, CD_3CN, 298 K, diffusion delay Δ = 110 ms, diffusion gradient length δ = 1700 μs).

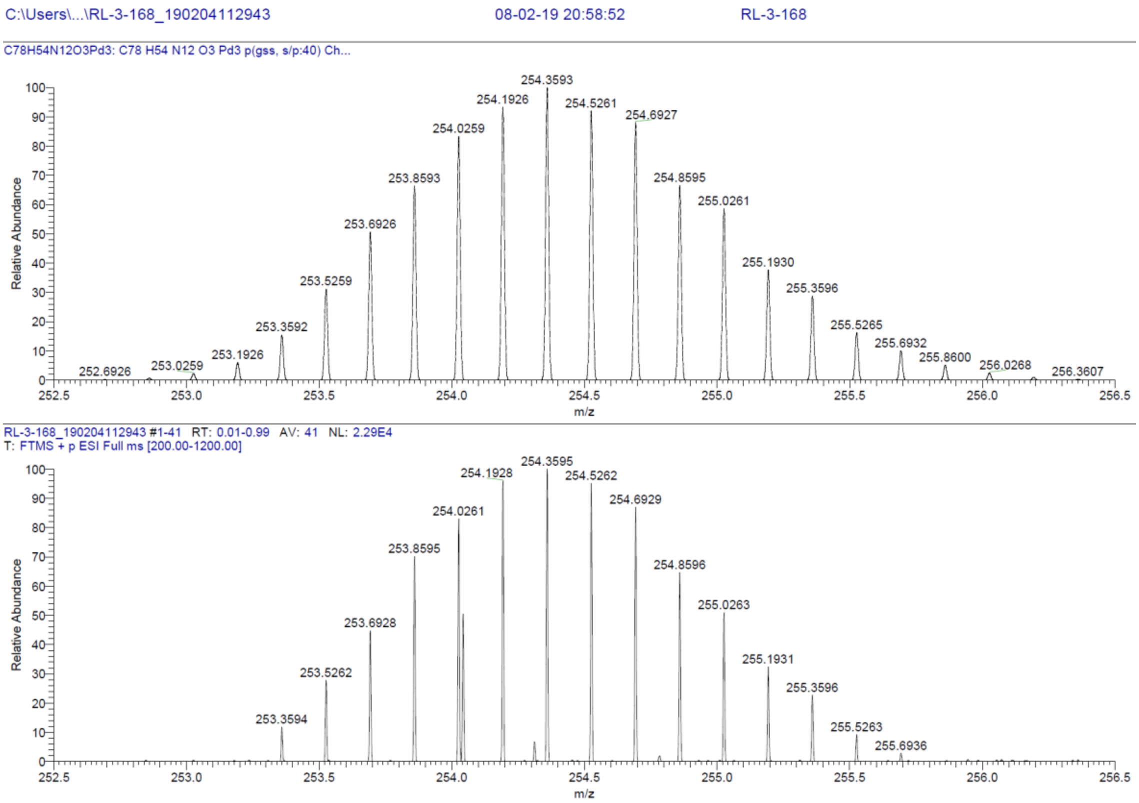

Figure S15A. Top: simulated isotopic pattern, bottom: recorded ESI-HRMS of [**5·T1**]$^{6+}$.

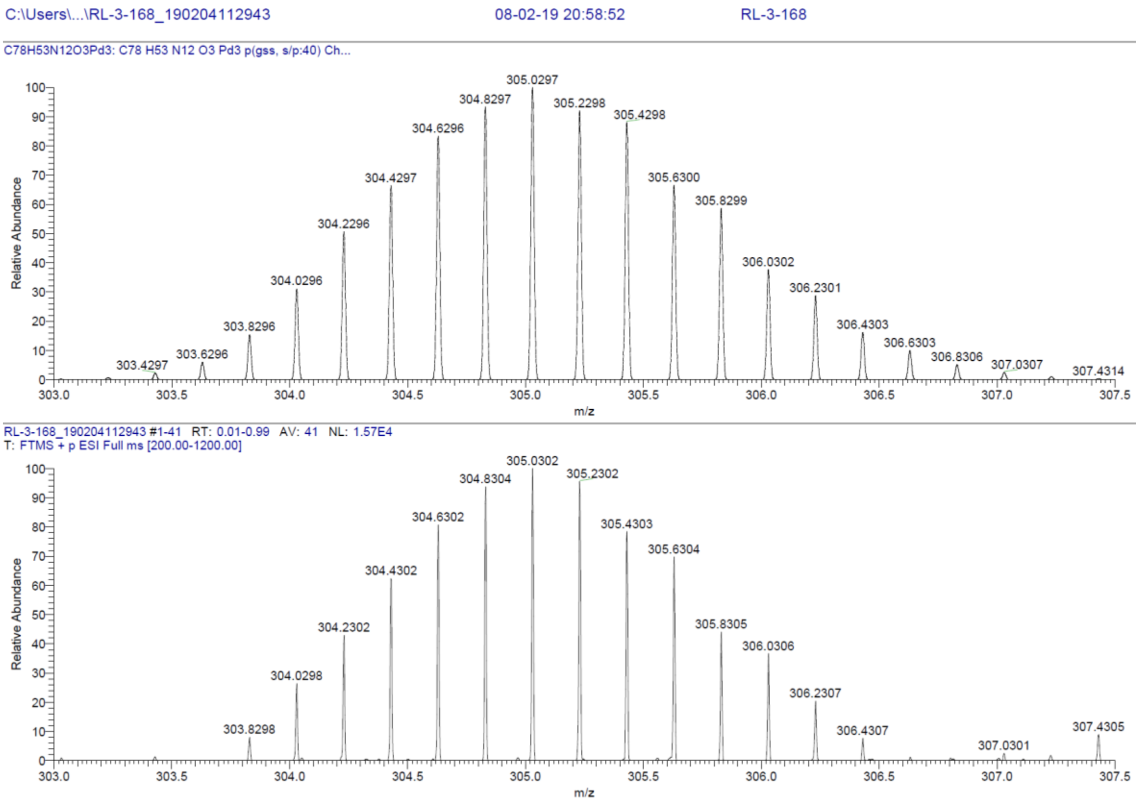

Figure S15B. Top: simulated isotopic pattern, bottom: ESI-HRMS of [**5·T1** - H]$^{5+}$.

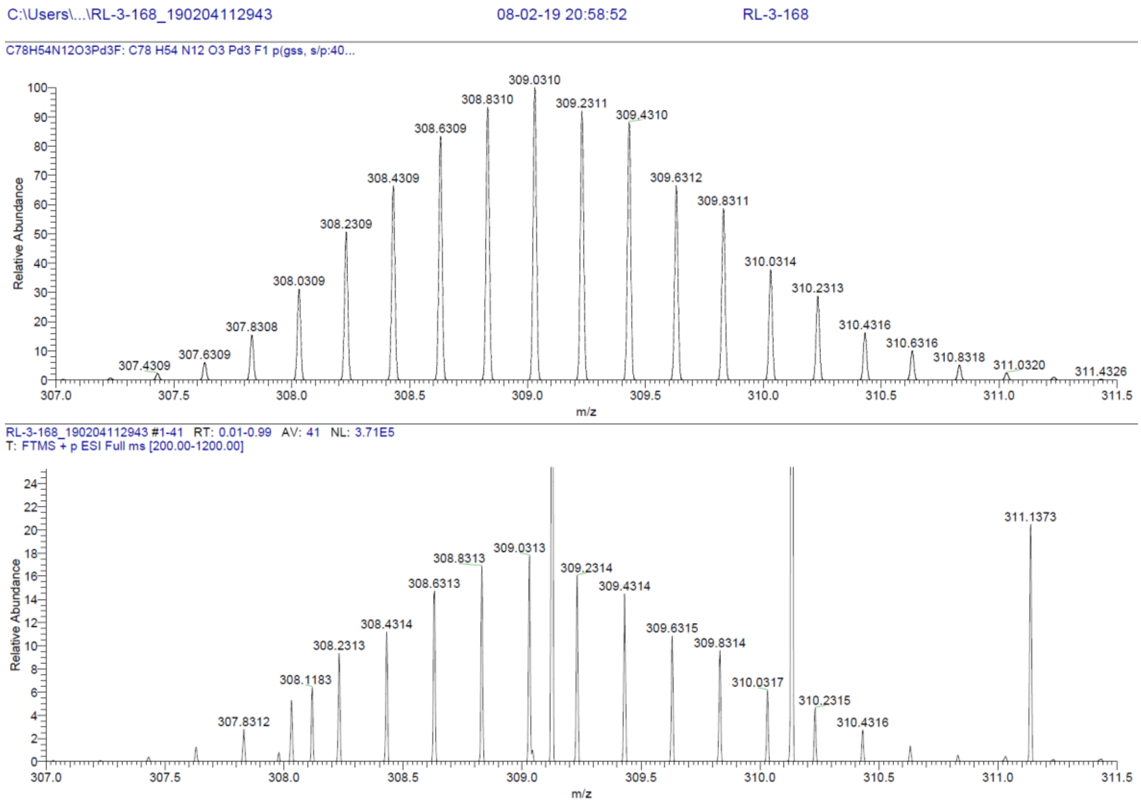

Figure S15C. Top: simulated isotopic pattern, bottom: ESI-HRMS of [**5·T1** + F]$^{5+}$. Fluoride is suspected to originate from BF_4 fragmentation in ESI-MS conditions. The three intense peaks correspond to [**T1** + H]$^{+}$.

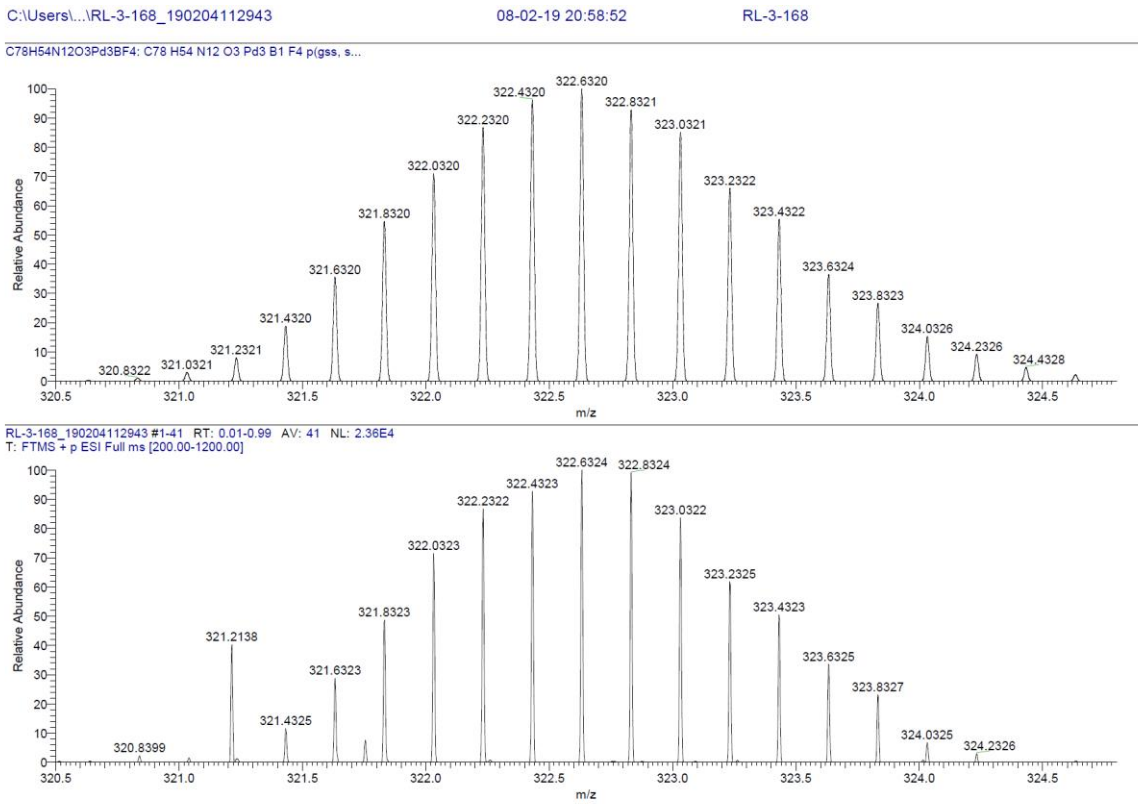

Figure S15D. Top: simulated isotopic pattern, bottom: ESI-HRMS of [**5·T1** + BF_4]$^{5+}$.

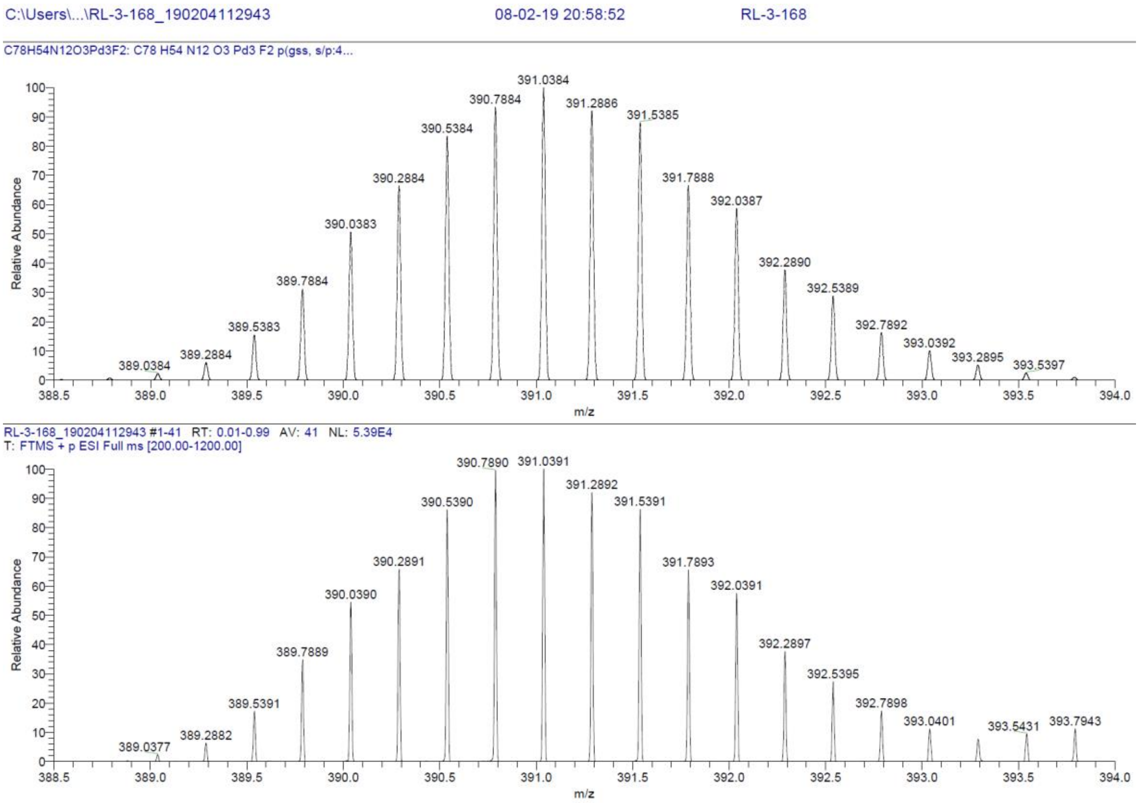

Figure S15E. Top: simulated isotopic pattern, bottom: ESI-HRMS of [**5·T1** + 2 F]$^{4+}$. Fluoride is suspected to originate from BF_4 fragmentation in ESI-MS conditions.

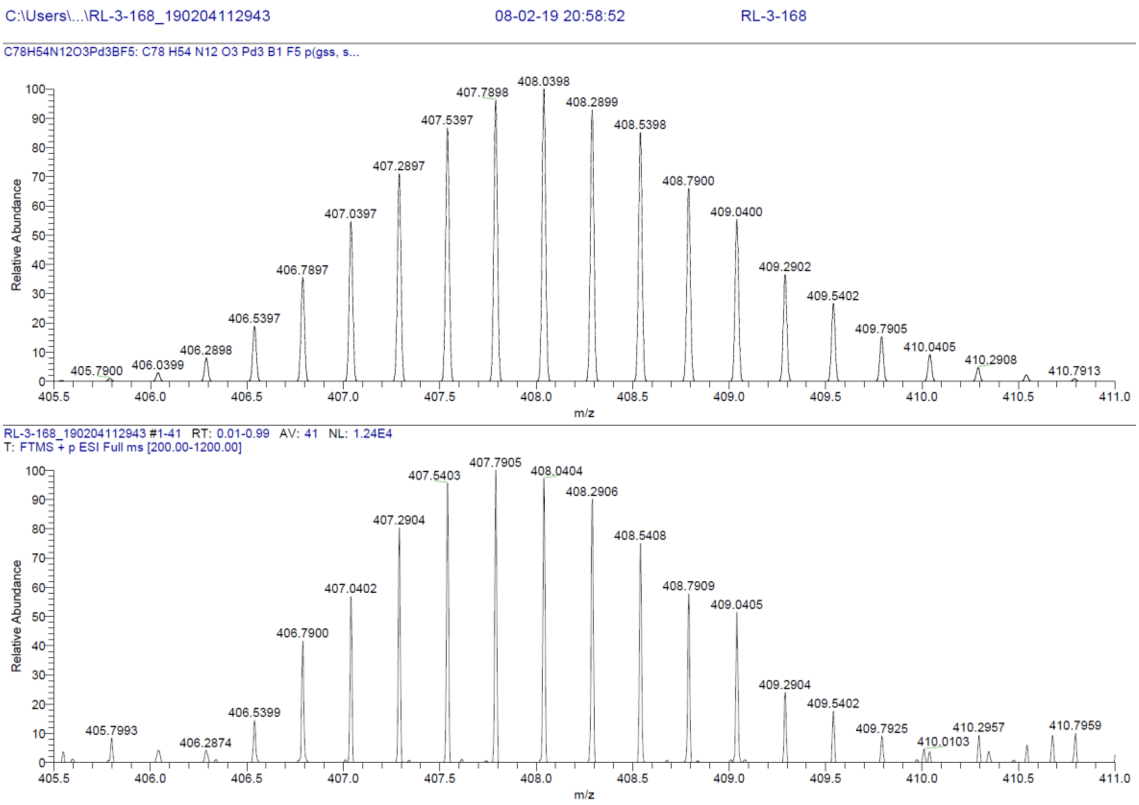

Figure S15F. Top: simulated isotopic pattern, bottom: ESI-HRMS of [**5·T1** + F + BF_4]$^{4+}$. Fluoride is suspected to originate from BF_4 fragmentation in ESI-MS conditions.

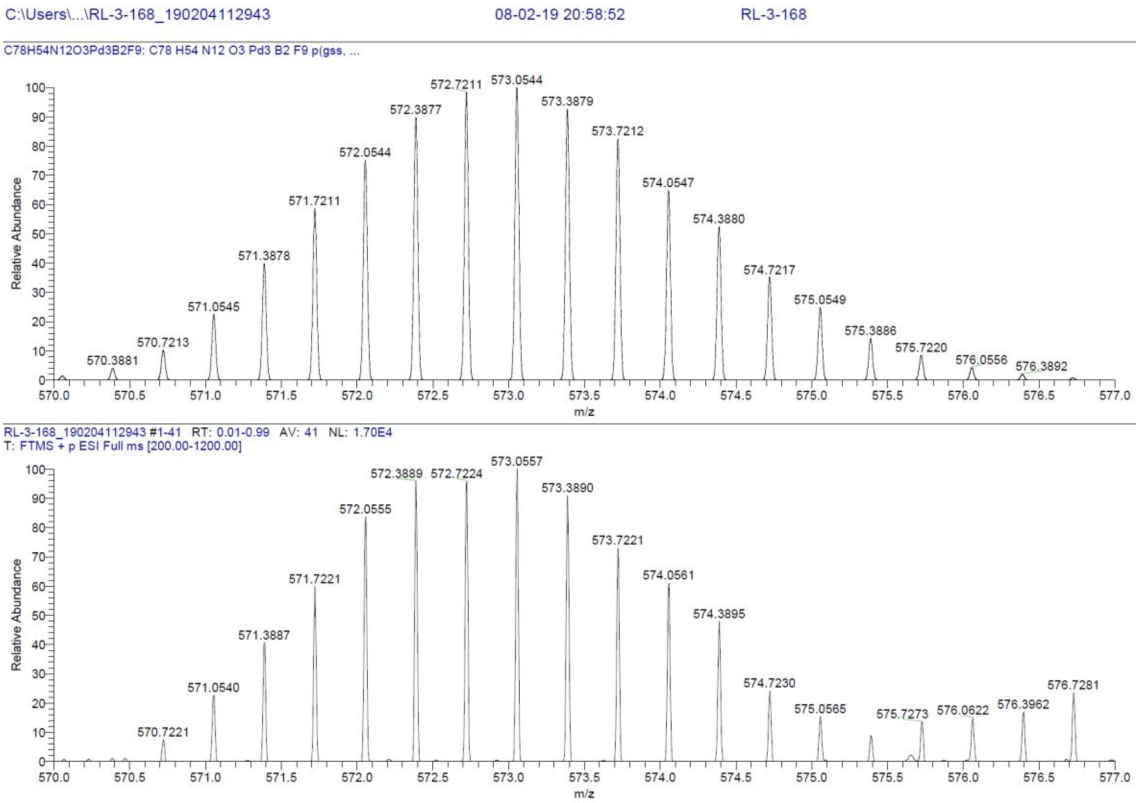

Figure S15G. Top: simulated isotopic pattern, bottom: ESI-HRMS of [**5·T1** + F + 2 BF_4]$^{3+}$. Fluoride is suspected to originate from BF_4 fragmentation in ESI-MS conditions.

1.4 Synthesis and characterization of templated macrocycle Pd_4[4+4] **6·T2**

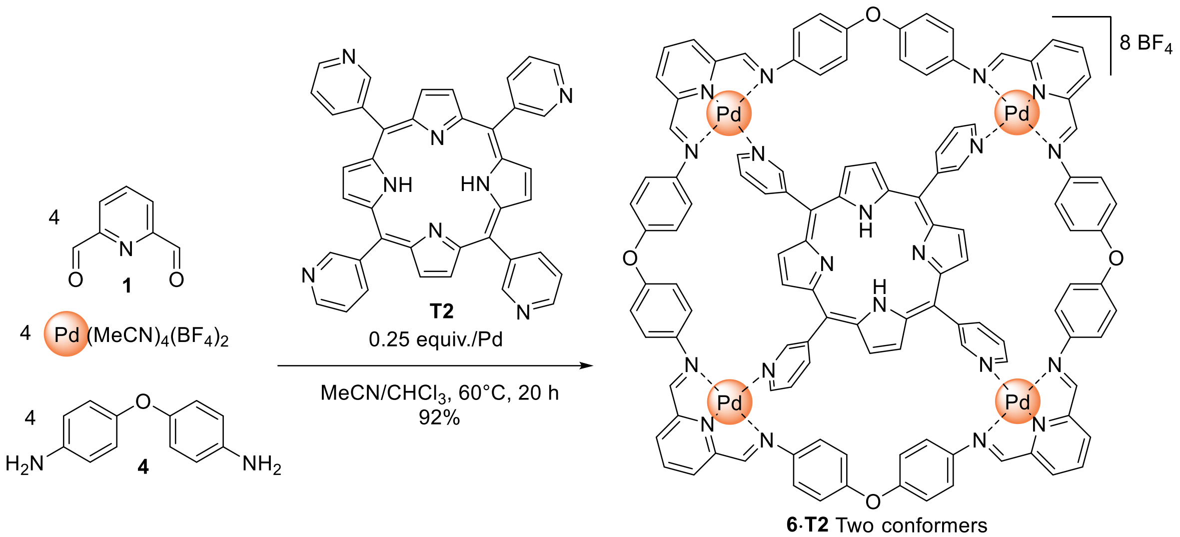

To a stirred suspension of 2,6-diformylpyridine **1** (13.6 mg, 0.101 mmol) and 4,4'-oxydianiline **4** (20.3 mg, 0.101 mmol) in 44 mL MeCN were added a solution of $[Pd(MeCN)_4](BF_4)_2$ (45.6 mg, 0.103 mmol) in 1 mL MeCN and a solution of tetrakis(3-pyridyl)porphyrin **T2** (15.8 mg, 0.0255 mmol) in 5 mL $CHCl_3$. The brown mixture was stirred at 60°C for 20 h. The solution was cooled down to *r.t.*, concentrated to a volume of *ca.* 3 mL with a rotary evaporator and slowly poured into 10 mL of *i*Pr_2O. The mixture was shaken and left to rest 10 minutes for complete precipitation then the precipitate was collected by centrifugation, washed with 5 mL Et_2O and dried under vacuum affording **6·T2(BF$_4$)$_8$** as a brown solid (68.2 mg, 0.0232 mmol, FW = 2936.15 g/mol). Yield: 92%.

^{1}H NMR (500 MHz, CD_3CN, 298 K, two conformers) δ (ppm) = 9.82 (dd, *J* = 5.9, 0.9 Hz, 1H, partial-cone), 9.71 (d, *J* = 2.0 Hz, 2H, partial-cone), 9.67 (dd, *J* = 6.0, 1.3 Hz, 4H, 1,2-alternate), 9.57 (d, *J* = 5.7 Hz, 2H, partial-cone), 9.40 (d, *J* = 2.0 Hz, 4H, 1,2-alternate), 9.33 (d, *J* = 2.0 Hz, 1H, partial-cone), 9.31 (dd, *J* = 6.0, 1.4 Hz, 1H, partial-cone), 9.29 (d, *J* = 1.9 Hz, 1H, partial-cone), 8.93 (dt, *J* = 7.8, 1.7 Hz, 1H, partial-cone), 8.66 (dt, *J* = 7.7, 1.6 Hz, 4H, 1,2-alternate), 8.64 (dt, *J* = 7.9, 1.7 Hz, 1H, partial-cone), 8.61 – 8.53 (m), 8.46 (t, *J* = 8.1 Hz, 1H, partial-cone), 8.44 (s, 2H, partial-cone), 8.43 (s, 4H, partial-cone), 8.39 (s, 4H, 1,2-alternate), 8.38 (s, 4H, 1,2-alternate), 8.30 (d, *J* = 7.8 Hz, 6H, partial-cone), 8.28 – 8.26 (m), 8.26 (dd, *J* = 4.8, 0.9 Hz, 4H, 1,2-alternate), 8.16 (d, *J* = 8.0 Hz, 2H, partial-cone), 8.12 (dd, *J* = 7.8, 6.0 Hz, 1H, partial-cone), 8.08 – 8.02 (m), 7.95 (dd, *J* = 7.8, 5.9 Hz, 2H), 7.91 (d, *J* = 5.0 Hz, 2H, partial-cone), 7.88 (bs, 2H, partial-cone), 7.81 (bs, 4H, 1,2-alternate), 7.76 (d, *J* = 8.8 Hz, 4H, partial-cone), 7.66 (d, *J* = 8.9 Hz, 8H, 1,2-alternate), 7.50 – 7.26 (m), 7.26 – 7.22 (m), -3.25 (s, 2H, partial-cone), -3.29 (s, 2H, 1,2-alternate).

^{13}C NMR (126 MHz, CD_3CN, 298 K, two conformers) δ (ppm) = 176.00, 175.74, 175.31, 174.68, 174.53, 174.24, 159.29, 159.07, 158.67, 158.42, 158.35, 157.90, 155.84, 155.82, 155.79, 155.72, 155.71, 155.51, 154.11, 153.15, 152.98, 152.58, 152.27, 152.18, 151.84, 151.45, 146.46, 146.37, 146.31, 146.27, 146.19, 145.86, 145.13, 144.20, 143.75, 143.45, 143.39, 143.12, 142.61, 142.01, 141.66, 141.37, 131.65, 131.61, 131.52, 131.43, 127.53, 126.94, 126.82, 126.62, 125.57, 125.38, 125.30, 125.25, 125.20, 124.98, 122.76, 121.29, 121.13, 120.94, 120.46, 119.86, 115.55, 115.50, 115.16.

ESI-HRMS for **6·T2** [$(C_{116}H_{78}N_{20}O_4Pd_4)^{8+}$] m/z = [**6·T2**]$^{8+}$, calcd: 280.1585, found: 280.1583; [**6·T2** + BF_4]$^{7+}$, calcd: 332.4674, found: 332.4680; [**6·T2** + 2 BF_4]$^{6+}$, calcd: 402.3793, found: 402.3801; [**6·T2** + 3 BF_4]$^{5+}$, calcd: 500.2560, found: 500.2573; [**6·T2** + 4 BF_4]$^{4+}$, calcd: 647.0711, found: 647.0727.

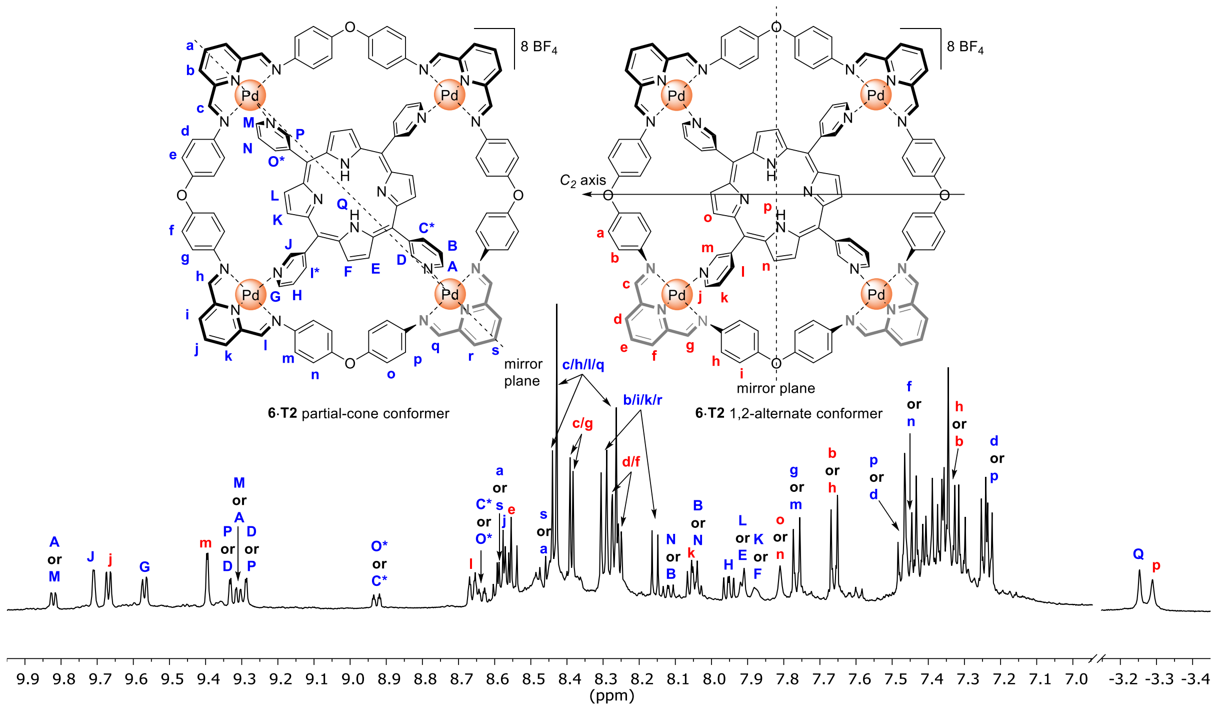

Figure S16. ^{1}H NMR spectrum of **6·T2** (500 MHz, CD_3CN, 298 K). Numerous overlapping signals prevented complete assignment. The C_{2h} symmetric conformer was identified by the presence of one set of ^{1}H NMR signals for the pyridyl moieties of the porphyrin template **T2** and two sets for the imines and aromatic protons of the macrocycle **6**; indeed, only one set of signals would have been expected for the highly symmetric cone (C_{4v}) and 1,3-alternate (D_{2d}) conformers.

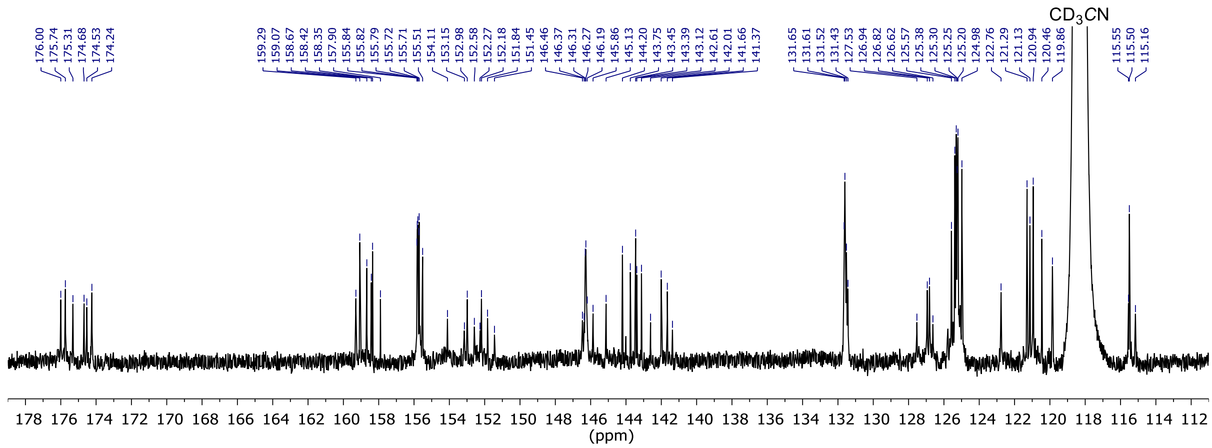

Figure S17. ^{13}C NMR spectrum of **6·T2** (126 MHz, CD_3CN, 298 K).

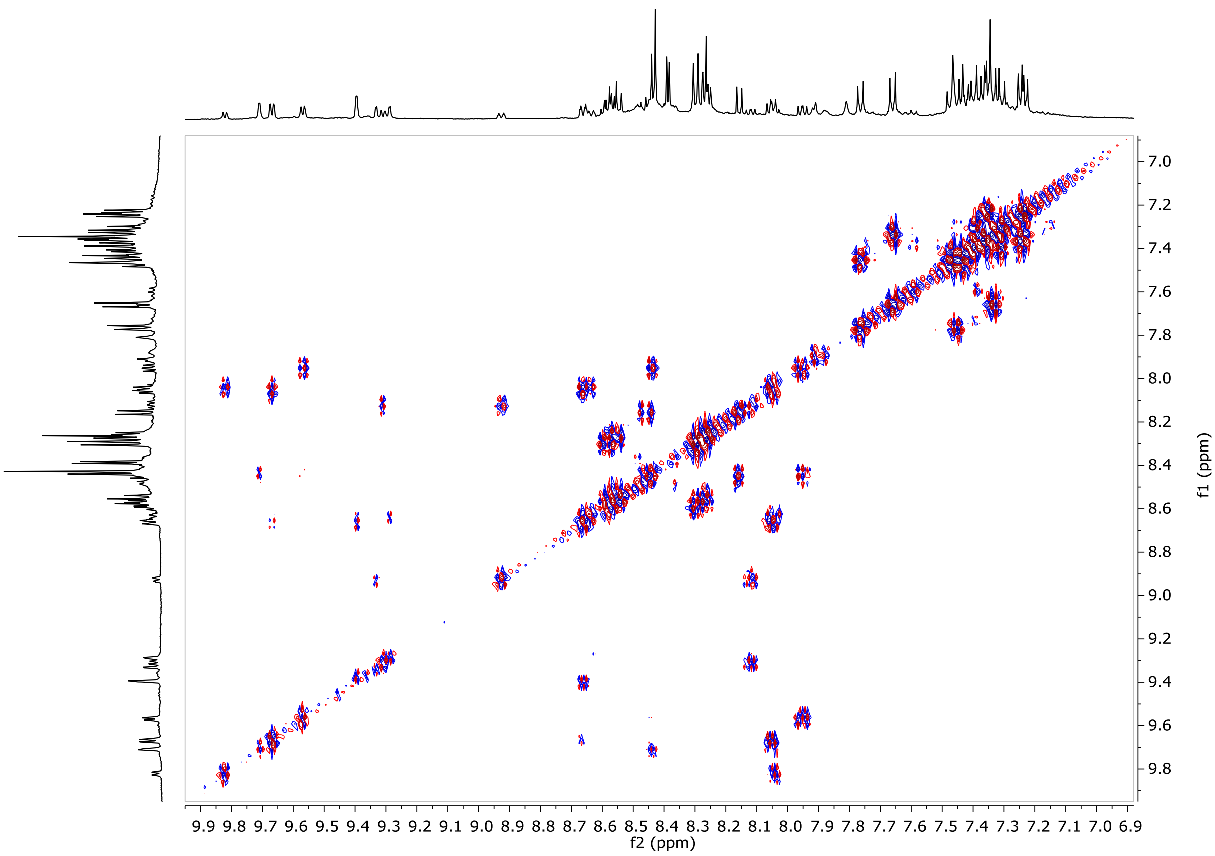

Figure S18. dqfCOSY spectrum of **6·T2** (500 MHz, CD_3CN, 298 K).

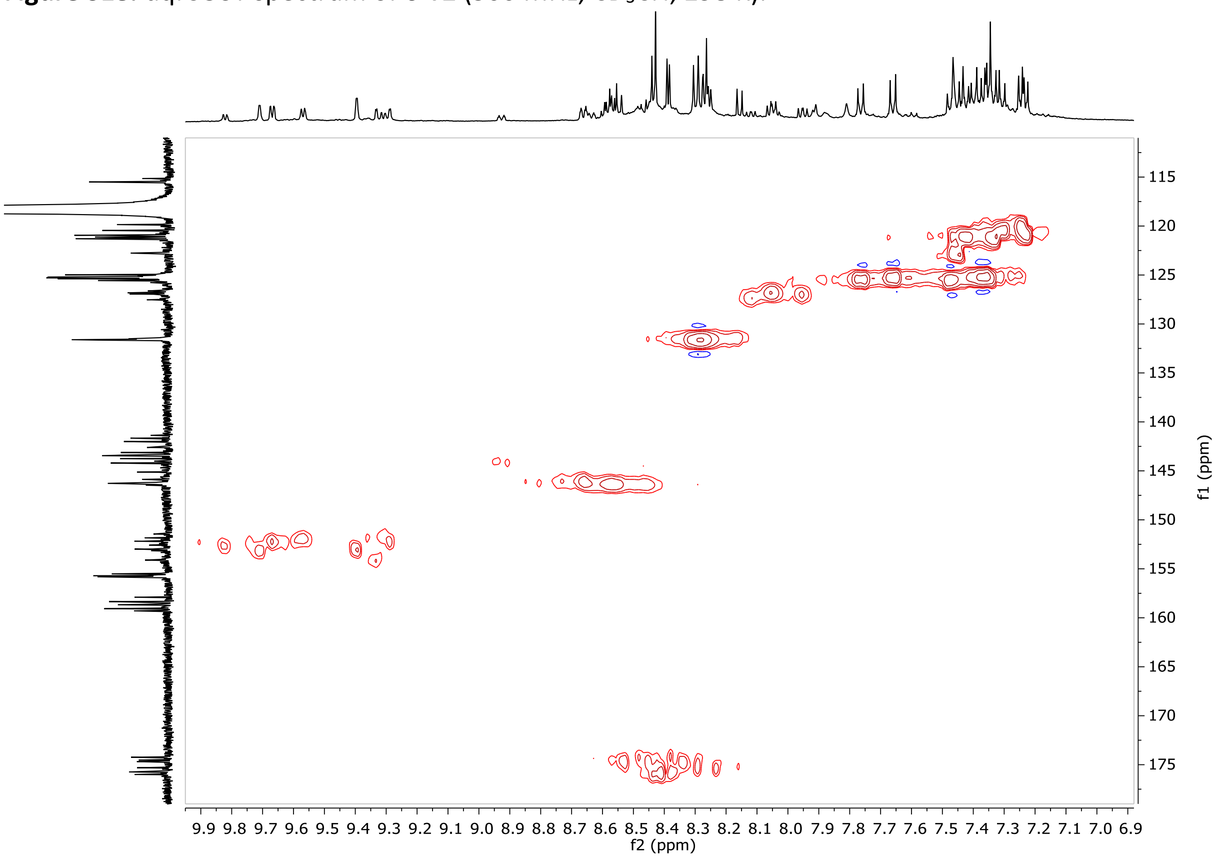

Figure S19. Edited ^{1}H-^{13}C HSQC spectrum of **6·T2** (11.7 Tesla, CD_3CN, 298 K). The unusual shape of the correlation spot for the N=CH is most likely caused by a ^{1}J coupling constant value out of the usual range covered by standard HSQC parameters.

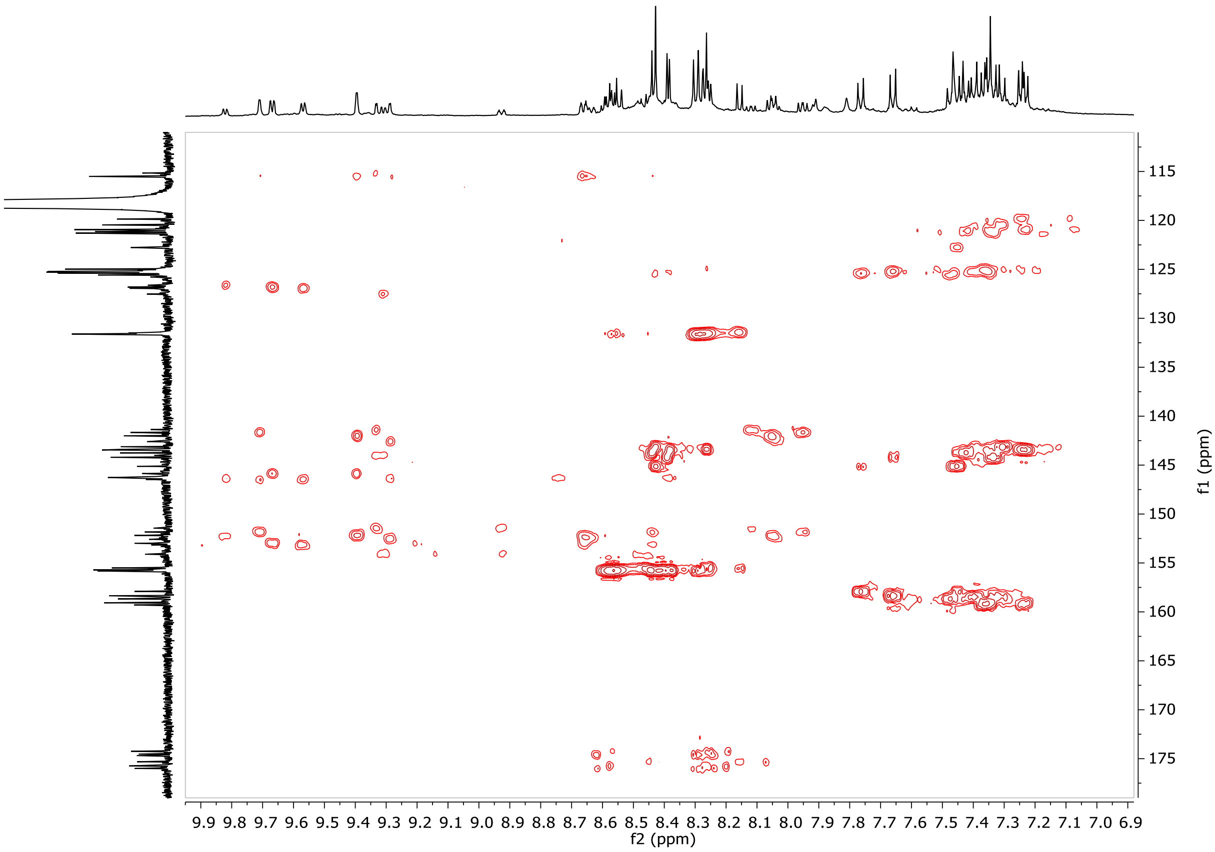

Figure S20. ^{1}H-^{13}C HMBC spectrum of **6·T2** (11.7 Tesla, CD_3CN, 298 K).

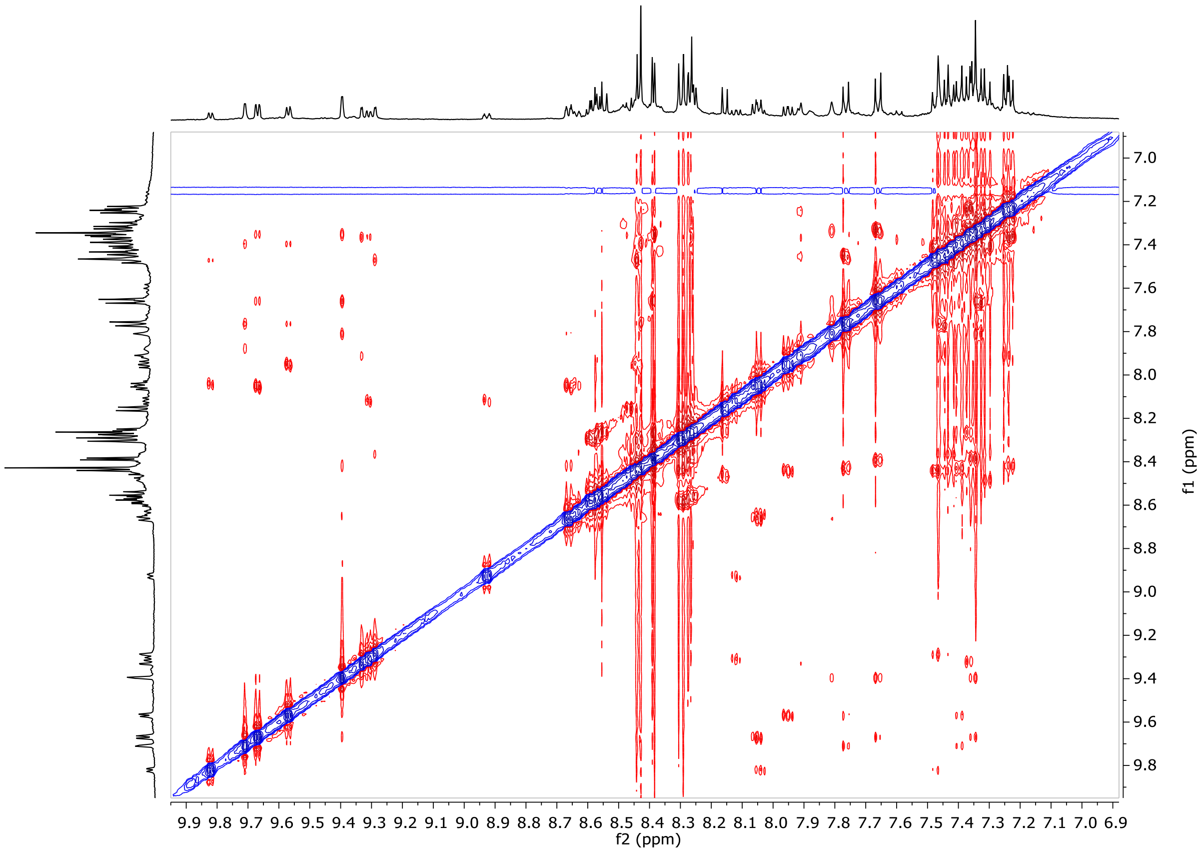

Figure S21. ROESY spectrum of **6·T2** (τ_m: 500 ms, 500 MHz, CD_3CN, 298 K).

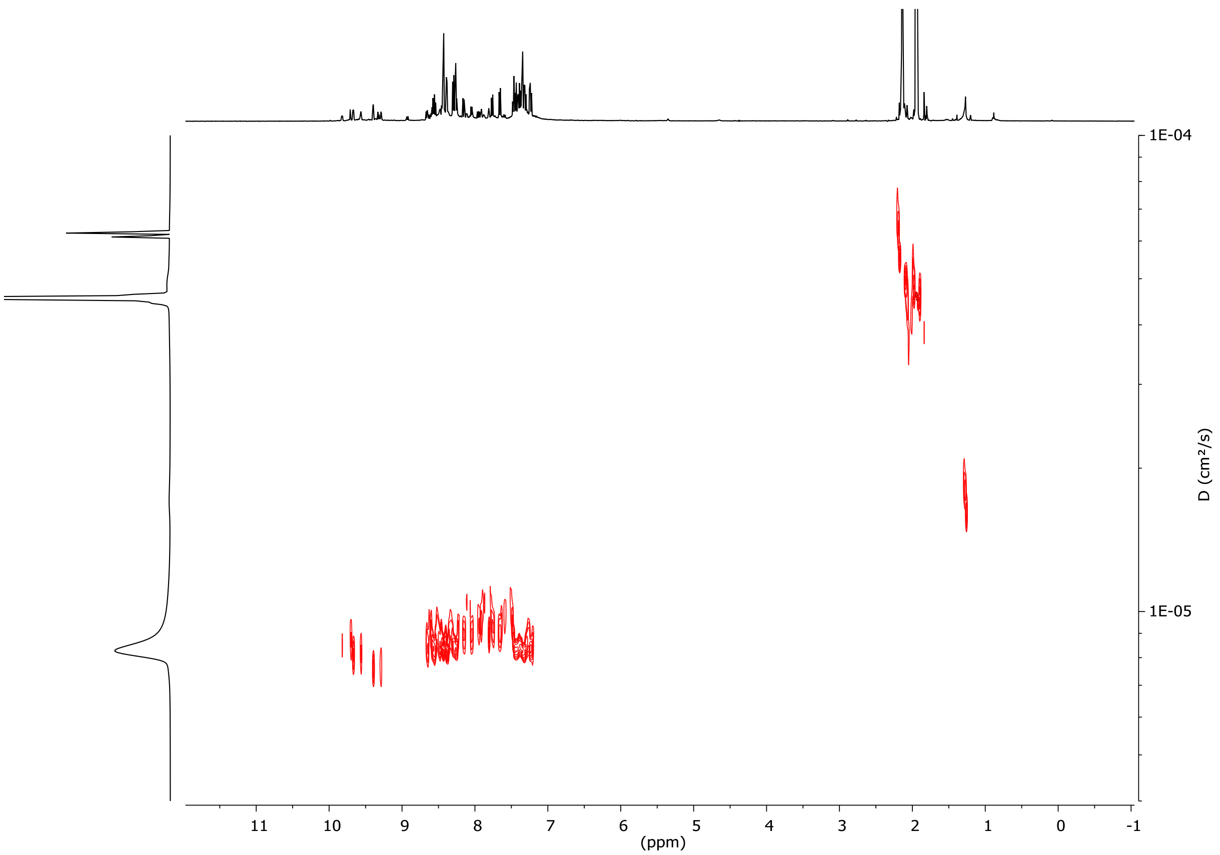

Figure S22. ^{1}H DOSY spectrum of **6·T2** (500 MHz, CD_3CN, 298 K, diffusion delay Δ = 100 ms, diffusion gradient length δ = 1700 μs).

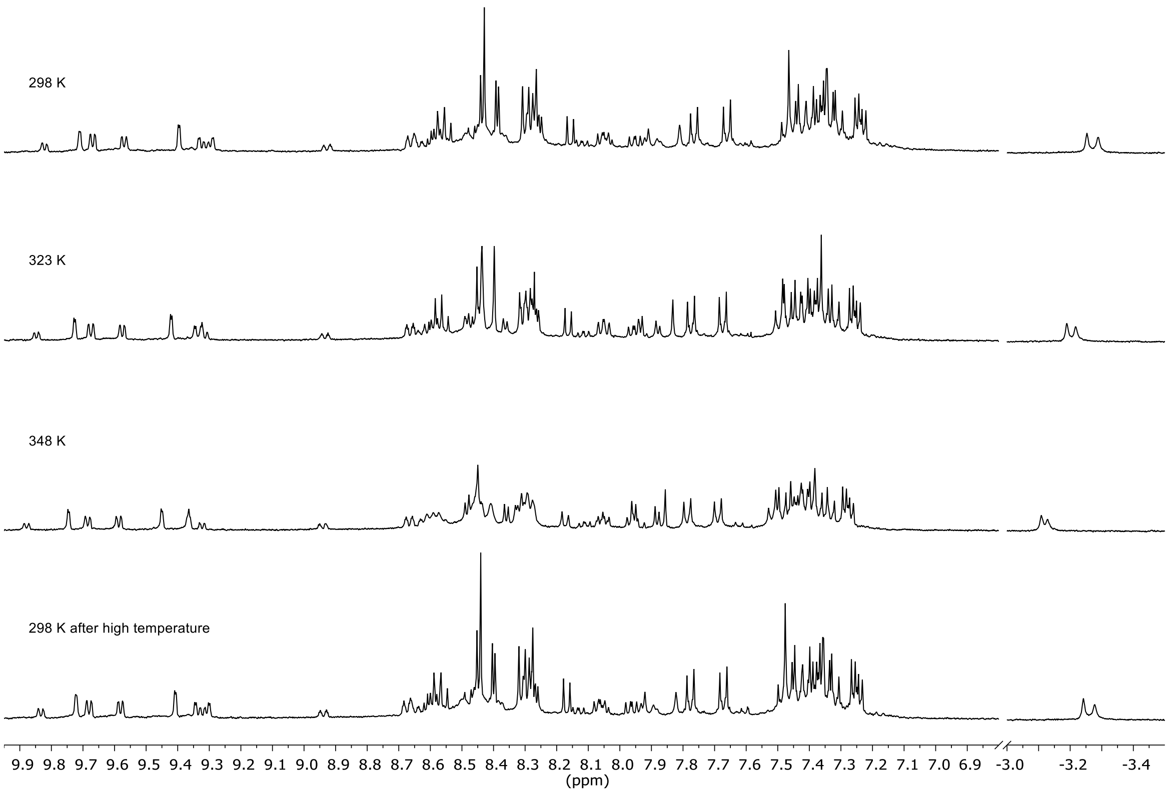

Figure S23. Variable temperature ^{1}H NMR spectra of **6·T2** (400 MHz, CD_3CN) showing slight broadening of signals at 348 K but no coalescence of signals between the two conformers. The bottom spectrum shows that no degradation occurred during the VT experiment.

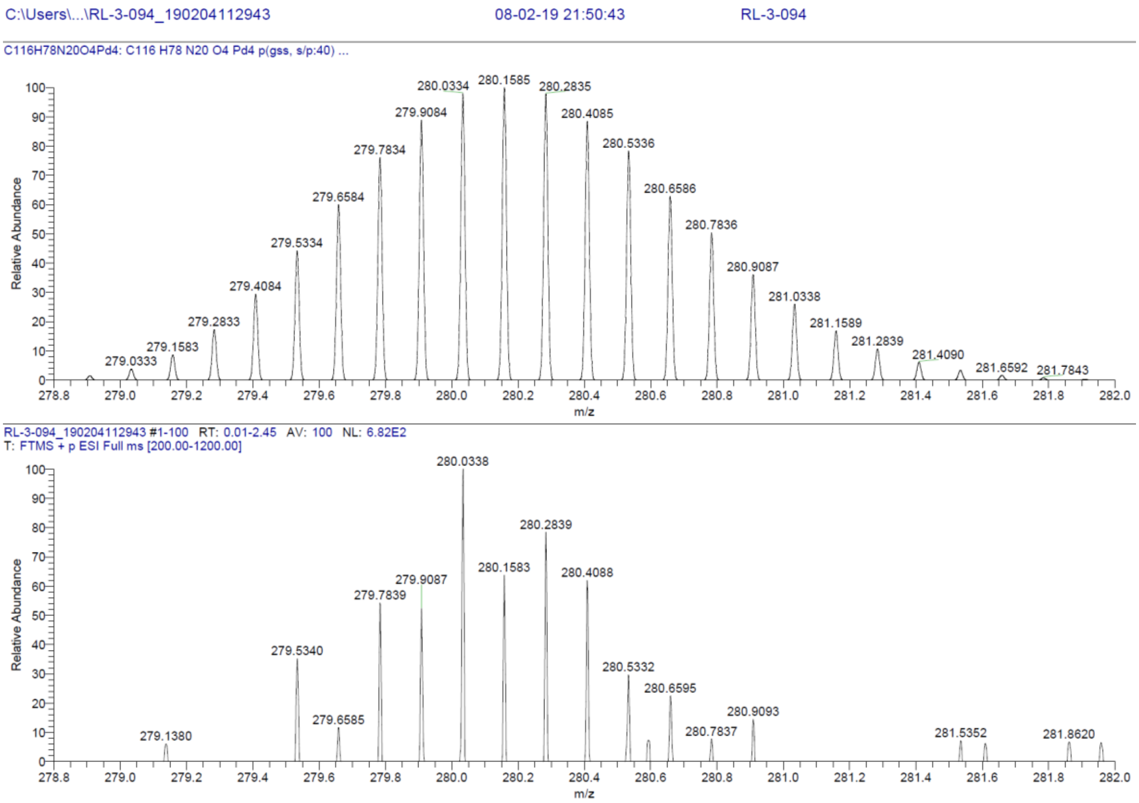

Figure S24A. Top: simulated isotopic pattern, bottom: recorded ESI-HRMS of [**6·T2**]$^{8+}$. The signal was weak for this charge state but intense enough to identify the species.

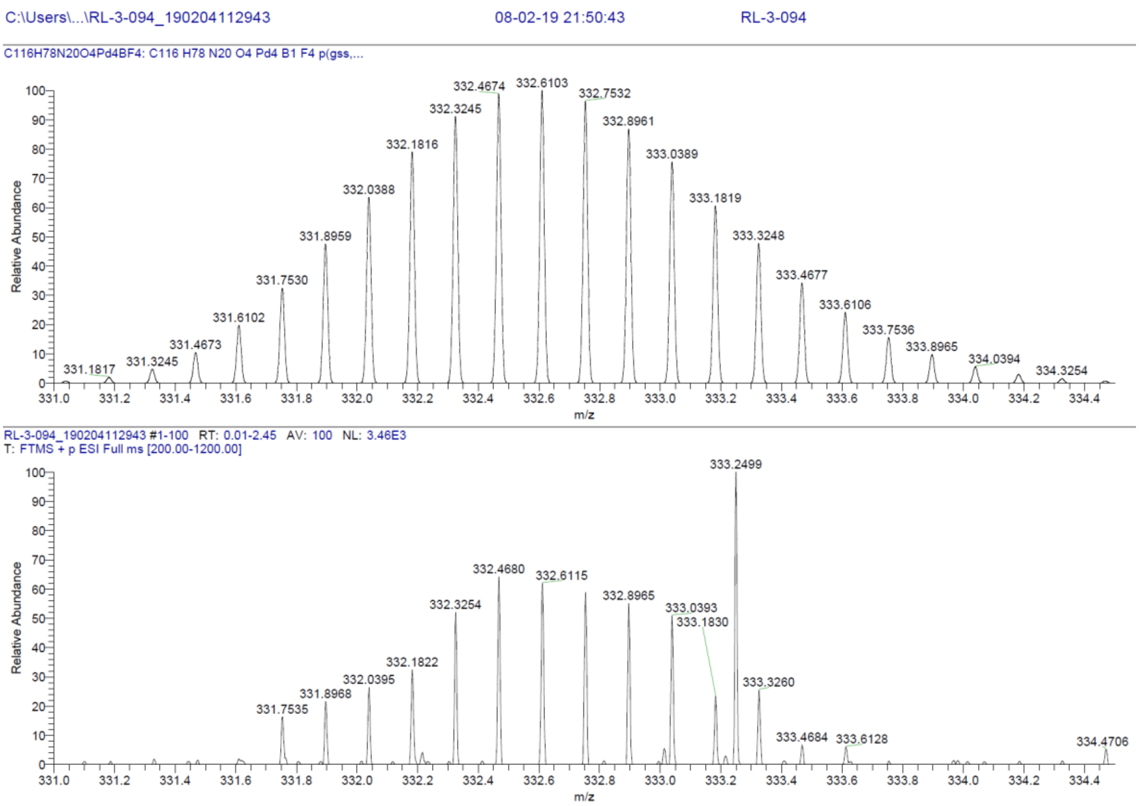

Figure S24B. Top: simulated isotopic pattern, bottom: ESI-HRMS of [**6·T2** + BF_4]$^{7+}$. The signal was weak for this charge state but intense enough to identify the species. The peak at 333.2499 m/z corresponds to an impurity present during the analysis.

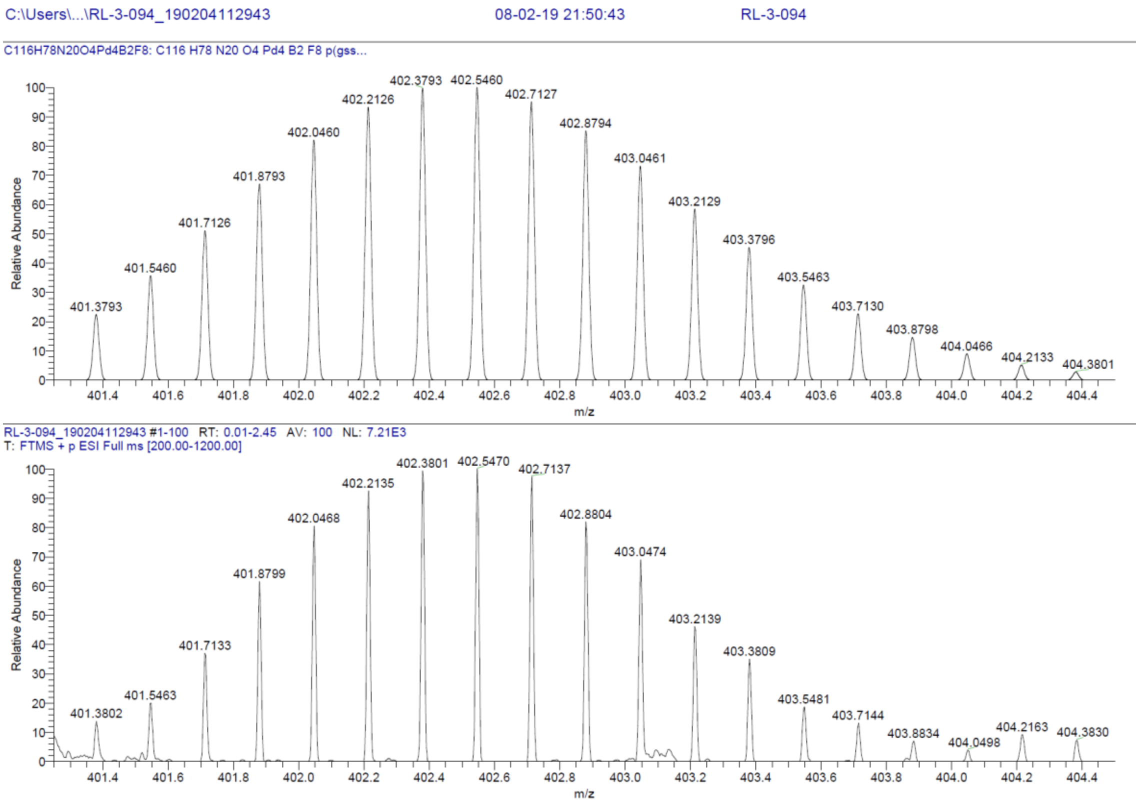

Figure S24C. Top: simulated isotopic pattern, bottom: ESI-HRMS of [**6·T2** + 2 BF_4]$^{6+}$.

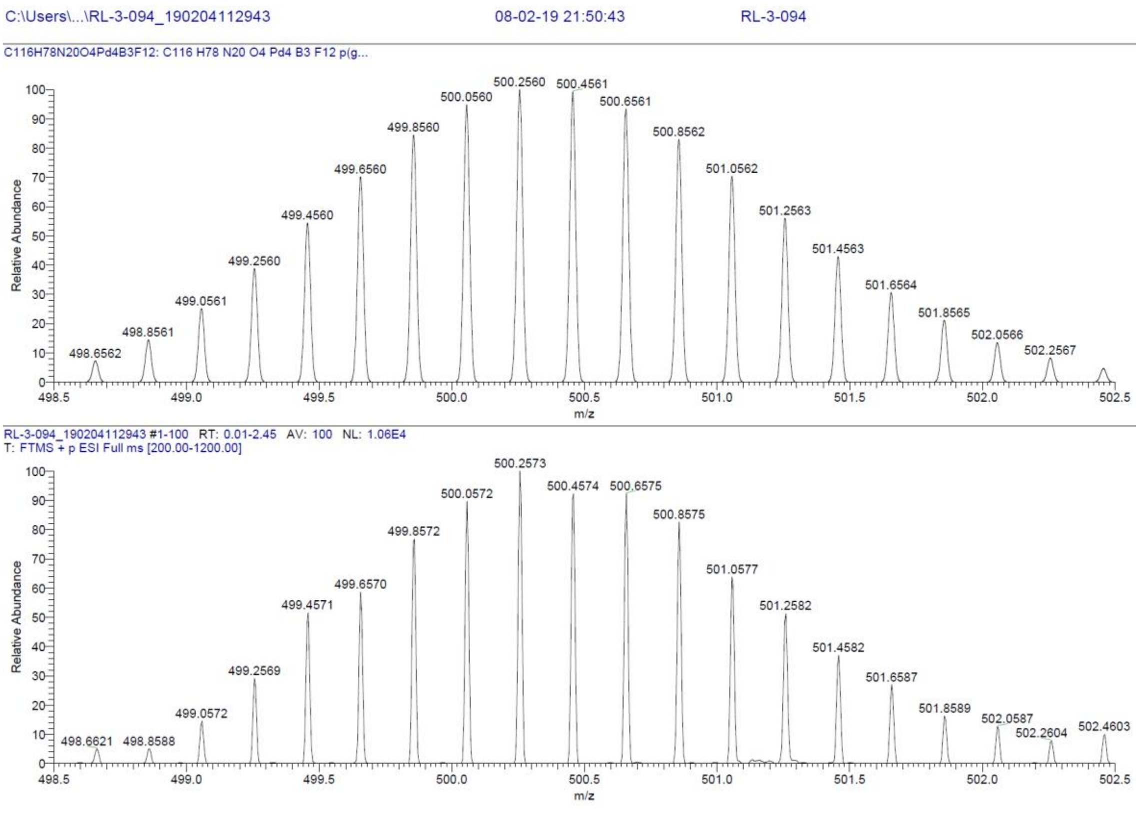

Figure S24D. Top: simulated isotopic pattern, bottom: ESI-HRMS of [**6·T2** + 3 BF_4]$^{5+}$.

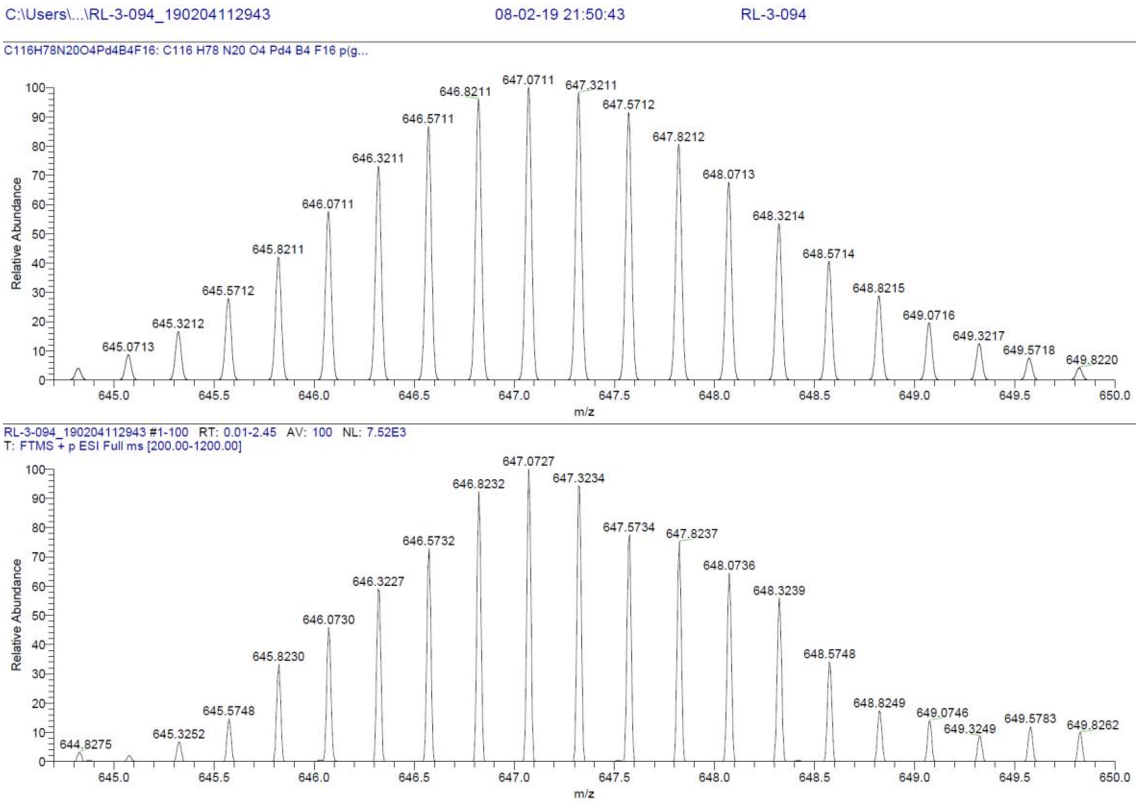

Figure S24E. Top: simulated isotopic pattern, bottom: ESI-HRMS of [**6·T2** + 4 BF_4]$^{4+}$.

1.5 Synthesis and characterization of reduced macrocycle Pd_3[3+3] **7·T1**

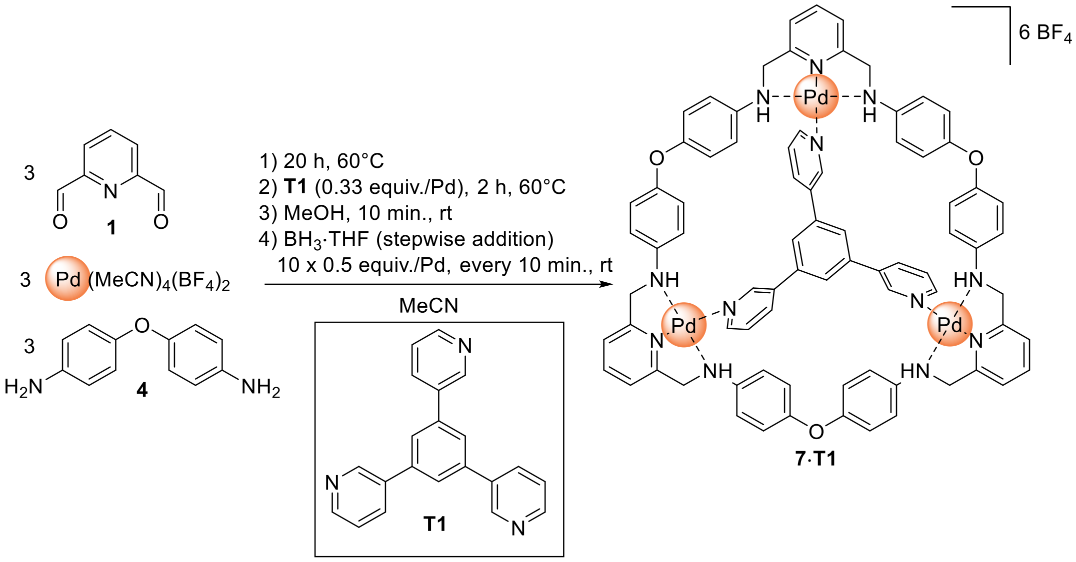

To a stirred suspension of 2,6-diformylpyridine **1** (27.5 mg, 0.203 mmol) and 4,4'-oxydianiline **4** (40.2 mg, 0.201 mmol) in 50 mL MeCN was added a solution of [Pd(MeCN)$_4$](BF_4)$_2$ (90.6 mg, 0.204 mmol) in 1 mL MeCN. The orange mixture was stirred at 60°C for 20 h. 1,3,5-tris(3-pyridyl)benzene **T1** (23.1 mg, 0.0672 mmol) was added and the mixture was stirred at 60°C for 2 h. The solution was cooled down to *r.t.* under stirring and 10 mL MeOH were added. After 10 minutes, BH_3·THF (1M) was added stepwise (10 additions of 100 µL, one every 10 min., total 1.00 mmol) and the reaction was monitored by ESI-MS (see Figure S27). The mixture was concentrated to a volume of *ca.* 5 mL with a rotary evaporator, filtered and slowly poured into 30 mL of Et_2O. The precipitate was collected by centrifugation, washed with 5 mL Et_2O and dried under vacuum affording **7·T1(BF_4)$_6$** as a yellowish grey solid (142 mg, purity and yield undetermined at this stage, FW = 2059.55 g/mol).

^{1}H NMR (500 MHz, CD_3CN, 298 K, mixture of stereoisomers and conformers) δ (ppm) = 9.20 – 5.80 (m), 5.60 – 4.20 (m).

ESI-HRMS for **7·T1** [($C_{78}H_{66}N_{12}O_3Pd_3$)$^{6+}$] m/z = [**7·T1** + BF_4]$^{5+}$, calcd: 325.0507, found: 325.0513; [**7·T1** + 2 BF_4]$^{4+}$, calcd: 428.0645, found: 428.0644; [**7·T1** + 3 BF_4]$^{3+}$, calcd: 599.4207, found: 599.4202; [**7·T1** + 4 BF_4]$^{2+}$, calcd: 942.6330, found: 942.6333.

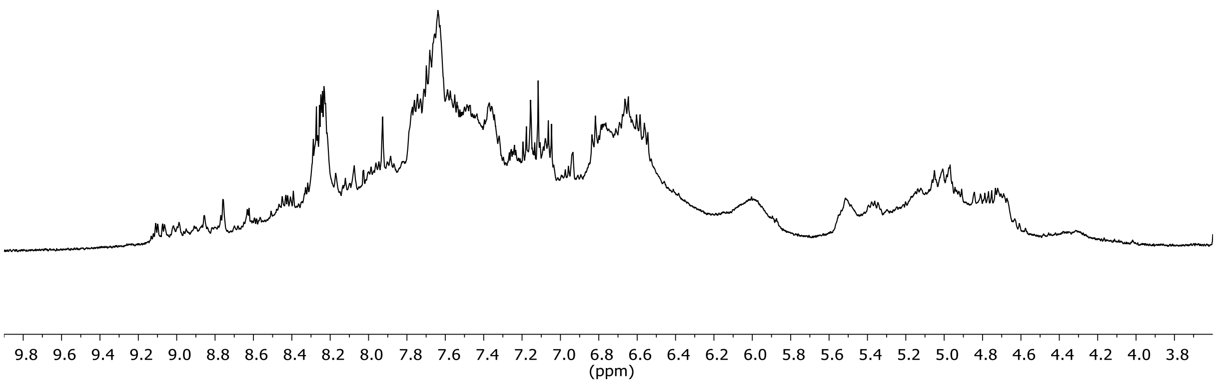

Figure S25. ^{1}H NMR spectrum of **7·T1** (500 MHz, CD_3CN, 298 K). The large number of stereoisomers and potential conformers prevents NMR characterization (see Figure S26).

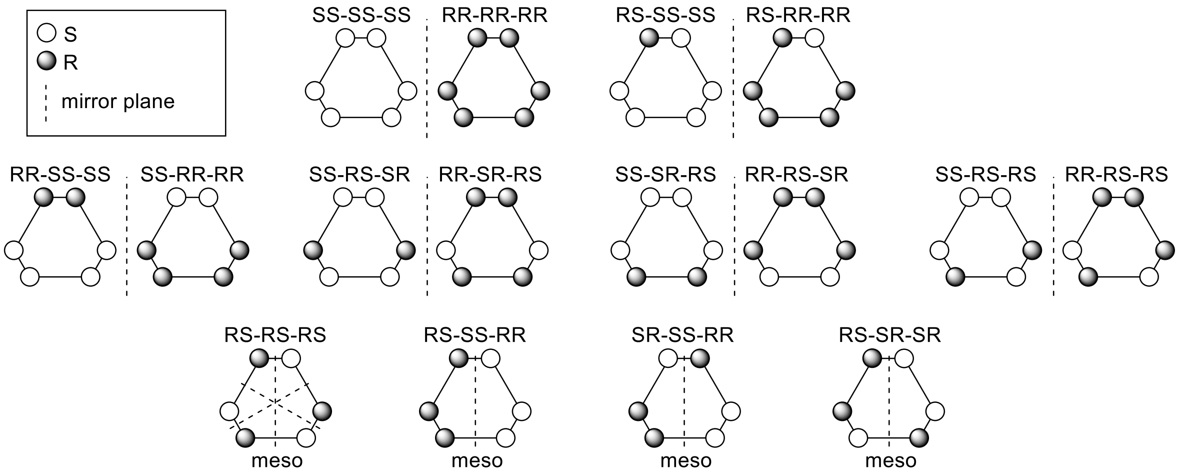

Figure S26. Expected 16 stereoisomers originating from the 6 NH stereocenters on **7·T1** including 6 pairs of enantiomers and 4 meso compounds.

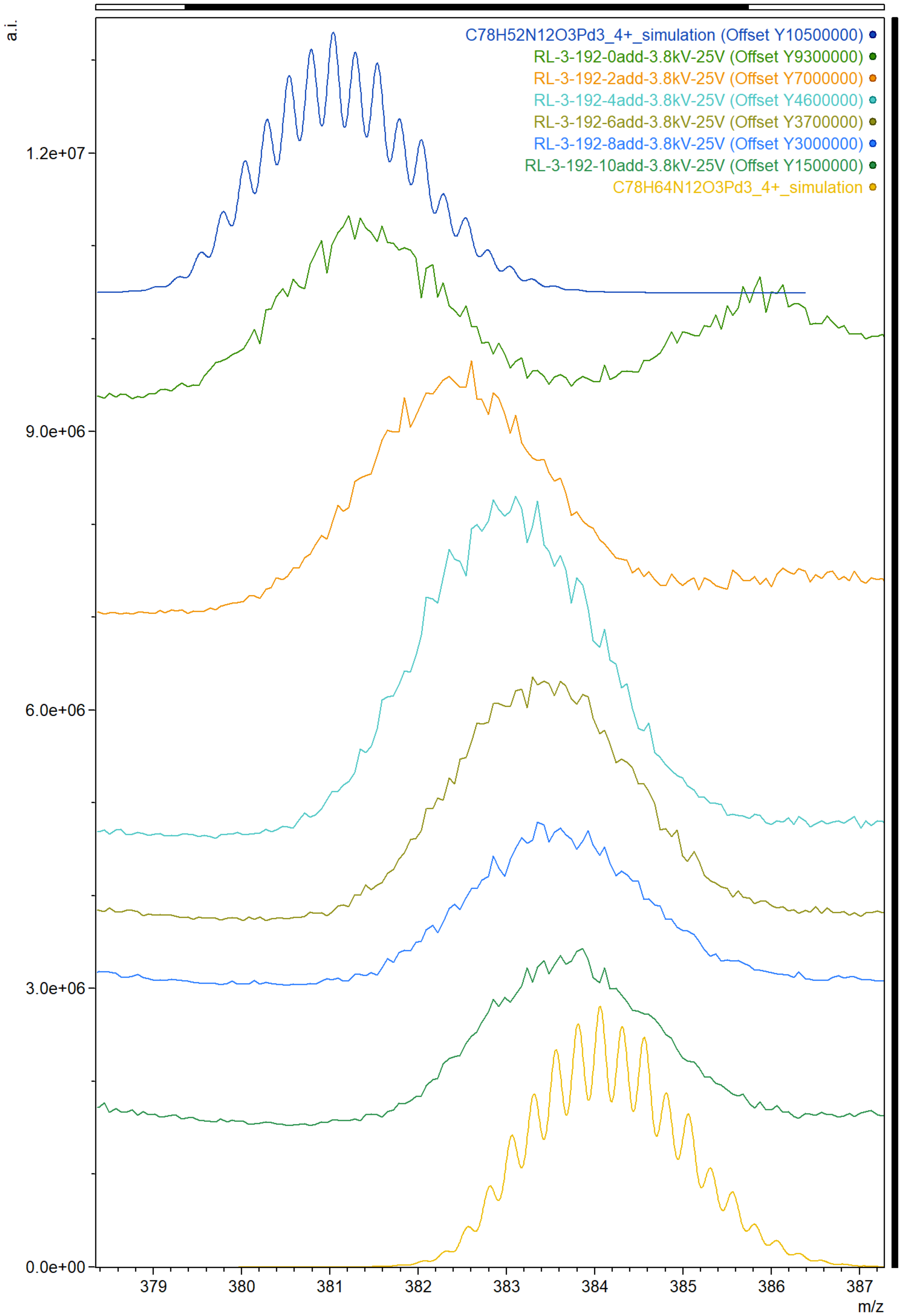

Figure S27. ESI-LRMS monitoring of the reduction of **5·T1** leading to **7·T1**. Zoom on the region around [**5·T1**-2H]$^{4+}$ and [**7·T1**-2H]$^{4+}$. Spectra from top to bottom: simulated for [**5·T1**-2H]$^{4+}$, before addition of BH_3, after 2, 4, 6, 8, 10 additions, simulated for [**7·T1**-2H]$^{4+}$. No change was observed between 8 and 10 additions, therefore the reaction was stopped even if the peak after 10 additions does not match perfectly the simulated spectrum of the product.

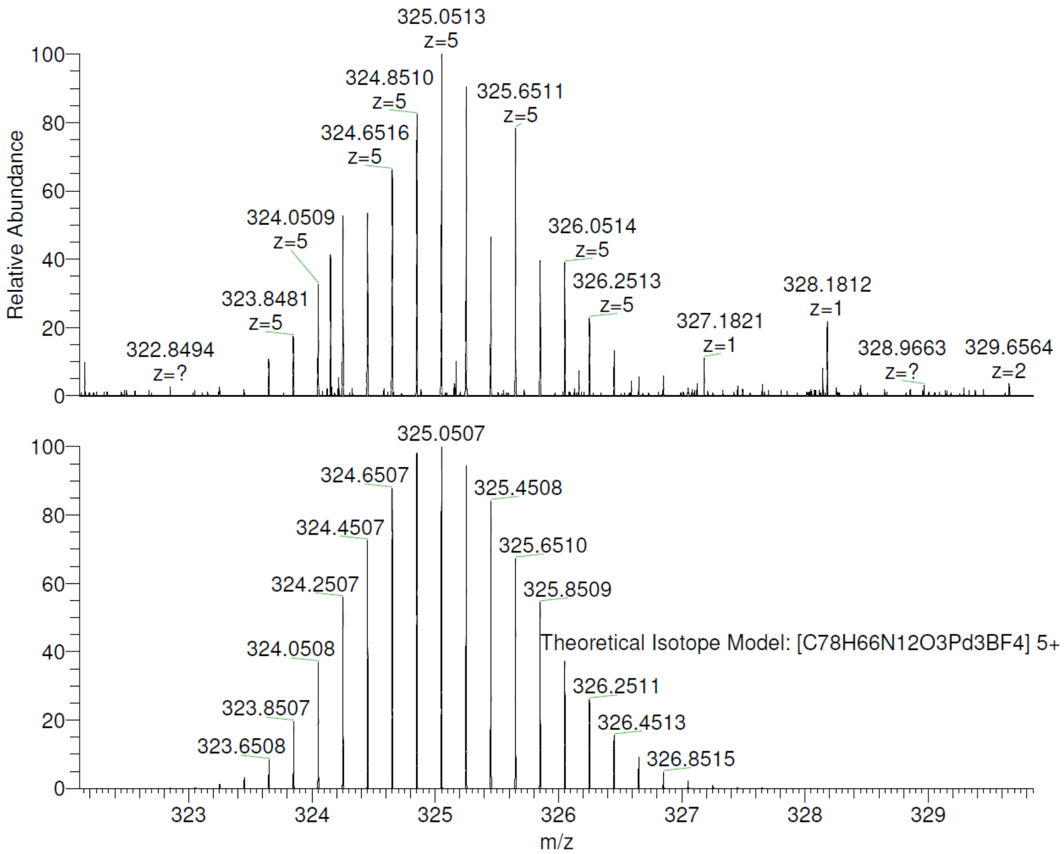

Figure S28A. Top: ESI-HRMS of [**7·T1** + BF_4]$^{5+}$, bottom: simulated isotopic pattern. The signal was weak for this charge state but intense enough to identify the species.

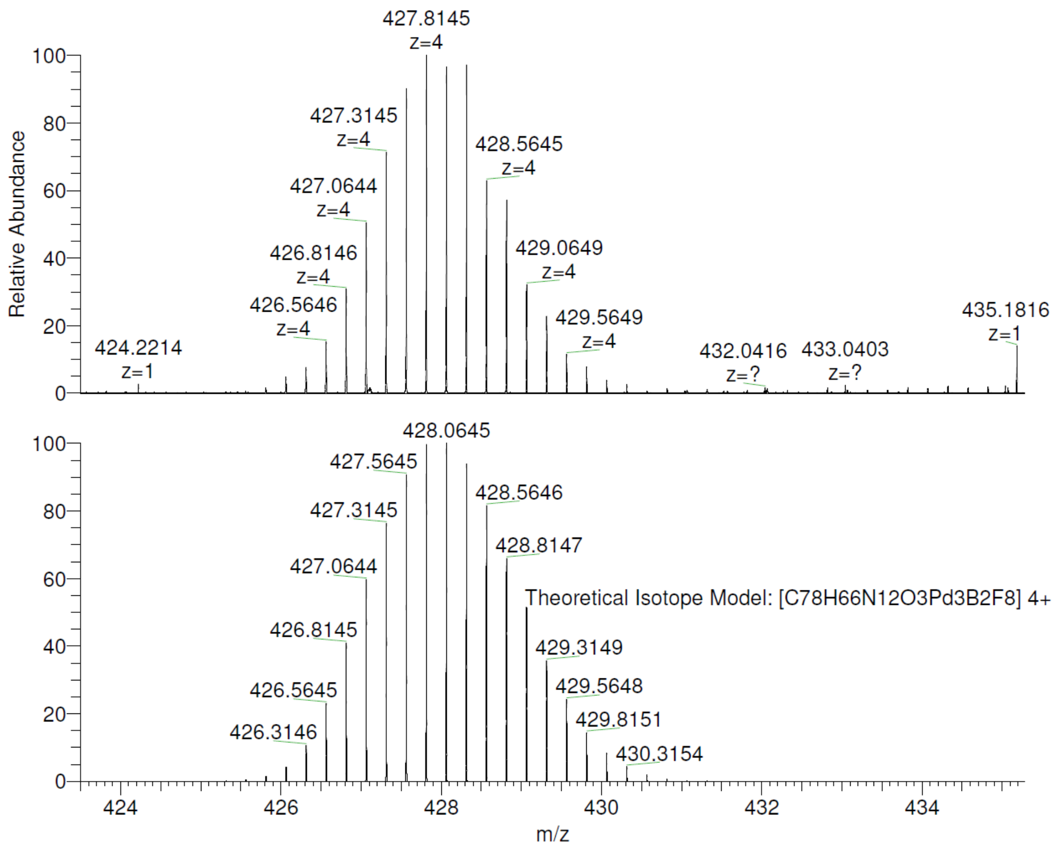

Figure S28B. Top: ESI-HRMS of [**7·T1** + 2 BF_4]$^{4+}$, bottom: simulated isotopic pattern.

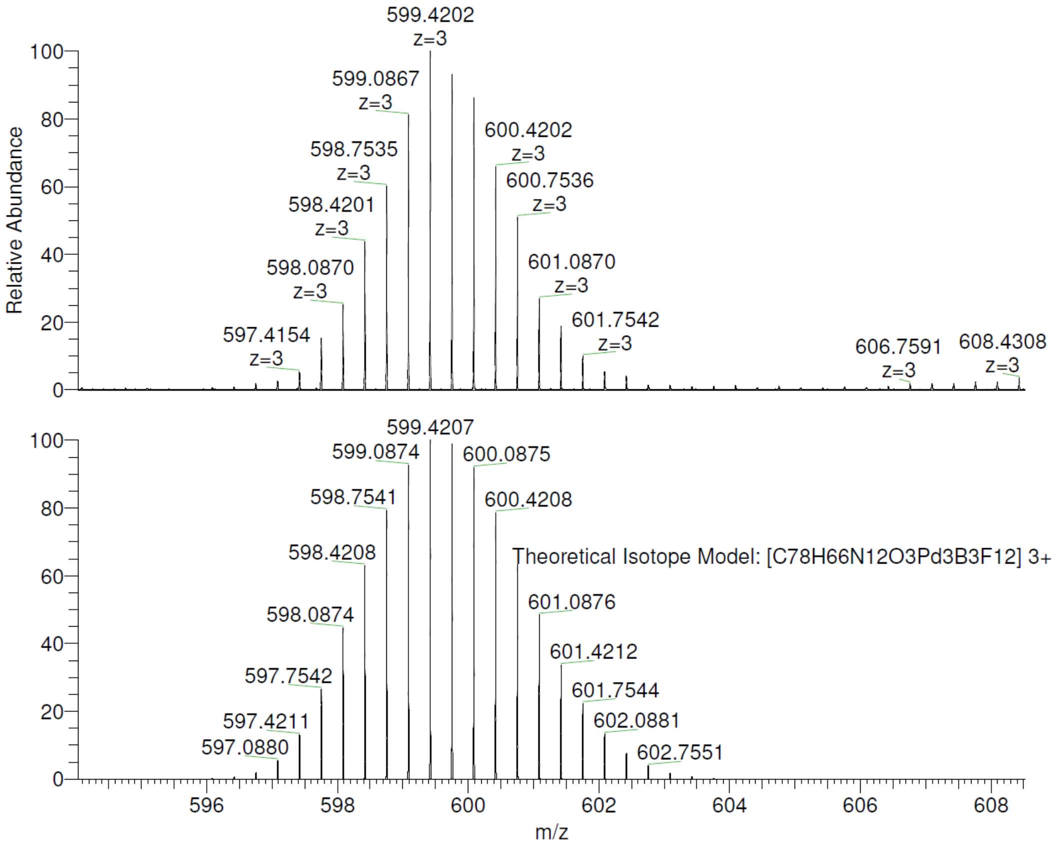

Figure S28C. Top: ESI-HRMS of [**7·T1** + 3 BF_4]$^{3+}$, bottom: simulated isotopic pattern.

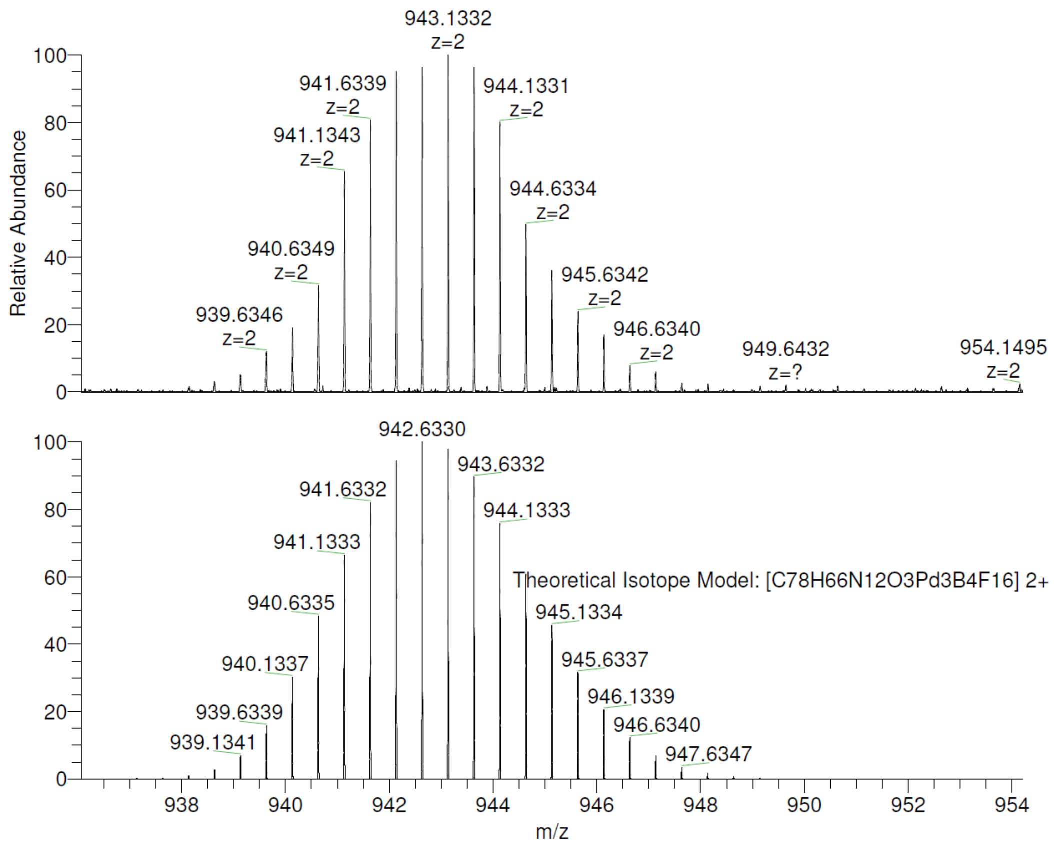

Figure S28D. Top: ESI-HRMS of [**7·T1** + 4 BF_4]$^{2+}$, bottom: simulated isotopic pattern.

1.6 Synthesis and characterization of reduced macrocycle Pd_4[4+4] **8·T2**

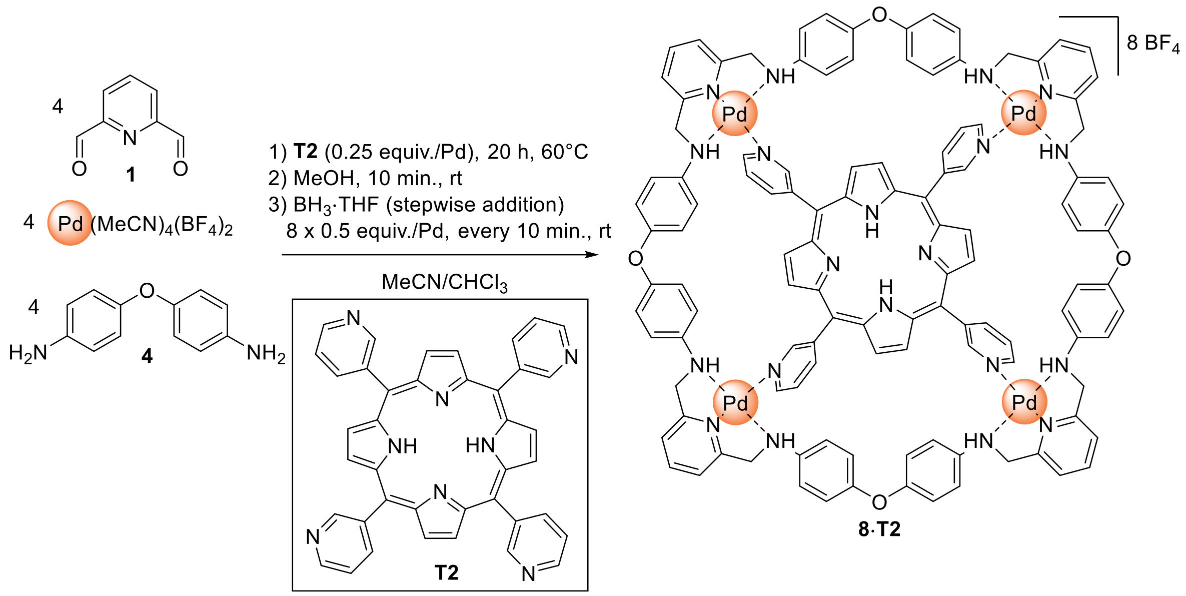

To a stirred suspension of 2,6-diformylpyridine **1** (27.2 mg, 0.201 mmol) and 4,4'-oxydianiline **4** (40.4 mg, 0.202 mmol) in 45 mL MeCN were added a solution of $[Pd(MeCN)_4](BF_4)_2$ (91.1 mg, 0.205 mmol) in 1 mL MeCN and a solution of tetrakis(3-pyridyl)porphyrin **T2** (32.0 mg, 0.0517 mmol) in 5 mL $CHCl_3$. The brown mixture was stirred at 60°C for 20 h. The solution was cooled down to *r.t.* under stirring and 10 mL MeOH were added. After 10 minutes, BH_3·THF (1M) was added stepwise (8 additions of 100 µL, one every 10 min., total 0.800 mmol) and the reaction was monitored by ESI-MS (see Figure S31). The mixture was concentrated to a volume of *ca.* 5 mL with a rotary evaporator, filtered and slowly poured into 30 mL of Et_2O. The precipitate was collected by centrifugation, washed with 10 mL Et_2O and dried under vacuum affording **8·T2(BF$_4$)$_8$** as a brown solid (153 mg, purity and yield undetermined at this stage, FW = 2952.27 g/mol).

^{1}H NMR (500 MHz, CD_3CN, 298 K, mixture of stereoisomers and conformers) δ (ppm) = 9.70 – 6.50 (m), 6.30 – 5.80 (m), 5.70 – 4.50 (m), -3.15 – -3.45 (m, $NH^{porphyrin}$).

ESI-HRMS for **8·T2** [$(C_{116}H_{94}N_{20}O_4Pd_4)^{8+}$] m/z = [**8·T2** + 3 BF_4]$^{5+}$, calcd: 503.4810, found: 503.4801; [**8·T2** + 4 BF_4]$^{4+}$, calcd: 651.1024, found: 651.1014; [**8·T2** + 5 BF_4]$^{3+}$, calcd: 897.1380, found: 897.1366; [**8·T2** + 6 BF_4]$^{2+}$, calcd: 1389.2089, found: 1389.2063.

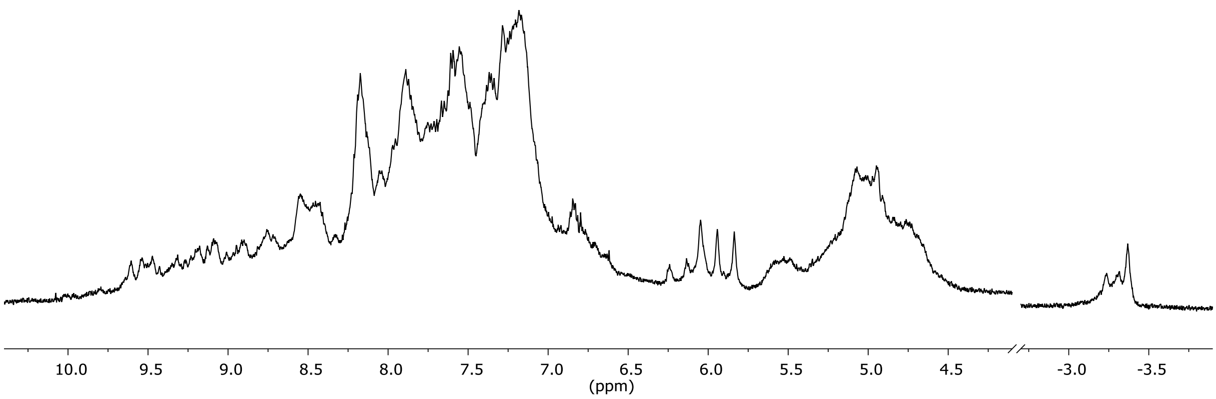

Figure S29. ^{1}H NMR spectrum of **8·T2** (500 MHz, CD_3CN, 298 K). The large number of stereoisomers and potential conformers prevents NMR characterization (see Figure S30).

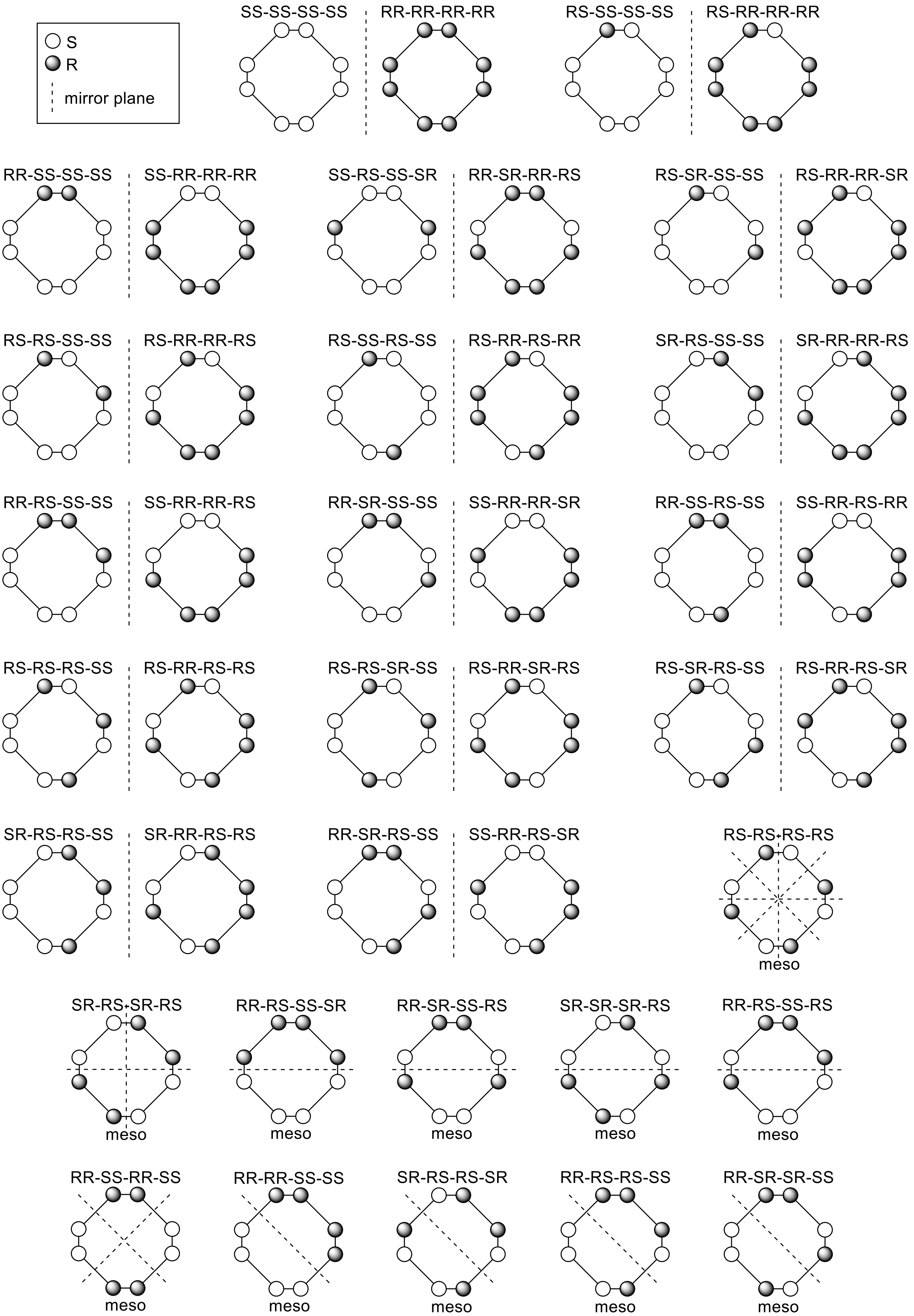

Figure S30. Expected 43 stereoisomers originating from the 8 NH stereocenters on **8·T2** including 16 pairs of enantiomers and 11 meso compounds.

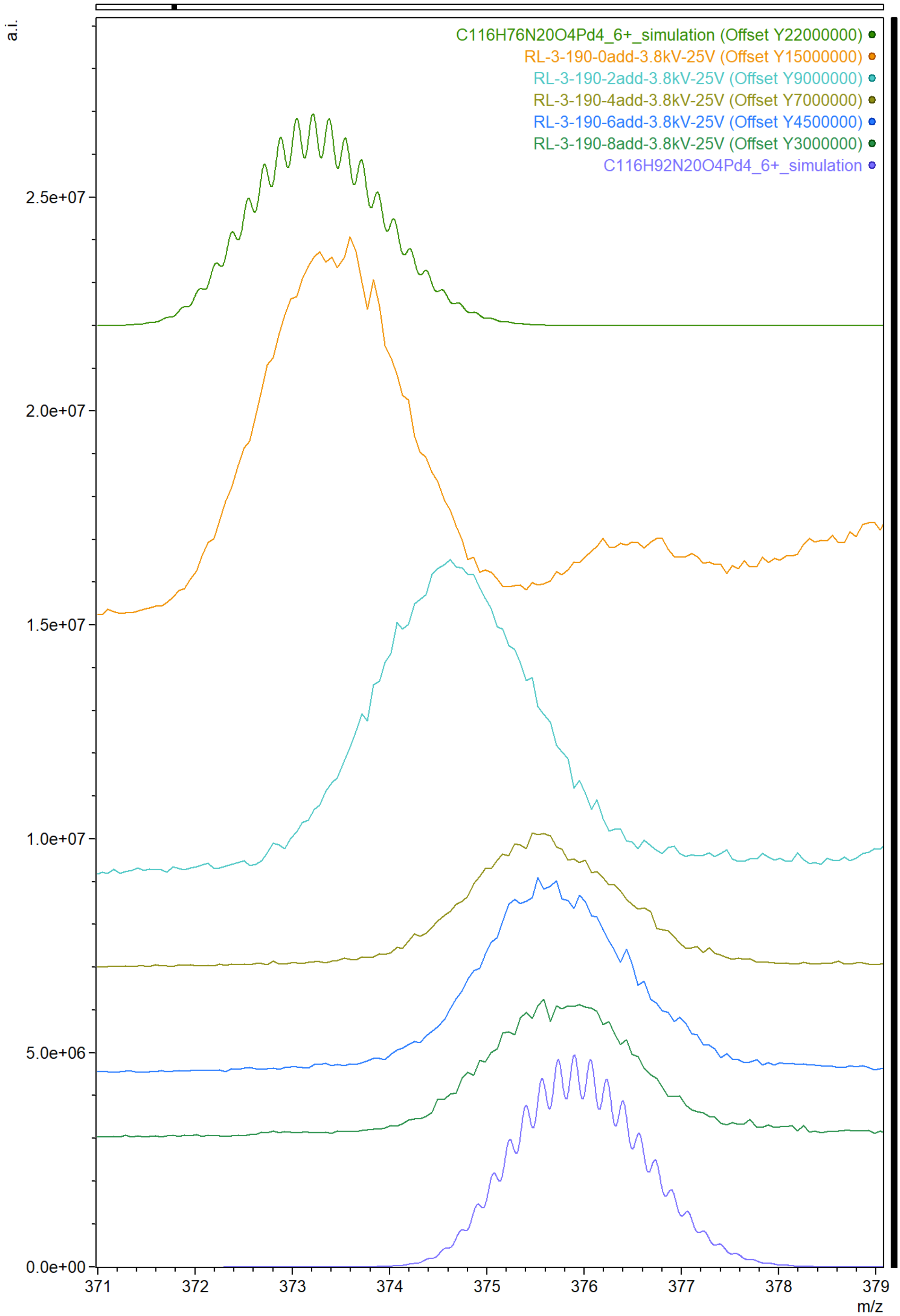

Figure S31. ESI-LRMS monitoring of the reduction of **6·T2** leading to **8·T2**. Zoom on the region around [**6·T2**-2H]$^{6+}$ and [**8·T2**-2H]$^{6+}$. Spectra from top to bottom: simulated for [**6·T2**-2H]$^{6+}$, before addition of BH_3, after 2, 4, 6, 8 additions, simulated for [**8·T2**-2H]$^{6+}$.

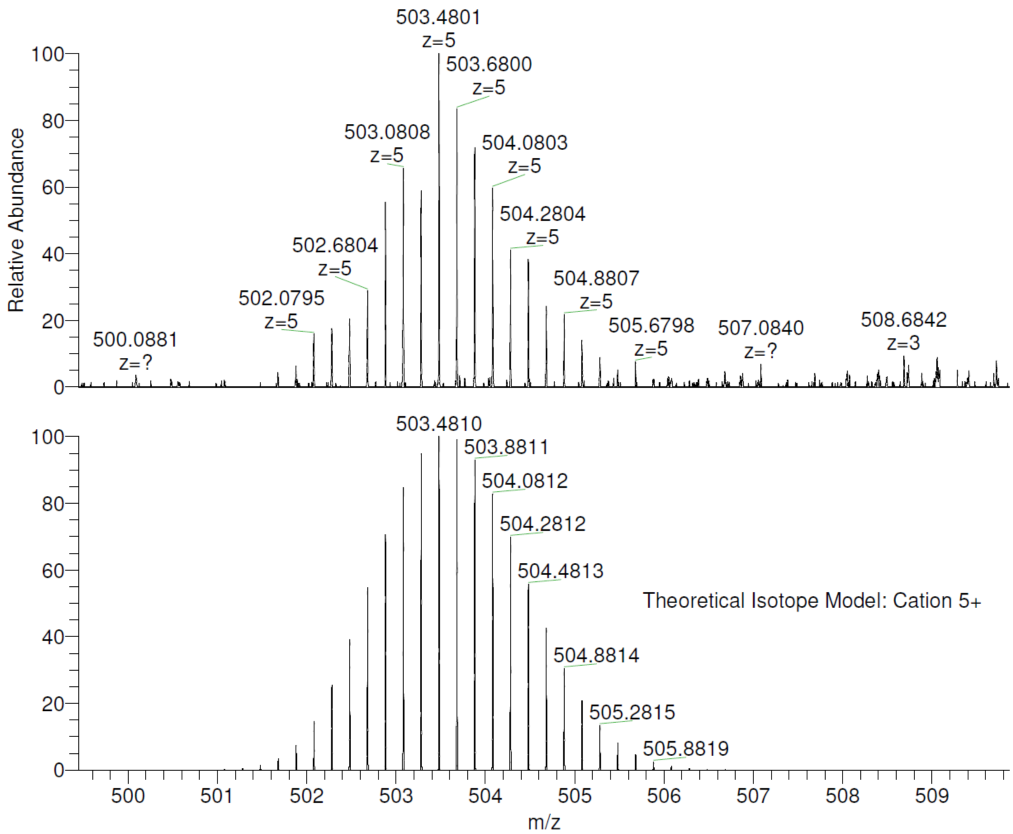

Figure S32A. Top: ESI-HRMS of [**8·T2** + 3 BF_4]$^{5+}$, bottom: simulated isotopic pattern for [$C_{116}H_{94}N_{20}O_4Pd_4B_3F_{12}$]$^{5+}$. The signal was weak for this charge state but intense enough to identify the species.

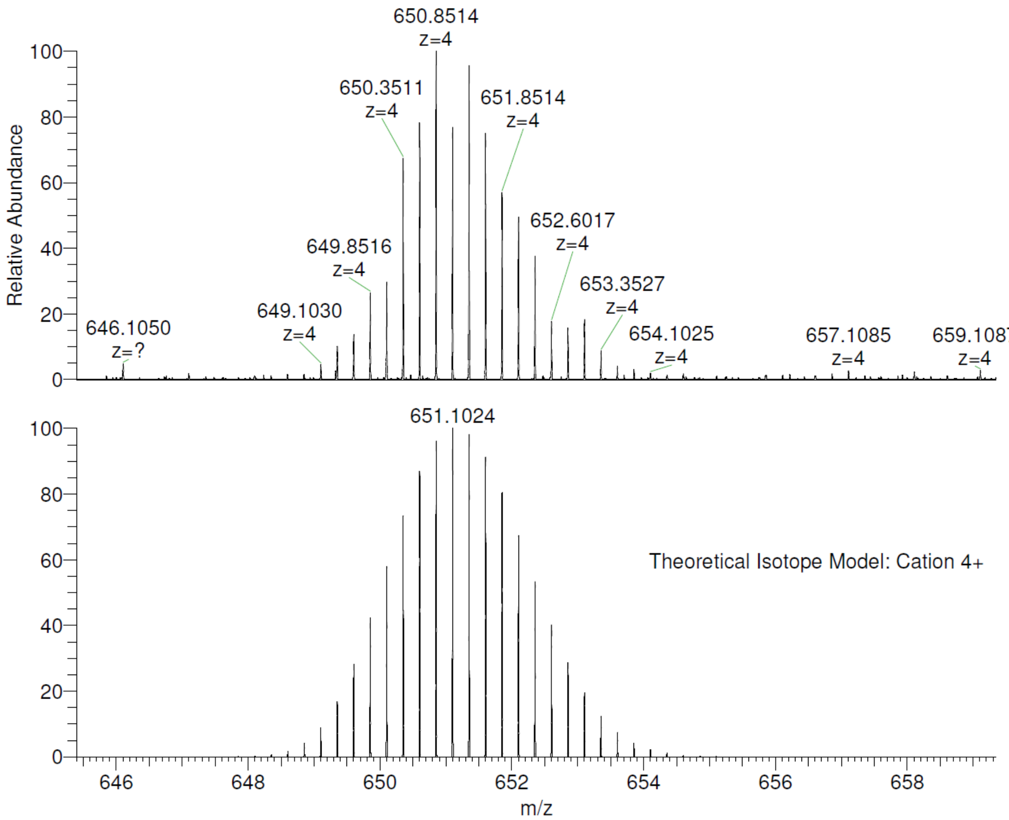

Figure S32B. Top: ESI-HRMS of [**8·T2** + 4 BF_4]$^{4+}$, bottom: simulated isotopic pattern for [$C_{116}H_{94}N_{20}O_4Pd_4B_4F_{16}$]$^{4+}$.

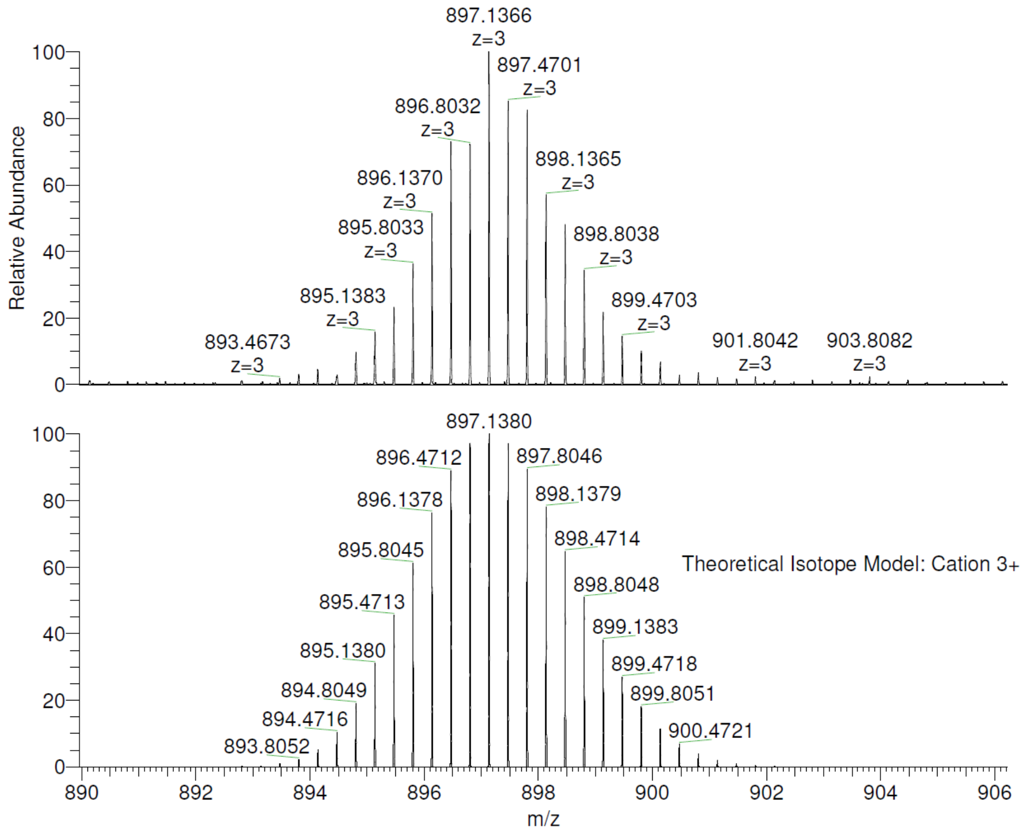

Figure S32C. Top: ESI-HRMS of [**8·T2** + 5 BF_4]$^{3+}$, bottom: simulated isotopic pattern for [$C_{116}H_{94}N_{20}O_4Pd_4B_5F_{20}$]$^{3+}$.

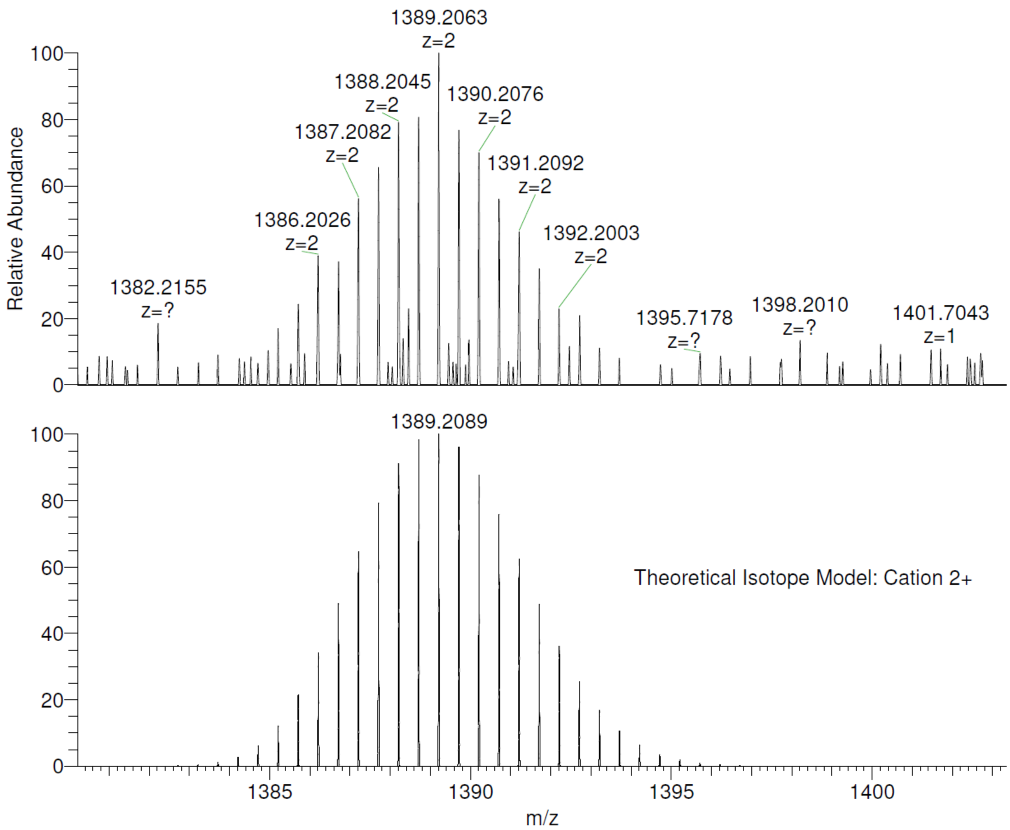

Figure S32D. Top: ESI-HRMS of [**8·T2** + 6 BF_4]$^{2+}$, bottom: simulated isotopic pattern for [$C_{116}H_{94}N_{20}O_4Pd_4B_6F_{24}$]$^{2+}$. The signal was weak for this charge state but intense enough to identify the species.

1.7 Synthesis and characterization of demetallated macrocycle [3+3] **9**

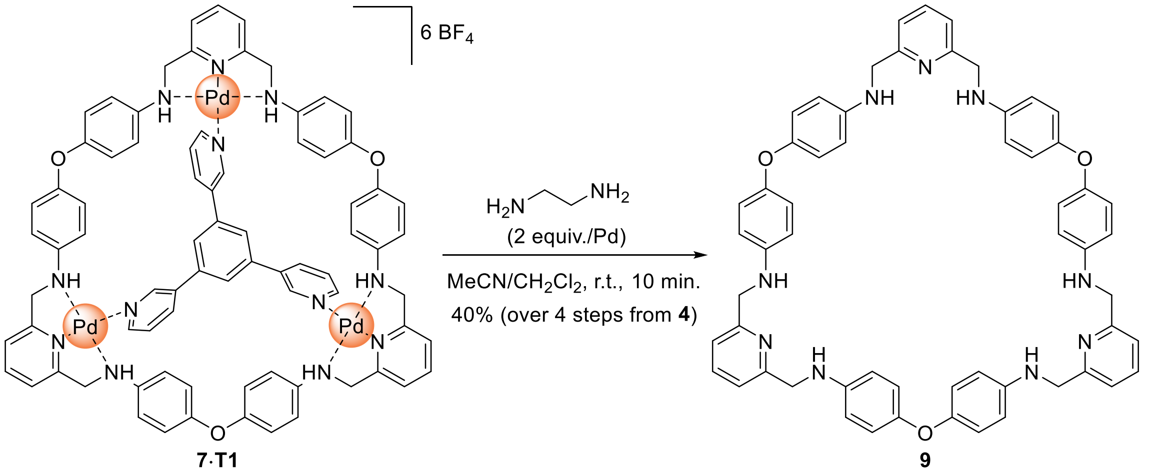

To a stirred solution of **7·T1** (crude, 64.0 mg, ≤30 µmol) in 6 mL MeCN/CH_2Cl_2, 1:1, was added ethylenediamine (12.0 µL, d = 0.897 g/mL, 179 µmol). The mixture was stirred at *r.t.* for 10 min., filtered to remove insoluble material and the solvents were evaporated under vacuum. The resulting solid was dissolved in 3 mL CH_2Cl_2, filtered and subjected to preparative layer chromatography (PLC) (SiO_2, CH_2Cl_2/MeOH, 85:15). The first band was separated in three sections: the central section contained pure **9** while the top and bottom sections contained **9** and impurities. The second band contained pure **T1** (8.7 mg, 28 µmol). The impure fractions of **9** were combined and subjected to as second PLC (SiO_2, CH_2Cl_2/acetone, 1:1). The main central band contained pure **9**. Pure fractions of **9** from both PLCs were combined and dried under vacuum affording a slightly yellow solid (11.0 mg, 12.1 µmol, FW = 910.10 g/mol). Yield over 4 steps (from **4**): 40%.

^{1}H NMR (400 MHz, $CDCl_3$, 298 K) δ (ppm) = 7.60 (t, *J* = 7.7 Hz, 3H), 7.20 (d, *J* = 7.7 Hz, 6H), 6.83 (d, *J* = 8.9 Hz, 12H), 6.61 (d, *J* = 8.9 Hz, 12H), 4.50 – 5.00 (br, 6H), 4.41 (s, 12H).

^{13}C NMR (126 MHz, $CDCl_3$, 298 K) δ (ppm) = 158.13, 150.26, 143.82, 137.36, 120.24, 119.69, 114.28, 50.05.

ESI-HRMS for **9** [$C_{57}H_{51}N_9O_3 + H^+$] m/z = calcd 910.4188, found 910.4181.

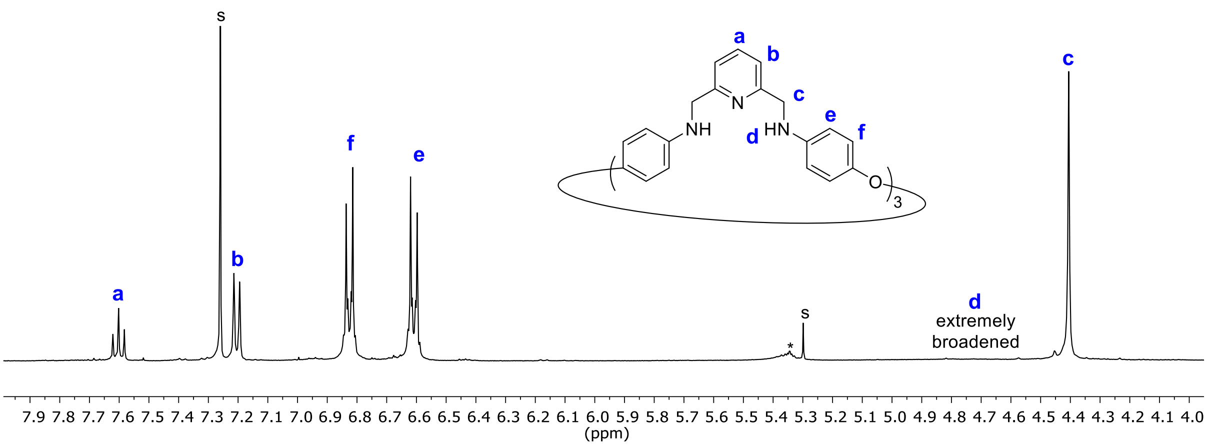

Figure S33. ^{1}H NMR spectrum of **9** (400 MHz, $CDCl_3$, 298 K). s: residual solvents; *impurity from PLC silica binder.

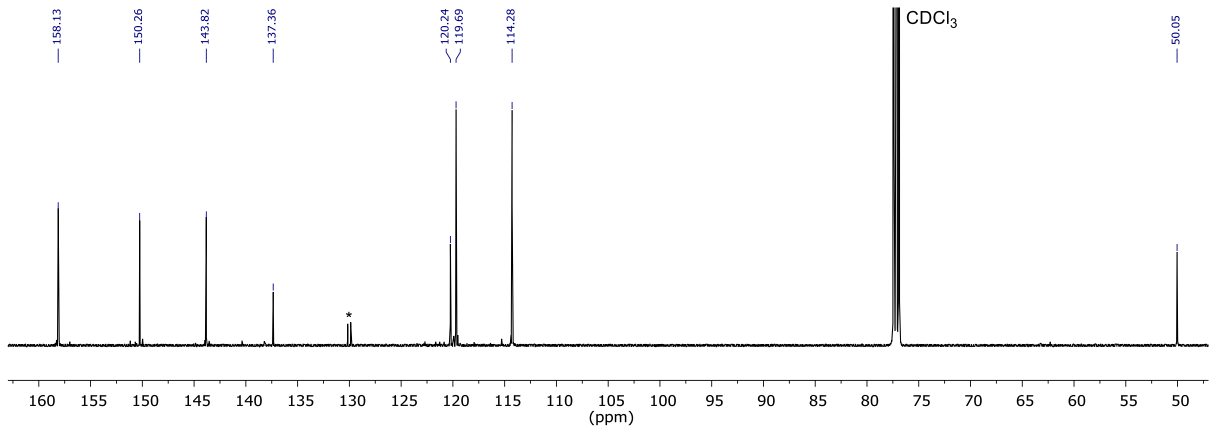

Figure S34. ^{13}C NMR spectrum of **9** (126 MHz, $CDCl_3$, 298 K). *impurity from PLC silica binder.

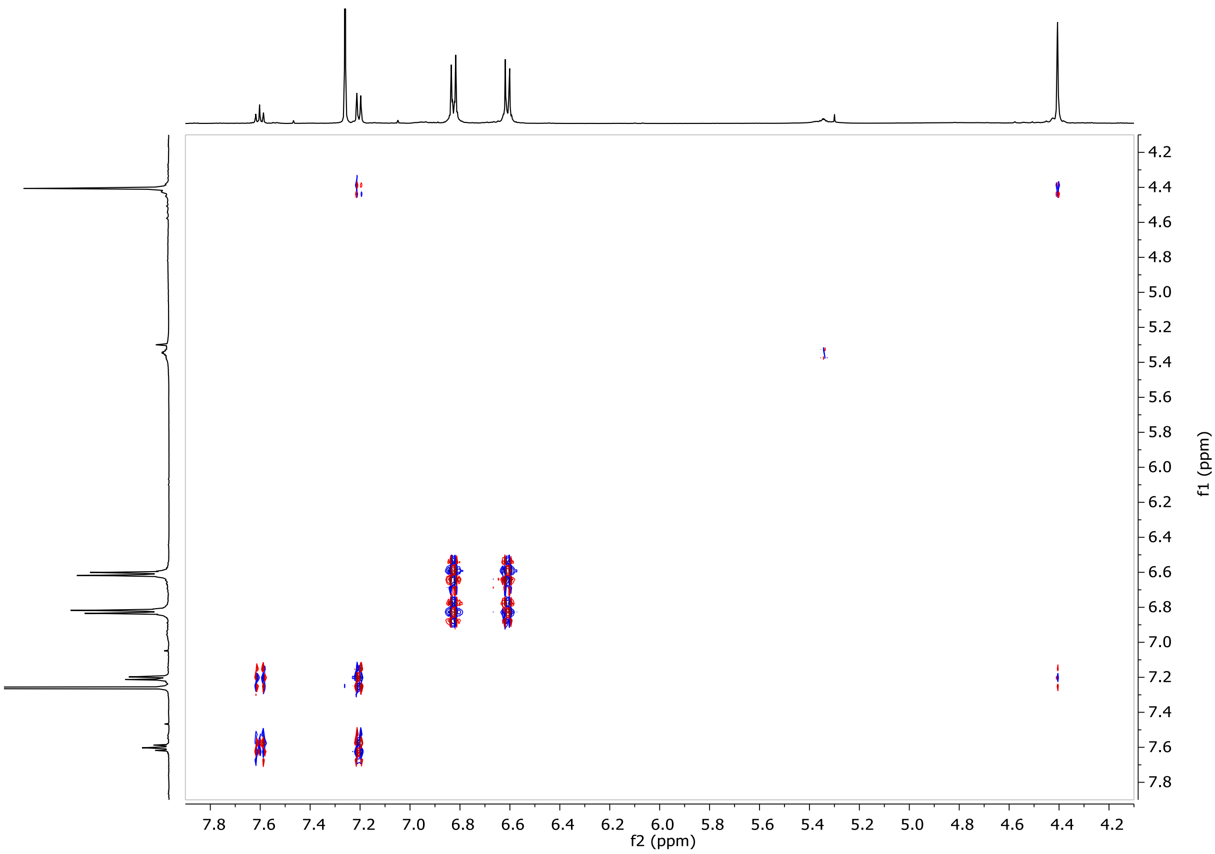

Figure S35. dqfCOSY spectrum of **9** (500 MHz, $CDCl_3$, 298 K).

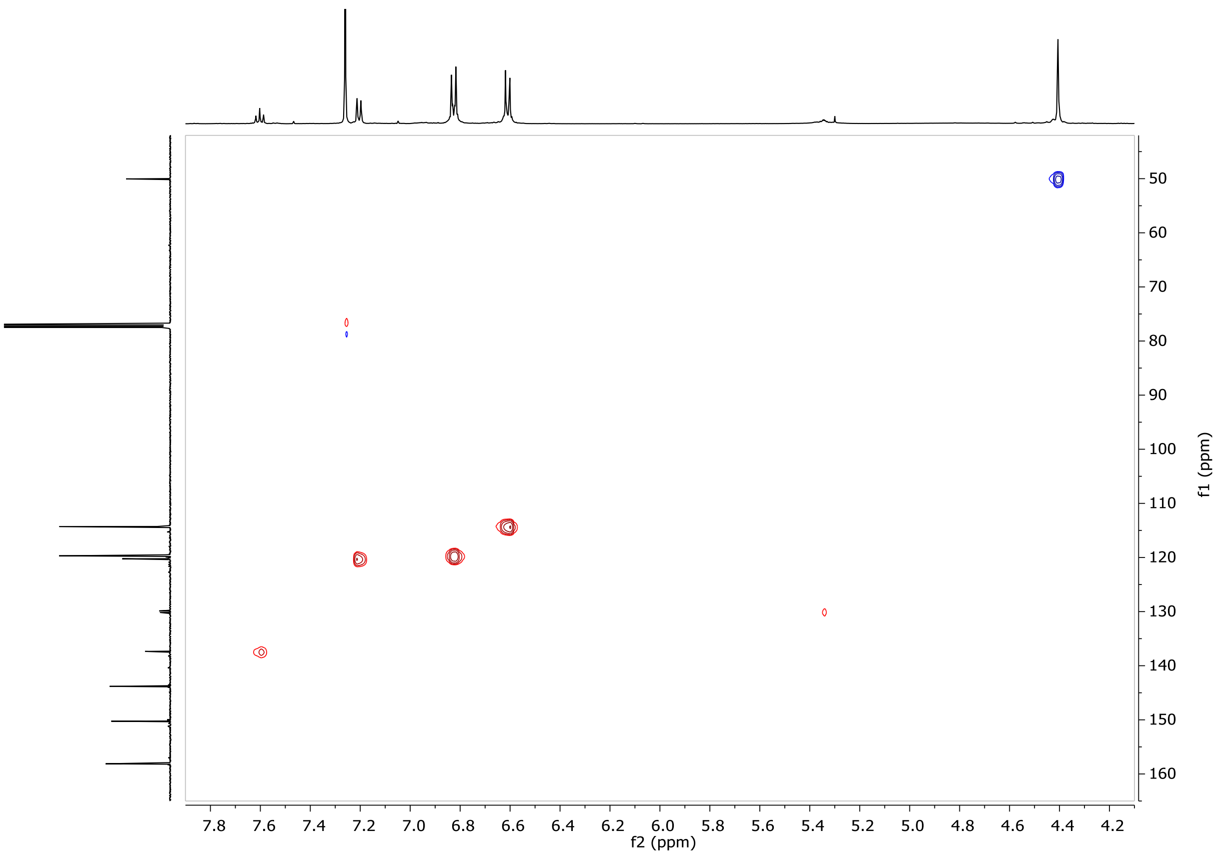

Figure S36. Edited ^{1}H-^{13}C HSQC spectrum of **9** (11.7 Tesla, $CDCl_3$, 298 K).

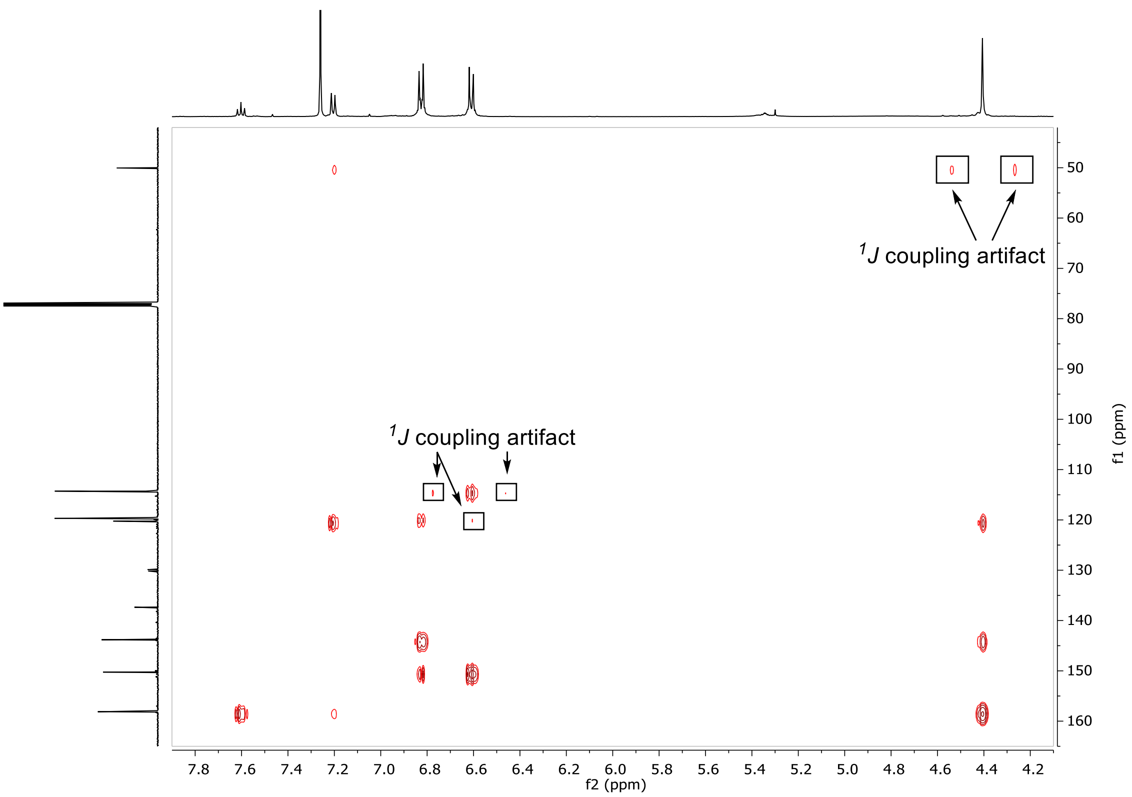

Figure S37. ^{1}H-^{13}C HMBC spectrum of **9** (11.7 Tesla, $CDCl_3$, 298 K). The ^{1}J coupling artifacts are caused by ^{1}J coupling constant values out of the range filtered by standard HMBC parameters.

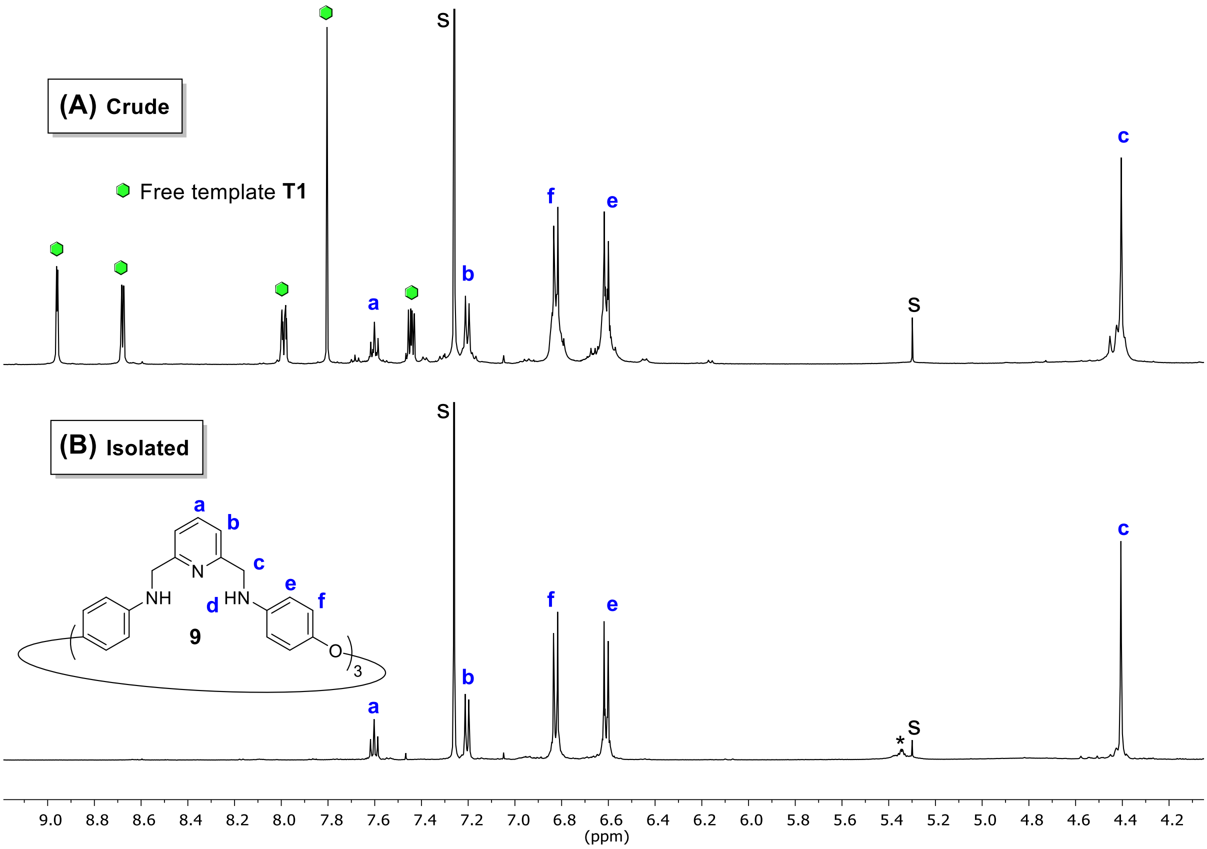

Figure S38. ^{1}H NMR spectra (500 MHz, $CDCl_3$, 298 K) of **9** (A) as crude material after demetallation, and (B) isolated by PLC. s: residual solvents, *impurity from PLC silica binder. This comparison shows that the crude material contains mainly **9** and the free template **T1** as proof of the good selectivity of the synthesis method despite the relatively low isolated yield resulting from tedious purification process to remove the minor impurities.

1.8 Synthesis and characterization of demetallated macrocycle [4+4] **10**

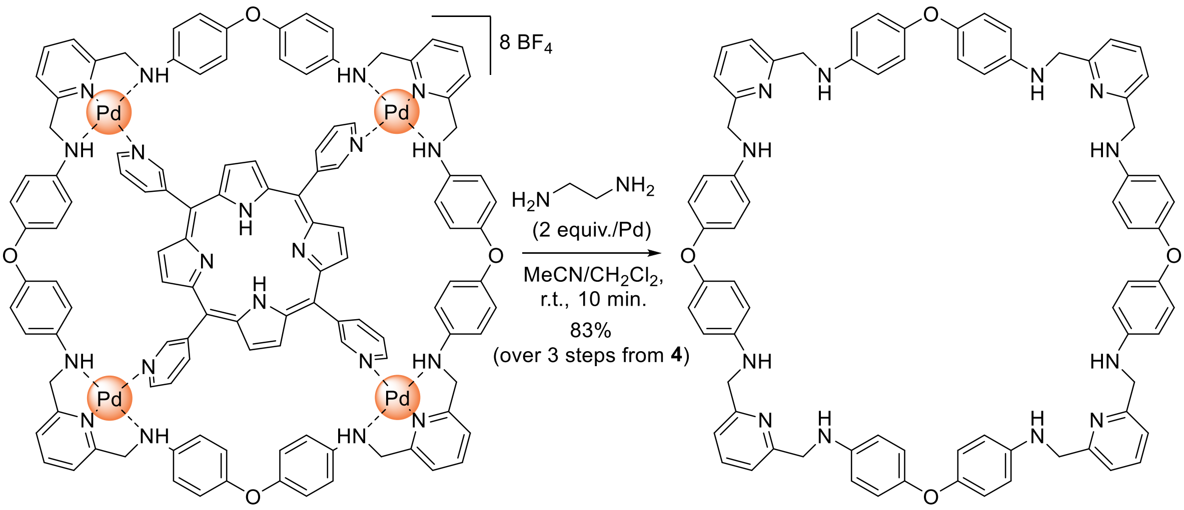

8·T2 **10**

To a stirred solution of **8·T2** (crude, 61.9 mg, ≤20 µmol) in 6 mL MeCN/CH_2Cl_2, 1:1, was added ethylenediamine (11.0 µL, d = 0.897 g/mL, 164 µmol). The mixture was stirred at *r.t.* for 10 min., filtered to remove insoluble material and solvents were evaporated under vacuum. The resulting solid was dissolved in 3 mL CH_2Cl_2, filtered and subjected to preparative layer chromatography (PLC) (SiO_2, CH_2Cl_2/MeOH, 85:15). The first band contained pure **10** while the second band contained pure **T2** (11 mg, 18 µmol). A small overlapping section was not collected. The pure fraction of **10** was dried under vacuum affording an off-white solid (13.9 mg, 16.9 µmol, FW = 1213.46 g/mol). Yield over 3 steps (from **4**): 83%.

^{1}H NMR (500 MHz, $CDCl_3$, 298 K) δ (ppm) = 7.57 (t, *J* = 7.7 Hz, 4H), 7.18 (d, *J* = 7.7 Hz, 8H), 6.81 (d, *J* = 8.9 Hz, 16H), 6.58 (d, *J* = 8.9 Hz, 16H), 4.59 (br, 8H), 4.39 (s, 16H).

^{13}C NMR (126 MHz, $CDCl_3$, 298 K) δ (ppm) = 158.25, 150.18, 143.81, 137.32, 120.11, 119.68, 114.25, 49.98.

ESI-HRMS for **10** [$C_{76}H_{68}N_{12}O_4 + H^+$] m/z = calcd 1213.5559, found 1213.5549.

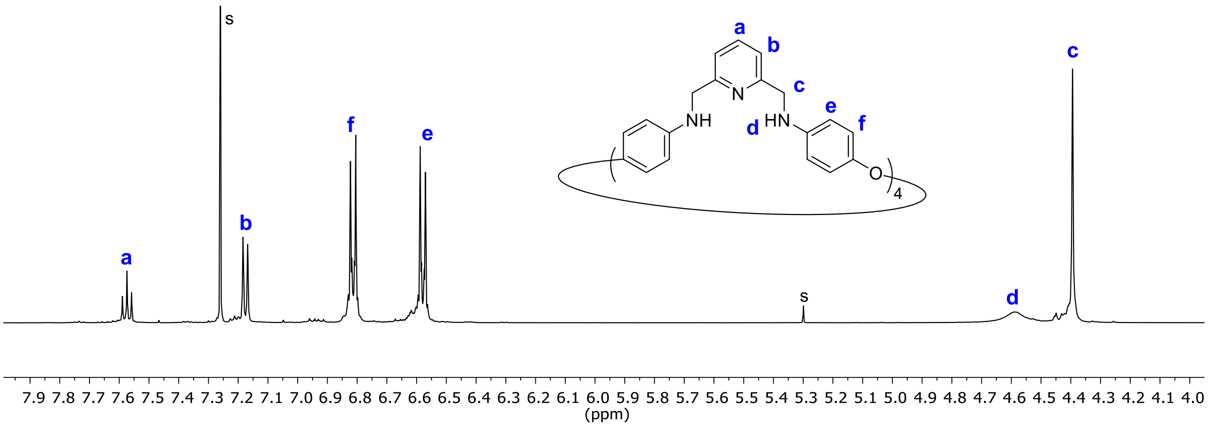

Figure S39. ^{1}H NMR spectrum of **10** (500 MHz, $CDCl_3$, 298 K). s: residual solvents.

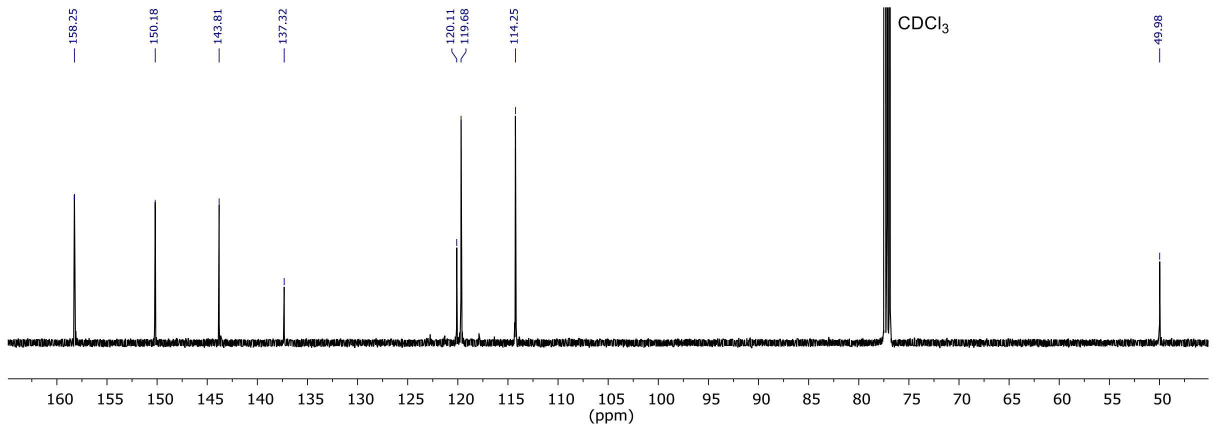

Figure S40. ^{13}C NMR spectrum of **10** (126 MHz, $CDCl_3$, 298 K).

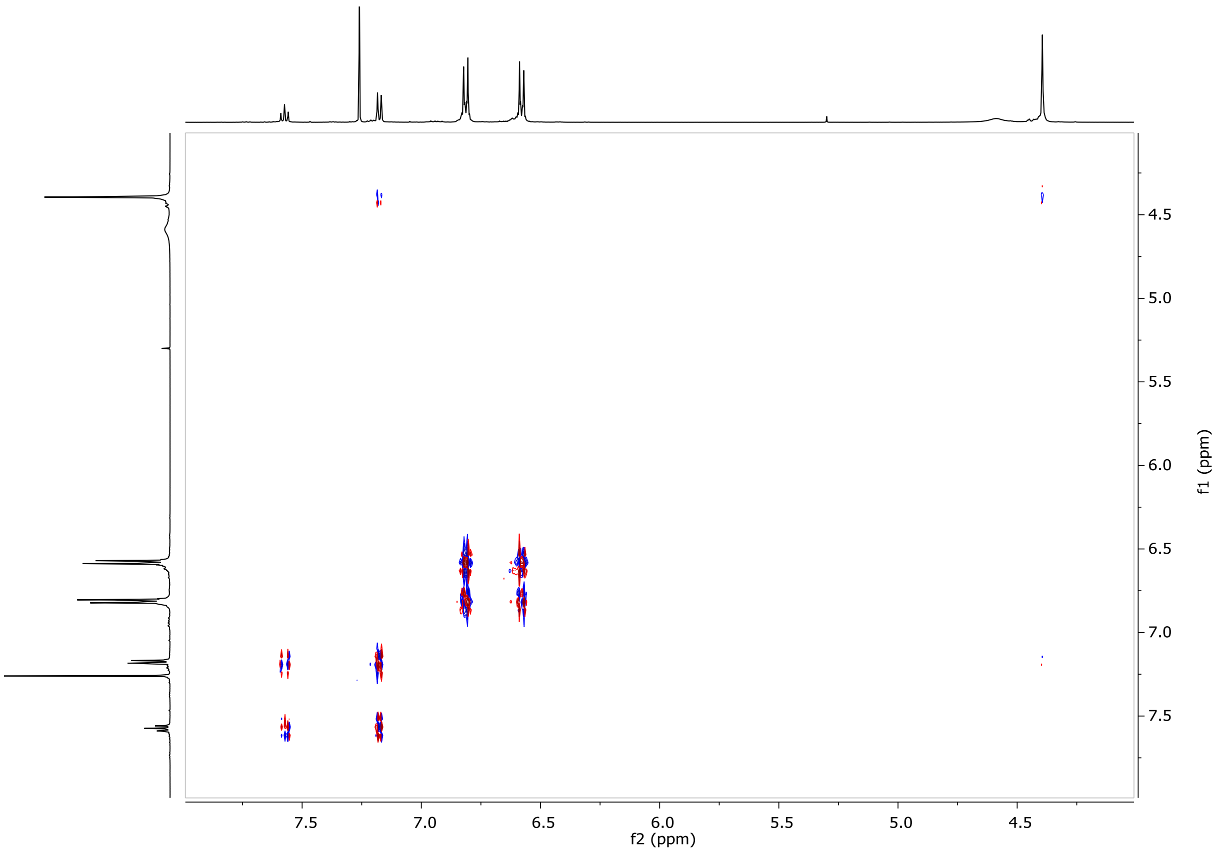

Figure S41. dqfCOSY spectrum of **10** (500 MHz, $CDCl_3$, 298 K).

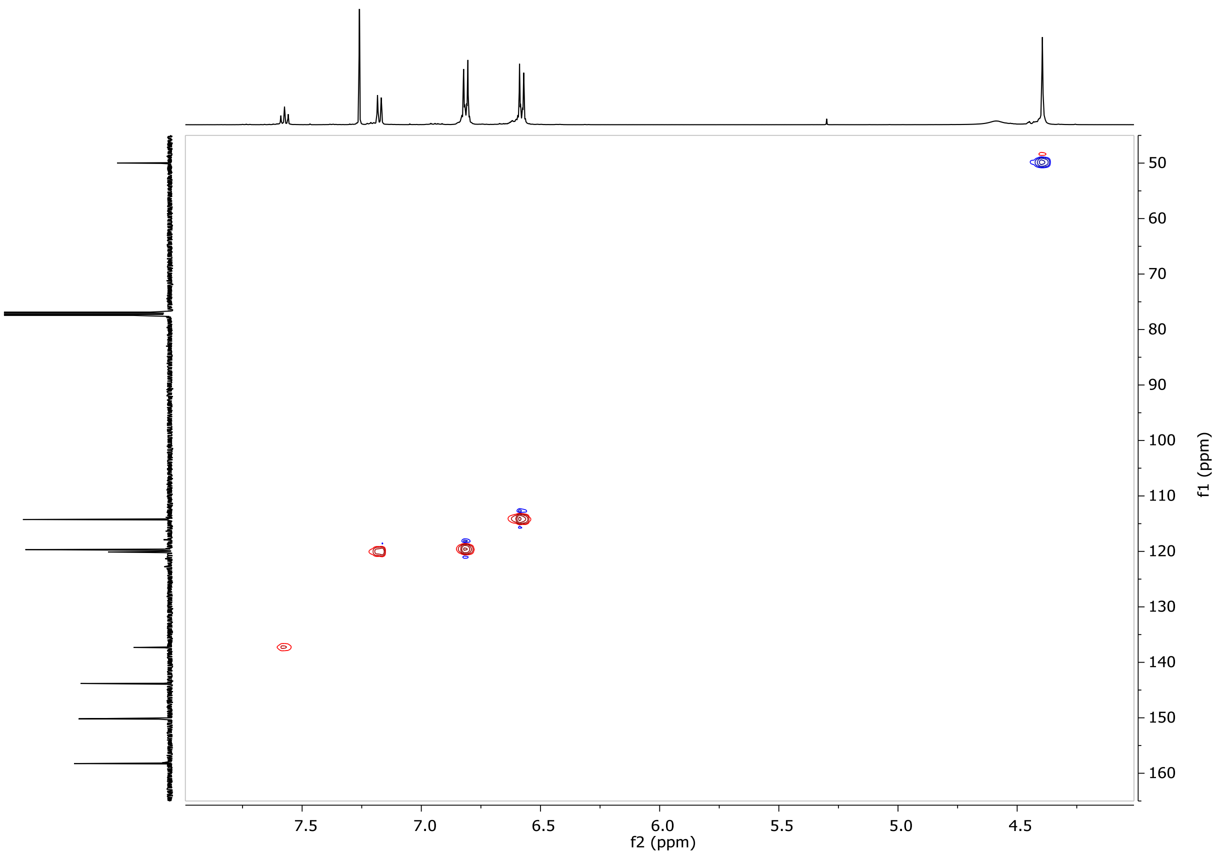

Figure S42. Edited ^{1}H-^{13}C HSQC spectrum of **10** (11.7 Tesla, $CDCl_3$, 298 K).

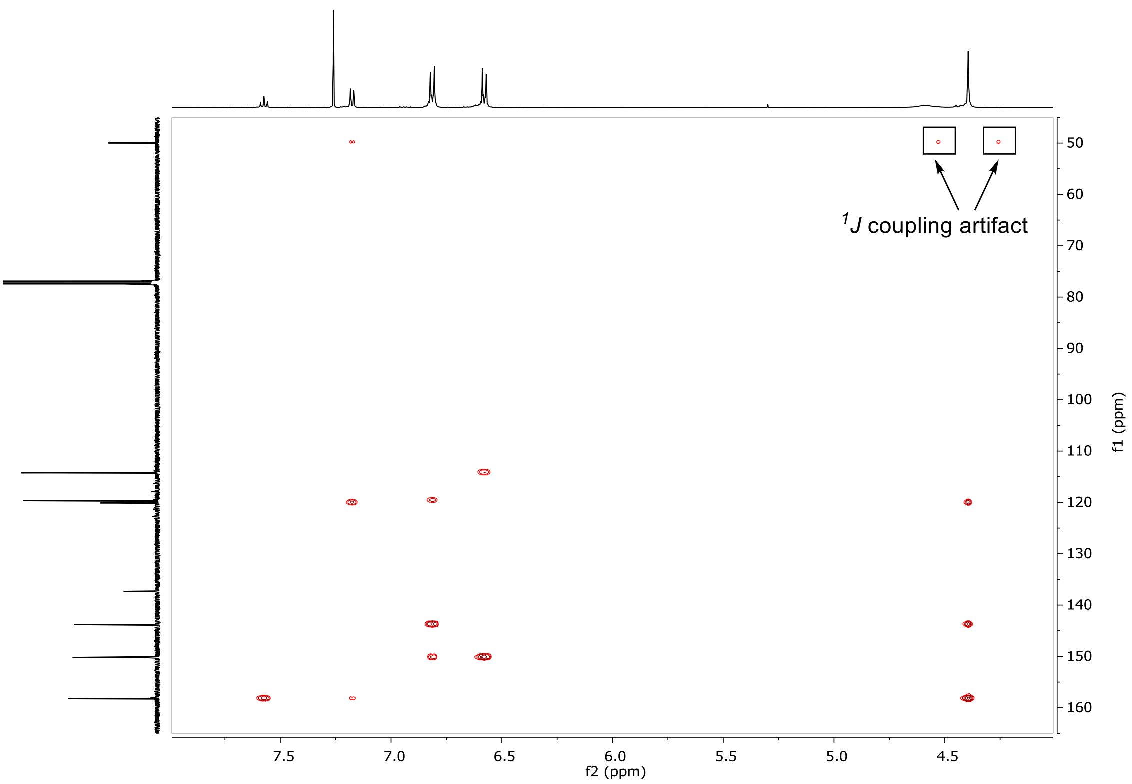

Figure S43. ^{1}H-^{13}C HMBC spectrum of **10** (11.7 Tesla, $CDCl_3$, 298 K). The ^{1}J coupling artifacts are caused by ^{1}J coupling constant values out of the range filtered by standard HMBC parameters.

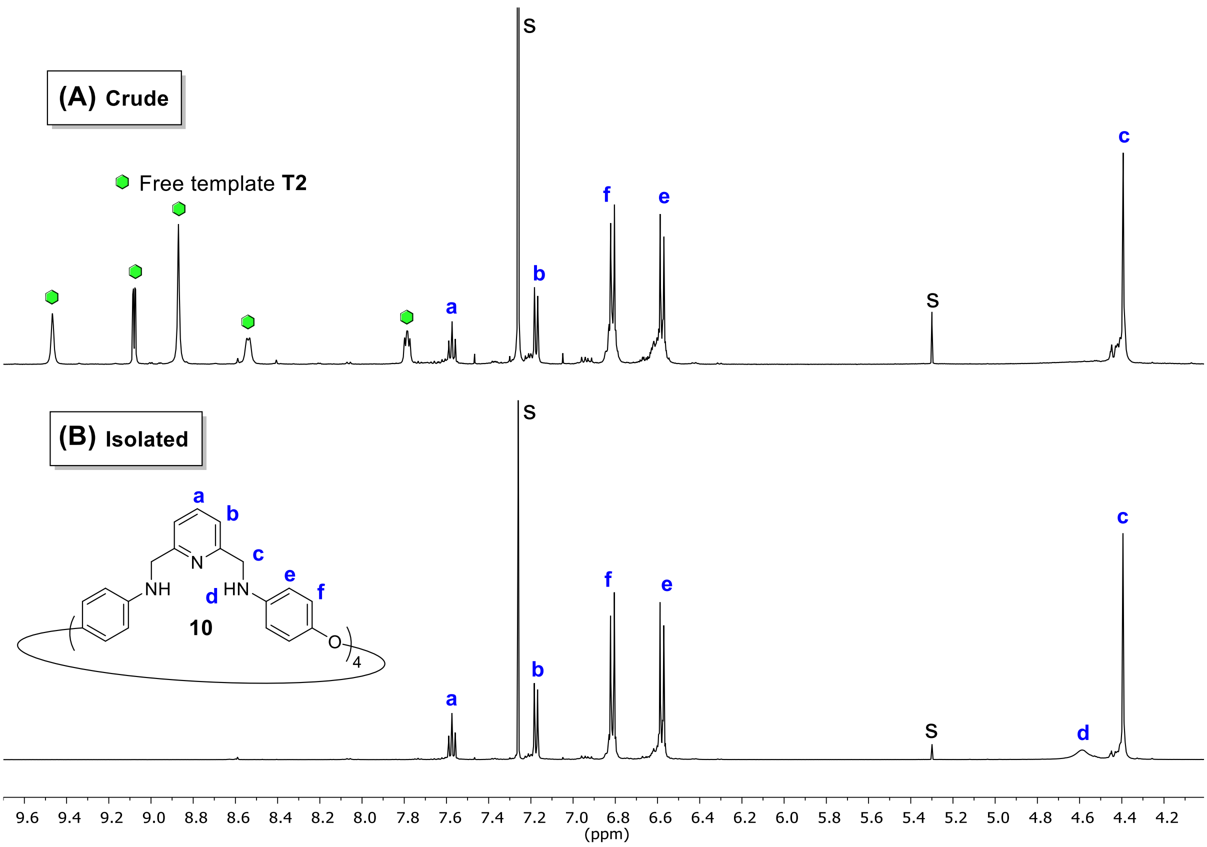

Figure S44. ^{1}H NMR spectra (500 MHz, $CDCl_3$, 298 K) of **10** (A) as crude material after demetallation, and (B) isolated by PLC. s: residual solvents. This comparison shows that the crude material contains mainly **10** and the free template **T2** as proof of the good selectivity of the synthesis method.

1.9 Synthesis and characterization of bridged macrocycles **5_2·T3$_3$**

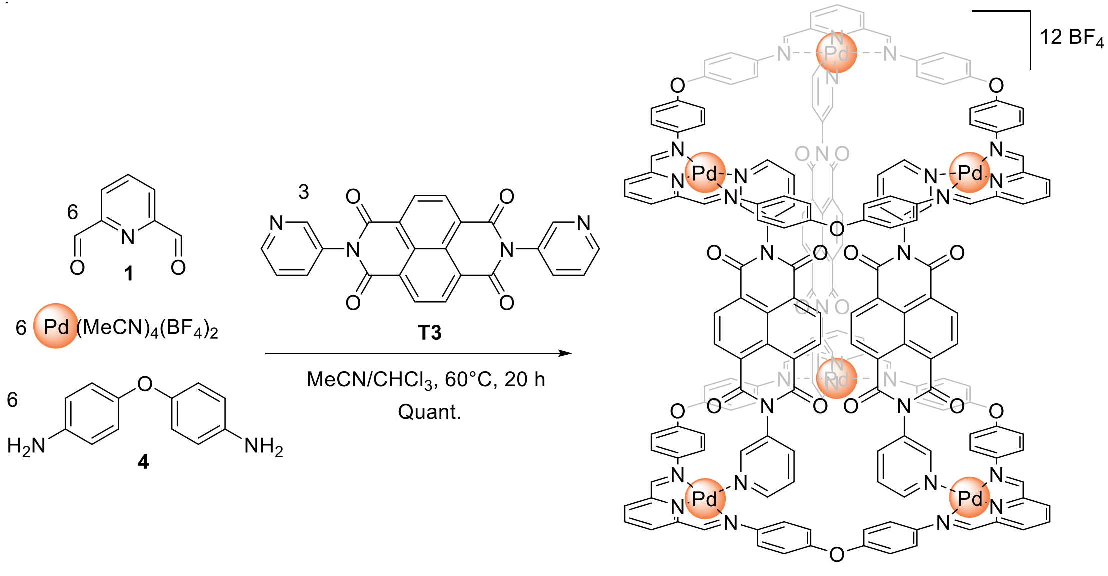

5_2·T3$_3$

To a stirred suspension of 2,6-diformylpyridine **1** (13.7 mg, 0.101 mmol), 4,4'-oxydianiline **4** (20.5 mg, 0.102 mmol) and bis(3-pyridyl)naphthalene diimide **T3** (21.1 mg, 0.0502 mmol) in a mixture of 45 mL MeCN and 5 mL $CHCl_3$ was added a solution of [Pd(MeCN)$_4$](BF_4)$_2$ (46.3 mg, 0.104 mmol) in 1 mL MeCN. The orange mixture was stirred at 60°C for 20 h. The solution was cooled down to *r.t.*, concentrated to a volume of *ca.* 3 mL with a rotary evaporator, filtered and slowly poured into 30 mL of Et_2O. The mixture was shaken and left to rest 10 minutes to maximize precipitation then the precipitate was collected by centrifugation. The orange colored supernatant was concentrated to a volume of *ca.* 1 mL, filtered, poured into 30 mL Et_2O and left to rest for 1 h to complete precipitation. This second precipitate was collected by centrifugation. The combined precipitates were washed with 5 mL Et_2O and dried under vacuum affording **5_2·T3$_3$(BF$_4$)$_{12}$** as an orange solid (79.4 mg, 0.0168 mmol, FW = 4734.32 g/mol). Quantitative yield.

^{1}H NMR (500 MHz, CD_3CN, 298 K) δ (ppm) = 8.57 (t, *J* = 8.1 Hz, 6H), 8.47 (s, 24H, overlapping singlets), 8.45 (d, *J* = 6.6 Hz, 6H), 8.32 (d, *J* = 2.0 Hz, 6H), 8.28 (d, *J* = 8.1 Hz, 12H), 7.49 (d, *J* = 8.4 Hz, 6H), 7.17 (dd, *J* = 8.2, 5.7 Hz, 6H), 7.13 (d, *J* = 8.6 Hz, 24H), 6.95 (br, 24H).

^{13}C NMR (126 MHz, CD_3CN, 298 K) δ (ppm) = 172.90, 163.60, 155.80, 152.37, 152.20, 146.21, 142.02, 135.91, 131.43, 128.10, 127.55, 125.71. The number of peaks observed is smaller than the expected 17 peaks because of broadening and/or overlapping.

ESI-HRMS for **5_2·T3$_3$** [($C_{186}H_{114}N_{30}O_{18}Pd_6$)$^{12+}$] m/z = [**$5_2$·T3$_3$** + 4 BF_4]$^{8+}$, calcd: 505.2918, found: 505.2923; [**5_2·T3$_3$** + 5 BF_4]$^{7+}$, calcd: 589.9055, found: 589.9070; [**5_2·T3$_3$** + 6 BF_4]$^{6+}$, calcd: 702.7238, found: 702.7263.

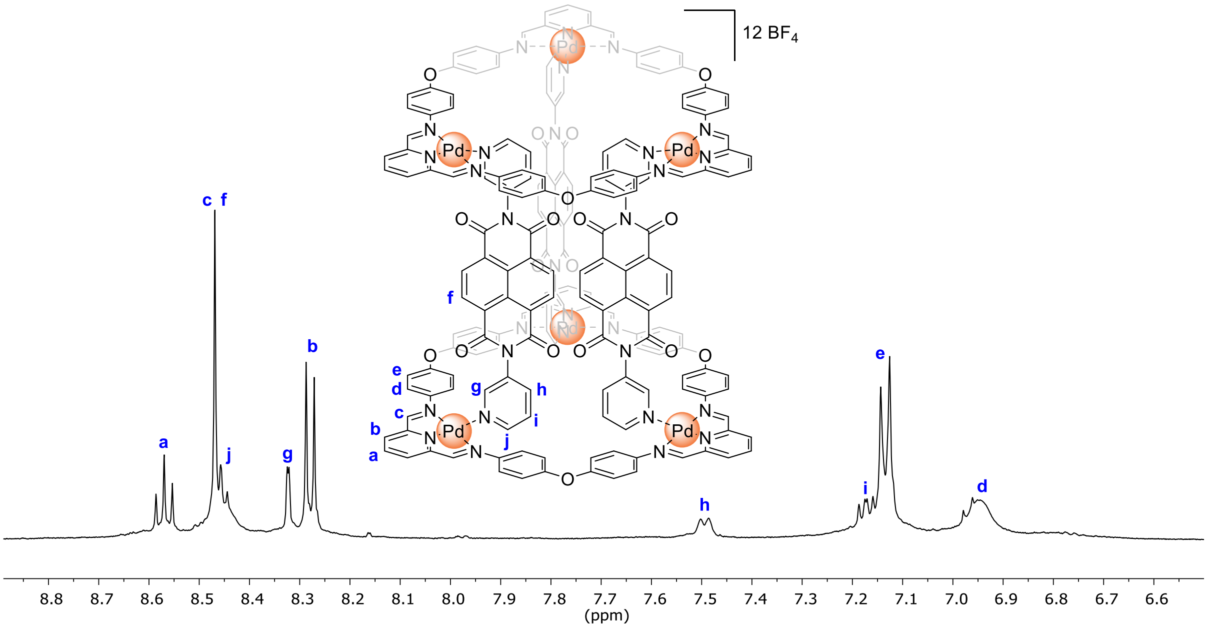

Figure S45. ^{1}H NMR spectrum of $\mathbf{5_2{\cdot}T3_3}$ (500 MHz, CD_3CN, 298 K).

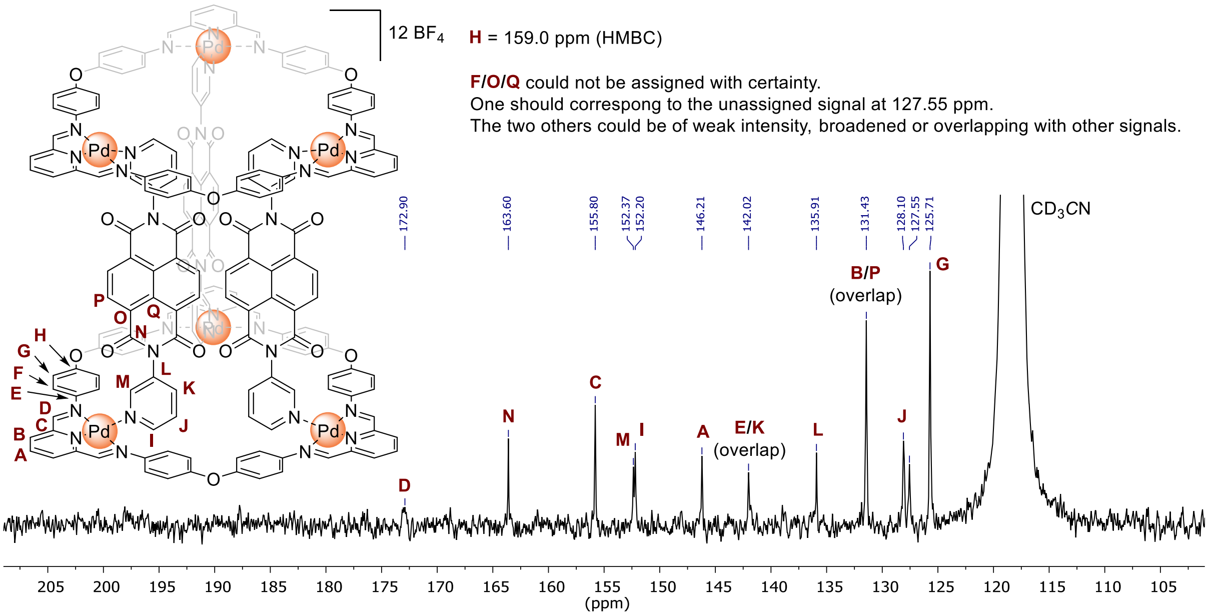

Figure S46. ^{13}C NMR spectrum of $\mathbf{5_2{\cdot}T3_3}$ (126 MHz, CD_3CN, 298 K). Assignment based on HSQC, HMBC spectra and chemical shifts.

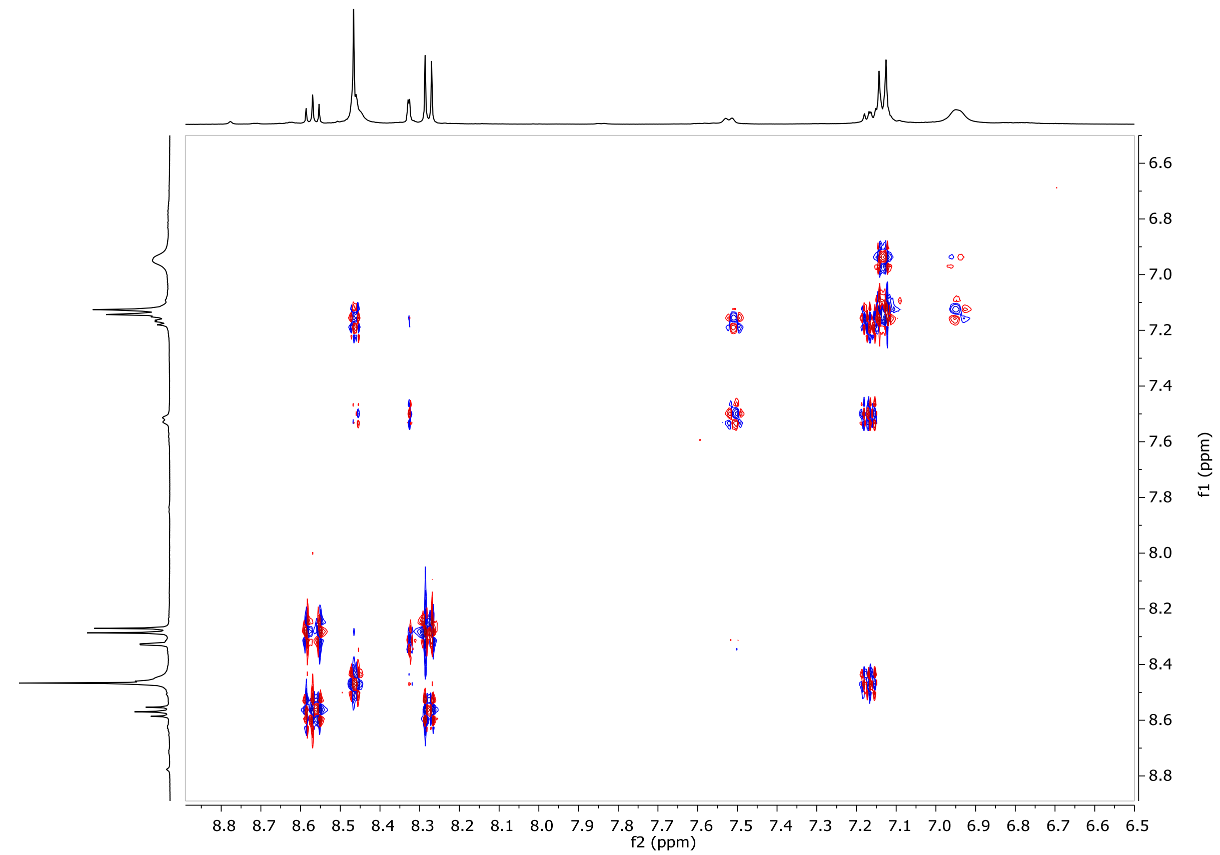

Figure S47. dqfCOSY spectrum of $\mathbf{5_2{\cdot}T3_3}$ (500 MHz, CD_3CN, 298 K).

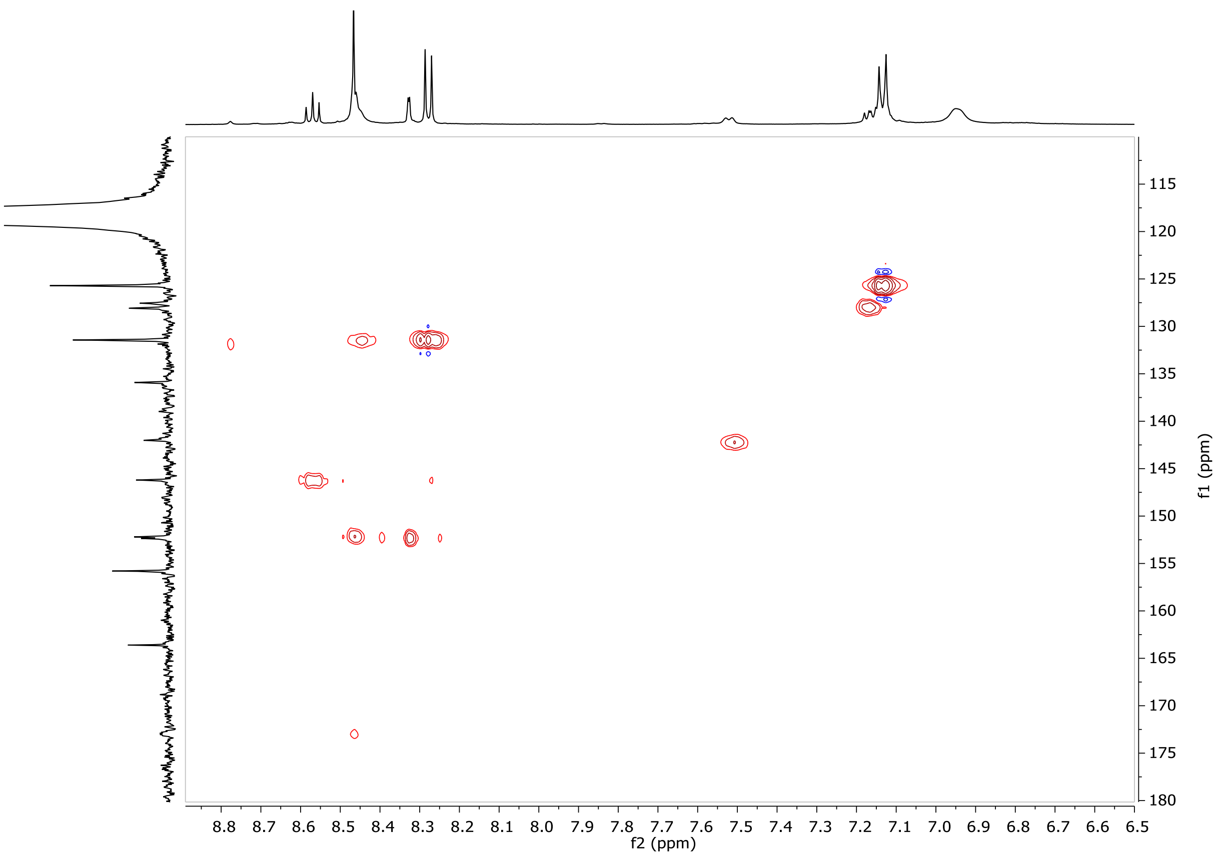

Figure S48. Edited ^{1}H-^{13}C HSQC spectrum of $\mathbf{5_2{\cdot}T3_3}$ (11.7 Tesla, CD_3CN, 298 K).

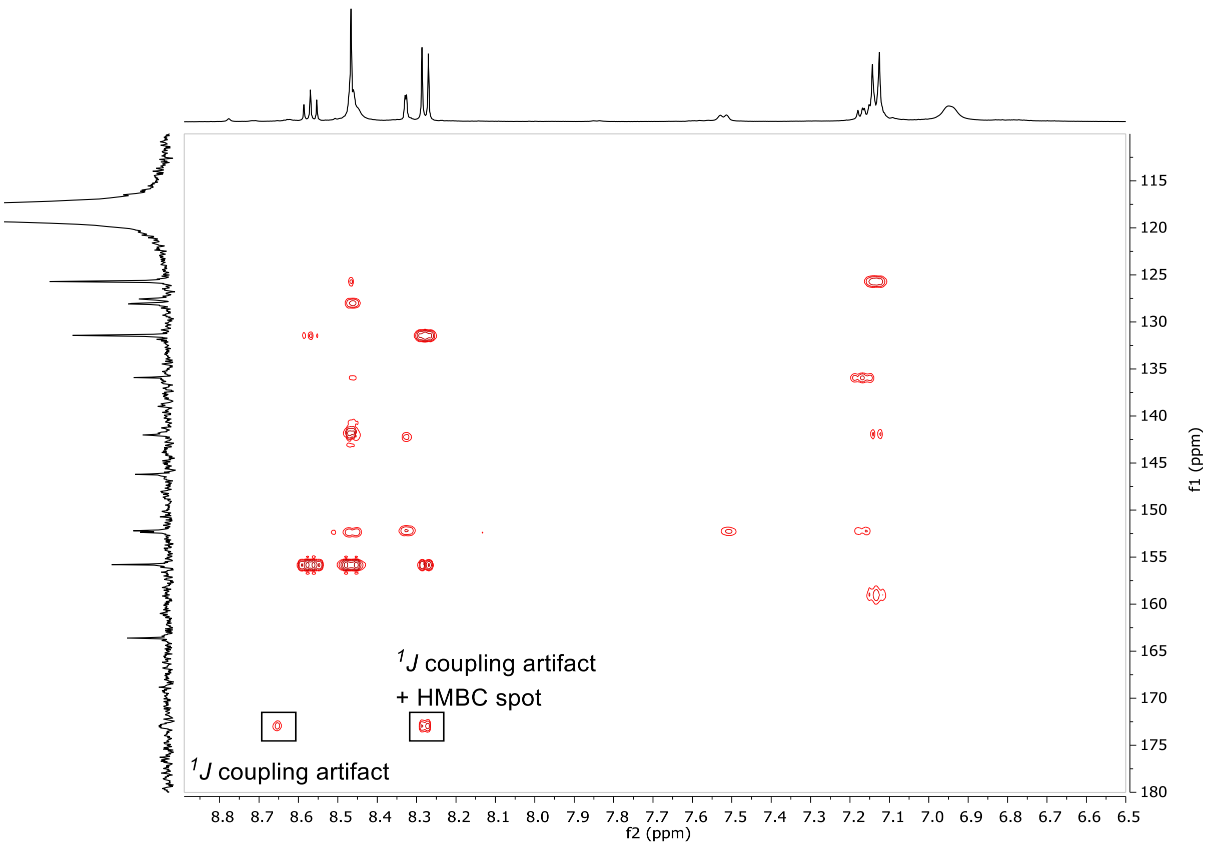

Figure S49. ^{1}H-^{13}C HMBC spectrum of **5_2·T3_3** (11.7 Tesla, CD_3CN, 298 K). The ^1J coupling artifacts are caused by ^1J coupling constant values out of the range filtered by standard HMBC parameters.

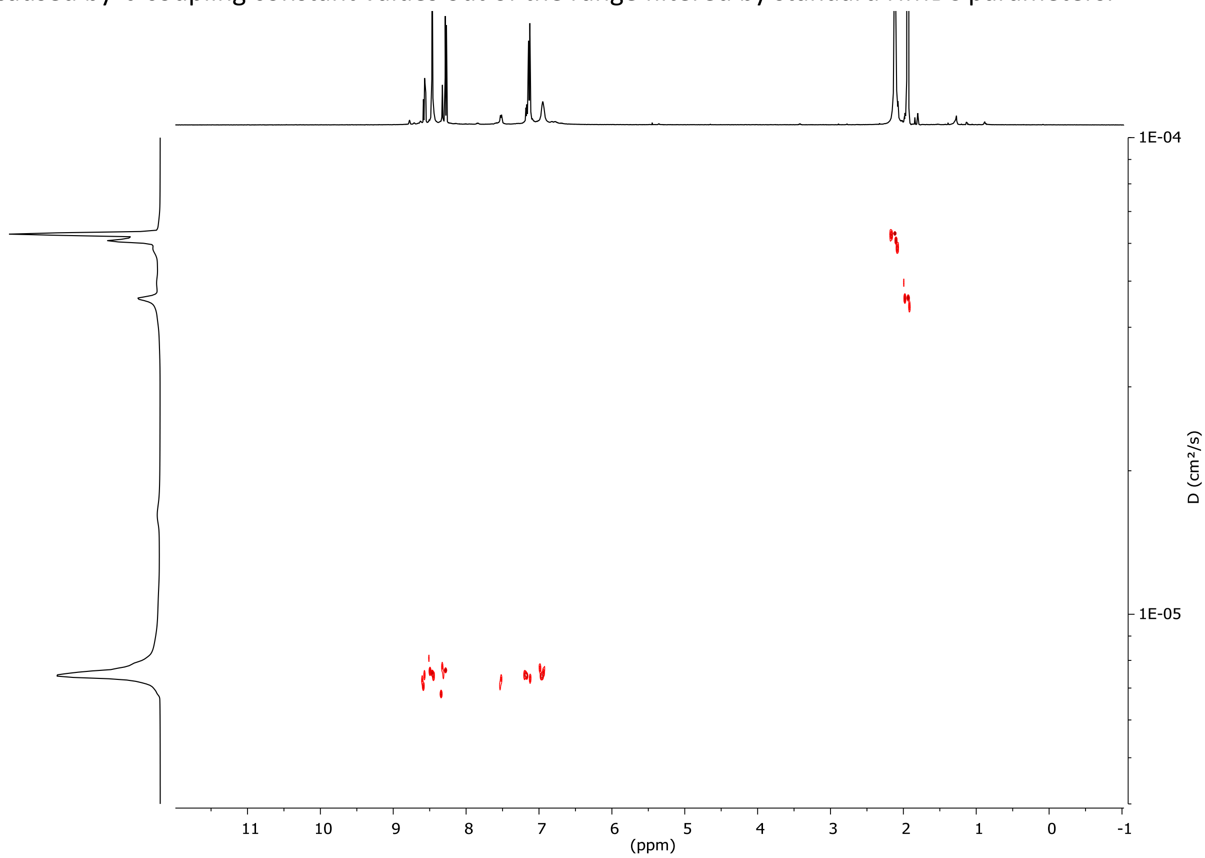

Figure S50. ^{1}H DOSY spectrum of **5_2·T3_3** (500 MHz, CD_3CN, 298 K, diffusion delay Δ = 32 ms, diffusion gradient length δ = 3000 μs).

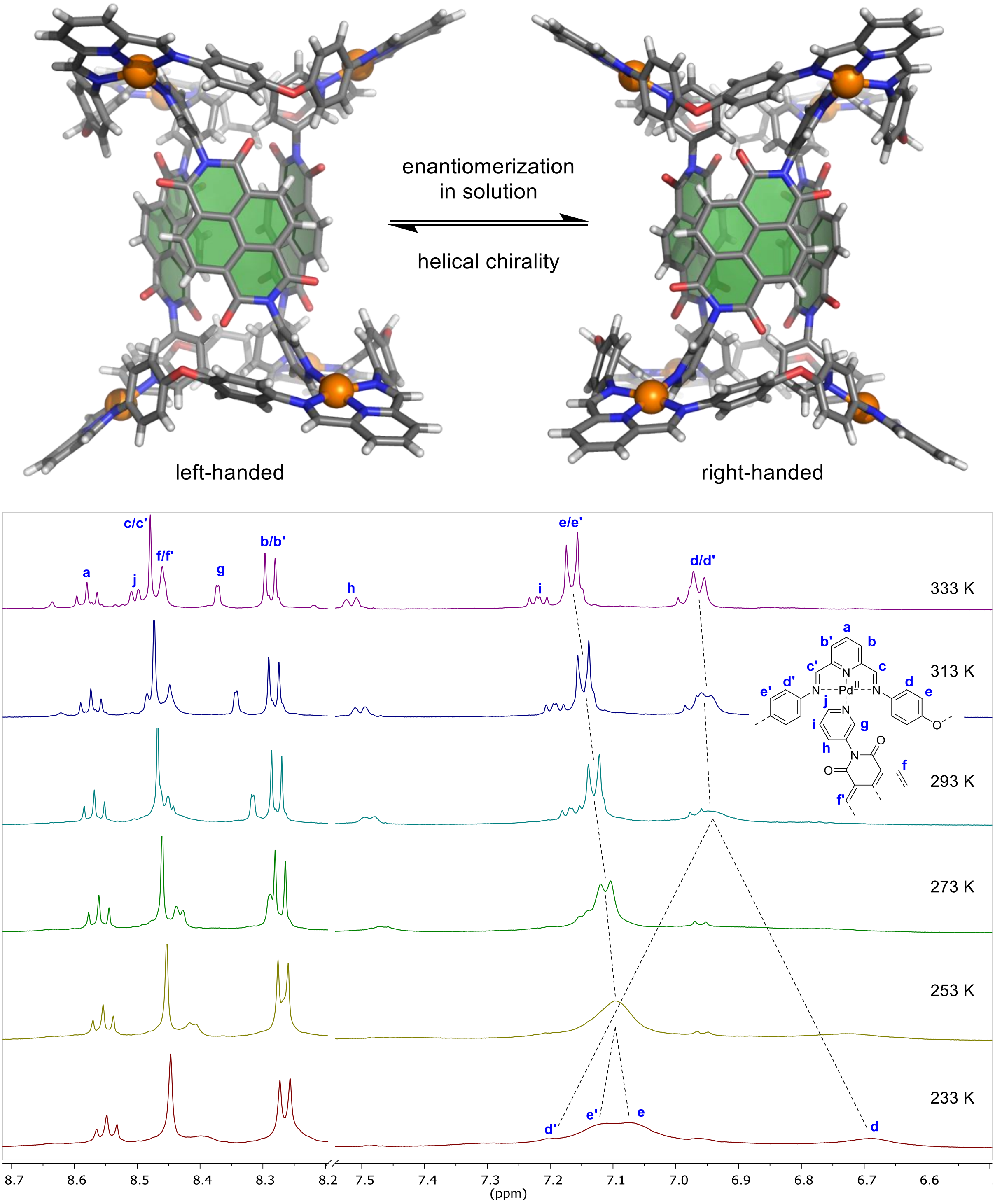

Figure S51. Variable temperature ^{1}H NMR spectra of $\mathbf{5_2{\cdot}T3_3}$ (500 MHz, CD_3CN) showing desymmetrization at low temperature which is consistent with the helical chirality observed in the solid state.

Considering a coalescence temperature T_c = 273±5 K for signals d and d' (Δν = 308 Hz), the enantiomerization activation barrier can be estimated to $\Delta G^{\ddagger}$ = 52±2 kJ mol^{-1} at 273 K with the formula $\Delta G^{\ddagger} = R\,T_c\,[22.96 + \mathit{ln}(T_c/\Delta\nu)]$.[4]

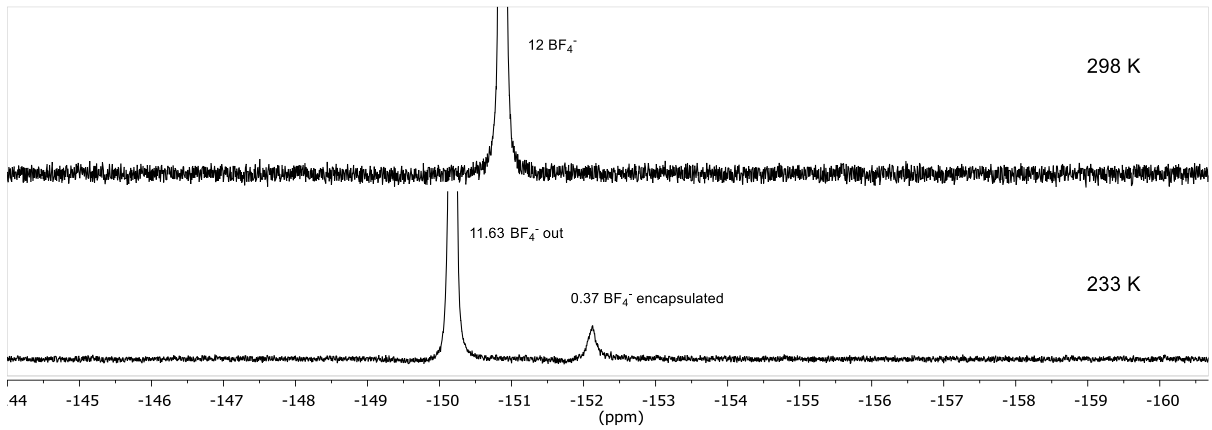

Figure S52. Variable temperature ^{19}F NMR spectra of **5_2·T3$_3$** (471 MHz, CD_3CN) showing one signal of BF_4^- at 298 K indicating fast in-out exchange of BF_4^- in **5_2·T3$_3$** cavity and two signals at 233 K indicating slow in-out exchange. Δδ = –1.9 ppm. Spectra were not calibrated.

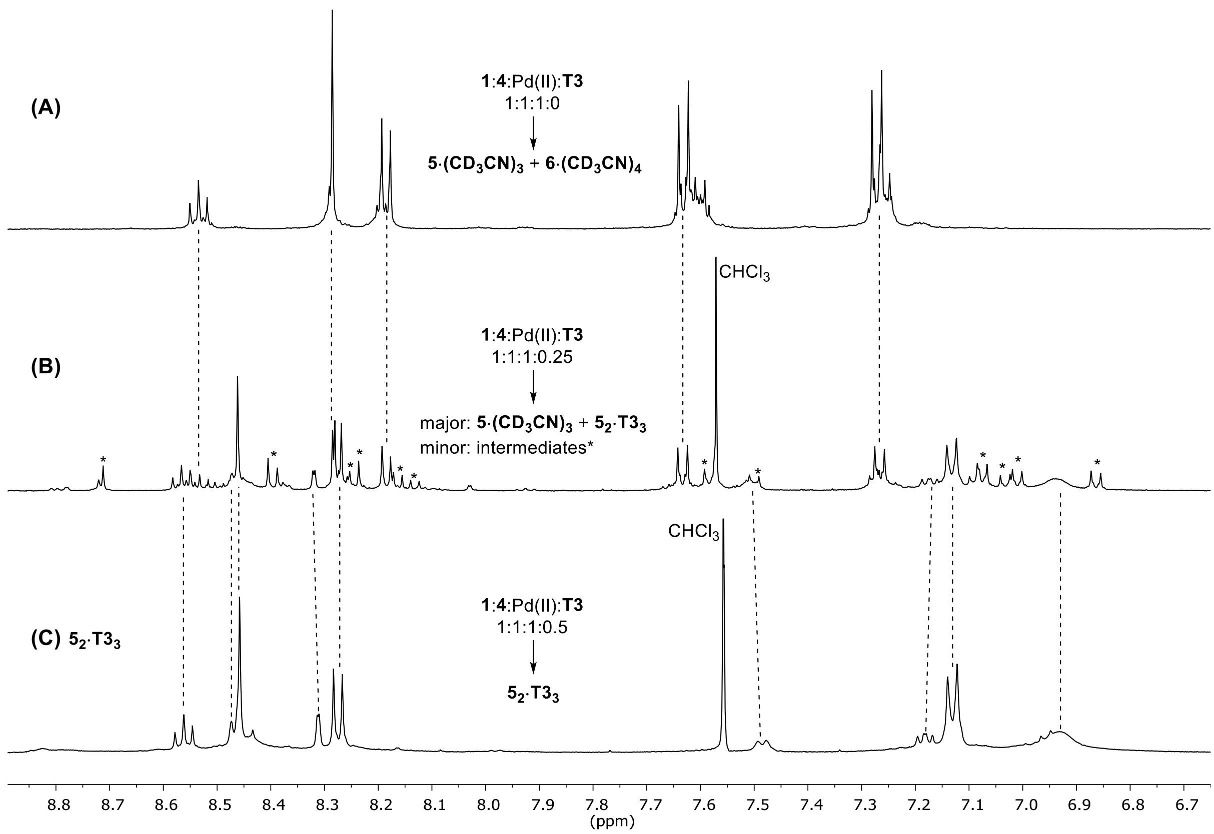

Figure S53. ^{1}H NMR spectra (500 MHz, 298 K) showing the assemblies formed with subcomponents **1**, **4**, Pd(II) and various amounts of template **T3** (60°C, 20 h). (A) 0 equiv. of **T3** leading to free macrocycles **5·(CD$_3$CN)$_3$** and **6·(CD$_3$CN)$_4$** (CD_3CN), (B) 0.25 equiv./Pd of **T3** leading predominantly to free macrocycle **5·(CD$_3$CN)$_3$** and fully bridged macrocycles **5_2·T3$_3$** with minor species suspected to be intermediates with one or two bridging **T3** ($CD_3CN/CDCl_3$, 10:1), and (C) 0.5 equiv./Pd of **T3** leading to fully bridged macrocycles **5_2·T3$_3$** ($CD_3CN/CDCl_3$, 5:1). $CDCl_3$ was used for the stock solution of **T3** but does not have significant effect on the assembly outcome.

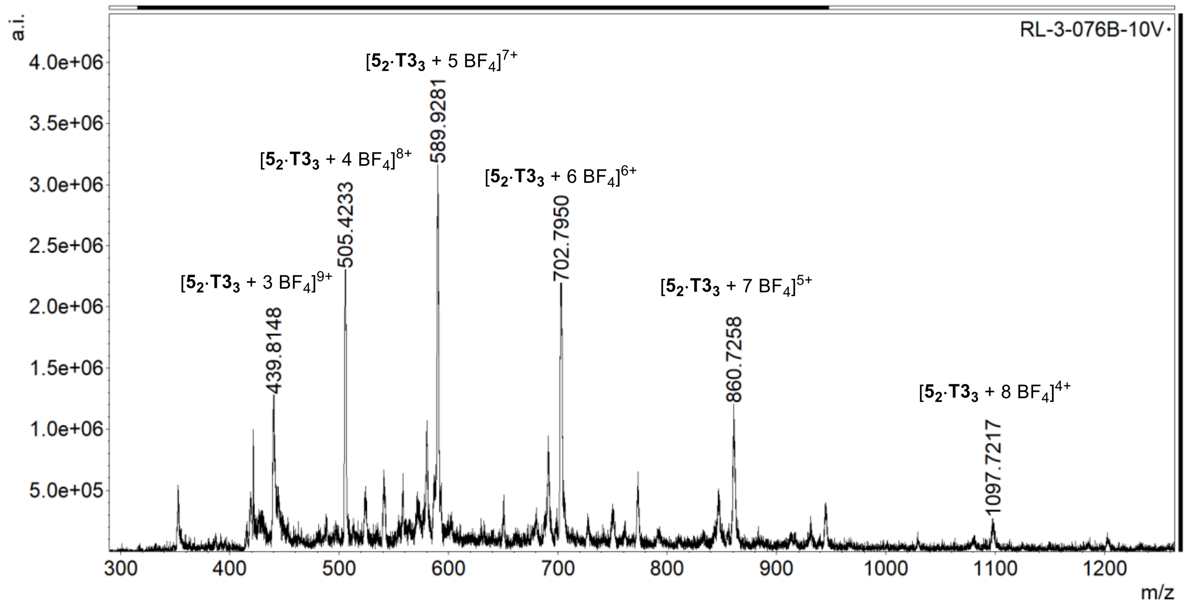

Figure S54. ESI-LRMS of $\mathbf{5_2{\cdot}T3_3}$ showing the different charge states corresponding to the loss of BF_4^- anions.

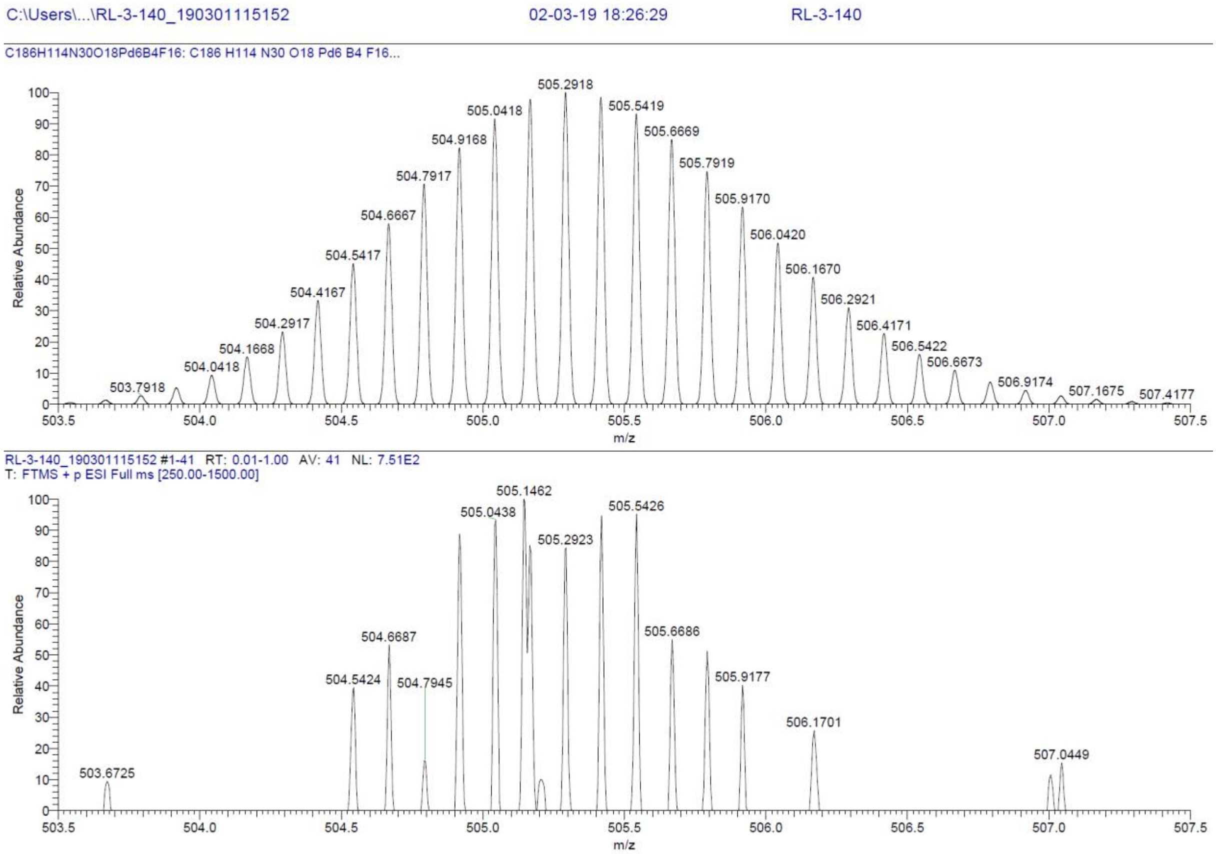

Figure S55A. Top: simulated isotopic pattern, bottom: ESI-HRMS of $[\mathbf{5_2{\cdot}T3_3} + 4\ BF_4]^{8+}$. The signal was weak in ESI-HRMS analysis conditions but intense enough to identify the species.

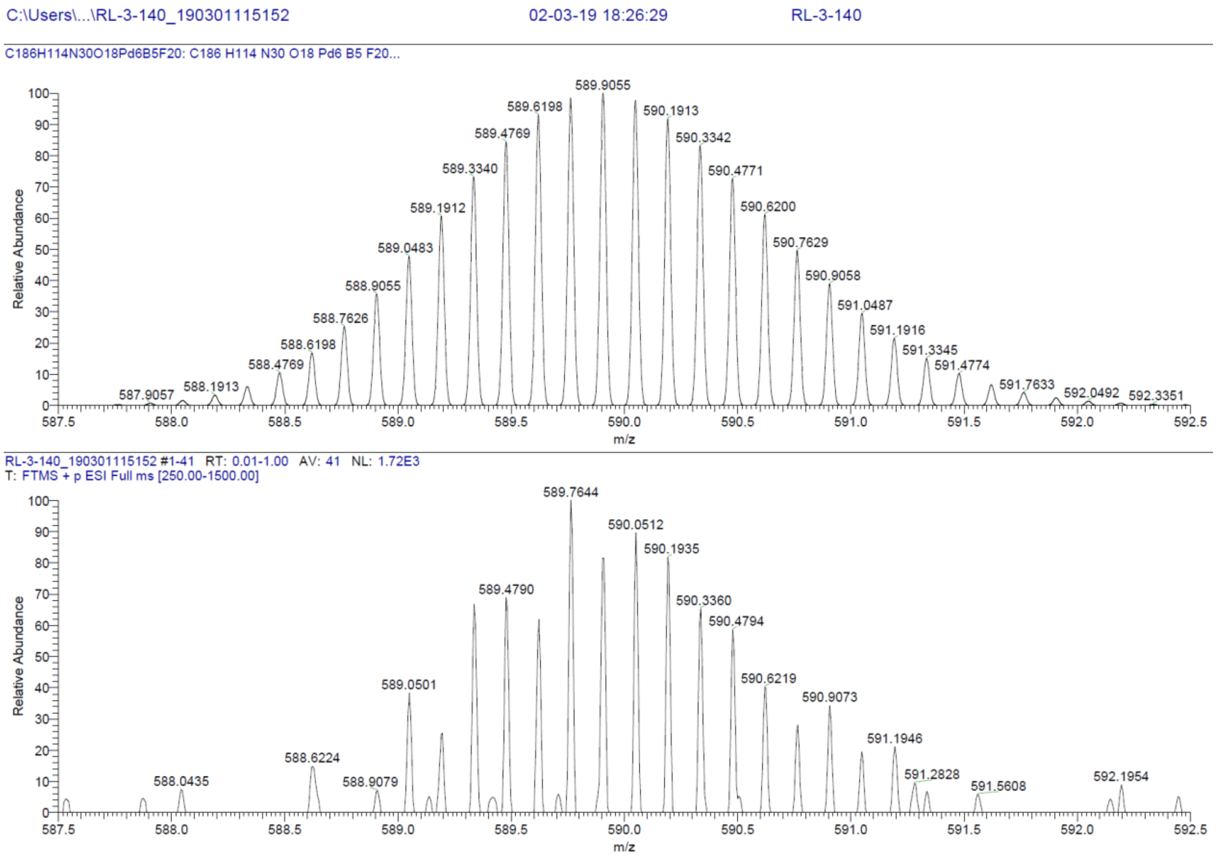

Figure S55B. Top: simulated isotopic pattern, bottom: ESI-HRMS of [$\mathbf{5_2{\cdot}T3_3}$ + 5 BF_4]$^{7+}$. The signal was weak in ESI-HRMS analysis conditions but intense enough to identify the species.

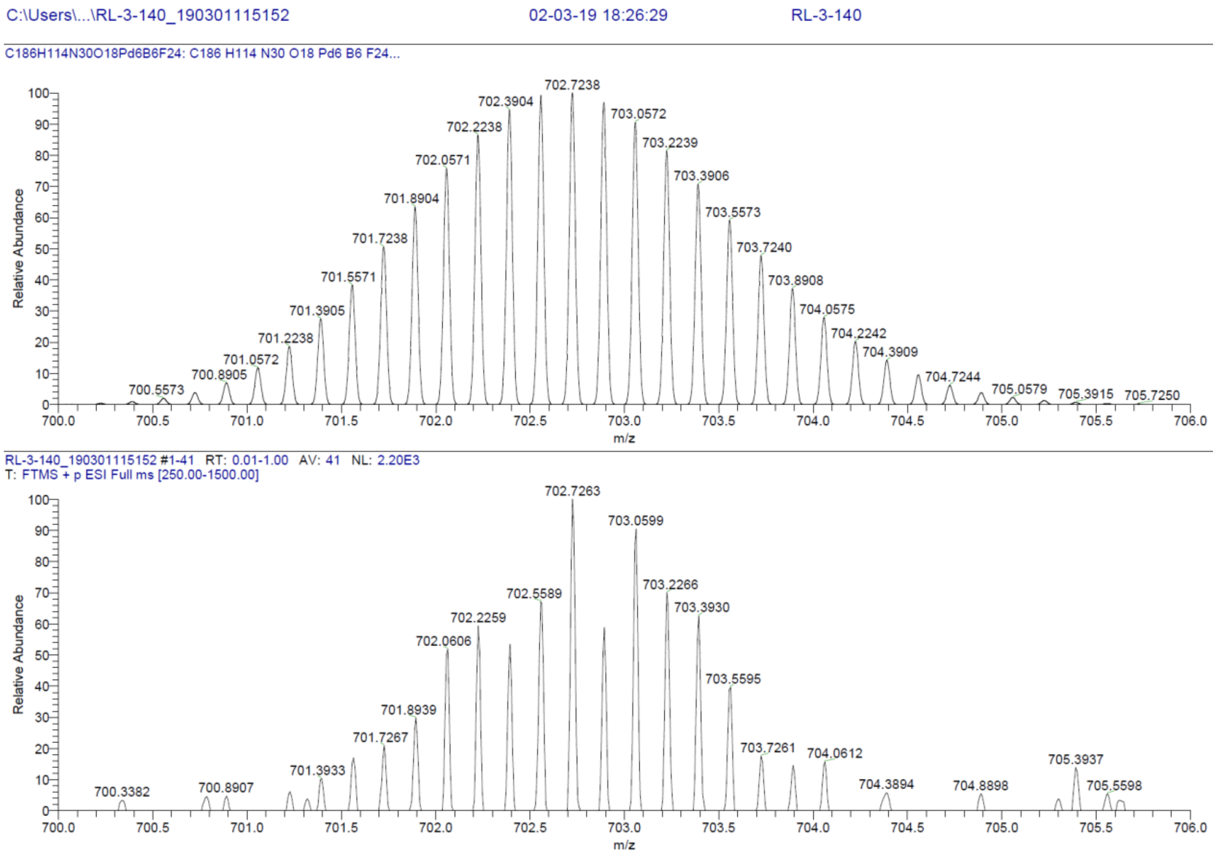

Figure S55C. Top: simulated isotopic pattern, bottom: ESI-HRMS of [$\mathbf{5_2{\cdot}T3_3}$ + 6 BF_4]$^{6+}$. The signal was weak in ESI-HRMS analysis conditions but intense enough to identify the species.

1.10 Synthesis and characterization of cages Pd_6[4+6] **12·(MeCN)$_6$** and Pd_9[6+9] **13·(MeCN)$_9$**

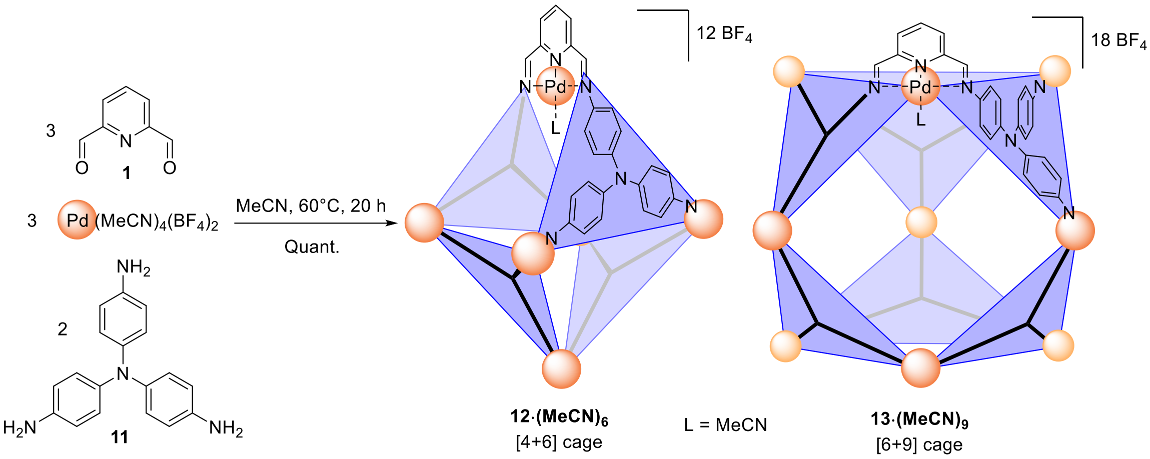

To a stirred suspension of 2,6-diformylpyridine **1** (27.5 mg, 0.203 mmol), 1,3,5-tris(4-aminophenyl)amine **11** (39.8 mg, 0.137 mmol) in 50 mL MeCN was added a solution of $[Pd(MeCN)_4](BF_4)_2$ (93.9 mg, 0.211 mmol) in 1 mL MeCN. The black mixture was stirred at 60°C for 20 h. The solution was cooled down to *r.t.*, concentrated to a volume of *ca.* 5 mL with a rotary evaporator, filtered and slowly poured into 30 mL of Et_2O. The mixture was shaken and left to rest 10 minutes to complete precipitation. The precipitate was collected by centrifugation, washed with 5 mL Et_2O and dried under vacuum affording a mixture of **12·(MeCN)$_6$(BF$_4$)$_{12}$** and **13·(MeCN)$_9$(BF$_4$)$_{18}$** as a black solid (124.6 mg, 0.203 mmol on Pd basis, FW/Pd = 613.75 g/mol). Quantitative yield.

^{1}H NMR (500 MHz, CD_3CN, 298 K, mixture of **12·(CD$_3$CN)$_6$** and **13·(CD$_3$CN)$_9$**) δ (ppm) = 8.55 – 8.45 (m, 6H for **12**, 9H for **13**), 8.35 (s, 12H for **12**), 8.31 (s, 12H for **13**), 8.30 (s, 6H for **13**), 8.20 – 8.13 (m, 12 H for **12**, 18H for **13**), 7.60 – 7.50 (m, 24H for **12**, 36H for **13**), 7.30 (d, *J* = 9.1 Hz, 12H for **13**), 7.28 (d, *J* = 8.9 Hz, 24H for **13**), 7.20 (d, *J* = 9.0 Hz, 24H for **12**).

^{13}C NMR (126 MHz, CD_3CN, 298 K, mixture of **12·(CD$_3$CN)$_6$** and **13·(CD$_3$CN)$_9$**) δ (ppm) =. 172.43, 157.16, 156.95, 156.85, 150.38, 149.73, 149.53, 146.43, 146.36, 143.26, 143.17, 131.37, 131.26, 126.21, 125.70, 125.56, 125.36. The number of peaks observed is smaller than the expected 8 peaks for **12** and 16 peaks for **13** because of broadening and/or overlapping.

ESI-LRMS for **12·Cl$_6$** [$(C_{114}H_{78}Cl_6N_{22}Pd_6)^{6+}$] m/z = [**12·Cl$_6$**]$^{6+}$, calcd: 434.53, found: 434.34; [**12·Cl$_6$** + BF_4]$^{5+}$, calcd: 538.80, found: 538.65; [**12·Cl$_6$** + 2 BF_4]$^{4+}$, calcd: 695.20, found: 695.44.

ESI-LRMS for **13·Cl$_9$** [$(C_{171}H_{117}Cl_9N_{33}Pd_9)^{9+}$] m/z = [**13·Cl$_9$**]$^{9+}$, calcd: 434.53, found: 434.34; [**13·Cl$_9$** + BF_4]$^{8+}$, calcd: 499.70, found: 499.51; [**13·Cl$_9$** + 2 BF_4]$^{7+}$, calcd: 583.48, found: 583.15; [**13·Cl$_9$** + 3 BF_4]$^{6+}$, calcd: 695.19, found: 695.44; [**13·Cl$_9$** + 4 BF_4]$^{5+}$, calcd: 851.59, found: 851.08.

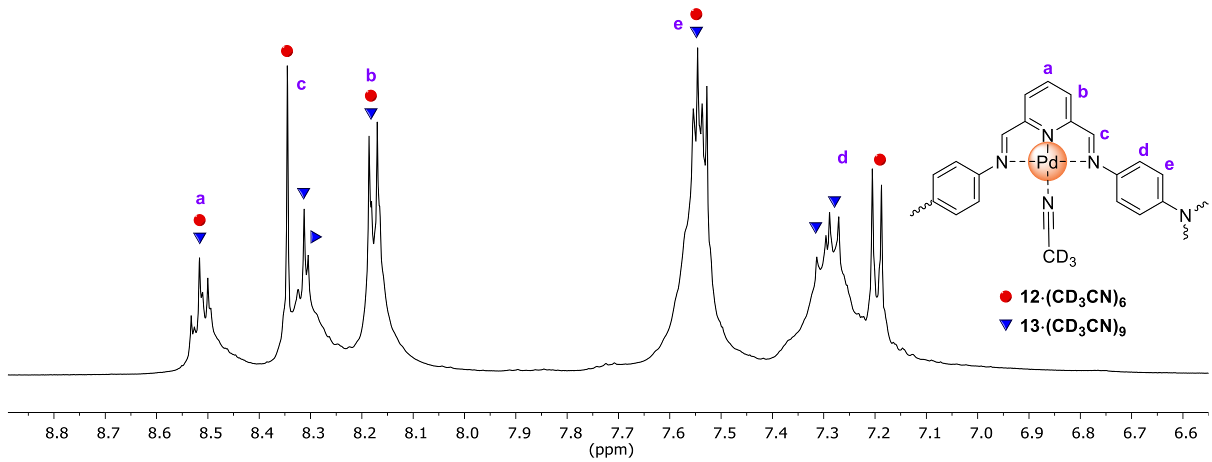

Figure S56. ^{1}H NMR spectrum of mixture of **12·(CD$_3$CN)$_6$** and **13·(CD$_3$CN)$_9$** (500 MHz, CD$_3$CN, 298 K).

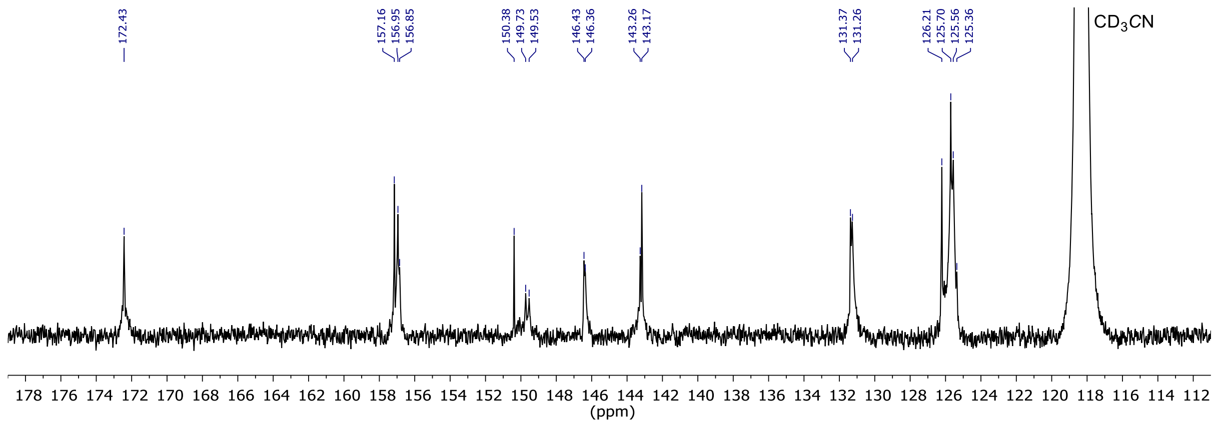

Figure S57. ^{13}C NMR spectrum of mixture of **12·(CD$_3$CN)$_6$** and **13·(CD$_3$CN)$_9$** (126 MHz, CD$_3$CN, 298 K).

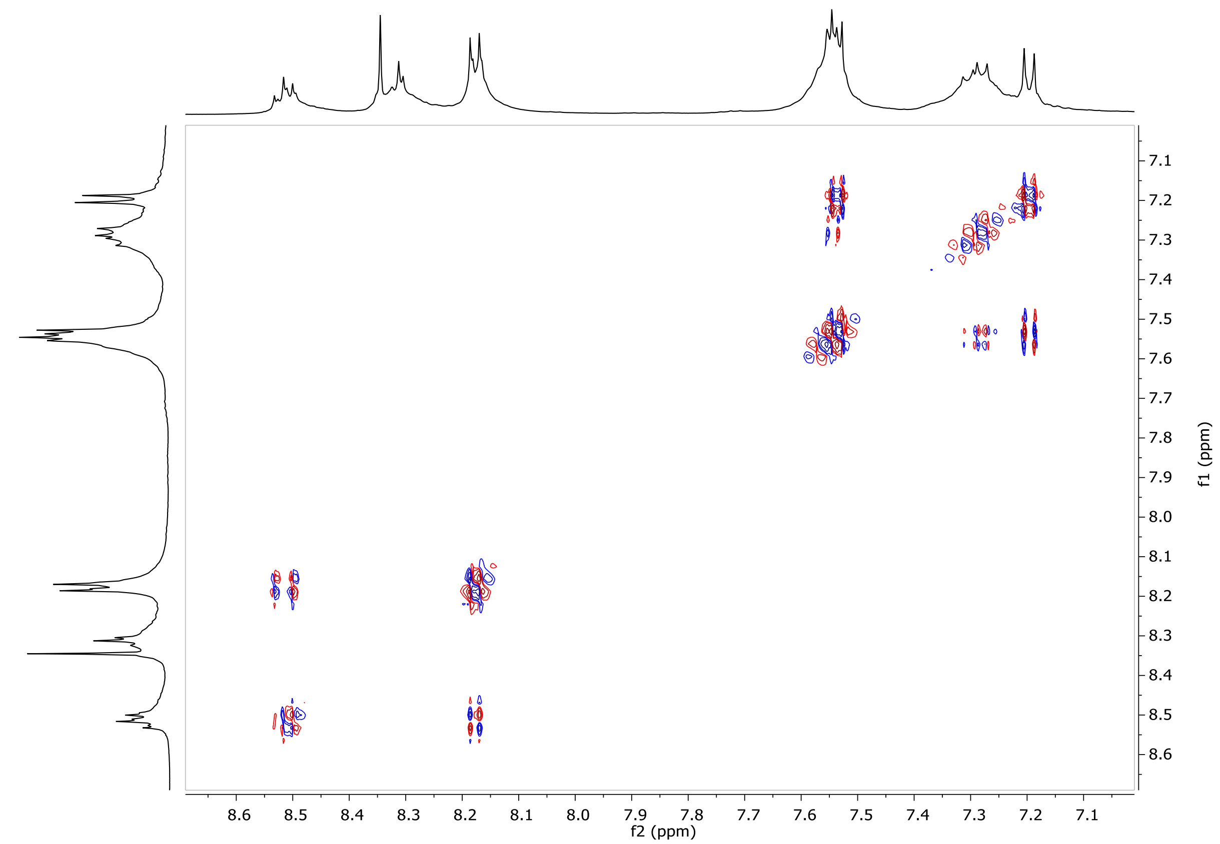

Figure S58. dqfCOSY spectrum of mixture of **12·(CD$_3$CN)$_6$** and **13·(CD$_3$CN)$_9$** (500 MHz, CD$_3$CN, 298 K).

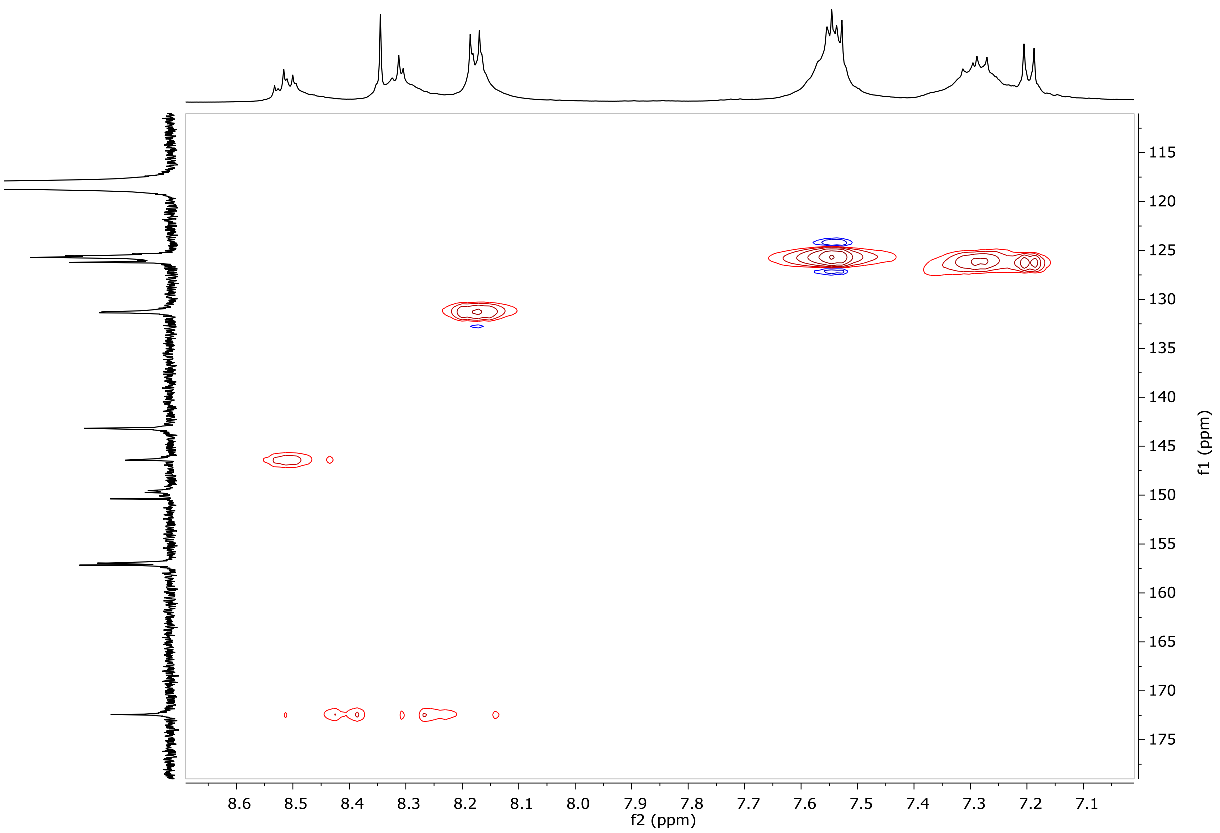

Figure S59. Edited ^{1}H-^{13}C HSQC spectrum of mixture of **12·(CD$_3$CN)$_6$** and **13·(CD$_3$CN)$_9$** (11.7 Tesla, CD$_3$CN, 298 K). The unusual shape of the correlation spot for the N=CH is most likely caused by a ^1J coupling constant value out of the usual range covered by standard HSQC parameters.

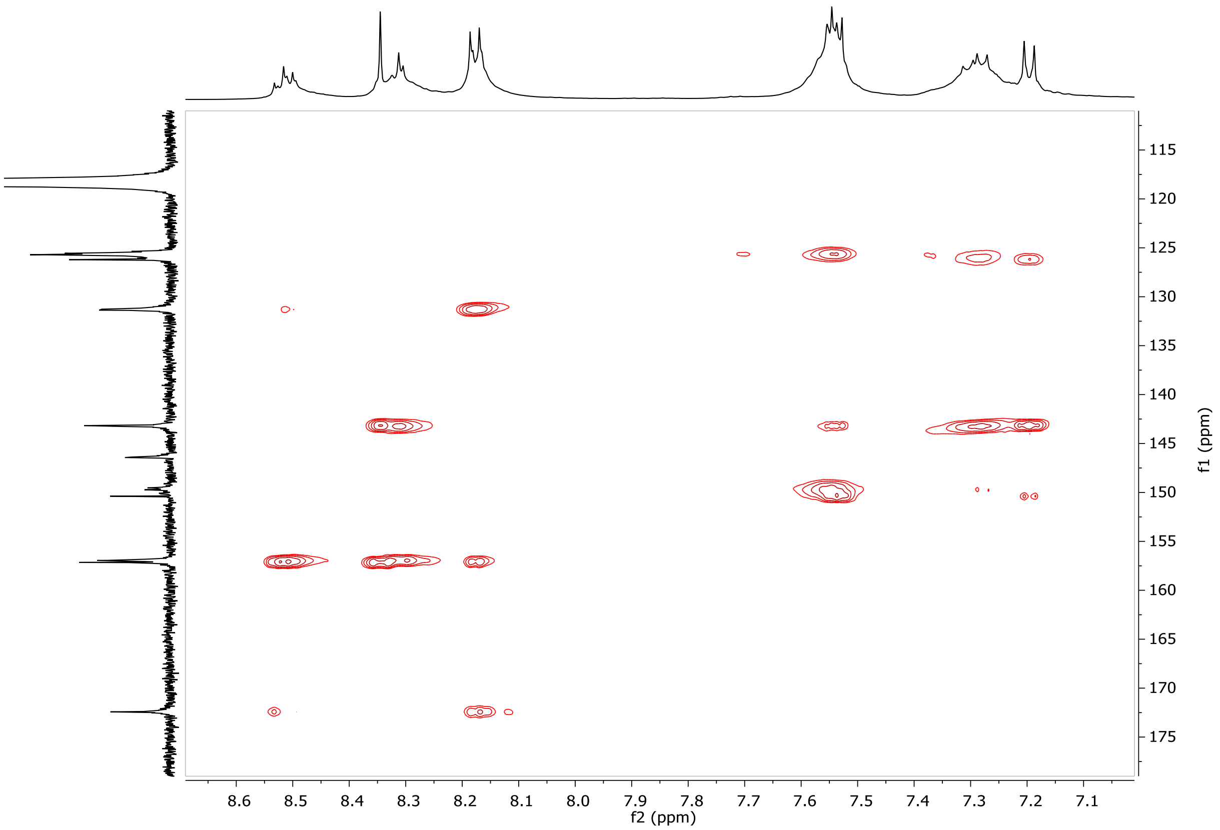

Figure S60. ^{1}H-^{13}C HMBC spectrum of mixture of **12·(CD$_3$CN)$_6$** and **13·(CD$_3$CN)$_9$** (11.7 Tesla, CD_3CN, 298 K).

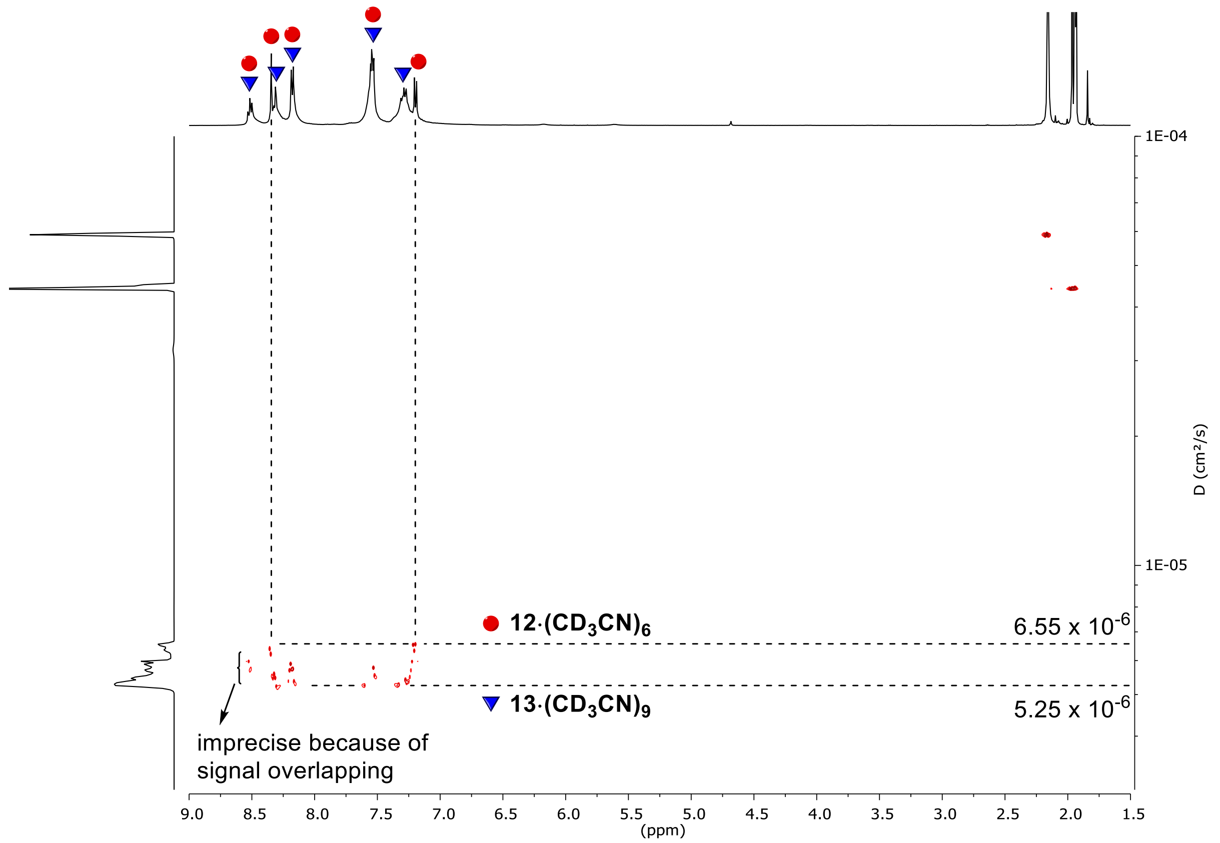

Figure S61A. ^{1}H DOSY spectrum of mixture of **12·(CD$_3$CN)$_6$** and **13·(CD$_3$CN)$_9$** (500 MHz, CD_3CN, 298 K, diffusion delay Δ = 50 ms, diffusion gradient length δ = 3000 μs).

The theoretical radii for a sphere containing **12** and a spheroid containing **13** would be 13.4 Å and 14.7 Å, respectively, based on the crystal structure of **12·Cl$_6$** and a PM3 model of **13·Cl$_9$** (see Figure S61B).

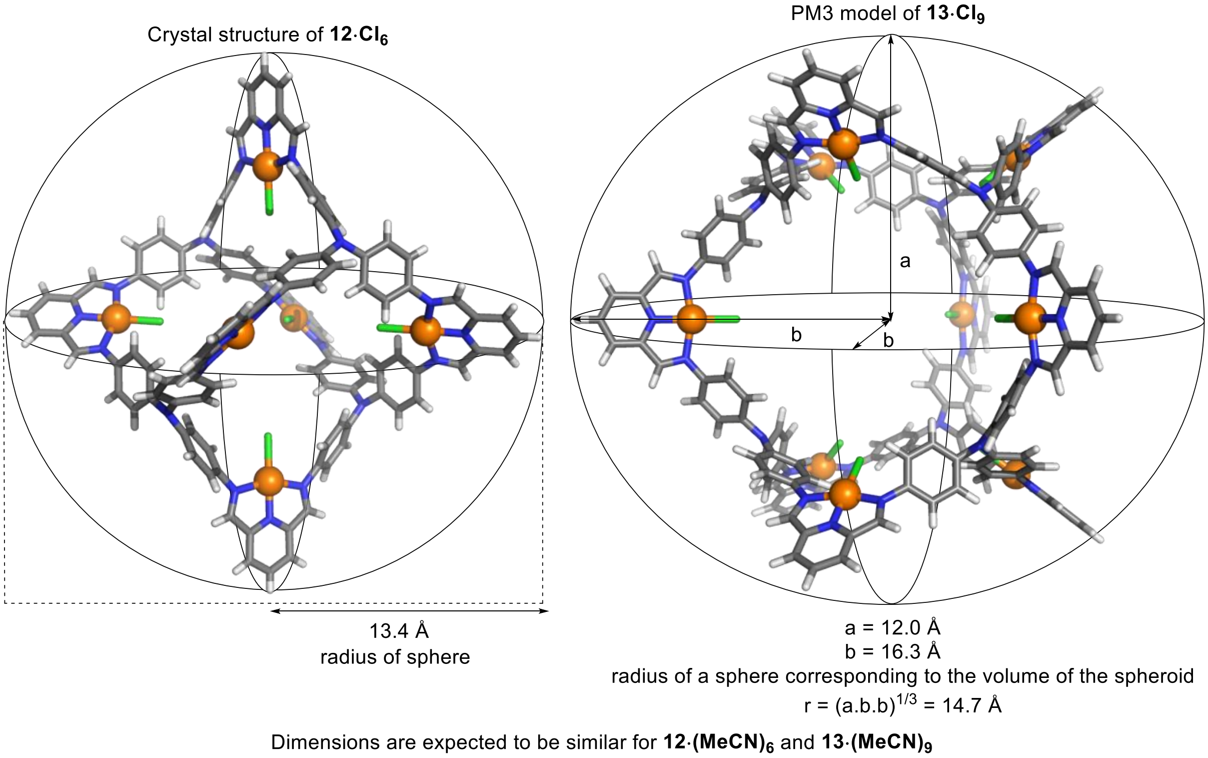

Figure S61B. Radii of a theoretical sphere containing cage **12** and a spheroid containing cage **13**.

The Stokes-Einstein equation can generally be used to determine the effective radius of a spherical particle moving through a fluid by thermal motion (or diffusion):

$r = \frac{k_B\,T}{6\,\pi\,\eta\,D}$, where r is the effective radius (in m), k_B the Boltzmann constant (in $J{\cdot}K^{-1}$), T the temperature (in K), η the fluid viscosity (in Pa·s), and *D* the diffusion coefficient of the particle (in $m^2{\cdot}s^{-1}$).

Following the Stokes-Einstein equation and with a CD_3CN viscosity of 3.41×10^{-4} Pa·s,[5] the diffusion coefficients calculated following the DOSY experiment of Figure S61A correspond to solvodynamic radii of 9.8 Å and 12.2 Å for Pd_6[4+6] **12·(MeCN)$_6$** and Pd_9[6+9] **13·(MeCN)$_9$**, respectively (assuming perfect sphere behavior). These calculated solvodynamic radii are smaller than the corresponding particle radii which we infer is due to the shape of cages **12·(MeCN)$_6$** and **13·(MeCN)$_9$**. Indeed, these cages are hollow with open faces, which leads to a smaller contact surface area compared to the corresponding closed spheres. Therefore, such open cage structures are expected to diffuse more rapidly than the corresponding closed spheres.

The radius values obtained with the Stokes-Einstein equation hold limited physical meaning for particles that deviate strongly from the behavior of a closed spherical particle. As we are not aware of a suitable theoretical model to correlate the diffusion coefficients with the radii of such open cage structures, we interpret the diffusion coefficients qualitatively, noting that larger assembly **13** diffuses more slowly than smaller assembly **12**.

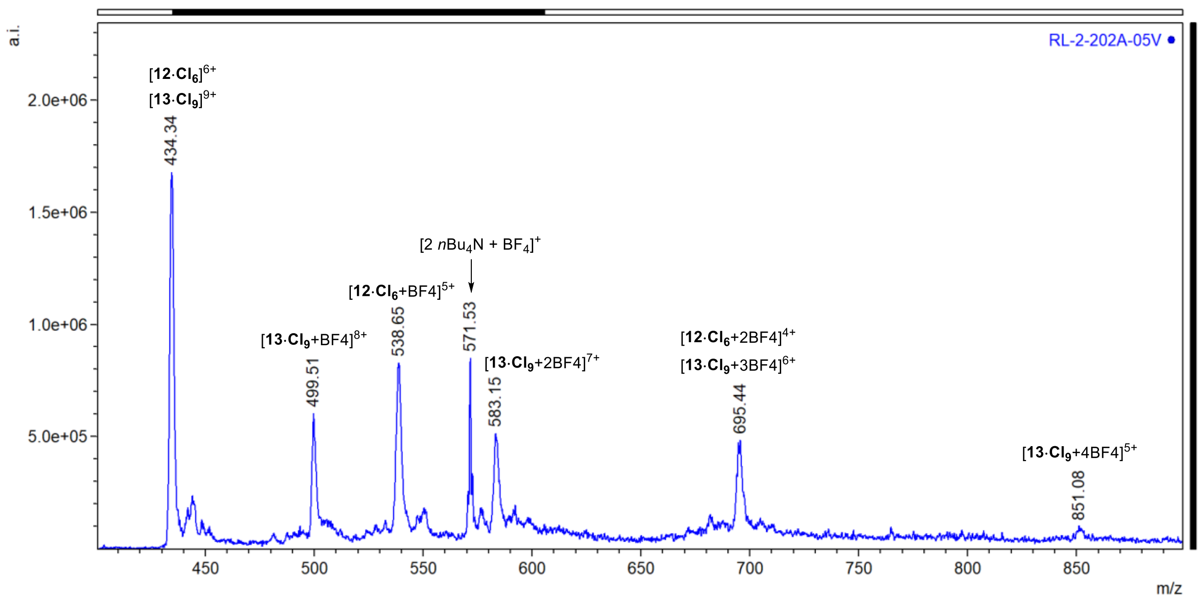

Figure S62. ESI-LRMS of mixture of **12·Cl$_6$** and **13·Cl$_9$** showing the different charge states corresponding to the loss of BF_4^- anions.

1.11 Enrichment of cages Pd_6[4+6] **12·Cl₆** and Pd_9[6+9] **13·Cl₉**

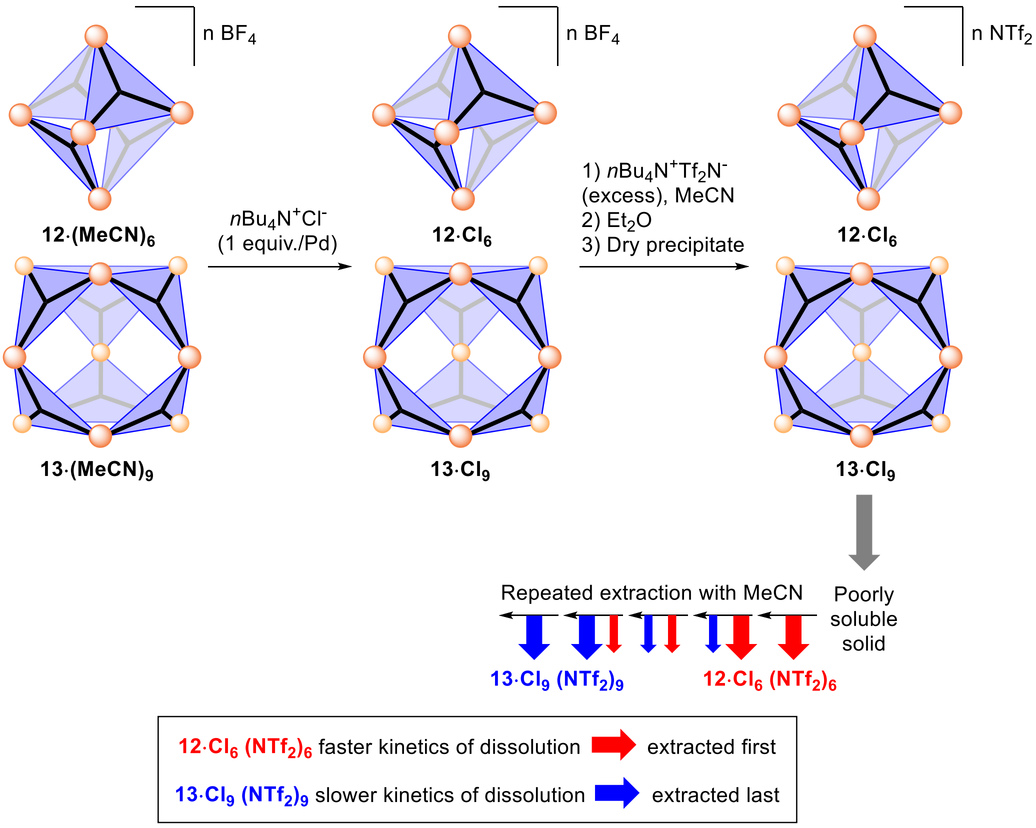

To a stirred solution of **12·(MeCN)$_6$(BF$_4$)$_{12}$** and **13·(MeCN)$_9$(BF$_4$)$_{18}$** (124 mg, 0.202 mmol in Pd) in 50 mL MeCN at *r.t.* was added a solution of nBu$_4$N$^+$Cl$^-$ in MeCN (0.10 M, 2.00 mL, 0.200 mmol). nBu$_4$N$^+$NTf$_2^-$ (523 mg, 1.00 mmol) was added and the mixture was concentrated to a volume of *ca.* 5 mL with a rotary evaporator and slowly poured into 30 mL of Et$_2$O. The mixture was shaken and left to rest 10 minutes to complete precipitation. The precipitate was collected by centrifugation, washed with 5 mL Et$_2$O and dissolved in a minimum amount of MeCN *without drying*. Two more cycles of nBu$_4$N$^+$NTf$_2^-$ addition, concentration, precipitation, washing and dissolution were performed. The final precipitate was dried under vacuum affording a poorly soluble black solid containing a mixture of **12·Cl$_6$(NTf$_2$)$_6$** and **13·Cl$_9$(NTf$_2$)$_9$**. Repeated extractions of the solid with 5 mL MeCN were performed, regularly replacing the MeCN (initially after one hour and gradually increasing the extraction time up to one month) and isolating each extract fraction. The extract fractions were gently dried by blowing N$_2$ affording solids of <10 mg each. ^{1}H NMR analysis in CD$_3$CN showed enrichment in **12·Cl$_6$(NTf$_2$)$_6$** for the early fractions and **13·Cl$_9$(NTf$_2$)$_9$** for the late fractions. The amount of material dissolved over time decreased exponentially, thus the solid was never fully dissolved but some product could continuously be extracted (over 10 extractions for 3 months). Sonication and heating to 60 °C over periods of less than an hour did not show significant effect on the kinetics of dissolution.

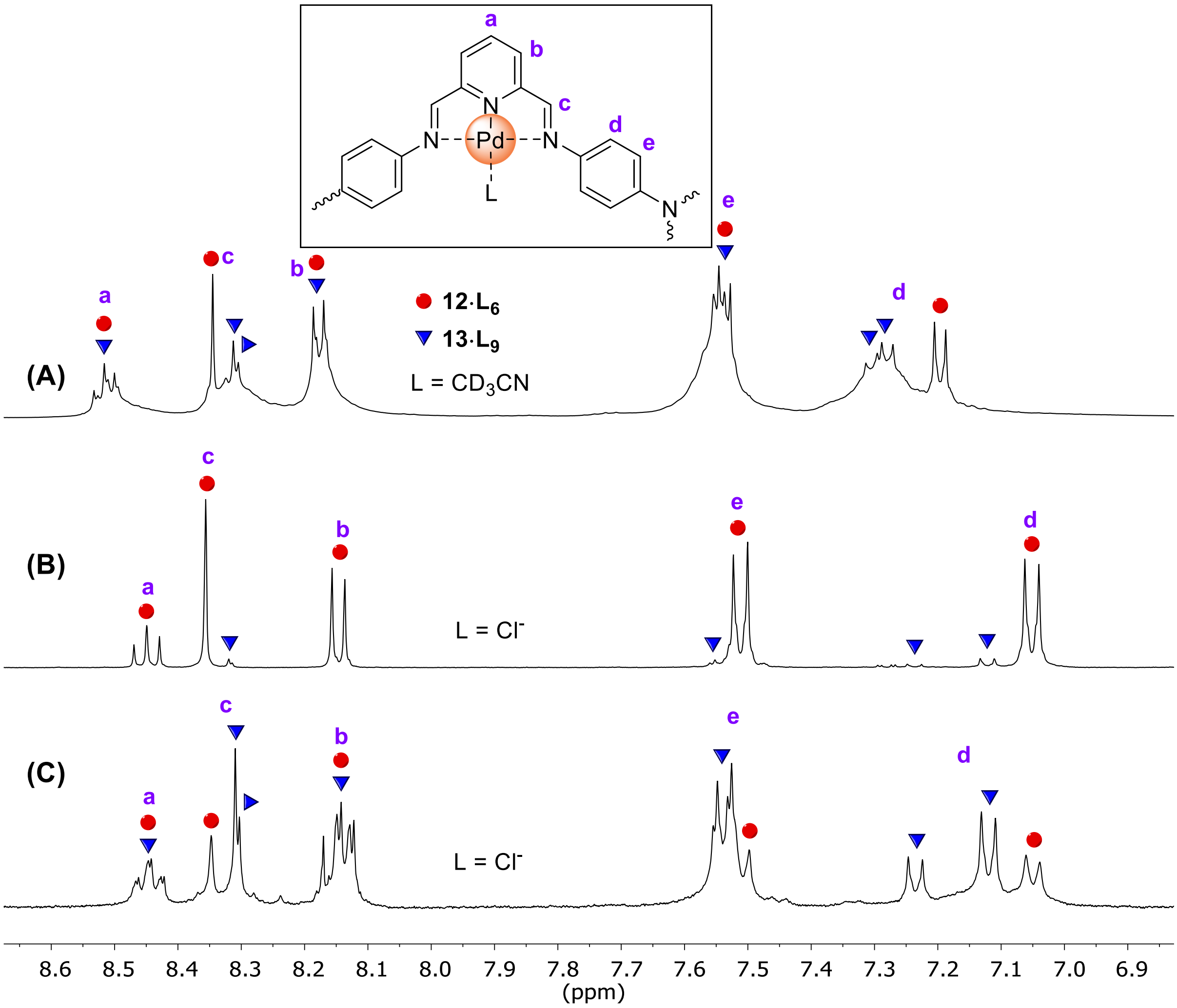

Figure S63. ^{1}H NMR spectra (CD_3CN, 298 K) of (A) **12·(MeCN)$_6$(BF$_4$)$_{12}$** and **13·(MeCN)$_9$(BF$_4$)$_{18}$** (500 MHz), (B) enriched **12·Cl$_6$(NTf$_2$)$_6$** from first extraction (400 MHz), and (C) enriched **13·Cl$_9$(NTf$_2$)$_9$** from fifth extraction (400 MHz).

1.12 Synthesis and characterization of templated cage **13·T3₃·Cl₃**

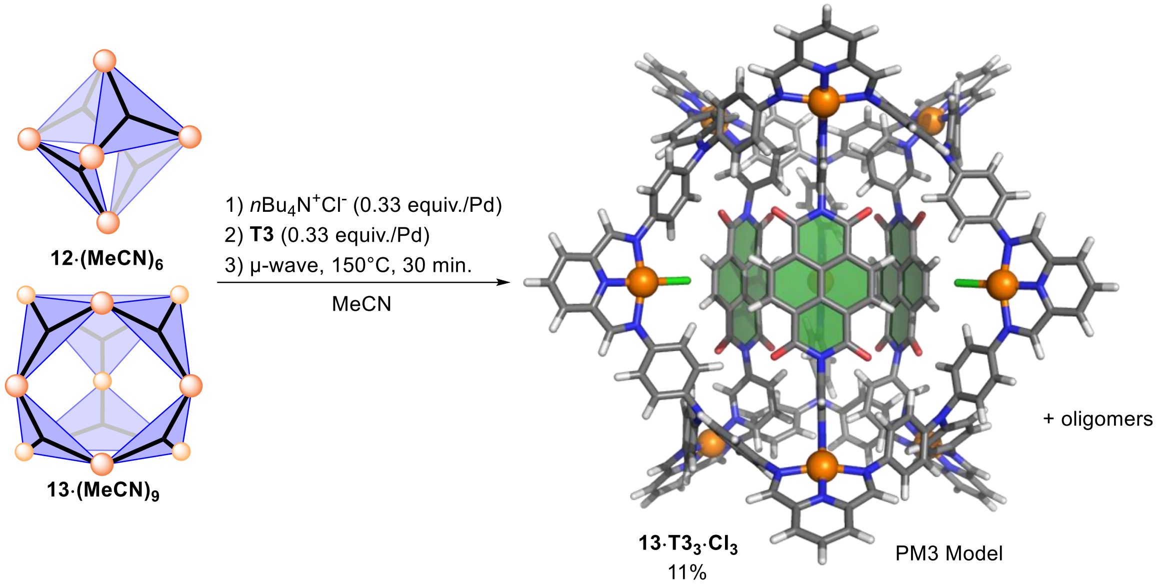

To a stirred solution of **12·(MeCN)$_6$(BF$_4$)$_{12}$** and **13·(MeCN)$_9$(BF$_4$)$_{18}$** (6.1 mg, 10 µmol in Pd) in 4 mL MeCN at *r.t.* were added bis(3-pyridyl)naphthalene diimide **T3** (1.4 mg, 3.3 µmol) and a solution of *n*Bu$_4$N$^+$Cl$^-$ in MeCN (0.10 M, 30 µL, 3.0 µmol). The mixture was stirred and heated under microwave radiation at 150°C for 30 min. The solvent was removed under vacuum and the crude product was analyzed by ^{1}H NMR spectroscopy showing a yield of 11% based on signal integration comparison with *n*Bu$_4$N$^+$. Further purification was precluded due to the high amount of oligomeric byproducts in the sample.

The synthesis of **13·T3·Cl$_3$** was attempted under stirring at *r.t.* or at 60°C (oil bath) for 24 h but the yield of **13·T3·Cl$_3$** was in the range 8-10% according to NMR analysis (see Table S1). The synthesis of **13·T3·Cl$_3$** was also attempted through aniline exchange without improving the yield (see Figure S80).

^{1}H NMR (500 MHz, CD$_3$CN, 298 K) δ (ppm) = 8.80 (d, *J* = 5.7 Hz, 6H), 8.63 (d, *J* = 2.1 Hz, 6H), 8.53 (t, *J* = 8.1 Hz, 6H), 8.50 (s, 12H), 8.46 (t, *J* = 8.0 Hz, 3H), 8.40 (s, 12H), 8.37 (s, 6H), 8.23 (d, *J* = 8.2 Hz, 12H), 8.18 (d, *J* = 7.9 Hz, 6H), 7.81 (d, *J* = 8.1 Hz, 6H), 7.66 (d, *J* = 8.4 Hz, 12H), 7.31 (dd, *J* = 8.2, 5.7 Hz, 6H), 7.21 (d, *J* = 8.4 Hz, 12H), 7.11 (d, *J* = 8.5 Hz, 24H), 6.94 (d, *J* = 8.6 Hz, 24H).

ESI-LRMS for **13·T3·Cl$_3$** [(C$_{243}$H$_{153}$Cl$_3$N$_{45}$O$_{12}$Pd$_9$)$^{15+}$] m/z = [**13·T3·Cl$_3$** + 2 BF$_4$]$^{13+}$, calcd: 394.83, found: 394.92; [**13·T3·Cl$_3$** + 3 BF$_4$]$^{12+}$, calcd: 434.96, found: 434.99; [**13·T3·Cl$_3$** + 4 BF$_4$]$^{11+}$, calcd: 482.40, found: 482.40; [**13·T3·Cl$_3$** + 5 BF$_4$]$^{10+}$, calcd: 539.32, found: 539.31; [**13·T3·Cl$_3$** + 6 BF$_4$]$^{9+}$, calcd: 608.89, found: 608.87; [**13·T3·Cl$_3$** + 7 BF$_4$]$^{8+}$, calcd: 695.85, found: 695.89; [**13·T3·Cl$_3$** + 8 BF$_4$]$^{7+}$, calcd: 807.65, found: 807.69; [**13·T3·Cl$_3$** + 9 BF$_4$]$^{6+}$, calcd: 956.73, found: 956.90; [**13·T3·Cl$_3$** + 10 BF$_4$]$^{5+}$, calcd: 1165.44, found: 1165.56.

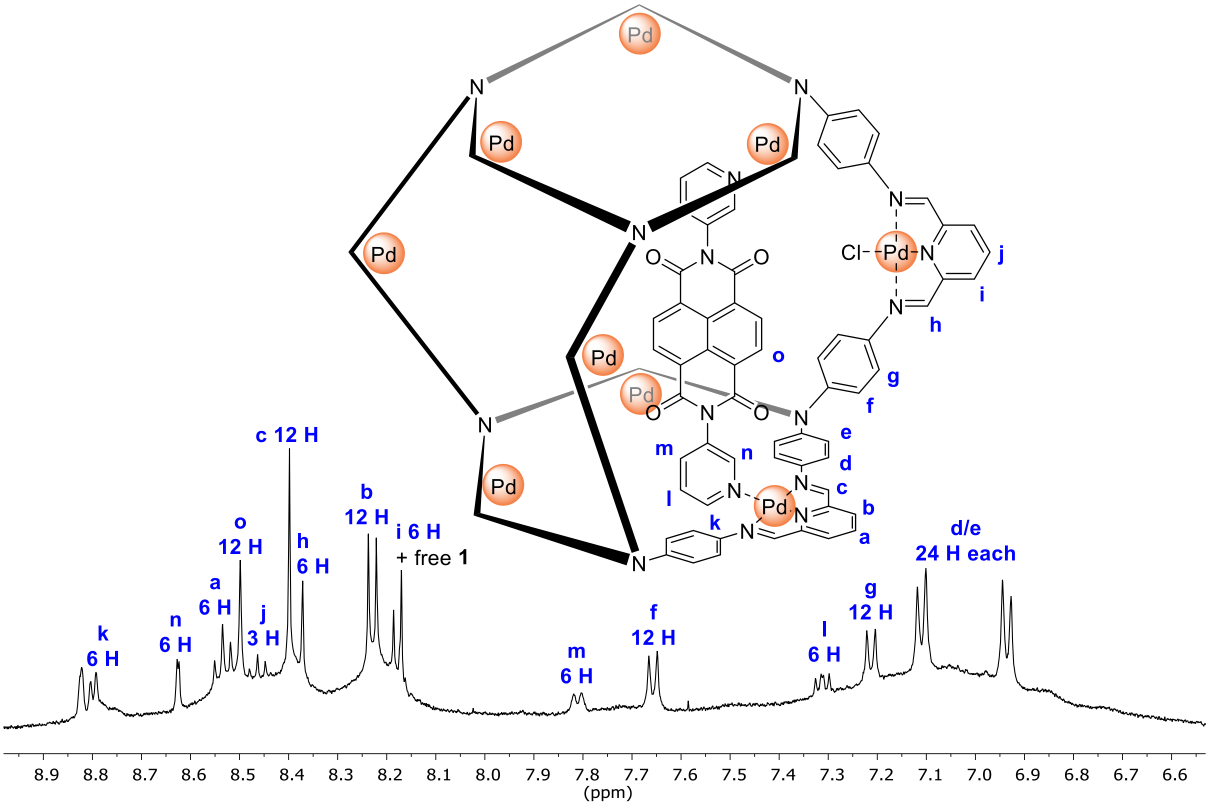

Figure S64. ^{1}H NMR spectrum of **13·T3·Cl₃** (500 MHz, CD_3CN, 298 K, crude mixture). ^{1}H signal assignment is based on integration, multiplicity and expected chemical shifts. Broad signals correspond presumably to oligomeric species. The low concentration of **13·T3·Cl₃** prevented full 2D NMR characterization in reasonable spectrometer usage time.

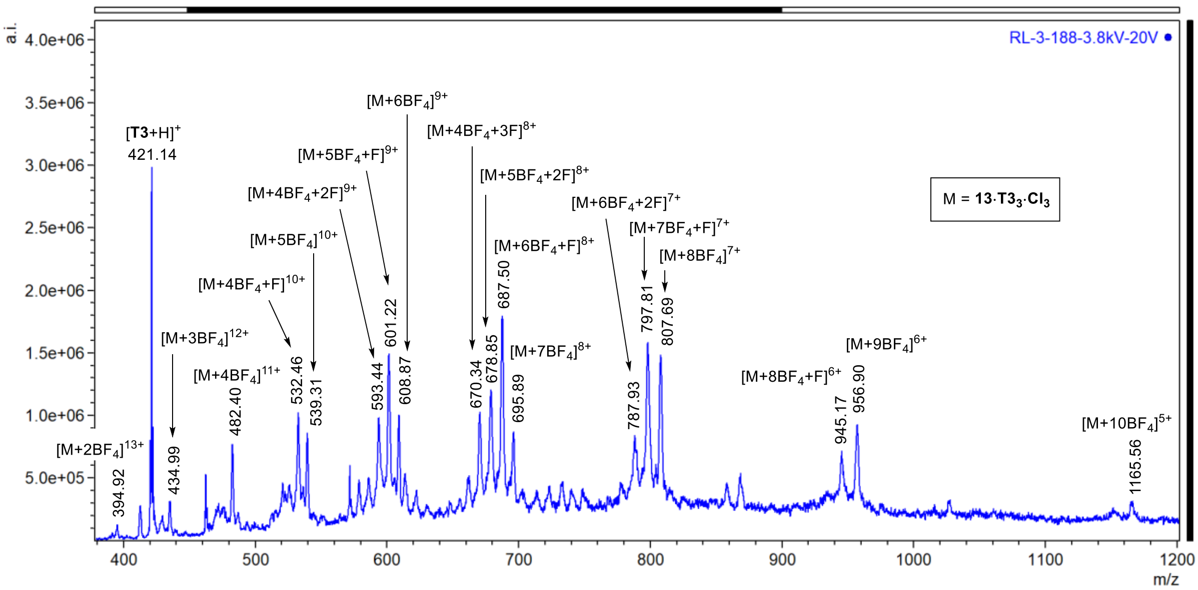

Figure S65. ESI-LRMS of **13·T3·Cl₃** (crude mixture) showing the different charge states corresponding to the loss of BF_4^- anions. Fluoride is suspected to originate from BF_4^- fragmentation in ESI-MS conditions.

Table S1. Templates tested to form templated covalent cages. Conditions were CD_3CN, 60 °C, 18 h at a concentration of 2 mM in Pd unless otherwise stated.

#	Starting Material	Template (equiv/Pd)	Expected structure	Result
1	**1**/**11**/[Pd(MeCN)$_4$](BF$_4$)$_2$; 3:2:3	**T1** (0.167)	**12·T1·(MeCN)$_3$**	Complex mixture
2	**1**/**11**/[Pd(MeCN)$_4$](BF$_4$)$_2$; 3:2:3	**T1** (0.222)	**13·T1$_2$·(MeCN)$_3$**	Complex mixture
3	**12·(MeCN)$_6$(BF$_4$)$_{12}$** + **13·(MeCN)$_9$(BF$_4$)$_{18}$**	**T1** (0.167)	**12·T1·(MeCN)$_3$**	Complex mixture
4	**12·(MeCN)$_6$(BF$_4$)$_{12}$** + **13·(MeCN)$_9$(BF$_4$)$_{18}$**	**T1** (0.222)	**13·T1$_2$·(MeCN)$_3$**	Complex mixture
5[a]	**1**/**11**/[Pd(MeCN)$_4$](BF$_4$)$_2$; 3:2:3	**T2** (0.111)	**13·T2·(MeCN)$_5$**	Complex mixture
6[a]	**1**/**11**/[Pd(MeCN)$_4$](BF$_4$)$_2$; 3:2:3	**T2** (0.167)	Pd$_{12}$ cage**·T2$_2$·(MeCN)$_4$**	Complex mixture
7[a]	**12·(MeCN)$_6$(BF$_4$)$_{12}$** + **13·(MeCN)$_9$(BF$_4$)$_{18}$**	**T2** (0.111)	**13·T2·(MeCN)$_5$**	Complex mixture
8[a]	**12·(MeCN)$_6$(BF$_4$)$_{12}$** + **13·(MeCN)$_9$(BF$_4$)$_{18}$**	**T2** (0.167)	Pd$_{12}$ cage**·T2$_2$·(MeCN)$_4$**	Complex mixture
9	**1**/**11**/[Pd(MeCN)$_4$](BF$_4$)$_2$; 3:2:3	**T3** (0.33)	**13·T3$_3$·(MeCN)$_3$** or Pd$_{12}$ cage**·T3$_4$·(MeCN)$_4$**	Complex mixture
10	**1**/**11**/[Pd(MeCN)$_4$](BF$_4$)$_2$; 3:2:3	**T3** (0.50)	Pd$_{12}$ cage**·T3$_6$**	Complex mixture
11	**12·(MeCN)$_6$(BF$_4$)$_{12}$** + **13·(MeCN)$_9$(BF$_4$)$_{18}$**	**T3** (0.33)	**13·T3$_3$·(MeCN)$_3$** or Pd$_{12}$ cage**·T3$_4$·(MeCN)$_4$**	Complex mixture
12	**12·(MeCN)$_6$(BF$_4$)$_{12}$** + **13·(MeCN)$_9$(BF$_4$)$_{18}$**	**T3** (0.50)	Pd$_{12}$ cage**·T3$_6$**	Complex mixture
13[b]	**12·(MeCN)$_6$(BF$_4$)$_{12}$** + **13·(MeCN)$_9$(BF$_4$)$_{18}$**	**T3** (0.33) + *n*Bu$_4$Cl (0.33)	**13·T3$_3$·Cl$_3$**	**13·T3$_3$·Cl$_3$** + oligomers
14[c]	**12·(MeCN)$_6$(BF$_4$)$_{12}$** + **13·(MeCN)$_9$(BF$_4$)$_{18}$**	**T3** (0.33) + *n*Bu$_4$Cl (0.33)	**13·T3$_3$·Cl$_3$**	**13·T3$_3$·Cl$_3$** + oligomers
15[d]	**12·(MeCN)$_6$(BF$_4$)$_{12}$** + **13·(MeCN)$_9$(BF$_4$)$_{18}$**	**T3** (0.33) + *n*Bu$_4$Cl (0.33)	**13·T3$_3$·Cl$_3$**	**13·T3$_3$·Cl$_3$** + oligomers
16	**15e** then **11** (0.67 equiv/Pd) after addition of template	**T3** (0.33) + *n*Bu$_4$Cl (0.33)	**13·T3$_3$·Cl$_3$**	**13·T3$_3$·Cl$_3$** + oligomers

[a] Tests in CD_3CN and $CD_3CN/CDCl_3$, 9:1 did not show noticeable difference in result.

[b] CD_3CN gave the expected result but tests in $CD_3CN/CDCl_3$ (1:1), CD_3NO_2 and $CD_3NO_2/CDCl_3$ (1:1) led to unidentified precipitate.

[c] Stirred at room temperature for 18 h.

[d] Stirred at 150 °C under microwave radiation for 30 min.

1.13 Reduction and demetallation of cages $Pd_6[4+6]$ **12·Cl₆** and $Pd_9[6+9]$ **13·Cl₉**

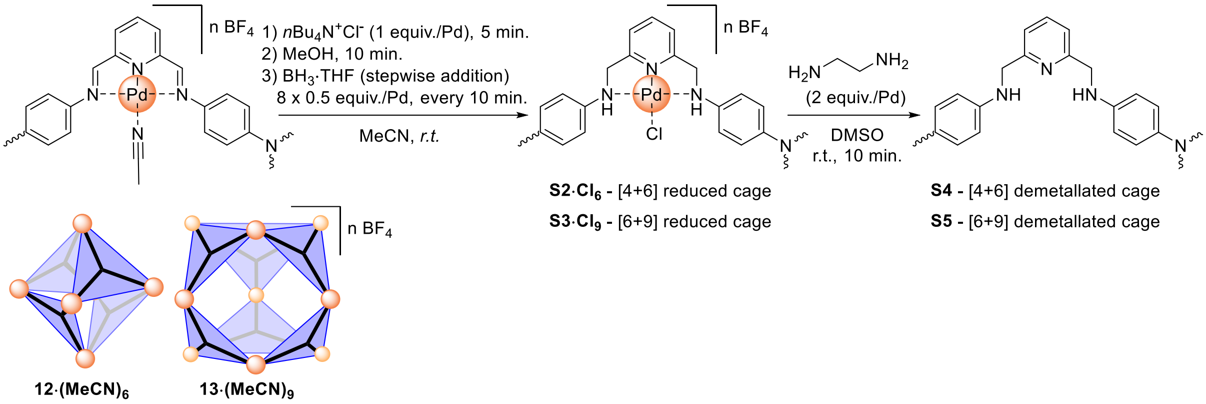

The reduction and demetallation of cages **12·Cl₆** and **13·Cl₉** was performed. ESI-MS monitoring of the reduction step shows that the reaction proceeds smoothly, similarly to the reduction of macrocycles **5·T1** and **6·T2** (see Figures S66 and S67). The demetallation occurs swiftly upon addition of ethylenediamine as shown by NMR monitoring (see Figure S68). Unfortunately, the numerous stereoisomers of reduced cages **S2·Cl₆** and **S3·Cl₉** prevented NMR characterization and purity assessment and the low solubility of the final demetallated cages **S4** and **S5** after precipitation prevented further characterization and purity assessment. Therefore, no yield could be determined.

Procedure:

To a stirred solution of **12·(MeCN)₆(BF₄)₁₂** and **13·(MeCN)₉(BF₄)₁₈** (124 mg, 0.202 mmol in Pd) in 50 mL MeCN at *r.t.* was added a solution of nBu$_4$N$^+$Cl$^-$ in MeCN (0.10 M, 2.00 mL, 0.200 mmol). After 5 min. 10 mL MeOH was added to the mixture. After 10 minutes, BH_3·THF (1M) was added stepwise (8 additions of 100 µL, one every 10 min., total 0.80 mmol) and the reaction was monitored by ESI-MS (see Figures S66 and S67). The mixture was filtered and slowly poured into 60 mL of Et_2O. The precipitate was collected by centrifugation, washed with 5 mL Et_2O *without drying*. The solid was dissolved in 10 mL MeCN by sonication. The solution was slowly poured into 30 mL Et_2O, left to rest for 30 min. and the precipitate was collected by centrifugation then washed with 5 mL Et_2O and dried under vacuum affording a black solid (87.2 mg, presumably mixture of **S2·Cl₆** and **S3·Cl₉**).

Note: the two precipitations were performed to remove nBu$_4$N$^+$BF$_4^-$ byproduct.

To a solution of the mixture of **S2·Cl₆** and **S3·Cl₉** (2.0 mg, expected 3.8 µmol in Pd) in 0.5 mL DMSO-*d₆* at *r.t.* was added ethylenediamine (7.6 µmol, stock solution in DMSO-*d₆*) under ^{1}H NMR spectroscopy monitoring (see Figure S68). The mixture was poured into 5 mL H_2O and the precipitate was collected by centrifugation. The solid material obtained could not be dissolved despite a wide range of solvents tested under heating and sonication: DMSO, DMF, pyridine, toluene, chlorobenzene, CH_2Cl_2, $CHCl_3$, CH_2ClCH_2Cl, $CHCl_2CHCl_2$, $CCl_2{=}CCl_2$, THF, MeOH, EtOH, MeCN, AcOEt, acetone, hexane. The solvent did not show coloration and spots deposited on TLC plates did not show the presence of product after drying.

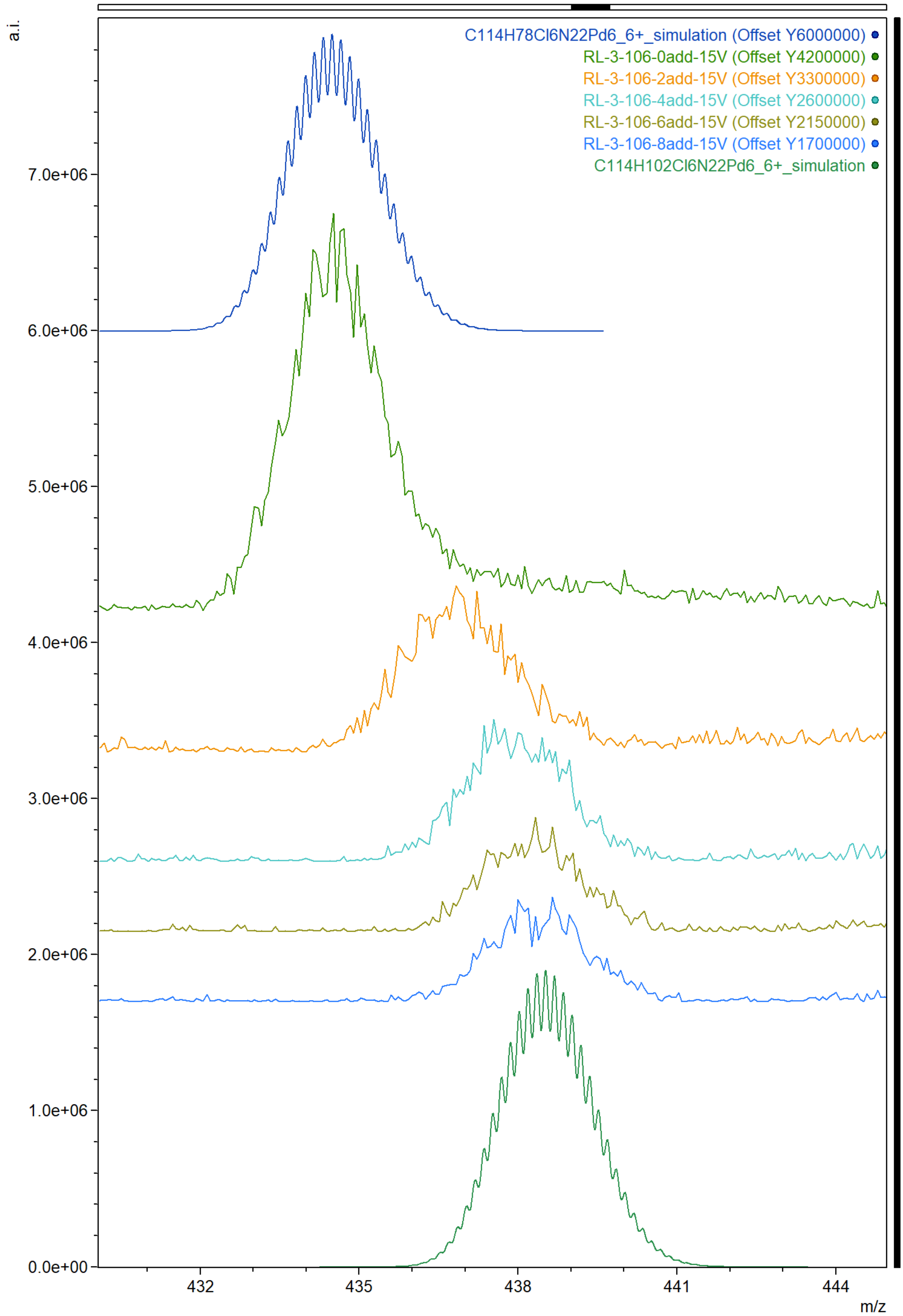

Figure S66. ESI-LRMS monitoring of the reduction of cages **12·Cl$_6$** and **13·Cl$_9$**. Zoom on the region around [**12·Cl$_6$**]$^{6+}$ and [**S2·Cl$_6$**]$^{6+}$. Spectra from top to bottom: simulated for [**12·Cl$_6$**]$^{6+}$, before addition of BH_3, after 2, 4, 6, 8 additions, simulated for [**S2·Cl$_6$**]$^{6+}$.

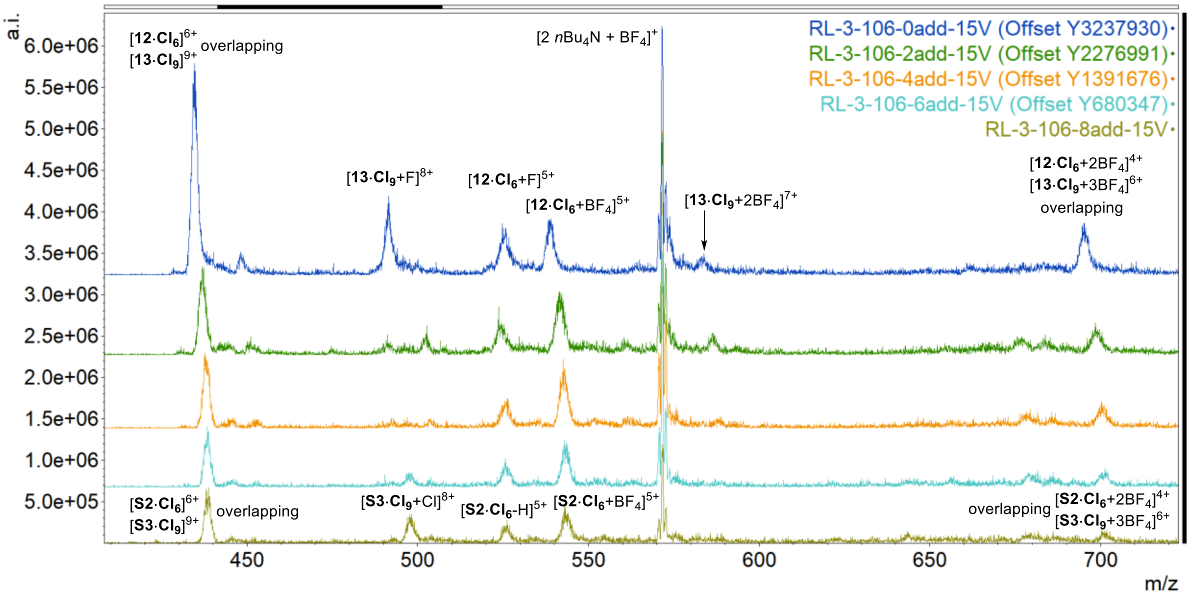

Figure S67. ESI-LRMS monitoring of the reduction of cages **12·Cl$_6$** and **13·Cl$_9$**. Full spectra showing that both [4+6] and [6+9] cages are reduced. Fluoride is suspected to originate from BF_4^- fragmentation in ESI-MS conditions.

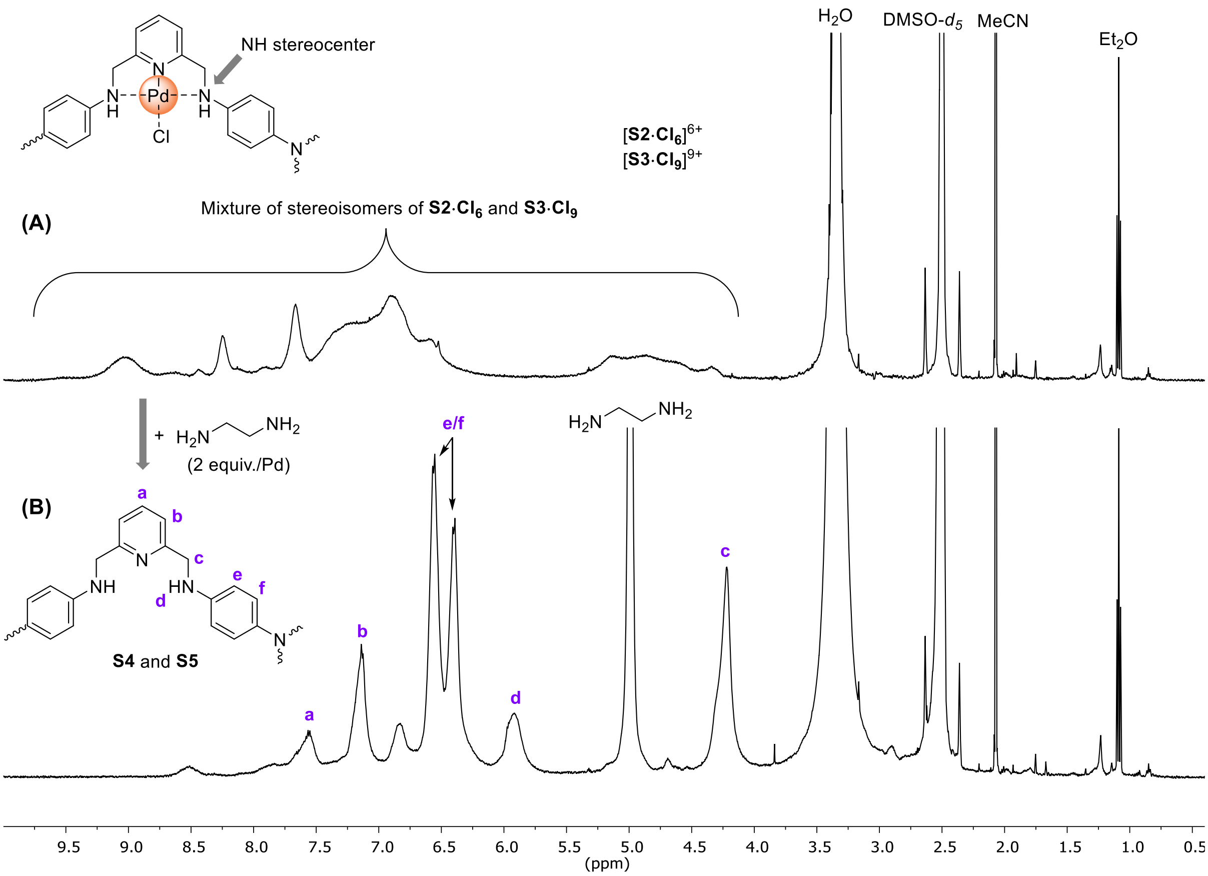

Figure S68. ^{1}H NMR spectra (500 MHz, DMSO-d_6, 298 K) of (A) the mixture of reduced cages **S2·Cl$_6$** and **S3·Cl$_9$**, and (B) after addition of ethylenediamine. The assignment proposed for **S4** and **S5** is based on expected chemical shifts and signals intensity. The broadening of the signals might be due to restricted conformational motion of the cages.

2. Anion binding by macrocycles 5 and 6

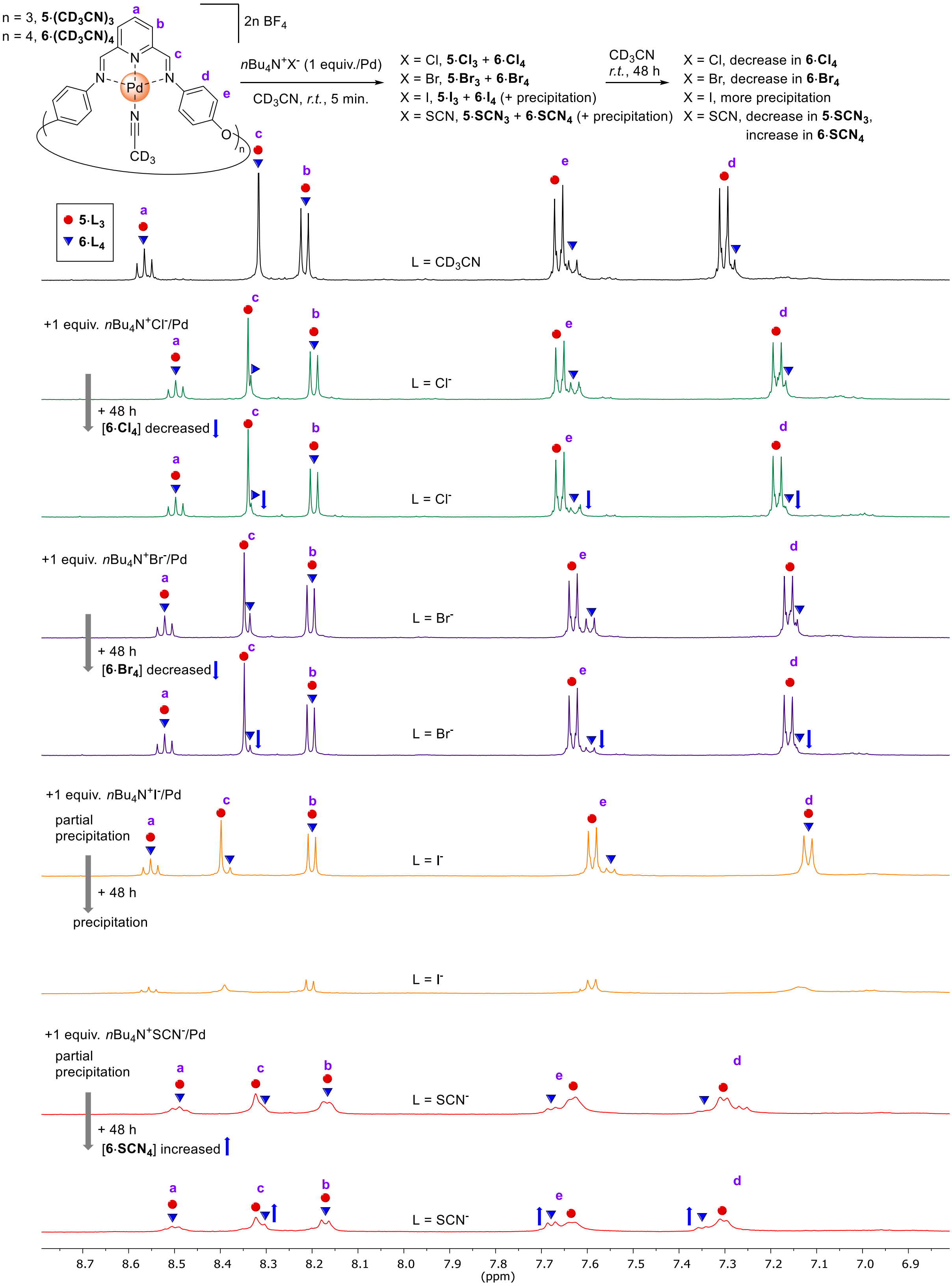

Figure S69. Effect of anions on macrocycles **5·(CD$_3$CN)$_3$** and **6·(CD$_3$CN)$_4$** analyzed by ^{1}H NMR spectroscopy (500 MHz, CD$_3$CN, 298 K).

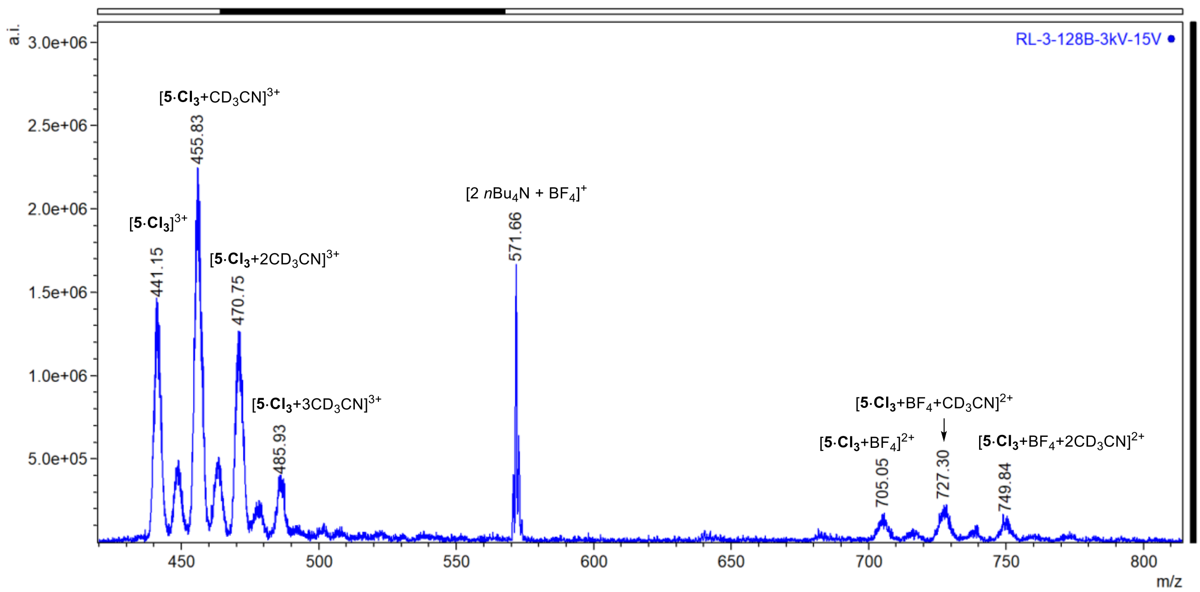

Figure S70. ESI-LRMS of **5·Cl₃** showing the different charge states corresponding to the loss of BF_4^- anions and solvent adduct peaks.

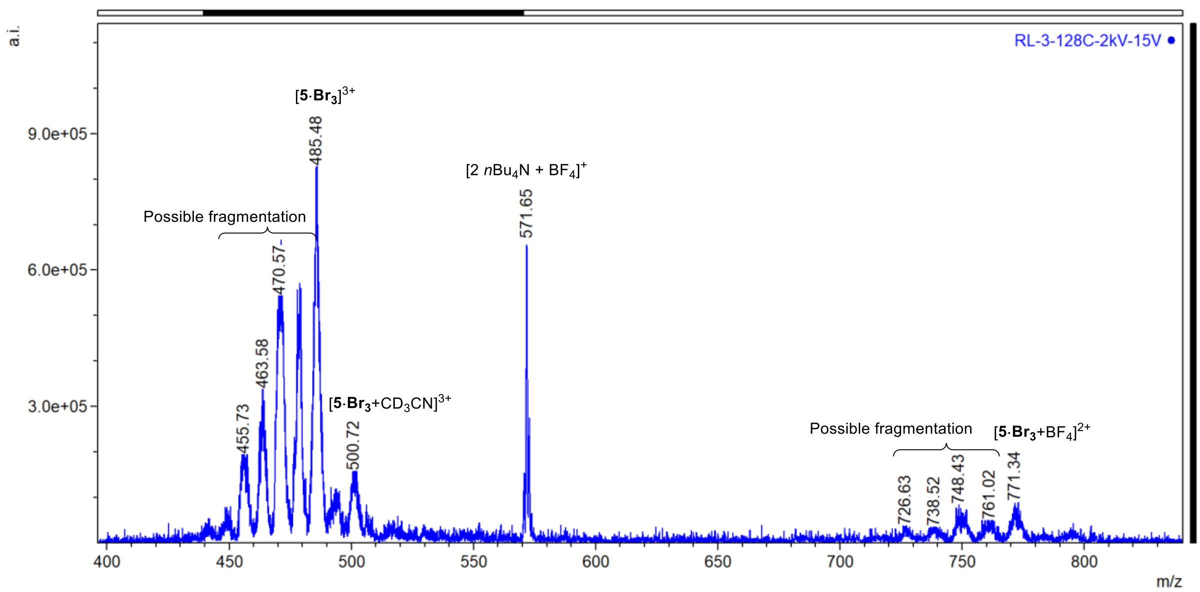

Figure S71. ESI-LRMS of **5·Br₃** showing the different charge states corresponding to the loss of BF_4^- anions, solvent adduct peak and peaks likely originating from fragmentation in ESI-MS conditions.

3. Anion binding by cages 12 and 13

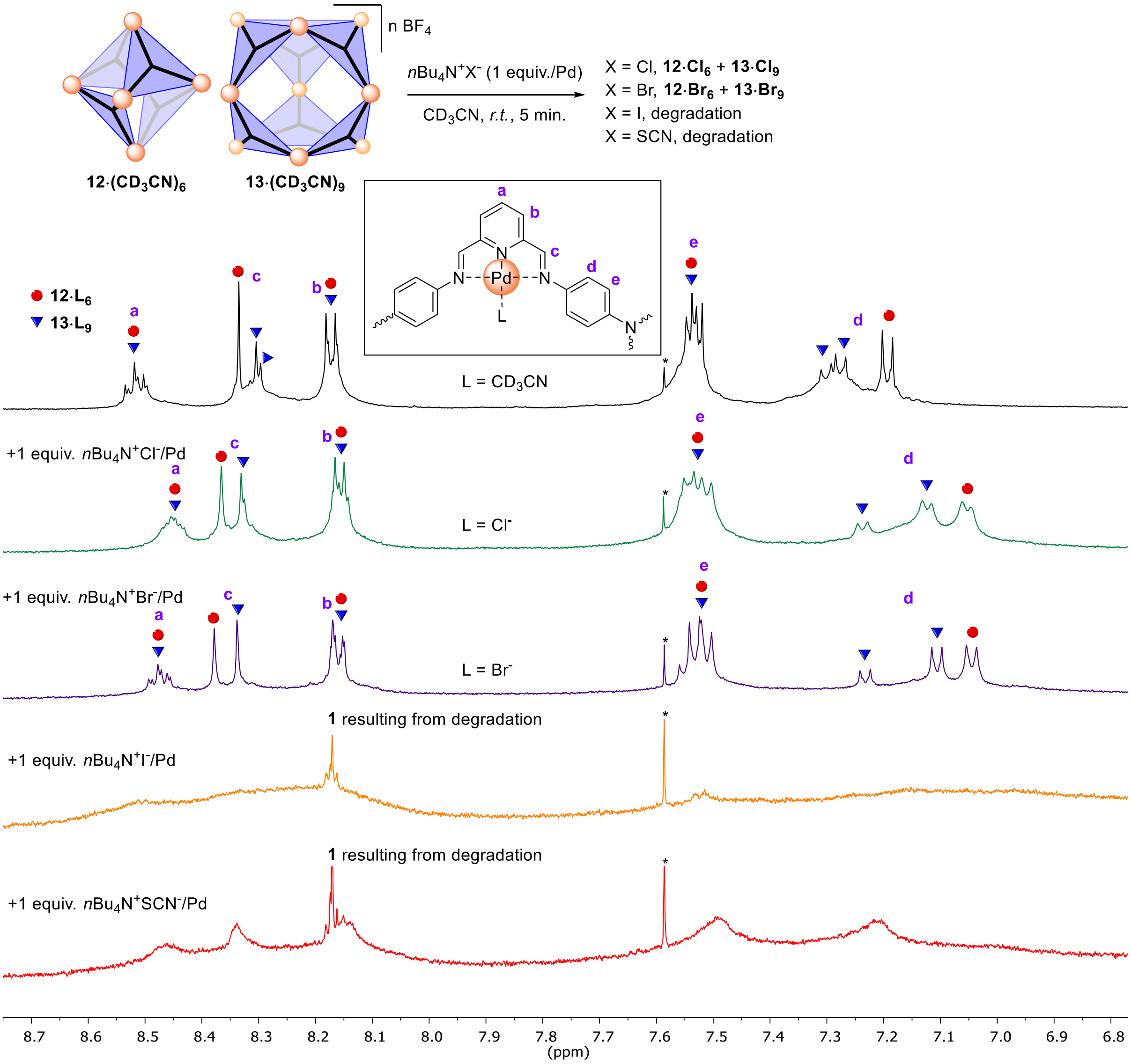

Figure S72. Effect of anions on cages **12·(CD$_3$CN)$_6$** and **13·(CD$_3$CN)$_9$** analyzed by ^{1}H NMR spectroscopy (500 MHz, CD$_3$CN, 298 K). Vertical scaling: x2 for Cl$^-$, x2 for Br$^-$, x5 for I$^-$, x5 for SCN$^-$. *trace of CHCl$_3$.

4. Cage assembly attempts with tris-anilines other than 11

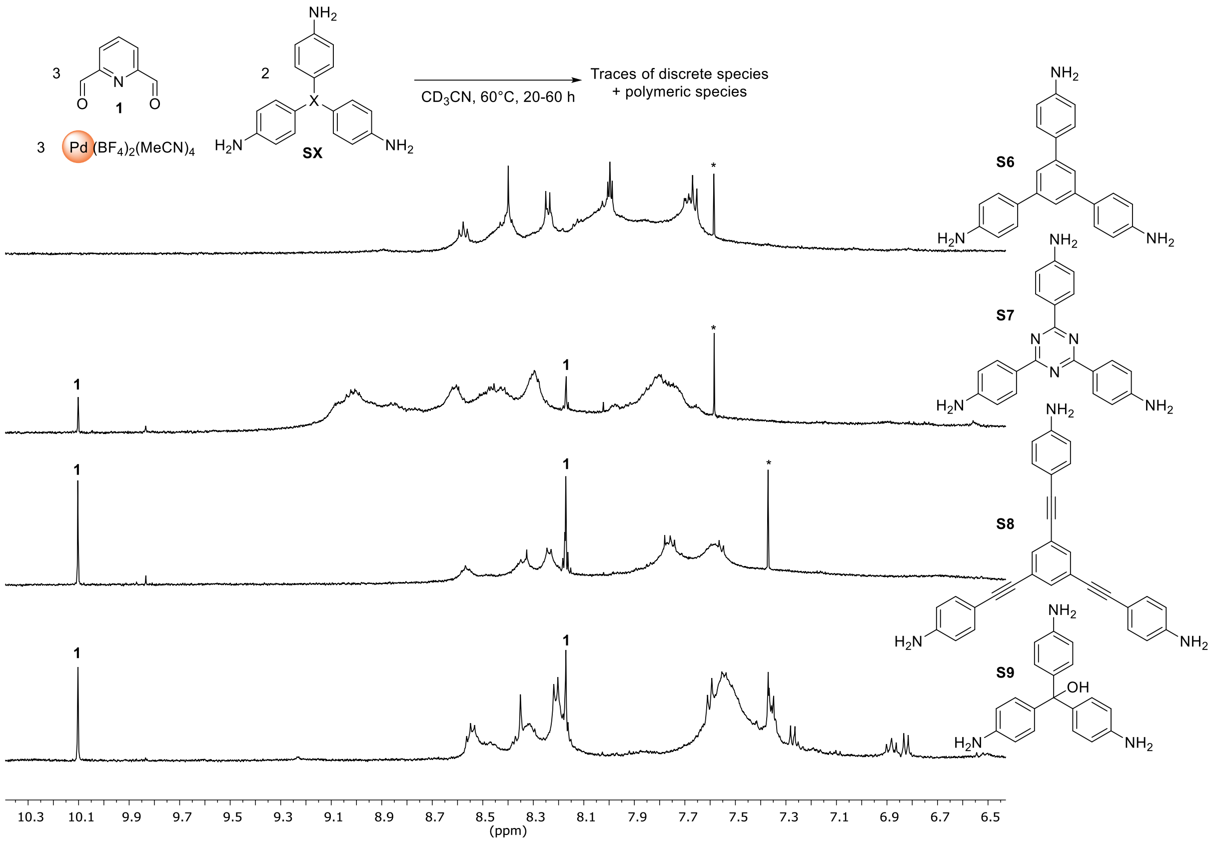

Figure S73. ^{1}H NMR spectra (500 MHz, CD_3CN, 298 K) of products from assembly of rigid tris-anilines with **1** and Pd(II). Sharp peaks are extremely small and only stand out because of the extreme broadening of signals for the main oligomeric products. Despite careful stoichiometry balance for the subcomponents, free **1** was observed in some cases which is suspected to originate from non-condensed anilines in the oligomeric species. For comparison purpose, the peaks of remaining **1** integrate for less than 10% of the original value (recorded before addition of Pd(II) and heating). *traces of solvents.

5. Aniline exchange

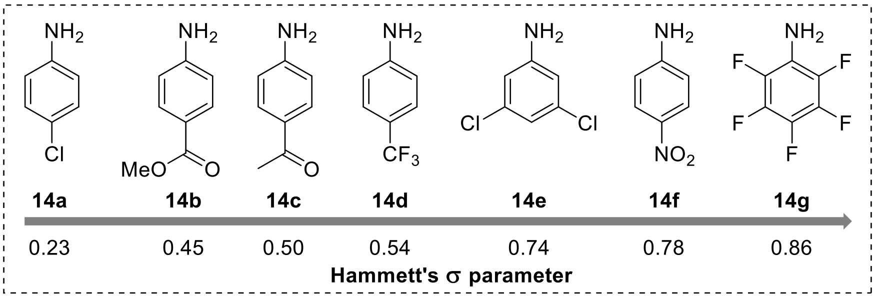

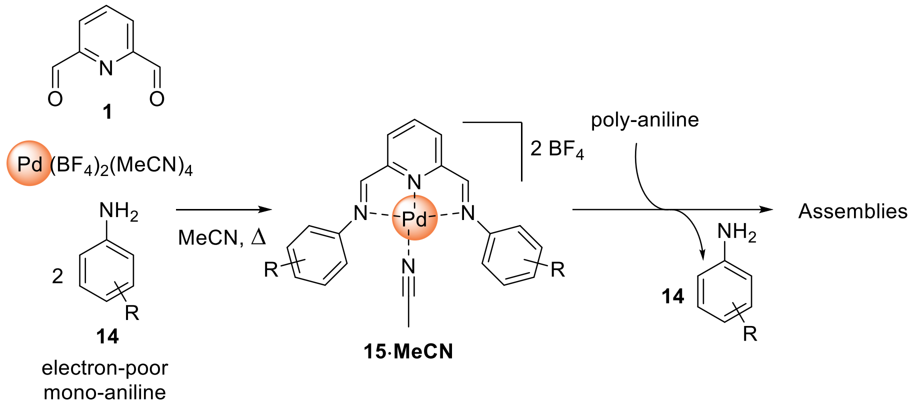

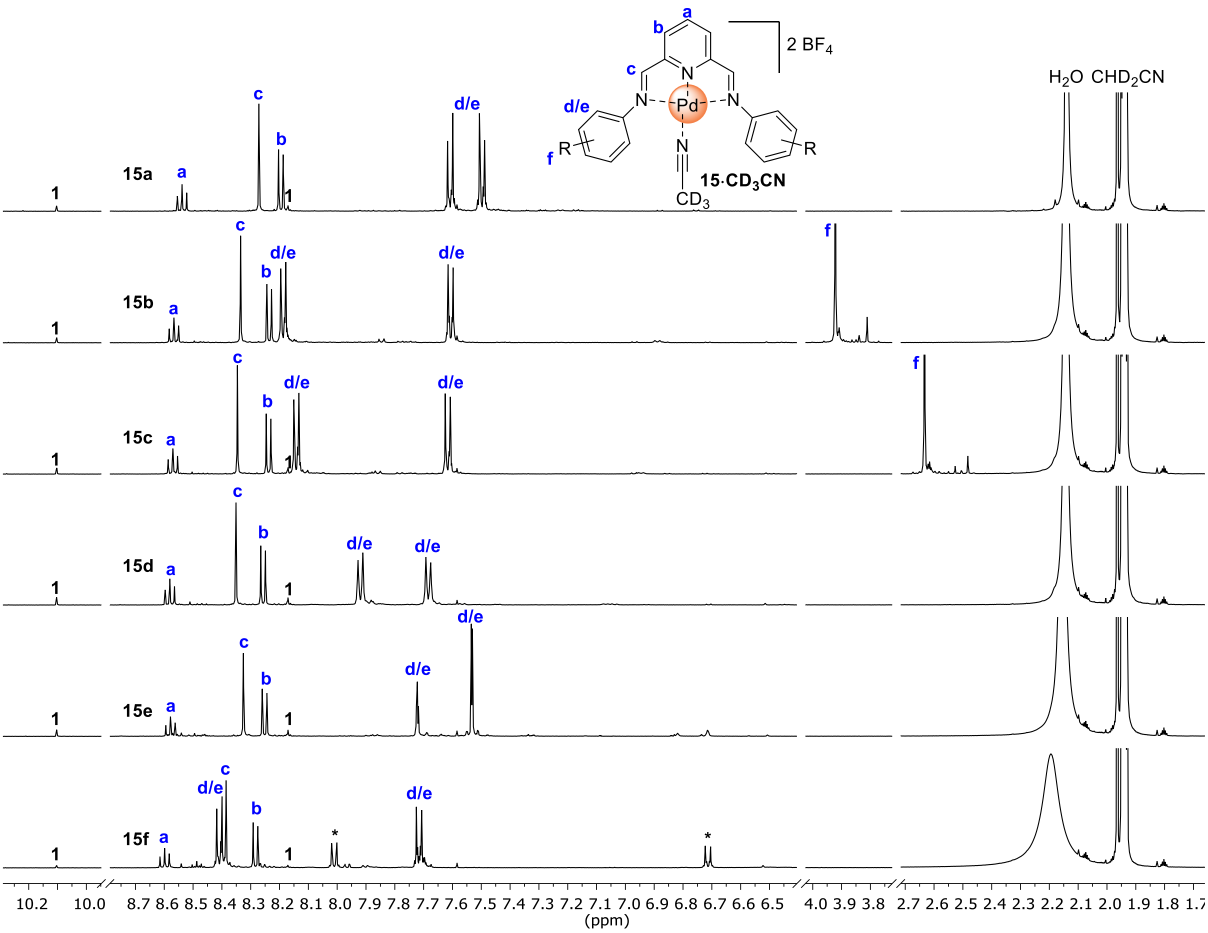

Figure S74. ^{1}H NMR spectra (500 MHz, CD_3CN, 298 K) of **15·CD₃CN** formed by heating reactants (**1**/**14**/Pd(II), 1:2:1 ratio) at 70°C for 14 h. Such reaction time is not necessary since completion was also observed after 1 h of heating in other experiments. * Unknown side product (δ close to **14f** signals).

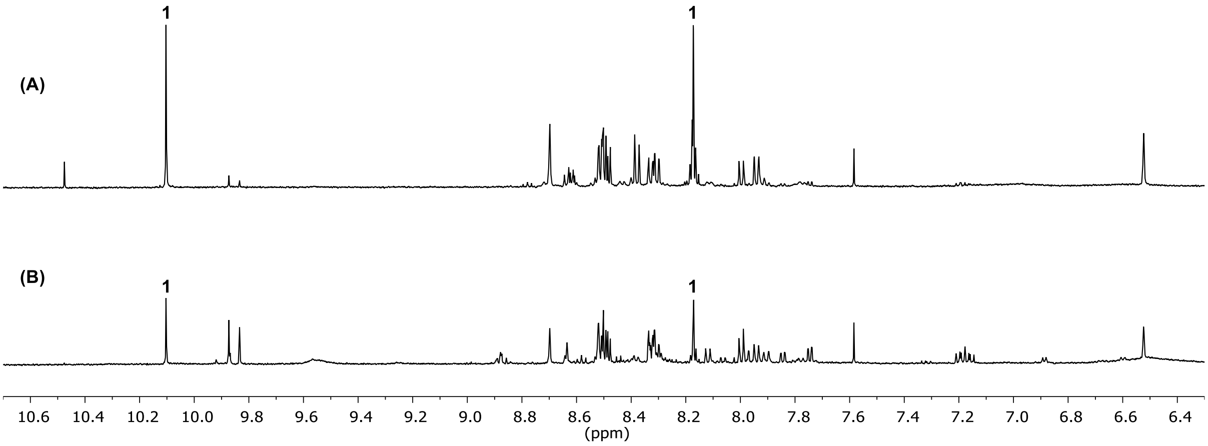

Figure S75. ^{1}H NMR spectra (500 MHz, CD_3CN, 298 K) of the heated mixture of **1**/**14g**/Pd(II) (1.0:2.2:1.0 ratio) at 70°C for (A) 2 h and (B) 24 h. Despite the excess of aniline **14g**, some unreacted **1** remains present and a complicated mixture of products is formed. Note that the failed clean formation of **15g** could result both from the low nucleophilicity of **14g** and from the bulkier *o*-fluorine substituents on **14g**.

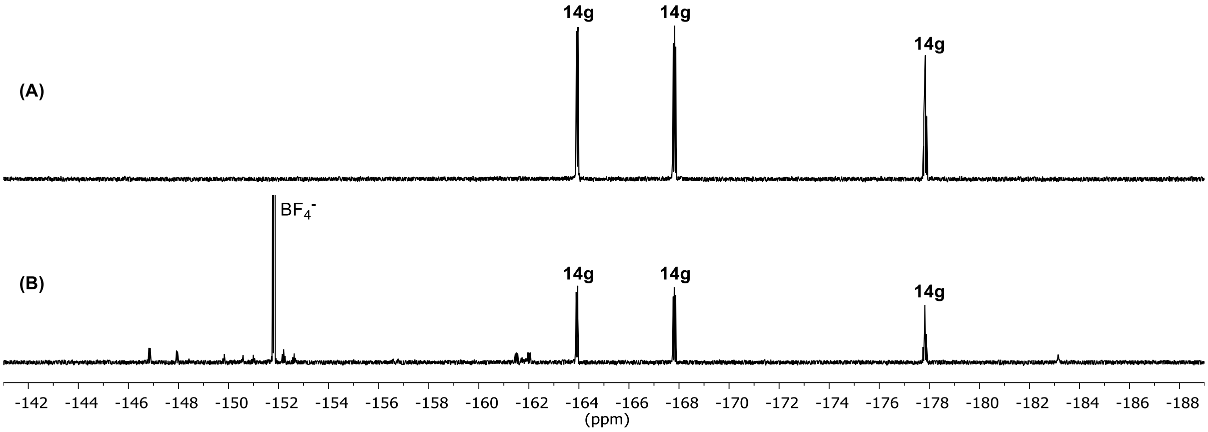

Figure S76. ^{19}F NMR spectra (376 MHz, CD_3CN, 298 K) of (A) **14g** and (B) the heated mixture of **1**/**14g**/Pd(II) (1.0:2.2:1.0 ratio) at 70°C for 2 h. Most starting material **14g** remains unreacted and a complicated mixture of products is formed. Note that the failed clean formation of **15g** could result both from the low nucleophilicity of **14g** and from the bulkier *o*-fluorine substituents on **14g**.

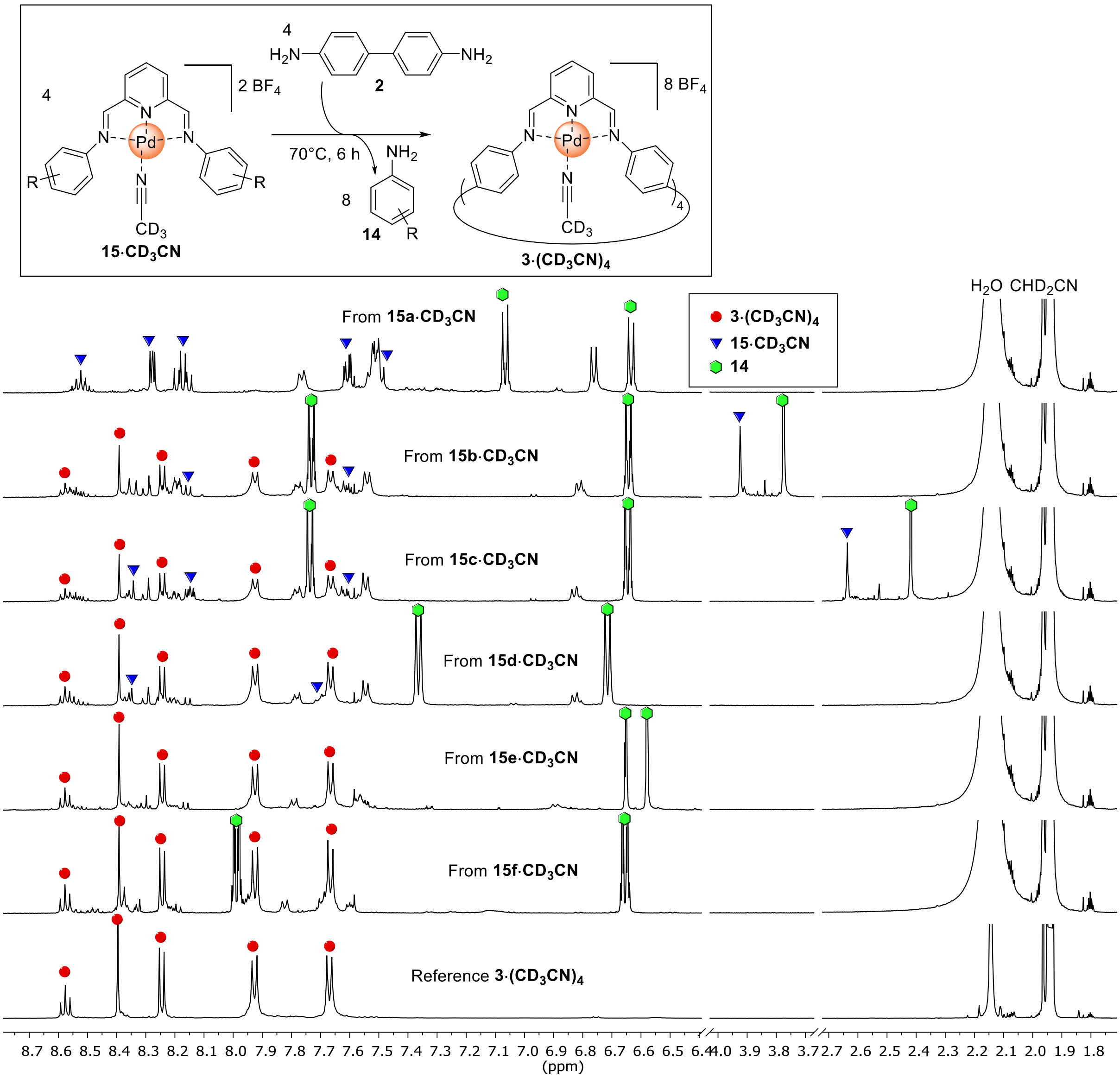

Figure S77. ^{1}H NMR spectra (500 MHz, CD_3CN, 298 K) showing the aniline exchange from mono-nuclear complexes **15·CD_3CN** to macrocycle **3·$(CD_3CN)_4$**. Non-assigned signals likely correspond to side products resulting from mixed anilines complexes. The most efficient exchanges are observed for **15e** and **15f** since all the starting material was consumed and minimal amount of side product was observed.

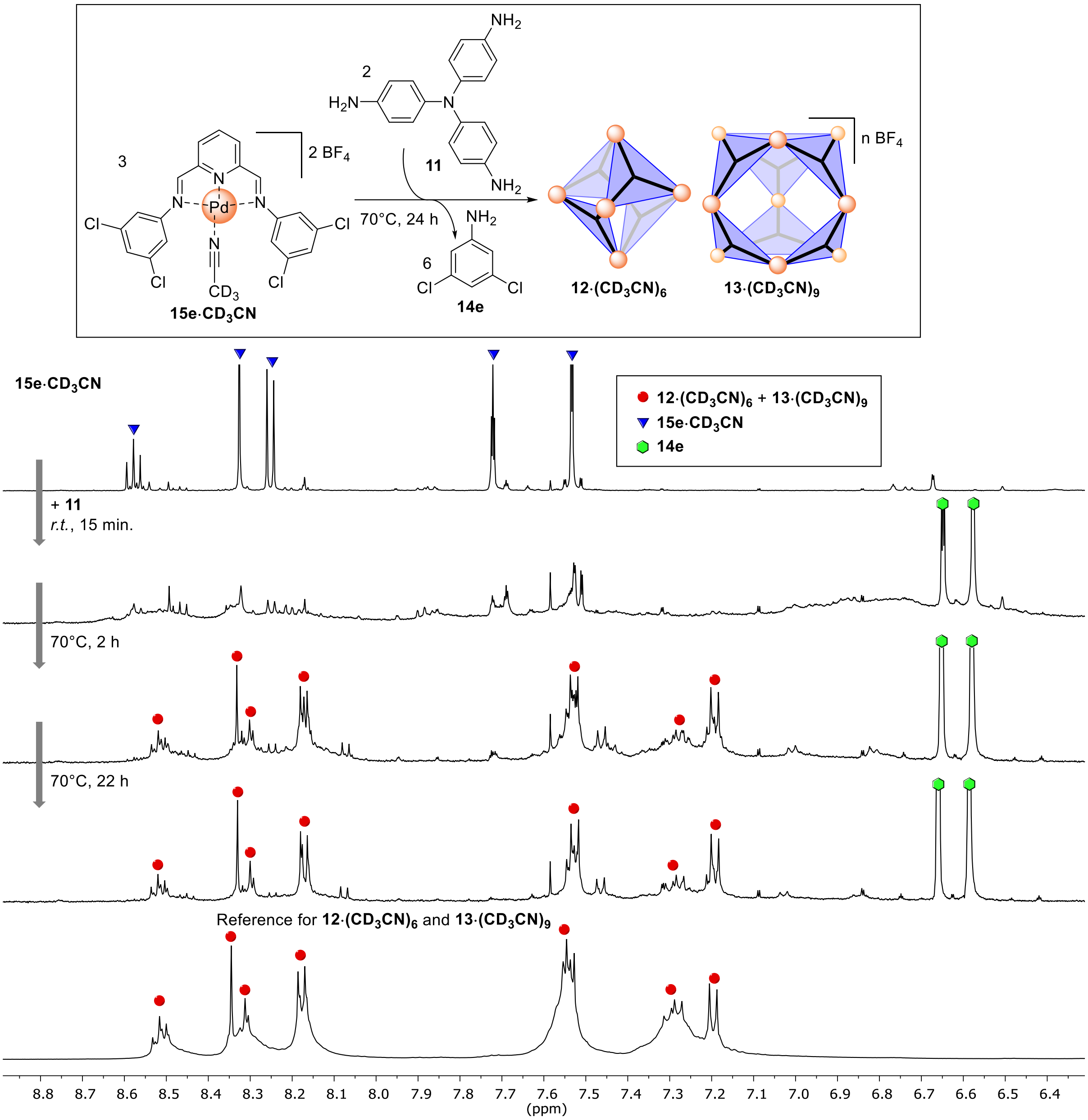

Figure S78. ^{1}H NMR spectra (500 MHz, CD_3CN, 298 K) showing different stages of the aniline exchange from mono-nuclear complex **15e·CD_3CN** to cages **12·$(CD_3CN)_6$** and **13·$(CD_3CN)_6$**. Non-assigned signals likely correspond to side products resulting from mixed anilines complexes. Top spectrum vertical scale divided by 4. The aniline exchange proceeds fast as shown by the large amount of **14e** released after 15 min. at *r.t.* and starting from **15e** leads almost cleanly to the desired cages contrary to **15f** (see Figure S79).

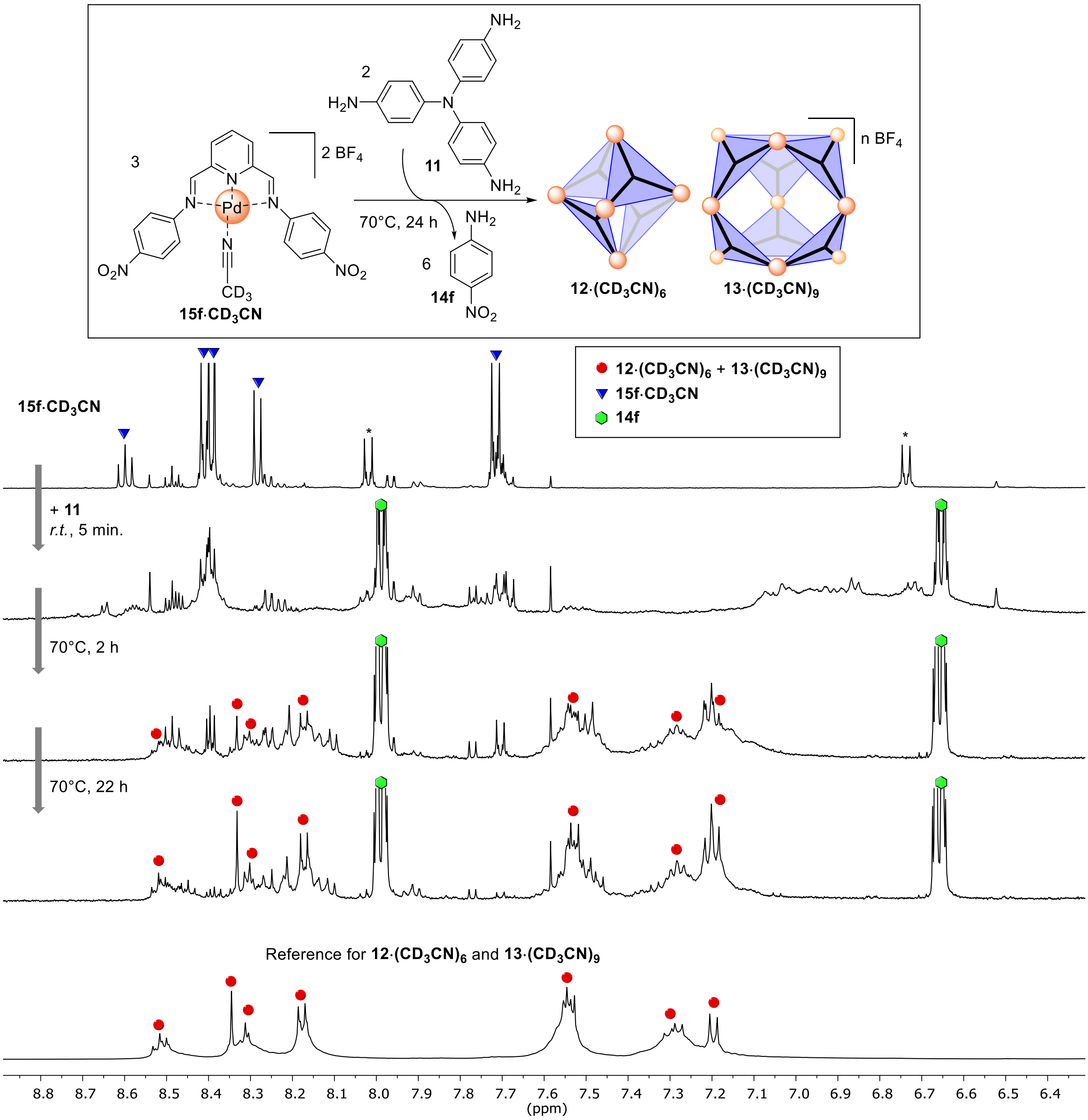

Figure S79. [1]H NMR spectra (500 MHz, CD_3CN, 298 K) showing different stages of the aniline exchange from mono-nuclear complex **15f·CD₃CN** to cages **12·(CD₃CN)₆** and **13·(CD₃CN)₆**. Non-assigned signals likely correspond to side products resulting from mixed anilines complexes. Top spectrum vertical scale divided by 4. The aniline exchange proceeds fast as shown by the large amount of **14f** released after 5 min. at *r.t.* but, in these conditions starting from **15f**, the cages are not cleanly formed.

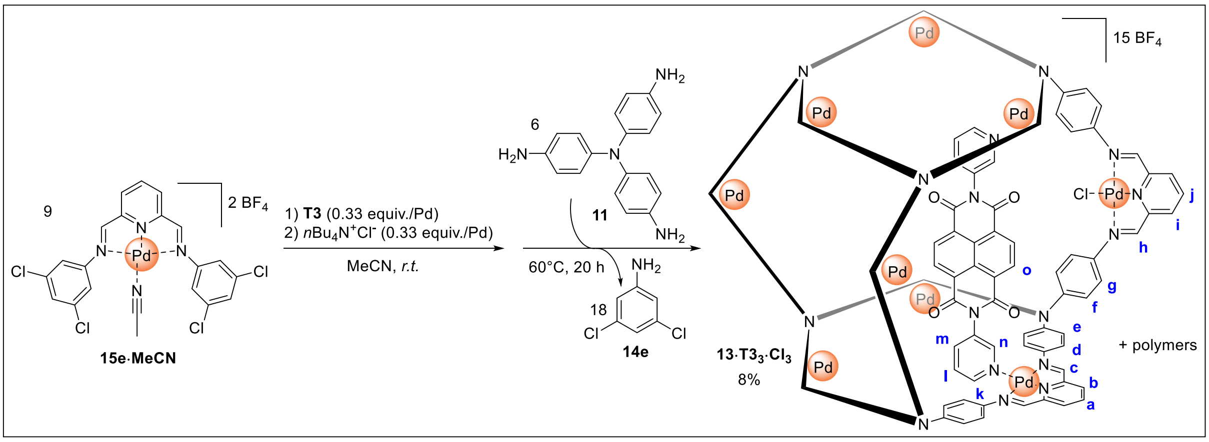

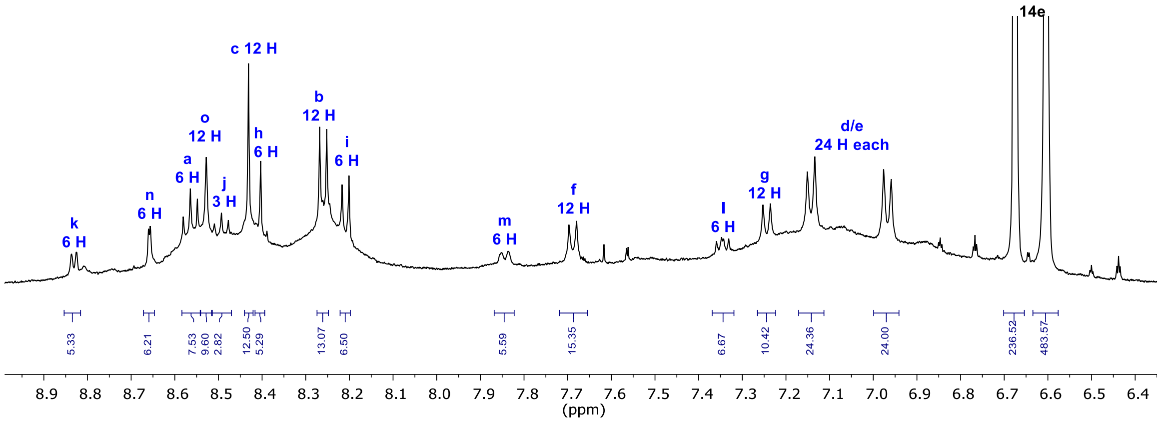

Figure S80. ^{1}H NMR spectrum (500 MHz, CD_3CN, 298 K) of the crude **13·T3₃·Cl₃** synthesized by aniline exchange from mono-nuclear complex **15e·MeCN**, template **T3** and chloride. The small deviation in integration of **13·T3₃·Cl₃** are likely caused by the broad signals overlapping with them despite linear correction of the integrals. Signals integral ratio between **13·T3₃·Cl₃** and **14e** indicate a yield of 8% for the desired cage. The rest of the side products are likely oligomeric species.

6. Potential cage formation from tetrakis-aniline building blocks

With a 90° divalent building block such as the bis(imino)pyridyl-Pd(II) studied herein and a planar tetravalent building block (90° between linkers), two symmetrical structures can be predicted (*i.e.* structures where all building blocks of the same type have the same role). These structures are either a [6+12] cuboctahedral cage or a linear planar polymer (Figure S81). The cage should be entropically favorable but the linear polymer can be favored if it is more favorable for the divalent and tetravalent building blocks to be in a same plane rather than perpendicular (which is the case in the cage structure).

We tested the assembly of **1**, Pd(II) and the tetrakis(4-aminophenyl)porphyrin subcomponent **S10** under typical assembly conditions (*i.e.* CD_3CN, 2 mM in Pd, 60°C) but ^1H NMR analysis only revealed extremely broadened signals likely corresponding to polymeric species and nothing was observed by ESI-MS analysis. This result suggests that polymeric species are favored.

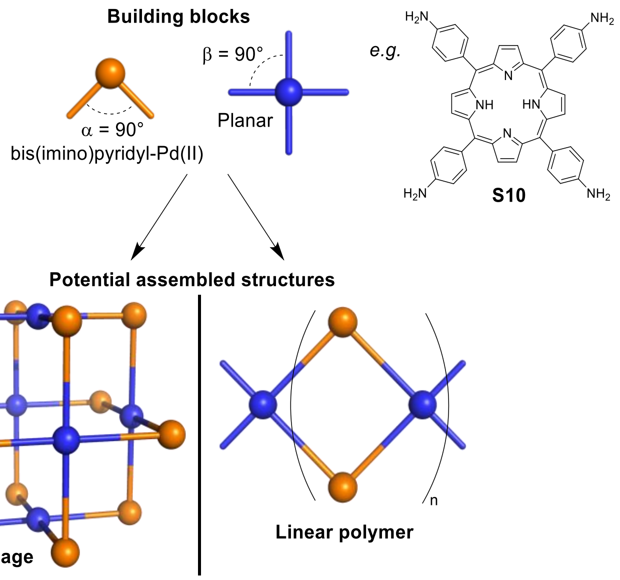

Figure S81. Potential symmetric structures resulting from the assembly of a divalent 90° bent and a tetravalent planar 90° building blocks.

The fact that polymeric species are favored from the self-assembly of **1** and **S10** building blocks can be put in parallel with the absence of report for the corresponding "classical" $Pd(II)_{12}$ coordination cage expected for the tetrakis-pyridyl ligand tetrakis(4-pyridyl)porphyrin while the capped linear oligomers, so-called "porphyrin tapes", were reported.[6] Indeed, aromatic rings stemming from porphyrin cores have a preferential out-of-plane orientation in regard to the porphyrin plane due to steric hindrance and such an orientation is expected to favor the linear polymer over the desired cage (see geometrical details in Figure S82). Other tetrakis-aniline compounds with different geometrical properties might lead to the expected Pd_{12} cage with bis(imino)pyridyl-Pd(II) building block but were not explored in the present study.

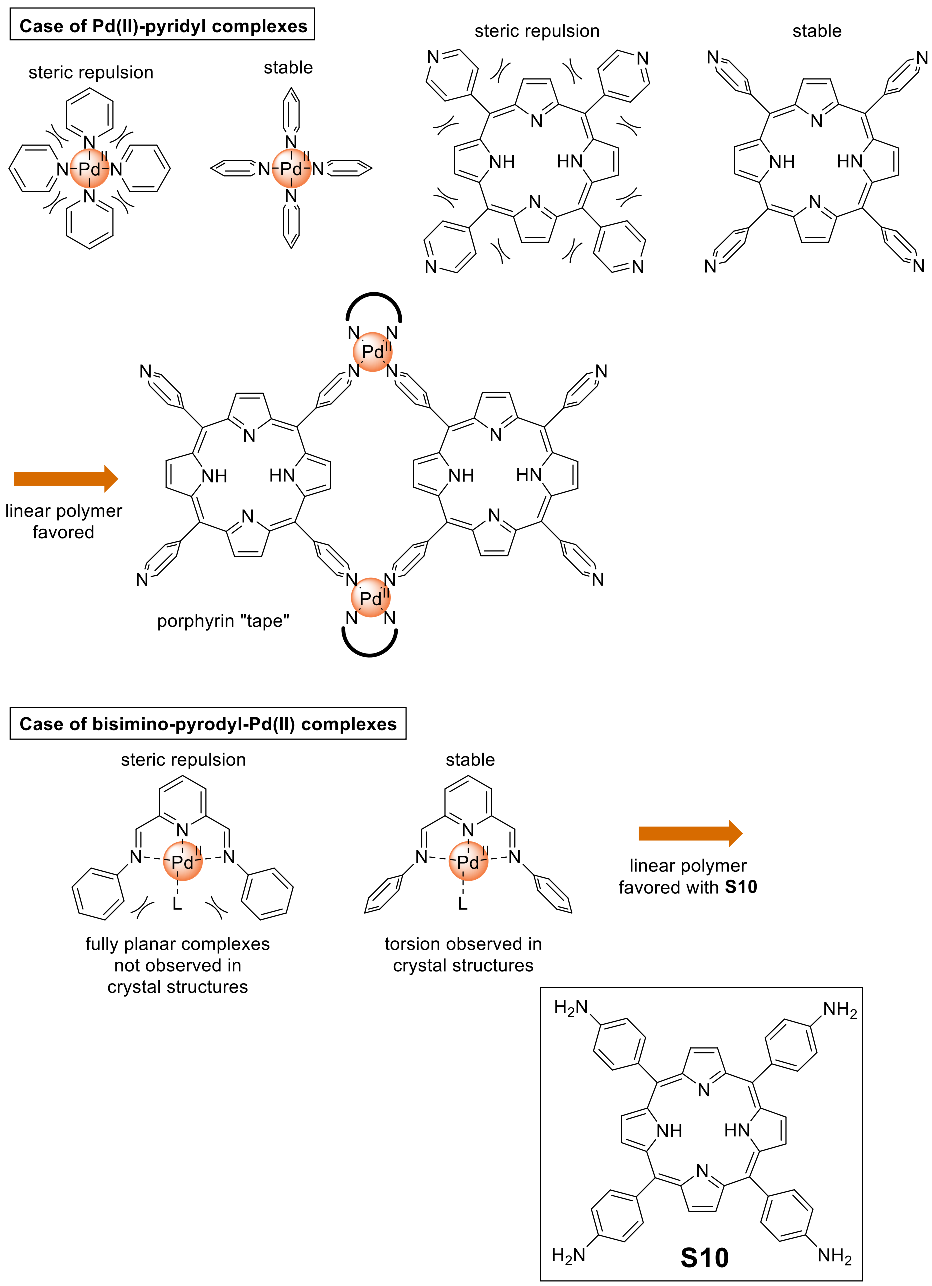

Figure S82. Geometrical constraints favoring linear polymers in Pd(II) complexes involving porphyrin as planar 90° tetravalent building blocks.

7. X-ray Crystallography

Data were collected at Beamline I19 of Diamond Light Source employing silicon double crystal monochromated synchrotron radiation (0.6889 Å) with ω and ψ scans at 100(2) K.[7] Data integration and reduction were undertaken with Xia2.[8] Subsequent computations were carried out using the WinGX-32 graphical user interface.[9] Multi-scan empirical absorption corrections were applied to the data using the AIMLESS[10] tool in the CCP4 suite.[11] The structures were solved by dual-space methods using SHELXT[12] then refined and extended with SHELXL.[13] In general, non-hydrogen atoms with occupancies greater than 0.5 were refined anisotropically. Carbon-bound hydrogen atoms were included in idealized positions and refined using a riding model. Disorder was modelled using standard crystallographic methods including constraints, restraints and rigid bodies where necessary. Crystallographic data along with specific details pertaining to the refinement follow. Crystallographic data have been deposited with the CCDC (1903235, 1903236 and 1903237).

7.1 [**3**]·8AsF_6·8MeCN·2H_2O

Formula $C_{92}H_{80}As_8F_{48}N_{20}O_2Pd_4$, *M* 3434.72, Monoclinic, space group C 2/c (#15), *a* 52.893(11), *b* 8.1609(16), *c* 38.856(8) Å, *β* 132.39(3)°, *V* 12388(6) Å^3, D_C 1.842 g cm^{-3}, *Z* 4, crystal size 0.050 by 0.050 by 0.050 mm, colour yellow, habit block, temperature 100(2) Kelvin, *λ*(Synchrotron) 0.6889 Å, *μ*(Synchrotron) 2.580 mm^{-1}, $T(\text{Analytical})_{min,max}$ 0.987469601804, 1.0, $2\vartheta_{max}$ 41.60, *hkl* range -54 54, -8 8, -40 39, *N* 31246, N_{ind} 7104(R_{merge} 0.1255), N_{obs} 4456(I > 2σ(I)), N_{var} 912, residuals* *R*1(*F*) 0.0772, $wR2(F^2)$ 0.2137, GoF(all) 0.956, $\Delta\rho_{min,max}$ -0.620, 1.154 e$^-$ Å^{-3}.

*$R1 = \Sigma||F_o| - |F_c||/\Sigma|F_o|$ for $F_o > 2\sigma(F_o)$; $wR2 = (\Sigma w(F_o^2 - F_c^2)^2/\Sigma(wF_c^2)^2)^{1/2}$ all reflections

$w=1/[\sigma^2(F_o^2)+(0.1429P)^2]$ where $P=(F_o^2+2F_c^2)/3$

Specific refinement details:

The crystals of [**3**]·8AsF_6·4MeCN·2H_2O were grown by diffusion at *r.t.* of *i*Pr_2O into an acetonitrile solution of [**3·(MeCN)$_4$**]·8BF_4 (0.5 mM) containing excess $K^+AsF_6^-$ (*ca.* 20 mM). The crystals employed immediately lost solvent after removal from the mother liquor and rapid handling prior to flash cooling in the cryostream was required to collect data. Despite these measures and the use of synchrotron radiation few reflections at greater than 0.97 Å resolution were observed. The asymmetric unit was found to contain one half of a **3·(MeCN)$_4$** assembly and associated counterions and solvent molecules. The hydrogen atoms of the half occupancy water molecules could not be located in the electron density map and were not included in the model.

The anions within the structure show evidence of significant disorder. The four anions (per asymmetric unit) were modelled as disordered over five lattice sites, one of which shows additional disorder of the fluorine atoms. Bond length and thermal parameter restraints were applied to facilitate a reasonable refinement of the disordered AsF_6^- anions. Even with these restraints some thermal parameters remain larger than ideal as a consequence of the high level of thermal motion or minor unresolved disorder of the anions and solvent molecules.

CheckCIF gives three A and fifteen B level alerts. These alerts (both A and B level) result from the limited data resolution, water molecules for which hydrogens were not modelled and thermal motion and/or unresolved disorder of some anions and solvent molecules as described above.

7.2 [$\mathbf{5_2{\cdot}T3_3}$]·11SbF_6·BF_4·7.75(C_6H_6)·5.25MeCN·H_2O [+ solvent]

Formula $C_{243}H_{178.25}BF_{70}N_{35.25}O_{19}Pd_6Sb_{11}$, *M* 7214.41, Triclinic, space group P -1 (#2), *a* 21.9773(8), *b* 22.3335(5), *c* 34.7471(9) Å, *α* 107.703(2)°, *β* 91.695(3)°, *γ* 116.031(2)°, *V* 14331.9(8) Å^3, D_c 1.672 g cm^{-3}, *Z* 2, crystal size 0.030 by 0.010 by 0.010 mm, colour yellow, habit needle, temperature 100(2) Kelvin, *λ*(Synchrotron) 0.6889 Å, *μ*(Synchrotron) 1.352 mm^{-1}, *T*(Analytical)$_{min,max}$ 0.975800029642, 1.0, 2ϑ_{max} 48.49, *hkl* range -26 25, -26 26, -41 41, *N* 133023, N_{ind} 48807(R_{merge} 0.0662), N_{obs} 27009(I > 2σ(I)), N_{var} 3893, residuals* *R*1(*F*) 0.0899, *wR*2(F^2) 0.3145, GoF(all) 1.054, $\Delta\rho_{min,max}$ -0.983, 1.490 e$^-$ Å^{-3}.

*$R1 = \Sigma||F_o| - |F_c||/\Sigma|F_o|$ for $F_o > 2\sigma(F_o)$; $wR2 = (\Sigma w(F_o^2 - F_c^2)^2/\Sigma(wF_c^2)^2)^{1/2}$ all reflections

$w=1/[\sigma^2(F_o^2)+(0.2000P)^2]$ where $P=(F_o^2+2F_c^2)/3$

Specific refinement details:

The crystals of [$\mathbf{5_2{\cdot}T3_3}$]·11SbF_6·BF_4·7.75(C_6H_6)·5.25MeCN·H_2O were grown by diffusion of benzene into an acetonitrile solution of [$\mathbf{5_2{\cdot}T3_3}$]·12BF_4 (0.17 mM) containing excess $K^+SbF_6^-$ (*ca.* 20 mM). The crystals employed immediately lost solvent after removal from the mother liquor and rapid handling prior to flash cooling in the cryostream was required to collect data. Data were obtained to 0.84 Å resolution. The asymmetric unit was found to contain one complete $\mathbf{5_2{\cdot}T3_3}$ assembly and associated counterions and solvent molecules. The structure shows evidence of a significant amount of thermal motion throughout. Therefore, bond lengths and angles within pairs of chemically identical organic ligands were restrained to be similar to each other and thermal parameter restraints (SIMU, RIGU) were applied to all atoms except for palladium and antimony.

The anions and solvent molecules within the structure show evidence of substantial disorder. The 11 SbF_6^- anions were modelled as disordered over 14 lattice sites. Nine of these lattice sites were further disordered over two or three positions. The occupancies of the disordered anions were allowed to refine freely and then fixed at the obtained values. Some additional minor occupancy positions of the anions could not be located in the electron density map and were not included in the model resulting in a discrepancy of 0.85 counterions per $\mathbf{5_2{\cdot}T3_3}$ assembly which were included as SbF_6^- in the formula. Some lower occupancy disordered atoms were modelled with isotropic thermal parameters and bond length and thermal parameter restraints were applied to facilitate realistic modelling of the disordered SbF_6^- anions. The content of the cavity was modelled as one BF_4^- anion disordered over three locations and one disordered water molecule. The disordered BF_4^- anion was restrained to have an idealized tetrahedral geometry and modelled with isotropic thermal parameters. Most acetonitrile solvent molecules were also modelled as disordered over two or more locations with bond length and thermal parameter restraints applied to ensure a reasonable refinement. Benzene solvent molecules were modelled as rigid groups (AFIX 66). The hydrogen atoms of the disordered water and acetonitrile molecules could not be located in the electron density map and were not included in the model.

The SQUEEZE[14] function of PLATON[15] was employed to account for a small quantity of highly disordered solvent, which gave a potential solvent accessible void of 401 Å^3 per unit cell (a total of approximately 116 electrons). Since the identity of these diffuse solvent molecules could not be assigned conclusively they were not included in the formula. Consequently, the molecular weight and density given above are likely to be slightly underestimated.

CheckCIF gives sixteen B level alerts. These alerts all result from thermal motion and/or unresolved disorder, especially of the anions and solvent molecules as described above.

7.3 [**12·Cl$_6$**]·6(AsF_6)·4C_6H_6 [+ solvent]

Formula $C_{138}H_{102}As_6Cl_6F_{36}N_{22}Pd_6$, *M* 4053.03, Orthorhombic, space group C m c m (#63), *a* 21.948(4), *b* 30.273(6), *c* 31.103(6) Å, *V* 20666(7) Å^3, D_c 1.303 g cm^{-3}, *Z* 4, crystal size 0.020 by 0.020 by 0.020 mm, colour dark brown, habit block, temperature 100(2) Kelvin, λ(Synchrotron) 0.6889 Å, μ(Synchrotron) 1.477 mm^{-1}, T(Analytical)$_{min,max}$ 0.991036337712, 1.0, $2\vartheta_{max}$ 34.86, *hkl* range -19 19, -25 26, -27 27, *N* 22836, N_{ind} 3798(R_{merge} 0.0490), N_{obs} 2179(I > 2σ(I)), N_{var} 589, residuals* $R1(F)$ 0.1278, $wR2(F^2)$ 0.3485, GoF(all) 1.074, $\Delta\rho_{min,max}$ -0.446, 1.105e$^-$ Å^{-3}.

*$R1 = \Sigma||F_o| - |F_c||/\Sigma|F_o|$ for $F_o > 2\sigma(F_o)$; $wR2 = (\Sigma w(F_o^2 - F_c^2)^2/\Sigma(wF_c^2)^2)^{1/2}$ all reflections

$w=1/[\sigma^2(F_o^2)+(0.2000P)^2+150.0000P]$ where $P=(F_o^2+2F_c^2)/3$

Specific refinement details:

The crystals of [**12·Cl$_6$**]·6(AsF_6)·4C_6H_6 were grown by diffusion of benzene into an acetonitrile solution of [**12·(MeCN)$_6$**]·12BF_4 and [**13·(MeCN)$_9$**]·18BF_4 (0.75 mM in Pd) containing nBu$_4$N$^+$Cl$^-$ (0.75 mM, 1 equiv./Pd) and excess $K^+AsF_6^-$ (*ca.* 7.5 mM). The crystals employed immediately lost solvent after removal from the mother liquor and rapid handling prior to flash cooling in the cryostream was required to collect data. The diffraction pattern was extremely broad and diffuse and few reflections were observed at better than 1.15 Å resolution despite the use of synchrotron radiation. As a result of the poorly diffracting ability of the crystals, the quality of the integration was also poor. Despite these limitations the quality of the data is more than sufficient to establish the connectivity of the structure. The asymmetric unit was found to contain one fourth of a **12·Cl$_6$** assembly and associated counterions and solvent molecules.

Due to the less than ideal resolution, extensive thermal parameter and bond length restraints were required to facilitate realistic modelling for the organic parts of the structure. The GRADE program[16] was employed using the GRADE Web Server[17] to generate a full set of bond distance and angle restraints (DFIX, DANG, FLAT) for the organic ligands. Two ligand phenyl rings were modelled as disordered over two equal occupancy locations and the remaining phenyl rings were all disordered around special positions by symmetry. The disordered atoms were modelled with isotropic thermal parameters. One benzene solvent molecule was modelled as a rigid group (AFIX 66) with partial occupancy. Thermal parameter restraints (SIMU, RIGU) were applied to all atoms except for palladium, arsenic and chlorine. Even with these restraints some thermal parameters remain larger than ideal as a consequence of the high level of thermal motion or minor unresolved disorder present throughout the structure.

The anions within the structure show evidence of significant disorder. One AsF_6^- anion was modelled as disordered over two locations and another anion was modelled with partial occupancy. The occupancies of the disordered anions were freely refined and then fixed at the obtained values. Some lower occupancy disordered atoms were modelled with isotropic thermal parameters and bond length and thermal parameter restraints were applied to facilitate realistic modelling of the disordered AsF_6^- anions. Further reflecting the solvent loss and poor diffraction properties there is a significant amount of void volume in the lattice containing smeared electron density from disordered solvent. Consequently the SQUEEZE[14] function of PLATON[15] was employed to remove the contribution of the electron density associated with this highly disordered solvent. This gave a potential solvent accessible void of 5668.6 Å^3 per unit cell (a total of approximately 853 electrons). Since the identity of the diffuse solvent molecules could not be assigned conclusively to acetonitrile or benzene, they were not included in the formula. Consequently, the molecular weight and density given above are likely to be slightly underestimated.

CheckCIF gives one A and five B level alerts. These alerts (both A and B level) all result from the limited data resolution, and thermal motion and/or unresolved disorder of some anions and solvent molecules as described above.

7.4 Calculation of angle α

The angle α defined in Figure S83 and referred in the manuscript is calculated (in degrees °) through formula (1) where *x*, *y* and *z* are the Cartesian coordinates of atoms a, b, c and d.

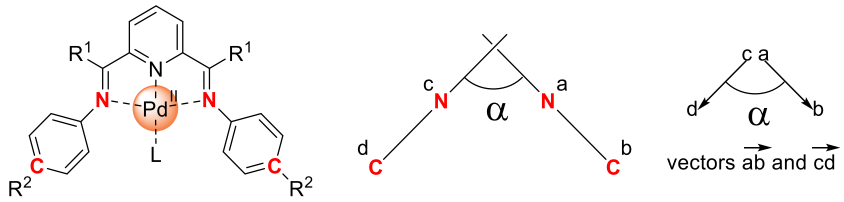

Figure S83. Definition of angle α.

$$\alpha = \frac{180}{\pi} \times \arccos \frac{(x_b - x_a)(x_d - x_c) + (y_b - y_a)(y_d - y_c) + (z_b - z_a)(z_d - z_c)}{\sqrt{[(x_b - x_a)^2 + (y_b - y_a)^2 + (z_b - z_a)^2] \times [(x_d - x_c)^2 + (y_d - y_c)^2 + (z_d - z_c)^2]}} \qquad (1)$$

8. Modelling

Geometry optimized structures were modelled with semi-empirical methods using PM3 or PM6 models on SCIGRESS software (Fujitsu Limited, Tokyo, Japan, 2013) version FJ 2.6 (EU 3.1.9) Build 5996.8255.20141202. The Cartesian coordinates given below can be pasted in a text file with .xyz extension.

Table S2. Cartesian coordinates (in Å) for the PM6 geometry optimized model of **5·T1-cone**.

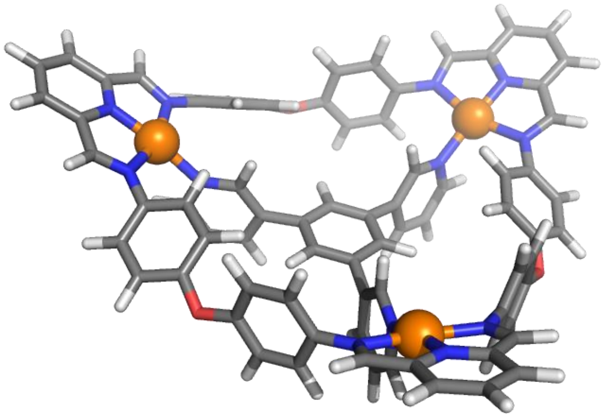

C	6.580000	15.848000	-8.826000	C	8.004000	15.334000	-12.945000
C	6.857000	16.184000	-7.483000	C	7.703000	15.677000	-11.626000
C	6.018000	17.072000	-6.826000	H	7.801000	12.541000	-10.211000
C	4.901000	17.614000	-7.506000	H	8.313000	11.926000	-12.588000
C	4.648000	17.279000	-8.849000	H	8.105000	16.124000	-13.696000
C	5.488000	16.388000	-9.519000	H	7.601000	16.727000	-11.338000
H	7.732000	15.744000	-6.981000	C	8.256000	12.606000	-18.485000
H	6.223000	17.339000	-5.783000	C	9.319000	12.714000	-19.400000
H	3.802000	17.733000	-9.372000	C	10.535000	13.252000	-18.945000
H	5.298000	16.131000	-10.558000	C	10.696000	13.676000	-17.615000
C	0.907000	20.626000	-5.556000	C	9.602000	13.550000	-16.739000
C	1.000000	21.749000	-4.713000	N	8.428000	13.031000	-17.200000
C	2.277000	22.196000	-4.338000	C	9.512000	13.917000	-15.298000
C	3.439000	21.538000	-4.776000	N	8.404000	13.608000	-14.669000
C	3.295000	20.421000	-5.618000	C	6.883000	12.071000	-18.708000
N	2.047000	20.022000	-6.002000	N	6.096000	11.984000	-17.663000
C	4.356000	19.544000	-6.184000	H	9.214000	12.381000	-20.444000
N	3.965000	18.501000	-6.877000	H	11.385000	13.341000	-19.648000
C	-0.315000	19.944000	-6.061000	H	11.659000	14.089000	-17.274000
N	-0.140000	18.853000	-6.768000	H	10.390000	14.434000	-14.859000
H	0.099000	22.266000	-4.348000	H	6.622000	11.786000	-19.747000
H	2.370000	23.080000	-3.678000	C	2.090000	10.718000	-17.889000
H	4.432000	21.891000	-4.458000	C	2.441000	11.930000	-18.494000
H	5.404000	19.844000	-5.986000	C	3.777000	12.336000	-18.449000
H	-1.287000	20.413000	-5.810000	C	4.729000	11.541000	-17.786000
C	-3.222000	16.628000	-8.557000	C	4.363000	10.313000	-17.197000
C	-2.126000	17.044000	-9.325000	C	3.037000	9.897000	-17.245000
C	-1.129000	17.800000	-8.707000	H	1.703000	12.522000	-19.043000
C	-1.237000	18.129000	-7.344000	H	4.072000	13.268000	-18.941000
C	-2.364000	17.725000	-6.590000	H	5.118000	9.676000	-16.728000
C	-3.357000	16.968000	-7.194000	H	2.726000	8.929000	-16.836000
H	-2.051000	16.794000	-10.381000	Pd	7.016000	12.683000	-15.923000
H	-0.271000	18.154000	-9.285000	C	-0.334000	10.890000	-17.882000
H	-2.459000	17.997000	-5.532000	C	-0.442000	12.138000	-17.250000
H	-4.245000	16.634000	-6.635000	C	-1.708000	12.712000	-17.125000
Pd	1.878000	18.363000	-6.990000	C	-2.841000	12.042000	-17.623000
C	7.610000	14.654000	-10.674000	C	-2.711000	10.794000	-18.276000
C	7.823000	13.301000	-11.002000	C	-1.458000	10.212000	-18.402000
C	8.115000	12.967000	-12.319000	H	0.436000	12.655000	-16.872000
C	8.185000	13.983000	-13.295000	H	-1.819000	13.694000	-16.655000

H	-3.590000	10.277000	-18.677000	C	-1.692000	11.221000	-12.612000
H	-1.324000	9.241000	-18.901000	C	-1.264000	12.513000	-12.975000
C	-7.156000	14.884000	-16.209000	C	0.045000	12.977000	-12.446000
C	-8.303000	15.170000	-16.970000	C	0.115000	13.705000	-11.249000
C	-8.378000	14.662000	-18.278000	C	1.364000	13.966000	-10.660000
C	-7.343000	13.882000	-18.819000	C	2.542000	13.528000	-11.286000
C	-6.213000	13.627000	-18.020000	C	2.470000	12.800000	-12.483000
N	-6.149000	14.145000	-16.760000	C	1.224000	12.541000	-13.073000
C	-4.993000	12.842000	-18.357000	C	3.688000	12.154000	-13.037000
N	-4.102000	12.690000	-17.406000	C	4.511000	12.741000	-14.019000
C	-6.855000	15.265000	-14.801000	N	5.612000	12.103000	-14.513000
N	-5.762000	14.774000	-14.268000	C	5.922000	10.858000	-14.040000
H	-9.130000	15.770000	-16.557000	C	5.149000	10.220000	-13.061000
H	-9.275000	14.875000	-18.892000	C	4.024000	10.874000	-12.555000
H	-7.424000	13.480000	-19.841000	C	1.435000	14.555000	-9.297000
H	-4.915000	12.463000	-19.395000	C	1.595000	15.930000	-9.046000
H	-7.584000	15.932000	-14.299000	N	1.673000	16.433000	-7.777000
C	-4.519000	15.615000	-10.341000	C	1.593000	15.566000	-6.723000
C	-4.596000	16.675000	-11.252000	C	1.429000	14.185000	-6.903000
C	-5.039000	16.410000	-12.549000	C	1.349000	13.676000	-8.199000
C	-5.372000	15.094000	-12.919000	H	-1.802000	14.296000	-14.127000
C	-5.305000	14.039000	-11.984000	H	-3.253000	9.724000	-12.835000
C	-4.875000	14.297000	-10.688000	H	-1.081000	10.600000	-11.944000
H	-4.370000	17.701000	-10.944000	H	4.296000	13.739000	-14.425000
H	-5.131000	17.233000	-13.265000	H	5.426000	9.219000	-12.700000
H	-5.614000	13.029000	-12.268000	H	3.407000	10.390000	-11.788000
H	-4.854000	13.510000	-9.925000	H	1.662000	16.653000	-9.869000
Pd	-4.684000	13.601000	-15.616000	H	1.367000	13.517000	-6.031000
O	-4.207000	15.759000	-8.992000	H	1.221000	12.598000	-8.359000
O	7.418000	14.859000	-9.311000	H	-4.619000	11.178000	-14.387000
O	0.826000	10.139000	-17.958000	H	6.818000	10.370000	-14.469000
N	-3.262000	12.795000	-14.322000	H	1.664000	16.004000	-5.708000
C	-2.083000	13.278000	-13.827000	H	-0.801000	14.028000	-10.750000
C	-3.660000	11.538000	-13.965000	H	3.509000	13.713000	-10.816000
C	-2.900000	10.730000	-13.107000	H	1.167000	11.960000	-13.995000

Table S3. Cartesian coordinates (in Å) for the PM6 geometry optimized model of **5·T1-partial-cone**.

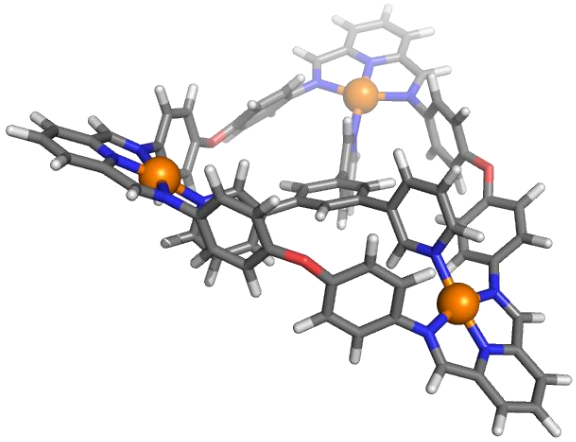

C	6.486000	15.914000	-8.886000
C	6.622000	16.077000	-7.488000
C	5.771000	16.948000	-6.825000
C	4.774000	17.639000	-7.551000
C	4.673000	17.491000	-8.946000
C	5.533000	16.624000	-9.625000
H	7.403000	15.519000	-6.951000
H	5.872000	17.087000	-5.742000
H	3.929000	18.067000	-9.504000
H	5.464000	16.523000	-10.706000
C	0.529000	20.288000	-5.651000
C	0.497000	21.423000	-4.820000
C	1.720000	21.996000	-4.429000
C	2.950000	21.458000	-4.841000
C	2.933000	20.324000	-5.675000
N	1.735000	19.800000	-6.066000
C	4.081000	19.547000	-6.229000
N	3.788000	18.462000	-6.905000
C	-0.608000	19.475000	-6.176000
N	-0.313000	18.366000	-6.811000
H	-0.455000	21.854000	-4.473000
H	1.714000	22.889000	-3.774000
H	3.898000	21.912000	-4.511000
H	5.096000	19.950000	-6.041000
H	-1.628000	19.875000	-5.995000
C	-3.173000	15.938000	-8.740000
C	-2.689000	17.092000	-9.387000
C	-1.766000	17.900000	-8.733000
C	-1.315000	17.540000	-7.445000
C	-1.787000	16.371000	-6.823000
C	-2.717000	15.552000	-7.476000
H	-3.091000	17.372000	-10.368000
H	-1.411000	18.817000	-9.212000
H	-1.462000	16.111000	-5.810000
H	-3.128000	14.672000	-6.972000
Pd	1.747000	18.107000	-6.986000
C	7.559000	14.715000	-10.726000
C	7.637000	13.350000	-11.070000
C	7.979000	13.005000	-12.371000
C	8.231000	14.017000	-13.323000
C	8.195000	15.373000	-12.949000
C	7.846000	15.730000	-11.643000
H	7.475000	12.589000	-10.300000
H	8.082000	11.951000	-12.648000
H	8.445000	16.159000	-13.671000
H	7.853000	16.782000	-11.339000
C	8.329000	12.392000	-18.440000
C	9.391000	12.468000	-19.360000
C	10.597000	13.050000	-18.936000
C	10.752000	13.553000	-17.633000
C	9.658000	13.462000	-16.752000
N	8.494000	12.897000	-17.184000
C	9.565000	13.903000	-15.330000
N	8.463000	13.607000	-14.684000
C	6.970000	11.810000	-18.629000
N	6.190000	11.729000	-17.576000
H	9.291000	12.077000	-20.385000
H	11.447000	13.110000	-19.644000
H	11.709000	13.996000	-17.317000
H	10.438000	14.452000	-14.921000
H	6.709000	11.489000	-19.658000
C	2.164000	10.477000	-17.757000
C	2.602000	11.527000	-18.603000
C	3.929000	11.917000	-18.568000
C	4.828000	11.270000	-17.684000
C	4.387000	10.206000	-16.881000
C	3.042000	9.810000	-16.900000
H	1.885000	11.995000	-19.291000
H	4.271000	12.730000	-19.218000
H	5.097000	9.657000	-16.258000
H	2.715000	8.963000	-16.298000
Pd	7.100000	12.566000	-15.892000
C	-4.459000	14.081000	-9.757000
C	-3.555000	13.020000	-9.640000
C	-3.889000	11.792000	-10.229000
C	-5.102000	11.639000	-10.921000
C	-6.039000	12.702000	-10.961000
C	-5.719000	13.920000	-10.391000
H	-2.629000	13.126000	-9.082000
H	-3.205000	10.944000	-10.136000
H	-7.010000	12.570000	-11.451000
H	-6.421000	14.766000	-10.410000
C	-5.318000	7.276000	-14.048000
C	-6.364000	6.342000	-14.171000
C	-7.475000	6.474000	-13.321000
C	-7.556000	7.509000	-12.373000
C	-6.485000	8.417000	-12.285000
N	-5.401000	8.253000	-13.099000
C	-6.358000	9.630000	-11.424000
N	-5.340000	10.422000	-11.652000
C	-4.096000	7.420000	-14.895000
N	-3.386000	8.509000	-14.728000
H	-6.329000	5.536000	-14.921000
H	-8.314000	5.756000	-13.412000
H	-8.445000	7.606000	-11.731000
H	-7.139000	9.772000	-10.649000

H	-3.895000	6.608000	-15.621000
C	-0.081000	9.713000	-17.046000
C	0.055000	8.547000	-16.292000
C	-1.045000	8.101000	-15.541000
C	-2.239000	8.838000	-15.536000
C	-2.364000	10.010000	-16.319000
C	-1.288000	10.450000	-17.071000
H	0.970000	7.949000	-16.326000
H	-0.960000	7.169000	-14.972000
H	-3.316000	10.548000	-16.353000
H	-1.364000	11.328000	-17.723000
Pd	-4.176000	9.743000	-13.228000
O	-4.276000	15.395000	-9.396000
O	7.303000	14.909000	-9.370000
O	0.819000	10.244000	-17.962000
N	-3.073000	11.442000	-13.509000
C	-1.840000	11.684000	-12.987000
C	-3.670000	12.408000	-14.270000
C	-3.044000	13.632000	-14.538000
C	-1.776000	13.883000	-14.000000
C	-1.163000	12.902000	-13.207000
C	0.160000	13.114000	-12.574000
C	0.228000	13.740000	-11.320000
C	1.463000	13.848000	-10.667000
C	2.629000	13.358000	-11.273000
C	2.552000	12.729000	-12.524000
C	1.321000	12.621000	-13.187000
C	3.758000	12.056000	-13.063000
C	4.602000	12.639000	-14.029000
N	5.716000	11.998000	-14.483000
C	6.017000	10.758000	-13.991000
C	5.214000	10.120000	-13.036000
C	4.075000	10.778000	-12.569000
C	1.534000	14.364000	-9.280000
C	1.625000	15.737000	-8.986000
N	1.718000	16.188000	-7.703000
C	1.714000	15.284000	-6.678000
C	1.615000	13.905000	-6.904000
C	1.526000	13.442000	-8.217000
H	-1.393000	10.882000	-12.381000
H	-3.547000	14.383000	-15.162000
H	-1.274000	14.836000	-14.200000
H	4.394000	13.634000	-14.452000
H	5.482000	9.124000	-12.662000
H	3.435000	10.300000	-11.818000
H	1.628000	16.497000	-9.781000
H	1.613000	13.205000	-6.057000
H	1.453000	12.367000	-8.417000
H	-4.677000	12.176000	-14.665000
H	6.933000	10.275000	-14.385000
H	1.798000	15.695000	-5.653000
H	-0.680000	14.120000	-10.849000
H	3.588000	13.441000	-10.759000
H	1.262000	12.139000	-14.164000

Table S4. Cartesian coordinates (in Å) for the PM6 geometry optimized model of **6·T2-cone**.

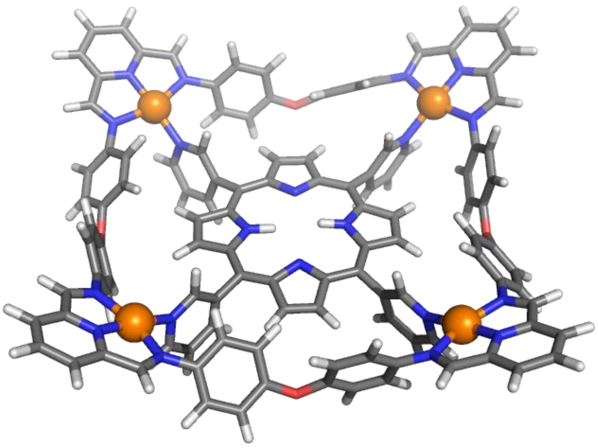

C	-6.349000	-0.230000	-8.173000	C	-9.756000	-10.741000	-7.154000
C	-7.261000	0.316000	-7.260000	C	-9.545000	-9.485000	-7.744000
C	-7.666000	1.639000	-7.440000	C	-8.913000	-8.487000	-6.979000
C	-7.172000	2.381000	-8.530000	N	-8.537000	-8.754000	-5.695000
C	-6.289000	1.799000	-9.465000	C	-8.528000	-7.110000	-7.389000
C	-5.866000	0.487000	-9.282000	N	-7.868000	-6.381000	-6.520000
H	-7.648000	-0.274000	-6.430000	C	-8.204000	-10.004000	-3.718000
H	-8.375000	2.096000	-6.743000	N	-7.631000	-8.913000	-3.270000
H	-5.927000	2.369000	-10.329000	H	-9.511000	-12.001000	-5.392000
H	-5.169000	0.008000	-9.986000	H	-10.249000	-11.542000	-7.741000
C	-8.534000	7.559000	-8.162000	H	-9.861000	-9.297000	-8.782000
C	-9.142000	8.370000	-9.139000	H	-8.805000	-6.806000	-8.419000
C	-9.452000	7.795000	-10.382000	H	-8.351000	-10.947000	-3.152000
C	-9.164000	6.447000	-10.654000	C	-6.196000	-8.482000	0.651000
C	-8.560000	5.677000	-9.644000	C	-5.726000	-9.571000	-0.106000
N	-8.276000	6.248000	-8.437000	C	-6.209000	-9.743000	-1.398000
C	-8.153000	4.246000	-9.687000	C	-7.140000	-8.820000	-1.922000
N	-7.574000	3.758000	-8.617000	C	-7.610000	-7.745000	-1.145000
C	-8.061000	7.942000	-6.805000	C	-7.143000	-7.574000	0.158000
N	-7.447000	7.023000	-6.097000	H	-4.994000	-10.267000	0.329000
H	-9.365000	9.431000	-8.945000	H	-5.858000	-10.592000	-1.997000
H	-9.928000	8.418000	-11.166000	H	-8.349000	-7.053000	-1.559000
H	-9.404000	6.015000	-11.639000	H	-7.509000	-6.754000	0.775000
H	-8.380000	3.692000	-10.620000	Pd	-7.567000	-7.395000	-4.710000
H	-8.242000	8.991000	-6.496000	C	-6.154000	-7.889000	3.009000
C	-5.494000	2.716000	8.216000	C	-7.522000	-8.009000	3.279000
C	-6.828000	3.047000	8.475000	C	-7.987000	-7.648000	4.545000
C	-7.262000	4.342000	8.186000	C	-7.088000	-7.156000	5.510000
C	-6.370000	5.274000	7.625000	C	-5.711000	-7.031000	5.216000
C	-5.026000	4.920000	7.364000	C	-5.239000	-7.392000	3.963000
C	-4.584000	3.638000	7.653000	H	-8.213000	-8.426000	2.542000
H	-7.511000	2.335000	8.945000	H	-9.051000	-7.759000	4.777000
H	-8.298000	4.622000	8.405000	H	-5.015000	-6.684000	5.985000
H	-4.330000	5.664000	6.968000	H	-4.172000	-7.350000	3.716000
H	-3.539000	3.344000	7.507000	C	-8.260000	-5.314000	10.426000
Pd	-7.334000	5.191000	-7.112000	C	-8.877000	-6.013000	11.479000
C	-6.388000	-2.589000	-7.573000	C	-9.315000	-7.327000	11.240000
C	-5.508000	-3.574000	-7.074000	C	-9.139000	-7.937000	9.988000
C	-6.022000	-4.815000	-6.729000	C	-8.512000	-7.197000	8.967000
C	-7.406000	-5.066000	-6.872000	N	-8.107000	-5.918000	9.211000
C	-8.269000	-4.069000	-7.361000	C	-8.165000	-7.631000	7.588000
C	-7.763000	-2.813000	-7.704000	N	-7.511000	-6.780000	6.832000
H	-4.434000	-3.363000	-7.024000	C	-7.713000	-3.931000	10.427000
H	-5.354000	-5.609000	-6.380000	N	-7.164000	-3.506000	9.315000
H	-9.339000	-4.267000	-7.484000	H	-9.013000	-5.553000	12.471000
H	-8.427000	-2.050000	-8.118000	H	-9.803000	-7.894000	12.058000
C	-8.724000	-9.974000	-5.111000	H	-9.480000	-8.971000	9.819000
C	-9.348000	-11.006000	-5.836000	H	-8.463000	-8.660000	7.304000

H	-7.818000	-3.354000	11.368000	C	-5.744000	1.962000	-2.643000
C	-5.605000	0.353000	8.779000	C	-5.853000	0.515000	-2.752000
C	-6.655000	-0.084000	7.962000	C	-5.796000	-0.204000	-4.064000
C	-7.169000	-1.365000	8.170000	C	-5.827000	-1.528000	-3.791000
C	-6.638000	-2.173000	9.192000	C	-5.903000	-1.681000	-2.309000
C	-5.605000	-1.702000	10.031000	N	-5.948000	-0.351000	-1.739000
C	-5.076000	-0.433000	9.819000	C	-5.848000	-2.851000	-1.617000
H	-7.069000	0.559000	7.185000	C	-5.872000	-3.005000	-0.174000
H	-7.990000	-1.735000	7.550000	N	-5.830000	-1.972000	0.765000
H	-5.210000	-2.323000	10.843000	C	-5.779000	-2.515000	2.052000
H	-4.265000	-0.038000	10.448000	C	-5.818000	-3.931000	1.914000
Pd	-7.165000	-4.963000	7.811000	C	-5.873000	-4.231000	0.549000
O	-4.881000	1.517000	8.536000	C	-5.628000	-1.764000	3.283000
O	-5.711000	-1.452000	-7.977000	C	-5.327000	-2.591000	4.493000
O	-5.519000	-8.310000	1.854000	C	-3.977000	-2.748000	4.858000
C	-5.755000	7.907000	-2.350000	C	-6.315000	-3.215000	5.283000
C	-4.959000	7.328000	-3.363000	N	-6.000000	-3.947000	6.394000
C	-5.540000	7.049000	-4.591000	C	-4.683000	-4.074000	6.743000
C	-6.909000	7.334000	-4.800000	C	-3.652000	-3.493000	5.993000
C	-7.687000	7.910000	-3.779000	C	-5.052000	4.221000	2.946000
C	-7.112000	8.190000	-2.537000	C	-3.685000	4.554000	2.979000
H	-3.890000	7.167000	-3.184000	C	-3.264000	5.682000	3.685000
H	-4.934000	6.642000	-5.406000	C	-4.219000	6.462000	4.352000
H	-8.742000	8.148000	-3.946000	N	-5.550000	6.147000	4.347000
H	-7.706000	8.673000	-1.757000	C	-5.957000	5.042000	3.654000
C	-5.593000	8.488000	0.009000	C	-5.467000	2.691000	-3.908000
C	-6.609000	7.708000	0.575000	C	-6.447000	3.412000	-4.625000
C	-6.964000	7.944000	1.904000	N	-6.162000	4.064000	-5.792000
C	-6.313000	8.957000	2.633000	C	-4.885000	4.012000	-6.277000
C	-5.320000	9.761000	2.033000	C	-3.863000	3.319000	-5.614000
C	-4.949000	9.521000	0.714000	C	-4.156000	2.655000	-4.423000
H	-7.120000	6.942000	-0.006000	C	-5.608000	-4.123000	-2.366000
H	-7.755000	7.353000	2.375000	C	-4.286000	-4.605000	-2.420000
H	-4.833000	10.568000	2.594000	C	-4.014000	-5.792000	-3.102000
H	-4.172000	10.123000	0.220000	C	-5.068000	-6.481000	-3.717000
C	-7.625000	8.791000	7.834000	N	-6.357000	-6.028000	-3.676000
C	-8.119000	9.834000	8.640000	C	-6.621000	-4.863000	-3.009000
C	-8.307000	11.096000	8.054000	H	-5.270000	-0.120000	5.637000
C	-8.010000	11.323000	6.699000	H	-5.192000	2.510000	5.010000
C	-7.522000	10.247000	5.935000	H	-5.991000	1.153000	0.078000
N	-7.357000	9.023000	6.517000	H	-5.401000	4.791000	-2.143000
C	-7.135000	10.232000	4.498000	H	-5.227000	5.367000	0.482000
N	-6.676000	9.102000	4.017000	H	-5.727000	0.289000	-5.016000
C	-7.294000	7.395000	8.225000	H	-5.793000	-2.359000	-4.473000
N	-6.765000	6.619000	7.308000	H	-5.822000	-0.978000	0.546000
H	-8.348000	9.675000	9.706000	H	-5.793000	-4.640000	2.720000
H	-8.692000	11.931000	8.672000	H	-5.893000	-5.212000	0.112000
H	-8.152000	12.322000	6.258000	H	-3.182000	-2.288000	4.255000
H	-7.273000	11.177000	3.934000	H	-7.382000	-3.137000	5.028000
H	-7.496000	7.115000	9.278000	H	-2.604000	-3.625000	6.296000
Pd	-6.570000	7.595000	5.468000	H	-2.951000	3.929000	2.454000
O	-5.009000	8.205000	-1.223000	H	-2.201000	5.960000	3.719000
C	-5.389000	0.352000	4.677000	H	-7.033000	4.814000	3.674000
C	-5.348000	1.666000	4.364000	H	-7.484000	3.471000	-4.265000
C	-5.545000	1.768000	2.884000	H	-2.846000	3.302000	-6.031000
N	-5.728000	0.559000	2.343000	H	-3.369000	2.105000	-3.891000
C	-5.614000	-0.409000	3.412000	H	-3.475000	-4.054000	-1.927000
C	-5.464000	3.027000	2.162000	H	-2.988000	-6.185000	-3.157000
C	-5.586000	3.155000	0.805000	H	-7.668000	-4.528000	-2.995000
N	-5.844000	2.141000	-0.149000	H	-4.463000	-4.663000	7.654000
C	-5.726000	2.655000	-1.464000	H	-3.922000	7.369000	4.914000
C	-5.495000	4.123000	-1.300000	H	-4.688000	4.547000	-7.226000
C	-5.410000	4.412000	0.014000	H	-4.888000	-7.427000	-4.263000

Table S5. Cartesian coordinates (in Å) for the PM6 geometry optimized model of **6·T2-partial-cone**.

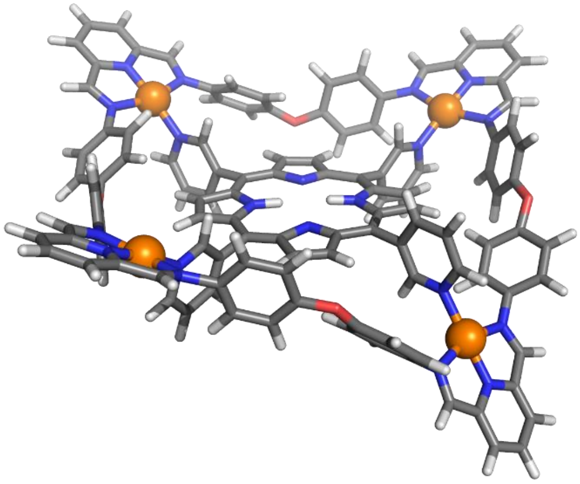

C	-6.259000	-0.233000	-7.960000	C	-10.088000	-10.741000	-5.521000
C	-7.614000	0.104000	-8.041000	C	-10.470000	-10.529000	-6.856000
C	-7.958000	1.449000	-8.199000	C	-10.119000	-9.352000	-7.537000
C	-6.954000	2.432000	-8.252000	C	-9.383000	-8.374000	-6.842000
C	-5.589000	2.072000	-8.180000	N	-9.046000	-8.582000	-5.536000
C	-5.236000	0.740000	-8.025000	C	-8.861000	-7.076000	-7.347000
H	-8.394000	-0.660000	-8.038000	N	-8.147000	-6.350000	-6.520000
H	-9.014000	1.726000	-8.284000	C	-8.802000	-9.735000	-3.489000
H	-4.812000	2.835000	-8.278000	N	-8.093000	-8.695000	-3.120000
H	-4.188000	0.422000	-8.007000	H	-10.357000	-11.678000	-5.007000
C	-7.944000	7.716000	-8.153000	H	-11.052000	-11.310000	-7.386000
C	-8.508000	8.508000	-9.172000	H	-10.412000	-9.209000	-8.589000
C	-8.912000	7.875000	-10.359000	H	-9.115000	-6.814000	-8.394000
C	-8.759000	6.489000	-10.535000	H	-9.031000	-10.623000	-2.866000
C	-8.185000	5.743000	-9.489000	C	-6.388000	-8.352000	0.705000
N	-7.805000	6.373000	-8.340000	C	-6.080000	-9.492000	-0.061000
C	-7.894000	4.285000	-9.439000	C	-6.655000	-9.627000	-1.319000
N	-7.271000	3.831000	-8.378000	C	-7.519000	-8.619000	-1.802000
C	-7.461000	8.139000	-6.813000	C	-7.826000	-7.492000	-1.018000
N	-6.912000	7.231000	-6.036000	C	-7.262000	-7.355000	0.252000
H	-8.629000	9.596000	-9.052000	H	-5.397000	-10.255000	0.341000
H	-9.357000	8.480000	-11.173000	H	-6.428000	-10.512000	-1.924000
H	-9.078000	6.009000	-11.474000	H	-8.515000	-6.733000	-1.396000
H	-8.218000	3.683000	-10.312000	H	-7.496000	-6.489000	0.872000
H	-7.614000	9.207000	-6.553000	Pd	-7.916000	-7.277000	-4.652000
C	-4.601000	8.670000	-0.001000	C	-6.135000	-7.820000	3.072000
C	-4.402000	9.736000	0.908000	C	-7.489000	-7.757000	3.415000
C	-3.543000	9.553000	1.977000	C	-7.831000	-7.402000	4.722000
C	-2.891000	8.306000	2.150000	C	-6.823000	-7.096000	5.655000
C	-3.077000	7.269000	1.225000	C	-5.460000	-7.169000	5.292000
C	-3.935000	7.449000	0.131000	C	-5.110000	-7.524000	3.998000
H	-4.928000	10.690000	0.749000	H	-8.271000	-8.029000	2.702000
H	-3.379000	10.373000	2.687000	H	-8.886000	-7.371000	5.011000
H	-2.543000	6.325000	1.345000	H	-4.681000	-6.979000	6.036000
H	-4.062000	6.655000	-0.600000	H	-4.062000	-7.629000	3.694000
Pd	-6.888000	5.345000	-6.981000	C	-7.872000	-5.056000	10.519000
C	-6.500000	-2.634000	-7.584000	C	-8.419000	-5.720000	11.633000
C	-6.146000	-3.763000	-8.347000	C	-8.782000	-7.070000	11.490000
C	-6.705000	-4.993000	-8.019000	C	-8.605000	-7.748000	10.273000
C	-7.599000	-5.084000	-6.930000	C	-8.050000	-7.041000	9.190000
C	-7.956000	-3.942000	-6.190000	N	-7.709000	-5.729000	9.345000
C	-7.407000	-2.701000	-6.520000	C	-7.744000	-7.530000	7.819000
H	-5.442000	-3.660000	-9.185000	N	-7.144000	-6.698000	7.002000
H	-6.443000	-5.879000	-8.608000	C	-7.429000	-3.642000	10.408000
H	-8.673000	-4.023000	-5.369000	N	-6.881000	-3.253000	9.278000
H	-7.685000	-1.807000	-5.960000	H	-8.559000	-5.204000	12.596000
C	-9.353000	-9.733000	-4.870000	H	-9.213000	-7.611000	12.356000

H	-8.892000	-8.808000	10.179000	C	-5.484000	4.341000	0.120000
H	-8.041000	-8.573000	7.585000	C	-5.427000	1.963000	-2.625000
H	-7.605000	-3.002000	11.297000	C	-5.512000	0.523000	-2.791000
C	-5.872000	0.821000	8.893000	C	-5.474000	-0.150000	-4.128000
C	-7.216000	0.467000	9.154000	C	-5.535000	-1.481000	-3.901000
C	-7.543000	-0.873000	9.275000	C	-5.607000	-1.686000	-2.424000
C	-6.540000	-1.861000	9.114000	N	-5.608000	-0.378000	-1.807000
C	-5.219000	-1.493000	8.816000	C	-5.606000	-2.881000	-1.775000
C	-4.875000	-0.139000	8.701000	C	-5.585000	-3.087000	-0.339000
H	-7.966000	1.255000	9.301000	N	-5.566000	-2.083000	0.632000
H	-8.576000	-1.159000	9.499000	C	-5.462000	-2.665000	1.899000
H	-4.443000	-2.255000	8.716000	C	-5.434000	-4.076000	1.715000
H	-3.834000	0.148000	8.543000	C	-5.509000	-4.334000	0.342000
Pd	-6.813000	-4.829000	7.884000	C	-5.371000	-1.950000	3.156000
O	-5.707000	2.193000	8.975000	C	-5.051000	-2.797000	4.344000
O	-5.733000	-1.510000	-7.879000	C	-3.705000	-3.157000	4.543000
O	-5.617000	-8.238000	1.859000	C	-6.012000	-3.228000	5.281000
C	-5.814000	8.379000	-2.131000	N	-5.669000	-3.960000	6.381000
C	-4.858000	7.766000	-2.944000	C	-4.353000	-4.282000	6.574000
C	-5.232000	7.378000	-4.238000	C	-3.353000	-3.903000	5.670000
C	-6.541000	7.598000	-4.692000	C	-5.371000	4.082000	3.079000
C	-7.504000	8.197000	-3.840000	C	-6.547000	4.694000	3.550000
C	-7.148000	8.579000	-2.558000	C	-6.455000	5.832000	4.353000
H	-3.821000	7.662000	-2.622000	C	-5.188000	6.344000	4.675000
H	-4.484000	6.942000	-4.905000	N	-4.038000	5.758000	4.231000
H	-8.530000	8.364000	-4.187000	C	-4.130000	4.643000	3.447000
H	-7.864000	9.071000	-1.887000	C	-5.105000	2.762000	-3.835000
C	-4.672000	2.918000	8.415000	C	-6.069000	3.490000	-4.566000
C	-3.962000	2.587000	7.257000	N	-5.731000	4.258000	-5.642000
C	-3.088000	3.536000	6.713000	C	-4.419000	4.320000	-6.022000
C	-2.928000	4.782000	7.338000	C	-3.416000	3.604000	-5.354000
C	-3.621000	5.084000	8.536000	C	-3.763000	2.817000	-4.255000
C	-4.500000	4.158000	9.073000	C	-5.505000	-4.135000	-2.583000
H	-4.075000	1.613000	6.784000	C	-4.224000	-4.635000	-2.882000
H	-2.523000	3.298000	5.809000	C	-4.102000	-5.805000	-3.633000
H	-3.475000	6.047000	9.040000	C	-5.263000	-6.458000	-4.072000
H	-5.059000	4.364000	9.998000	N	-6.515000	-5.987000	-3.788000
C	-0.228000	8.657000	4.754000	C	-6.631000	-4.841000	-3.052000
C	0.903000	9.362000	5.206000	H	-5.378000	-0.378000	5.591000
C	1.452000	9.012000	6.451000	H	-5.468000	2.279000	5.052000
C	0.887000	7.993000	7.236000	H	-5.640000	1.034000	0.053000
C	-0.243000	7.318000	6.739000	H	-5.432000	4.795000	-2.022000
N	-0.751000	7.656000	5.519000	H	-5.499000	5.293000	0.632000
C	-1.044000	6.249000	7.392000	H	-5.401000	0.375000	-5.063000
N	-2.069000	5.765000	6.730000	H	-5.515000	-2.290000	-4.610000
C	-1.015000	8.869000	3.511000	H	-5.606000	-1.083000	0.446000
N	-2.046000	8.085000	3.297000	H	-5.354000	-4.808000	2.497000
H	1.350000	10.173000	4.609000	H	-5.489000	-5.302000	-0.125000
H	2.343000	9.555000	6.824000	H	-2.938000	-2.854000	3.819000
H	1.322000	7.740000	8.216000	H	-7.080000	-2.990000	5.157000
H	-0.724000	5.942000	8.409000	H	-2.307000	-4.190000	5.848000
H	-0.679000	9.697000	2.852000	H	-7.529000	4.279000	3.290000
Pd	-2.323000	6.720000	4.879000	H	-7.361000	6.328000	4.730000
O	-5.615000	8.964000	-0.892000	H	-3.183000	4.195000	3.113000
C	-5.409000	0.121000	4.639000	H	-7.134000	3.462000	-4.291000
C	-5.446000	1.446000	4.373000	H	-2.373000	3.666000	-5.694000
C	-5.485000	1.590000	2.885000	H	-2.994000	2.247000	-3.720000
N	-5.518000	0.393000	2.290000	H	-3.327000	-4.112000	-2.525000
C	-5.445000	-0.603000	3.335000	H	-3.111000	-6.213000	-3.880000
C	-5.455000	2.877000	2.215000	H	-7.651000	-4.492000	-2.837000
C	-5.519000	3.043000	0.860000	H	-4.111000	-4.862000	7.486000
N	-5.581000	2.039000	-0.135000	H	-5.077000	7.246000	5.306000
C	-5.498000	2.613000	-1.425000	H	-4.180000	4.965000	-6.890000
C	-5.459000	4.092000	-1.205000	H	-5.202000	-7.387000	-4.671000

Table S6. Cartesian coordinates (in Å) for the PM6 geometry optimized model of **6·T2-1,2-alternate**.

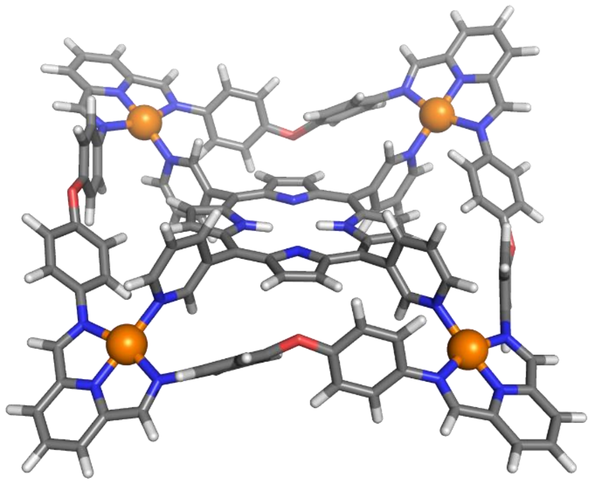

C	-6.335000	-0.242000	-7.782000
C	-7.687000	0.108000	-7.858000
C	-8.019000	1.452000	-8.036000
C	-7.004000	2.424000	-8.114000
C	-5.643000	2.052000	-8.044000
C	-5.303000	0.718000	-7.871000
H	-8.475000	-0.649000	-7.834000
H	-9.072000	1.739000	-8.118000
H	-4.859000	2.806000	-8.158000
H	-4.258000	0.390000	-7.856000
C	-8.081000	7.689000	-8.063000
C	-8.665000	8.460000	-9.086000
C	-9.056000	7.810000	-10.267000
C	-8.871000	6.427000	-10.435000
C	-8.279000	5.702000	-9.384000
N	-7.912000	6.348000	-8.239000
C	-7.961000	4.251000	-9.321000
N	-7.318000	3.821000	-8.261000
C	-7.606000	8.131000	-6.726000
N	-7.021000	7.244000	-5.952000
H	-8.812000	9.546000	-8.972000
H	-9.516000	8.399000	-11.085000
H	-9.180000	5.933000	-11.370000
H	-8.289000	3.632000	-10.180000
H	-7.796000	9.193000	-6.466000
C	-4.772000	8.879000	0.051000
C	-4.640000	9.966000	0.947000
C	-3.752000	9.858000	2.003000
C	-3.004000	8.665000	2.174000
C	-3.130000	7.606000	1.263000
C	-4.017000	7.710000	0.183000
H	-5.240000	10.875000	0.790000
H	-3.642000	10.694000	2.704000
H	-2.525000	6.705000	1.385000
H	-4.102000	6.901000	-0.537000
Pd	-6.948000	5.354000	-6.885000
C	-6.636000	-2.619000	-7.350000
C	-6.381000	-3.761000	-8.129000
C	-6.983000	-4.962000	-7.767000
C	-7.817000	-5.007000	-6.630000
C	-8.081000	-3.849000	-5.878000
C	-7.489000	-2.637000	-6.240000
H	-5.722000	-3.694000	-9.006000
H	-6.801000	-5.861000	-8.368000
H	-8.758000	-3.892000	-5.020000
H	-7.690000	-1.730000	-5.671000
C	-9.460000	-9.647000	-4.473000
C	-10.371000	-10.577000	-5.009000
C	-10.974000	-10.281000	-6.242000
C	-10.674000	-9.096000	-6.936000
C	-9.759000	-8.198000	-6.356000
N	-9.200000	-8.489000	-5.145000
C	-9.255000	-6.909000	-6.901000
N	-8.381000	-6.253000	-6.177000
C	-8.656000	-9.752000	-3.227000
N	-7.837000	-8.765000	-2.946000
H	-10.606000	-11.516000	-4.485000
H	-11.693000	-11.001000	-6.682000
H	-11.144000	-8.888000	-7.910000
H	-9.654000	-6.596000	-7.887000
H	-8.797000	-10.672000	-2.624000
C	-5.265000	-8.888000	0.380000
C	-5.268000	-9.983000	-0.514000
C	-6.130000	-9.957000	-1.598000
C	-6.976000	-8.838000	-1.796000
C	-6.972000	-7.767000	-0.888000
C	-6.114000	-7.789000	0.216000
H	-4.593000	-10.833000	-0.335000
H	-6.142000	-10.800000	-2.298000
H	-7.648000	-6.921000	-1.036000
H	-6.111000	-6.963000	0.927000
Pd	-7.887000	-7.266000	-4.410000
C	-4.262000	0.227000	8.277000
C	-2.938000	-0.208000	8.400000
C	-2.700000	-1.565000	8.621000
C	-3.779000	-2.467000	8.690000
C	-5.109000	-2.012000	8.559000
C	-5.356000	-0.663000	8.347000
H	-2.103000	0.496000	8.378000
H	-1.671000	-1.918000	8.745000
H	-5.943000	-2.714000	8.653000
H	-6.377000	-0.270000	8.292000
C	-2.838000	-7.756000	8.787000
C	-2.386000	-8.533000	9.871000
C	-2.121000	-7.884000	11.088000
C	-2.299000	-6.498000	11.231000
C	-2.754000	-5.767000	10.118000
N	-3.000000	-6.411000	8.940000
C	-3.026000	-4.309000	10.010000
N	-3.548000	-3.875000	8.888000
C	-3.169000	-8.191000	7.405000
N	-3.673000	-7.298000	6.583000
H	-2.246000	-9.622000	9.777000
H	-1.766000	-8.479000	11.954000

H	-2.090000	-6.006000	12.194000	C	-5.026000	4.318000	0.204000
H	-2.763000	-3.688000	10.890000	C	-5.136000	2.010000	-2.597000
H	-2.946000	-9.249000	7.155000	C	-5.233000	0.573000	-2.793000
C	-4.242000	-8.443000	2.571000	C	-5.221000	-0.072000	-4.143000
C	-2.931000	-8.420000	3.103000	C	-5.286000	-1.407000	-3.943000
C	-2.754000	-8.041000	4.421000	C	-5.338000	-1.642000	-2.470000
C	-3.875000	-7.662000	5.202000	N	-5.317000	-0.347000	-1.826000
C	-5.163000	-7.658000	4.649000	C	-5.350000	-2.849000	-1.842000
C	-5.356000	-8.052000	3.318000	C	-5.330000	-3.077000	-0.410000
H	-2.087000	-8.742000	2.478000	N	-5.371000	-2.094000	0.583000
H	-1.748000	-8.041000	4.854000	C	-5.319000	-2.701000	1.839000
H	-6.027000	-7.388000	5.261000	C	-5.234000	-4.105000	1.628000
H	-6.366000	-8.114000	2.910000	C	-5.236000	-4.335000	0.247000
Pd	-3.820000	-5.414000	7.496000	C	-5.370000	-2.016000	3.118000
O	-4.669000	1.542000	8.137000	C	-5.662000	-2.908000	4.281000
O	-5.832000	-1.526000	-7.675000	C	-7.009000	-3.116000	4.626000
O	-4.237000	-8.990000	1.300000	C	-4.663000	-3.559000	5.036000
C	-5.980000	8.476000	-2.060000	N	-4.967000	-4.380000	6.083000
C	-4.983000	7.945000	-2.882000	C	-6.284000	-4.574000	6.403000
C	-5.336000	7.522000	-4.171000	C	-7.323000	-3.957000	5.696000
C	-6.664000	7.631000	-4.609000	C	-4.983000	4.021000	3.144000
C	-7.667000	8.144000	-3.747000	C	-6.179000	4.493000	3.718000
C	-7.331000	8.557000	-2.470000	C	-6.159000	5.647000	4.502000
H	-3.938000	7.932000	-2.571000	C	-4.942000	6.315000	4.705000
H	-4.562000	7.148000	-4.846000	N	-3.770000	5.866000	4.167000
H	-8.706000	8.221000	-4.084000	C	-3.792000	4.734000	3.401000
H	-8.080000	8.985000	-1.789000	C	-4.913000	2.843000	-3.807000
C	-3.773000	2.557000	7.799000	C	-5.949000	3.519000	-4.489000
C	-2.954000	2.492000	6.664000	N	-5.705000	4.313000	-5.572000
C	-2.257000	3.638000	6.279000	C	-4.416000	4.451000	-6.008000
C	-2.382000	4.817000	7.037000	C	-3.344000	3.793000	-5.390000
C	-3.178000	4.853000	8.201000	C	-3.597000	2.981000	-4.283000
C	-3.887000	3.717000	8.583000	C	-5.296000	-4.094000	-2.668000
H	-2.864000	1.568000	6.091000	C	-4.049000	-4.541000	-3.141000
H	-1.610000	3.616000	5.400000	C	-3.981000	-5.711000	-3.900000
H	-3.250000	5.764000	8.806000	C	-5.161000	-6.417000	-4.174000
H	-4.524000	3.716000	9.479000	N	-6.381000	-5.997000	-3.722000
C	-0.383000	9.260000	4.775000	C	-6.445000	-4.851000	-2.979000
C	0.629000	10.106000	5.269000	H	-5.446000	-0.486000	5.582000
C	1.239000	9.771000	6.488000	H	-5.242000	2.167000	5.106000
C	0.849000	8.629000	7.209000	H	-5.161000	1.013000	0.071000
C	-0.164000	7.815000	6.671000	H	-5.051000	4.819000	-1.929000
N	-0.731000	8.143000	5.473000	H	-5.009000	5.258000	0.735000
C	-0.768000	6.584000	7.249000	H	-5.158000	0.471000	-5.069000
N	-1.716000	6.000000	6.557000	H	-5.282000	-2.200000	-4.671000
C	-1.210000	9.425000	3.551000	H	-5.418000	-1.091000	0.415000
N	-2.121000	8.513000	3.301000	H	-5.169000	-4.850000	2.398000
H	0.936000	11.012000	4.722000	H	-5.158000	-5.288000	-0.242000
H	2.037000	10.423000	6.894000	H	-7.810000	-2.625000	4.059000
H	1.328000	8.390000	8.171000	H	-3.595000	-3.429000	4.802000
H	-0.375000	6.251000	8.231000	H	-8.369000	-4.132000	5.983000
H	-1.004000	10.324000	2.935000	H	-7.122000	3.958000	3.546000
Pd	-2.163000	7.029000	4.790000	H	-7.083000	6.034000	4.955000
O	-5.814000	9.089000	-0.830000	H	-2.830000	4.397000	2.990000
C	-5.328000	0.025000	4.642000	H	-6.997000	3.427000	-4.168000
C	-5.224000	1.352000	4.405000	H	-2.322000	3.917000	-5.774000
C	-5.100000	1.522000	2.923000	H	-2.772000	2.455000	-3.787000
N	-5.113000	0.336000	2.305000	H	-3.134000	-3.978000	-2.911000
C	-5.266000	-0.677000	3.326000	H	-3.017000	-6.078000	-4.279000
C	-5.016000	2.819000	2.272000	H	-7.440000	-4.543000	-2.629000
C	-5.053000	3.005000	0.918000	H	-6.496000	-5.248000	7.257000
N	-5.127000	2.023000	-0.097000	H	-4.890000	7.239000	5.313000
C	-5.116000	2.627000	-1.377000	H	-4.252000	5.112000	-6.882000
C	-5.055000	4.100000	-1.126000	H	-5.145000	-7.349000	-4.771000

Table S7. Cartesian coordinates (in Å) for the PM6 geometry optimized model of **6·T2-1,3-alternate**.

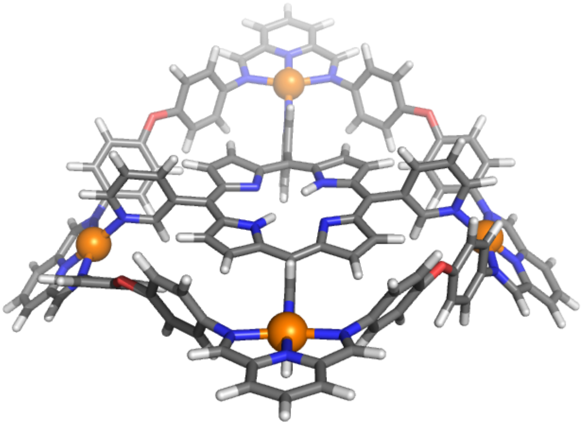

C	-6.621000	-0.512000	-8.057000
C	-7.828000	0.219000	-8.182000
C	-7.765000	1.589000	-8.363000
C	-6.505000	2.237000	-8.396000
C	-5.321000	1.503000	-8.244000
C	-5.373000	0.113000	-8.069000
H	-8.787000	-0.315000	-8.177000
H	-8.689000	2.163000	-8.488000
H	-4.349000	2.000000	-8.298000
H	-4.447000	-0.463000	-8.019000
C	-6.688000	7.619000	-8.589000
C	-6.954000	8.426000	-9.712000
C	-7.202000	7.793000	-10.941000
C	-7.184000	6.393000	-11.058000
C	-6.912000	5.632000	-9.906000
N	-6.686000	6.262000	-8.718000
C	-6.845000	4.153000	-9.763000
N	-6.464000	3.666000	-8.604000
C	-6.407000	8.037000	-7.191000
N	-6.083000	7.108000	-6.319000
H	-6.967000	9.525000	-9.638000
H	-7.413000	8.410000	-11.837000
H	-7.376000	5.913000	-12.031000
H	-7.140000	3.557000	-10.652000
H	-6.508000	9.122000	-6.974000
C	-4.722000	8.795000	-0.057000
C	-4.710000	9.915000	0.806000
C	-3.972000	9.853000	1.976000
C	-3.258000	8.671000	2.294000
C	-3.259000	7.578000	1.413000
C	-3.990000	7.636000	0.220000
H	-5.281000	10.816000	0.535000
H	-3.953000	10.717000	2.651000
H	-2.677000	6.685000	1.651000
H	-3.973000	6.801000	-0.474000
Pd	-6.112000	5.194000	-7.210000
C	-5.920000	-8.673000	0.686000
C	-6.104000	-9.787000	-0.164000
C	-5.437000	-9.821000	-1.378000
C	-4.598000	-8.742000	-1.748000
C	-4.406000	-7.654000	-0.881000
C	-5.066000	-7.617000	0.353000
H	-6.769000	-10.605000	0.149000
H	-5.571000	-10.681000	-2.044000
H	-3.733000	-6.841000	-1.161000
H	-4.913000	-6.778000	1.031000
C	-2.641000	-8.316000	-6.746000
C	-1.824000	-9.236000	-7.429000
C	-1.403000	-10.388000	-6.744000
C	-1.791000	-10.630000	-5.417000
C	-2.610000	-9.680000	-4.778000
N	-2.991000	-8.556000	-5.449000
C	-3.190000	-9.728000	-3.409000
N	-3.952000	-8.726000	-3.035000
C	-3.249000	-7.058000	-7.258000
N	-3.996000	-6.363000	-6.433000
H	-1.523000	-9.069000	-8.475000
H	-0.759000	-11.124000	-7.265000
H	-1.463000	-11.546000	-4.899000
H	-2.945000	-10.622000	-2.800000
H	-3.033000	-6.801000	-8.315000
C	-5.998000	-2.866000	-7.658000
C	-6.336000	-4.096000	-8.268000
C	-5.660000	-5.243000	-7.885000
C	-4.658000	-5.165000	-6.887000
C	-4.315000	-3.933000	-6.312000
C	-4.985000	-2.766000	-6.700000
H	-7.123000	-4.123000	-9.036000
H	-5.908000	-6.202000	-8.355000
H	-3.516000	-3.876000	-5.570000
H	-4.710000	-1.807000	-6.264000
Pd	-4.168000	-7.300000	-4.559000
C	-6.586000	-8.144000	3.001000
C	-7.797000	-8.118000	3.733000
C	-7.769000	-7.721000	5.058000
C	-6.542000	-7.328000	5.651000
C	-5.359000	-7.321000	4.899000
C	-5.374000	-7.731000	3.559000
H	-8.728000	-8.450000	3.253000
H	-8.696000	-7.717000	5.642000
H	-4.411000	-7.036000	5.362000
H	-4.441000	-7.788000	2.997000
C	-6.808000	-5.475000	10.713000
C	-7.089000	-6.219000	11.874000
C	-7.325000	-7.597000	11.741000
C	-7.283000	-8.226000	10.486000
C	-6.997000	-7.438000	9.355000
N	-6.779000	-6.100000	9.501000
C	-6.905000	-7.857000	7.933000
N	-6.525000	-6.963000	7.048000
C	-6.538000	-4.019000	10.586000
N	-6.208000	-3.560000	9.401000
H	-7.122000	-5.741000	12.867000
H	-7.548000	-8.200000	12.644000
H	-7.468000	-9.308000	10.398000
H	-7.183000	-8.909000	7.712000

H	-6.652000	-3.415000	11.510000
C	-5.818000	0.573000	8.683000
C	-6.995000	0.091000	9.307000
C	-7.111000	-1.263000	9.563000
C	-6.060000	-2.143000	9.195000
C	-4.890000	-1.644000	8.607000
C	-4.762000	-0.273000	8.341000
H	-7.788000	0.799000	9.586000
H	-8.019000	-1.645000	10.044000
H	-4.061000	-2.317000	8.374000
H	-3.838000	0.111000	7.910000
Pd	-6.204000	-5.093000	7.951000
O	-5.962000	1.920000	8.395000
O	-6.889000	-1.868000	-8.016000
O	-6.794000	-8.712000	1.758000
C	-5.626000	8.343000	-2.312000
C	-4.533000	7.770000	-2.963000
C	-4.691000	7.343000	-4.290000
C	-5.926000	7.490000	-4.935000
C	-7.036000	8.043000	-4.245000
C	-6.893000	8.459000	-2.933000
H	-3.550000	7.723000	-2.490000
H	-3.831000	6.936000	-4.828000
H	-8.005000	8.151000	-4.745000
H	-7.727000	8.917000	-2.384000
C	-4.973000	2.816000	8.043000
C	-3.589000	2.637000	8.056000
C	-2.769000	3.709000	7.680000
C	-3.341000	4.927000	7.281000
C	-4.746000	5.101000	7.298000
C	-5.564000	4.050000	7.669000
H	-3.135000	1.703000	8.398000
H	-1.682000	3.582000	7.704000
H	-5.181000	6.075000	7.051000
H	-6.653000	4.159000	7.728000
C	-0.935000	9.248000	5.176000
C	0.067000	10.048000	5.757000
C	0.569000	9.676000	7.015000
C	0.085000	8.541000	7.687000
C	-0.919000	7.776000	7.066000
N	-1.387000	8.146000	5.840000
C	-1.620000	6.570000	7.586000
N	-2.562000	6.051000	6.836000
C	-1.629000	9.434000	3.873000
N	-2.538000	8.550000	3.536000
H	0.451000	10.946000	5.247000
H	1.357000	10.294000	7.489000
H	0.484000	8.270000	8.678000
H	-1.310000	6.211000	8.588000
H	-1.321000	10.314000	3.272000
Pd	-2.808000	7.103000	5.036000
O	-5.648000	8.957000	-1.071000
C	-5.102000	0.254000	4.718000
C	-5.179000	1.573000	4.434000
C	-5.368000	1.690000	2.953000
N	-5.438000	0.482000	2.385000
C	-5.268000	-0.497000	3.438000
C	-5.414000	2.960000	2.252000
C	-5.430000	3.095000	0.891000
N	-5.446000	2.072000	-0.084000
C	-5.304000	2.620000	-1.382000
C	-5.237000	4.100000	-1.189000
C	-5.346000	4.377000	0.125000
C	-5.244000	1.941000	-2.566000
C	-5.487000	0.514000	-2.700000
C	-5.780000	-0.147000	-4.009000
C	-5.982000	-1.459000	-3.748000
C	-5.807000	-1.660000	-2.281000
N	-5.507000	-0.371000	-1.701000
C	-5.918000	-2.834000	-1.604000
C	-5.803000	-3.016000	-0.171000
N	-5.540000	-2.012000	0.765000
C	-5.500000	-2.570000	2.043000
C	-5.753000	-3.963000	1.907000
C	-5.947000	-4.235000	0.548000
C	-5.246000	-1.846000	3.275000
C	-4.828000	-2.713000	4.416000
C	-3.455000	-2.991000	4.538000
C	-5.720000	-3.283000	5.350000
N	-5.285000	-4.091000	6.360000
C	-3.945000	-4.353000	6.463000
C	-3.008000	-3.818000	5.572000
C	-5.480000	4.200000	3.065000
C	-6.732000	4.781000	3.337000
C	-6.791000	5.994000	4.028000
C	-5.599000	6.603000	4.442000
N	-4.377000	6.035000	4.215000
C	-4.320000	4.850000	3.538000
C	-4.802000	2.656000	-3.787000
C	-5.663000	3.400000	-4.622000
N	-5.204000	4.061000	-5.724000
C	-3.871000	3.995000	-6.026000
C	-2.965000	3.265000	-5.246000
C	-3.436000	2.589000	-4.120000
C	-6.232000	-4.076000	-2.370000
C	-7.571000	-4.477000	-2.524000
C	-7.859000	-5.639000	-3.241000
C	-6.806000	-6.385000	-3.791000
N	-5.501000	-6.008000	-3.646000
C	-5.219000	-4.870000	-2.945000
H	-4.971000	-0.229000	5.670000
H	-5.130000	2.415000	5.099000
H	-5.548000	1.073000	0.121000
H	-5.143000	4.784000	-2.018000
H	-5.380000	5.340000	0.614000
H	-5.832000	0.377000	-4.945000
H	-6.246000	-2.254000	-4.423000
H	-5.410000	-1.026000	0.548000
H	-5.801000	-4.672000	2.712000
H	-6.187000	-5.188000	0.114000
H	-2.738000	-2.567000	3.824000
H	-6.804000	-3.097000	5.293000
H	-1.940000	-4.049000	5.684000
H	-7.655000	4.288000	3.006000
H	-7.759000	6.469000	4.244000
H	-3.321000	4.420000	3.377000
H	-6.741000	3.470000	-4.412000
H	-1.902000	3.230000	-5.520000
H	-2.745000	2.010000	-3.495000
H	-8.383000	-3.882000	-2.083000
H	-8.899000	-5.972000	-3.376000
H	-4.158000	-4.599000	-2.847000
H	-3.627000	-5.014000	7.295000
H	-5.605000	7.575000	4.971000
H	-3.534000	4.551000	-6.923000
H	-6.996000	-7.311000	-4.365000

Table S8. Cartesian coordinates (in Å) for the PM3 geometry optimized model of **13·Cl₉**.

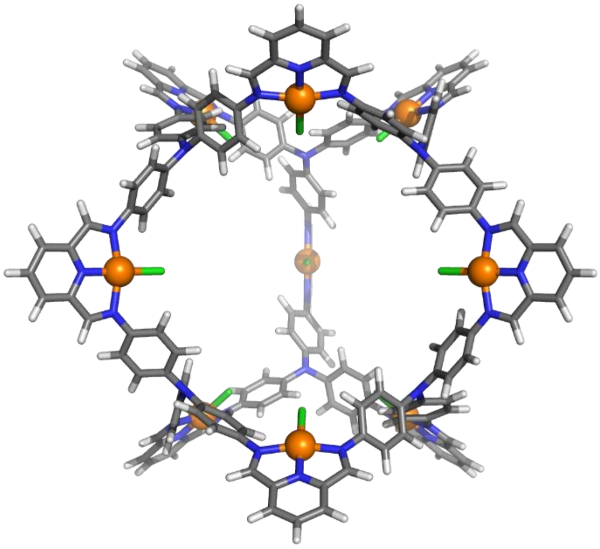

C	0.330000	0.031000	-1.861000	H	3.979000	14.841000	1.642000
C	-0.237000	-0.688000	-0.800000	C	10.639000	14.102000	6.714000
C	0.316000	-1.897000	-0.400000	C	10.842000	15.080000	7.695000
C	1.456000	-2.400000	-1.044000	C	9.804000	15.984000	7.953000
C	2.035000	-1.677000	-2.096000	C	8.587000	15.932000	7.263000
C	1.464000	-0.480000	-2.510000	C	8.420000	14.940000	6.289000
H	-1.119000	-0.300000	-0.274000	N	9.446000	14.077000	6.062000
H	-0.151000	-2.442000	0.431000	C	7.266000	14.649000	5.417000
H	2.959000	-2.019000	-2.587000	N	7.363000	13.639000	4.571000
H	1.924000	0.071000	-3.341000	C	11.540000	13.037000	6.231000
C	5.227000	8.990000	-11.107000	N	11.107000	12.241000	5.271000
C	6.451000	9.363000	-10.531000	H	11.790000	15.138000	8.247000
C	7.637000	9.220000	-11.240000	H	9.949000	16.758000	8.722000
C	7.611000	8.733000	-12.554000	H	7.785000	16.651000	7.480000
C	6.387000	8.372000	-13.137000	H	6.373000	15.291000	5.514000
C	5.207000	8.492000	-12.417000	H	12.537000	12.958000	6.698000
H	6.485000	9.754000	-9.505000	Pd	9.192000	12.712000	4.693000
H	8.586000	9.463000	-10.738000	C	3.606000	10.306000	-9.722000
H	6.342000	7.983000	-14.163000	C	2.769000	10.275000	-8.595000
H	4.259000	8.187000	-12.881000	C	2.411000	11.448000	-7.948000
C	12.433000	7.977000	-14.820000	C	2.862000	12.684000	-8.436000
C	12.828000	8.311000	-16.121000	C	3.678000	12.721000	-9.576000
C	11.882000	8.903000	-16.968000	C	4.052000	11.544000	-10.209000
C	10.572000	9.166000	-16.548000	H	2.403000	9.317000	-8.201000
C	10.215000	8.820000	-15.240000	H	1.799000	11.380000	-7.035000
N	11.154000	8.243000	-14.443000	H	4.040000	13.676000	-9.981000
C	8.931000	8.982000	-14.530000	H	4.705000	11.591000	-11.090000
N	8.859000	8.584000	-13.273000	C	1.636000	16.879000	-5.306000
C	13.201000	7.355000	-13.724000	C	1.190000	18.146000	-5.703000
N	12.588000	7.144000	-12.573000	C	1.041000	18.396000	-7.073000
H	13.850000	8.114000	-16.469000	C	1.322000	17.423000	-8.041000
H	12.178000	9.171000	-17.994000	C	1.767000	16.168000	-7.608000
H	9.846000	9.633000	-17.227000	N	1.902000	15.958000	-6.271000
H	8.089000	9.431000	-15.085000	C	2.127000	14.964000	-8.383000
H	14.256000	7.096000	-13.920000	N	2.503000	13.887000	-7.719000
Pd	10.637000	7.787000	-12.619000	C	1.872000	16.333000	-3.954000
C	4.122000	12.698000	1.987000	N	2.306000	15.090000	-3.858000
C	4.816000	11.686000	2.668000	H	0.963000	18.923000	-4.961000
C	5.879000	11.998000	3.505000	H	0.690000	19.387000	-7.399000
C	6.246000	13.336000	3.700000	H	1.195000	17.639000	-9.110000
C	5.550000	14.351000	3.027000	H	2.062000	15.021000	-9.483000
C	4.502000	14.035000	2.173000	H	1.669000	16.987000	-3.089000
H	4.535000	10.633000	2.530000	C	2.903000	13.140000	-0.141000
H	6.439000	11.174000	3.977000	C	1.754000	13.916000	-0.341000
H	5.824000	15.407000	3.156000	C	1.569000	14.592000	-1.540000

C	2.526000	14.491000	-2.559000
C	3.691000	13.741000	-2.349000
C	3.882000	13.081000	-1.141000
H	0.983000	13.982000	0.438000
H	0.657000	15.189000	-1.676000
H	4.449000	13.624000	-3.140000
H	4.797000	12.492000	-0.991000
Pd	2.512000	14.198000	-5.695000
C	3.028000	8.013000	-10.469000
C	3.316000	6.732000	-9.984000
C	2.346000	5.736000	-10.013000
C	1.083000	6.008000	-10.555000
C	0.810000	7.277000	-11.087000
C	1.775000	8.275000	-11.038000
H	4.301000	6.508000	-9.551000
H	2.581000	4.757000	-9.567000
H	-0.167000	7.505000	-11.532000
H	1.538000	9.271000	-11.434000
C	-2.627000	2.206000	-9.742000
C	-3.571000	1.716000	-10.652000
C	-3.578000	2.247000	-11.948000
C	-2.677000	3.242000	-12.349000
C	-1.748000	3.709000	-11.412000
N	-1.767000	3.173000	-10.161000
C	-0.699000	4.741000	-11.543000
N	0.061000	4.986000	-10.493000
C	-2.387000	1.846000	-8.331000
N	-1.425000	2.478000	-7.682000
H	-4.288000	0.938000	-10.358000
H	-4.315000	1.871000	-12.674000
H	-2.701000	3.644000	-13.370000
H	-0.605000	5.262000	-12.511000
H	-3.026000	1.065000	-7.883000
C	-0.558000	1.579000	-3.620000
C	-0.813000	0.540000	-4.527000
C	-1.116000	0.824000	-5.851000
C	-1.159000	2.153000	-6.298000
C	-0.900000	3.195000	-5.396000
C	-0.617000	2.908000	-4.069000
H	-0.768000	-0.507000	-4.200000
H	-1.311000	-0.010000	-6.538000
H	-0.884000	4.247000	-5.721000
H	-0.420000	3.738000	-3.375000
Pd	-0.463000	3.837000	-8.874000
C	-0.738000	2.187000	-1.223000
C	-2.113000	2.441000	-1.140000
C	-2.599000	3.342000	-0.202000
C	-1.714000	4.009000	0.658000
C	-0.341000	3.734000	0.594000
C	0.140000	2.818000	-0.334000
H	-2.815000	1.945000	-1.823000
H	-3.680000	3.531000	-0.159000
H	0.380000	4.261000	1.238000
H	1.218000	2.615000	-0.377000
C	-3.054000	8.142000	3.823000
C	-4.124000	8.226000	4.721000
C	-4.972000	7.118000	4.846000
C	-4.777000	5.946000	4.103000
C	-3.698000	5.899000	3.213000
N	-2.893000	6.992000	3.115000
C	-3.255000	4.817000	2.310000
N	-2.180000	5.027000	1.574000
C	-2.014000	9.133000	3.483000
N	-1.110000	8.803000	2.578000
H	-4.295000	9.135000	5.313000
H	-5.818000	7.170000	5.548000
H	-5.455000	5.089000	4.216000
H	-3.846000	3.885000	2.291000
H	-2.043000	10.108000	4.001000
C	1.985000	11.497000	1.473000
C	1.630000	11.355000	2.823000
C	0.607000	10.494000	3.192000
C	-0.074000	9.746000	2.220000
C	0.279000	9.882000	0.869000
C	1.289000	10.759000	0.502000
H	2.163000	11.920000	3.600000
H	0.351000	10.404000	4.256000
H	-0.207000	9.282000	0.084000
H	1.550000	10.856000	-0.561000
Pd	-1.394000	6.902000	1.873000
N	3.087000	12.323000	1.050000
N	4.032000	9.054000	-10.293000
N	-0.167000	1.331000	-2.256000
C	13.602000	9.136000	3.791000
C	13.502000	9.353000	5.172000
C	12.700000	10.375000	5.663000
C	11.973000	11.188000	4.782000
C	12.057000	10.964000	3.401000
C	12.879000	9.956000	2.912000
H	14.051000	8.714000	5.877000
H	12.643000	10.525000	6.750000
H	11.457000	11.549000	2.687000
H	12.941000	9.796000	1.827000
C	14.697000	5.383000	-9.329000
C	13.396000	4.966000	-9.651000
C	12.708000	5.550000	-10.707000
C	13.326000	6.541000	-11.482000
C	14.630000	6.953000	-11.169000
C	15.306000	6.384000	-10.099000
H	12.902000	4.186000	-9.058000
H	11.667000	5.243000	-10.893000
H	15.133000	7.733000	-11.757000
H	16.320000	6.730000	-9.858000
C	9.761000	-3.486000	0.011000
C	8.724000	-2.761000	0.616000
C	7.432000	-3.269000	0.646000
C	7.164000	-4.530000	0.096000
C	8.202000	-5.263000	-0.500000
C	9.487000	-4.741000	-0.549000
H	8.921000	-1.774000	1.057000
H	6.630000	-2.648000	1.075000
H	8.015000	-6.251000	-0.942000
H	10.284000	-5.319000	-1.036000
C	1.972000	-5.940000	0.058000
C	1.421000	-7.185000	0.381000
C	2.291000	-8.217000	0.756000
C	3.678000	-8.033000	0.815000
C	4.193000	-6.773000	0.486000
N	3.323000	-5.793000	0.124000
C	5.588000	-6.291000	0.463000
N	5.807000	-5.034000	0.127000
C	1.314000	-4.689000	-0.368000
N	2.074000	-3.640000	-0.623000
H	0.336000	-7.350000	0.341000
H	1.872000	-9.202000	1.012000
H	4.343000	-8.855000	1.112000
H	6.385000	-7.008000	0.730000
H	0.213000	-4.691000	-0.454000
Pd	4.064000	-4.046000	-0.322000
C	15.510000	3.406000	-8.018000
C	15.695000	2.878000	-6.730000
C	15.787000	1.508000	-6.533000
C	15.722000	0.636000	-7.630000
C	15.550000	1.160000	-8.920000
C	15.439000	2.530000	-9.111000
H	15.753000	3.545000	-5.859000

H	15.878000	1.130000	-5.502000
H	15.493000	0.499000	-9.795000
H	15.289000	2.920000	-10.127000
C	15.702000	-4.580000	-6.319000
C	16.379000	-5.626000	-6.955000
C	17.160000	-5.324000	-8.079000
C	17.277000	-4.018000	-8.572000
C	16.586000	-2.997000	-7.910000
N	15.837000	-3.323000	-6.823000
C	16.526000	-1.548000	-8.191000
N	15.799000	-0.788000	-7.392000
C	14.824000	-4.596000	-5.131000
N	14.293000	-3.454000	-4.739000
H	16.302000	-6.657000	-6.585000
H	17.698000	-6.137000	-8.588000
H	17.896000	-3.803000	-9.453000
H	17.096000	-1.168000	-9.056000
H	14.657000	-5.563000	-4.626000
C	11.865000	-3.137000	-1.277000
C	13.035000	-3.907000	-1.235000
C	13.817000	-4.047000	-2.374000
C	13.445000	-3.410000	-3.567000
C	12.260000	-2.664000	-3.618000
C	11.469000	-2.541000	-2.481000
H	13.352000	-4.391000	-0.302000
H	14.733000	-4.651000	-2.317000
H	11.955000	-2.131000	-4.532000
H	10.545000	-1.950000	-2.533000
Pd	14.884000	-1.881000	-5.921000
C	16.217000	5.693000	-7.381000
C	15.635000	6.701000	-6.603000
C	16.419000	7.468000	-5.748000
C	17.801000	7.248000	-5.682000
C	18.392000	6.273000	-6.500000
C	17.603000	5.498000	-7.340000
H	14.552000	6.879000	-6.640000
H	15.924000	8.210000	-5.103000
H	19.476000	6.097000	-6.478000
H	18.076000	4.721000	-7.955000
C	20.332000	9.790000	-1.680000
C	21.574000	10.434000	-1.719000
C	22.270000	10.458000	-2.935000
C	21.760000	9.860000	-4.094000
C	20.516000	9.223000	-4.018000
N	19.864000	9.221000	-2.823000
C	19.747000	8.506000	-5.056000
N	18.582000	7.990000	-4.715000
C	19.390000	9.602000	-0.559000
N	18.279000	8.926000	-0.787000
H	21.994000	10.907000	-0.821000
H	23.247000	10.962000	-2.980000
H	22.323000	9.889000	-5.036000
H	20.188000	8.431000	-6.065000
H	19.661000	10.034000	0.420000
C	15.411000	8.288000	2.282000
C	16.008000	9.549000	2.135000
C	16.962000	9.761000	1.149000
C	17.328000	8.721000	0.283000
C	16.732000	7.459000	0.424000
C	15.793000	7.245000	1.423000
H	15.722000	10.379000	2.793000
H	17.414000	10.757000	1.059000
H	16.965000	6.632000	-0.264000
H	15.339000	6.249000	1.523000
Pd	18.142000	8.312000	-2.735000
C	14.439000	6.798000	4.005000
C	15.621000	6.380000	4.631000
C	15.679000	5.138000	5.250000
C	14.559000	4.294000	5.239000
C	13.367000	4.725000	4.644000
C	13.306000	5.977000	4.042000
H	16.514000	7.019000	4.623000
H	16.618000	4.827000	5.728000
H	12.479000	4.075000	4.599000
H	12.367000	6.301000	3.573000
C	14.658000	-0.878000	6.698000
C	15.167000	-1.430000	7.880000
C	15.718000	-0.562000	8.832000
C	15.771000	0.824000	8.631000
C	15.254000	1.339000	7.437000
N	14.726000	0.470000	6.533000
C	15.182000	2.733000	6.953000
N	14.628000	2.951000	5.776000
C	14.030000	-1.533000	5.534000
N	13.641000	-0.773000	4.526000
H	15.137000	-2.513000	8.057000
H	16.122000	-0.981000	9.766000
H	16.208000	1.486000	9.390000
H	15.601000	3.526000	7.597000
H	13.916000	-2.631000	5.560000
C	11.753000	-2.428000	1.099000
C	11.406000	-2.887000	2.379000
C	12.035000	-2.369000	3.502000
C	13.014000	-1.374000	3.371000
C	13.368000	-0.916000	2.093000
C	12.752000	-1.450000	0.970000
H	10.630000	-3.653000	2.503000
H	11.742000	-2.748000	4.491000
H	14.107000	-0.111000	1.955000
H	13.044000	-1.082000	-0.023000
Pd	14.012000	1.210000	4.878000
N	11.069000	-2.874000	-0.087000
N	15.336000	4.829000	-8.156000
N	14.363000	8.036000	3.240000
Cl	3.232000	12.136000	-4.995000
Cl	4.937000	-1.990000	-0.843000
Cl	13.174000	2.105000	2.939000
Cl	13.750000	-0.201000	-4.848000
Cl	16.119000	7.235000	-2.649000
Cl	10.027000	7.257000	-10.474000
Cl	1.083000	4.625000	-7.375000
Cl	0.369000	6.775000	0.412000
Cl	8.898000	11.109000	3.080000

Table S9. Cartesian coordinates (in Å) for the PM3 geometry optimized model of **13·T3$_3$·Cl$_3$**.

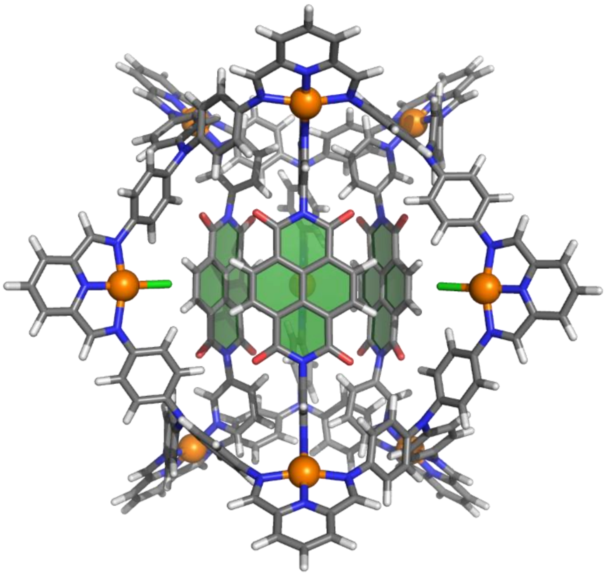

C	0.006000	0.302000	-1.933000
C	-0.527000	-0.571000	-0.977000
C	0.183000	-1.699000	-0.582000
C	1.439000	-1.990000	-1.142000
C	1.981000	-1.107000	-2.083000
C	1.268000	0.023000	-2.476000
H	-1.512000	-0.378000	-0.528000
H	-0.270000	-2.355000	0.176000
H	2.985000	-1.275000	-2.506000
H	1.711000	0.693000	-3.225000
C	4.913000	8.996000	-11.020000
C	6.098000	9.162000	-10.290000
C	7.339000	8.957000	-10.887000
C	7.421000	8.590000	-12.236000
C	6.232000	8.403000	-12.961000
C	4.994000	8.609000	-12.364000
H	6.063000	9.460000	-9.234000
H	8.248000	9.063000	-10.272000
H	6.250000	8.095000	-14.017000
H	4.084000	8.465000	-12.962000
C	12.328000	7.810000	-14.393000
C	12.728000	8.143000	-15.697000
C	11.791000	8.747000	-16.546000
C	10.485000	9.022000	-16.120000
C	10.124000	8.671000	-14.811000
N	11.051000	8.077000	-14.007000
C	8.837000	8.847000	-14.124000
N	8.722000	8.421000	-12.877000
C	13.109000	7.196000	-13.313000
N	12.529000	6.972000	-12.145000
H	13.751000	7.937000	-16.044000
H	12.090000	9.013000	-17.575000
H	9.762000	9.501000	-16.797000
H	8.022000	9.330000	-14.697000
H	14.176000	6.964000	-13.520000
Pd	10.519000	7.623000	-12.210000
C	3.821000	12.660000	1.880000
C	4.611000	11.581000	2.298000
C	5.741000	11.787000	3.088000
C	6.097000	13.082000	3.485000
C	5.316000	14.164000	3.047000
C	4.189000	13.957000	2.259000
H	4.349000	10.555000	2.011000
H	6.357000	10.917000	3.369000
H	5.573000	15.200000	3.317000
H	3.594000	14.825000	1.943000
C	10.530000	13.700000	6.536000
C	10.703000	14.627000	7.576000
C	9.640000	15.484000	7.887000
C	8.426000	15.430000	7.189000
C	8.294000	14.492000	6.154000
N	9.345000	13.674000	5.867000
C	7.143000	14.231000	5.279000
N	7.253000	13.295000	4.351000
C	11.466000	12.689000	6.031000
N	11.091000	11.906000	5.032000
H	11.650000	14.679000	8.135000
H	9.761000	16.220000	8.701000
H	7.597000	16.107000	7.448000
H	6.235000	14.842000	5.445000
H	12.453000	12.607000	6.533000
Pd	9.120000	12.391000	4.445000
C	3.259000	10.453000	-9.815000
C	2.181000	10.562000	-8.916000
C	1.881000	11.766000	-8.297000
C	2.662000	12.904000	-8.537000
C	3.713000	12.820000	-9.462000
C	4.005000	11.614000	-10.088000
H	1.547000	9.692000	-8.704000
H	1.006000	11.809000	-7.634000
H	4.313000	13.706000	-9.715000
H	4.833000	11.581000	-10.811000
C	1.485000	17.099000	-5.348000
C	1.057000	18.377000	-5.743000
C	0.932000	18.643000	-7.115000
C	1.220000	17.672000	-8.085000
C	1.646000	16.405000	-7.655000
N	1.757000	16.178000	-6.315000
C	1.991000	15.216000	-8.460000
N	2.365000	14.130000	-7.810000
C	1.684000	16.566000	-3.985000
N	2.130000	15.329000	-3.876000
H	0.823000	19.153000	-4.996000
H	0.595000	19.645000	-7.440000
H	1.114000	17.900000	-9.158000
H	1.908000	15.287000	-9.561000
H	1.436000	17.219000	-3.127000
C	2.521000	13.282000	-0.149000

C	1.306000	13.891000	-0.499000
C	1.181000	14.594000	-1.694000
C	2.273000	14.713000	-2.565000
C	3.514000	14.193000	-2.172000
C	3.634000	13.484000	-0.984000
H	0.436000	13.828000	0.171000
H	0.214000	15.061000	-1.932000
H	4.413000	14.347000	-2.783000
H	4.618000	13.082000	-0.701000
Pd	2.394000	14.448000	-5.755000
C	2.615000	8.148000	-10.583000
C	2.978000	6.800000	-10.422000
C	2.026000	5.791000	-10.503000
C	0.681000	6.104000	-10.736000
C	0.327000	7.437000	-10.987000
C	1.284000	8.445000	-10.915000
H	4.027000	6.528000	-10.234000
H	2.357000	4.750000	-10.394000
H	-0.704000	7.707000	-11.255000
H	0.980000	9.479000	-11.134000
C	-3.061000	2.299000	-9.897000
C	-4.021000	1.834000	-10.810000
C	-4.033000	2.381000	-12.102000
C	-3.119000	3.369000	-12.494000
C	-2.171000	3.812000	-11.556000
N	-2.186000	3.260000	-10.309000
C	-1.121000	4.838000	-11.709000
N	-0.326000	5.053000	-10.678000
C	-2.847000	1.905000	-8.490000
N	-1.868000	2.500000	-7.835000
H	-4.750000	1.059000	-10.521000
H	-4.784000	2.023000	-12.830000
H	-3.145000	3.788000	-13.513000
H	-1.060000	5.383000	-12.670000
H	-3.522000	1.146000	-8.051000
C	-1.092000	1.715000	-3.697000
C	-1.021000	0.678000	-4.645000
C	-1.291000	0.914000	-5.989000
C	-1.639000	2.199000	-6.429000
C	-1.760000	3.227000	-5.485000
C	-1.481000	2.991000	-4.147000
H	-0.754000	-0.341000	-4.330000
H	-1.237000	0.072000	-6.693000
H	-2.098000	4.229000	-5.779000
H	-1.587000	3.820000	-3.436000
Pd	-0.848000	3.845000	-9.053000
C	-1.286000	2.321000	-1.265000
C	-2.598000	2.819000	-1.317000
C	-3.066000	3.694000	-0.342000
C	-2.235000	4.087000	0.717000
C	-0.961000	3.512000	0.829000
C	-0.493000	2.646000	-0.151000
H	-3.278000	2.517000	-2.127000
H	-4.100000	4.059000	-0.414000
H	-0.317000	3.721000	1.693000
H	0.511000	2.212000	-0.042000
C	-3.492000	8.270000	3.893000
C	-4.586000	8.377000	4.767000
C	-5.466000	7.290000	4.869000
C	-5.278000	6.115000	4.127000
C	-4.174000	6.041000	3.262000
N	-3.338000	7.115000	3.185000
C	-3.764000	4.938000	2.370000
N	-2.656000	5.100000	1.672000
C	-2.442000	9.263000	3.590000
N	-1.514000	8.919000	2.717000
H	-4.752000	9.293000	5.358000
H	-6.332000	7.361000	5.553000
H	-5.982000	5.272000	4.220000
H	-4.408000	4.040000	2.320000
H	-2.490000	10.246000	4.096000
C	1.566000	11.628000	1.484000
C	1.440000	11.258000	2.836000
C	0.432000	10.396000	3.254000
C	-0.483000	9.872000	2.330000
C	-0.395000	10.270000	0.990000
C	0.617000	11.124000	0.575000
H	2.141000	11.656000	3.584000
H	0.361000	10.145000	4.321000
H	-1.132000	9.935000	0.249000
H	0.655000	11.415000	-0.483000
Pd	-1.802000	6.976000	2.030000
N	2.670000	12.418000	1.009000
N	3.621000	9.170000	-10.353000
N	-0.699000	1.523000	-2.327000
C	13.932000	8.980000	3.738000
C	14.027000	9.536000	5.020000
C	13.102000	10.486000	5.434000
C	12.058000	10.904000	4.589000
C	11.970000	10.349000	3.307000
C	12.902000	9.401000	2.888000
H	14.826000	9.232000	5.710000
H	13.213000	10.928000	6.440000
H	11.159000	10.635000	2.615000
H	12.815000	8.989000	1.874000
C	14.983000	5.233000	-9.101000
C	13.587000	5.143000	-9.033000
C	12.784000	5.712000	-10.019000
C	13.365000	6.379000	-11.103000
C	14.768000	6.457000	-11.173000
C	15.570000	5.896000	-10.186000
H	13.105000	4.617000	-8.199000
H	11.686000	5.638000	-9.915000
H	15.256000	6.953000	-12.030000
H	16.662000	5.980000	-10.274000
C	10.097000	-3.365000	0.030000
C	9.073000	-2.418000	0.150000
C	7.734000	-2.806000	0.136000
C	7.393000	-4.157000	0.010000
C	8.427000	-5.105000	-0.099000
C	9.762000	-4.719000	-0.093000
H	9.311000	-1.352000	0.261000
H	6.956000	-2.025000	0.210000
H	8.190000	-6.181000	-0.171000
H	10.541000	-5.488000	-0.183000
C	2.140000	-5.525000	-0.165000
C	1.607000	-6.793000	0.108000
C	2.486000	-7.818000	0.485000
C	3.866000	-7.599000	0.586000
C	4.360000	-6.317000	0.301000
N	3.485000	-5.337000	-0.052000
C	5.747000	-5.835000	0.313000
N	5.992000	-4.572000	0.004000
C	1.447000	-4.295000	-0.574000
N	2.164000	-3.199000	-0.762000
H	0.525000	-6.982000	0.028000
H	2.081000	-8.821000	0.706000
H	4.544000	-8.414000	0.880000
H	6.543000	-6.568000	0.561000
H	0.349000	-4.353000	-0.701000
Pd	4.179000	-3.581000	-0.446000
C	15.986000	3.250000	-7.941000
C	16.506000	2.666000	-6.770000
C	16.589000	1.288000	-6.631000
C	16.135000	0.442000	-7.651000
C	15.652000	1.010000	-8.838000

C	15.578000	2.391000	-8.978000
H	16.869000	3.298000	-5.950000
H	17.036000	0.882000	-5.714000
H	15.337000	0.376000	-9.679000
H	15.198000	2.808000	-9.923000
C	16.038000	-4.783000	-6.296000
C	16.730000	-5.837000	-6.913000
C	17.528000	-5.547000	-8.030000
C	17.649000	-4.243000	-8.533000
C	16.944000	-3.212000	-7.891000
N	16.176000	-3.528000	-6.809000
C	16.914000	-1.769000	-8.204000
N	16.167000	-0.998000	-7.438000
C	15.154000	-4.817000	-5.113000
N	14.590000	-3.683000	-4.742000
H	16.650000	-6.868000	-6.532000
H	18.078000	-6.368000	-8.526000
H	18.283000	-4.035000	-9.410000
H	17.526000	-1.405000	-9.051000
H	15.020000	-5.783000	-4.590000
C	12.260000	-3.260000	-1.190000
C	13.548000	-3.815000	-1.132000
C	14.298000	-3.994000	-2.290000
C	13.774000	-3.630000	-3.538000
C	12.450000	-3.176000	-3.612000
C	11.706000	-2.991000	-2.454000
H	13.980000	-4.127000	-0.169000
H	15.301000	-4.436000	-2.205000
H	11.972000	-2.972000	-4.579000
H	10.671000	-2.631000	-2.539000
Pd	15.181000	-2.102000	-5.978000
C	16.678000	5.589000	-7.318000
C	16.153000	6.811000	-6.862000
C	16.917000	7.664000	-6.075000
C	18.224000	7.314000	-5.714000
C	18.785000	6.144000	-6.245000
C	18.021000	5.295000	-7.041000
H	15.129000	7.108000	-7.129000
H	16.474000	8.618000	-5.758000
H	19.836000	5.883000	-6.053000
H	18.494000	4.394000	-7.457000
C	20.682000	10.028000	-1.744000
C	21.911000	10.704000	-1.808000
C	22.601000	10.717000	-3.029000
C	22.097000	10.076000	-4.170000
C	20.865000	9.409000	-4.072000
N	20.219000	9.416000	-2.872000
C	20.131000	8.654000	-5.106000
N	18.962000	8.142000	-4.771000
C	19.775000	9.850000	-0.592000
N	18.667000	9.163000	-0.793000
H	22.325000	11.212000	-0.922000
H	23.570000	11.245000	-3.093000
H	22.656000	10.096000	-5.120000
H	20.600000	8.540000	-6.102000
H	20.073000	10.286000	0.381000
C	15.897000	8.278000	2.348000
C	16.165000	9.612000	1.990000
C	17.080000	9.916000	0.988000
C	17.755000	8.892000	0.309000
C	17.533000	7.563000	0.693000
C	16.613000	7.263000	1.686000
H	15.654000	10.436000	2.508000
H	17.270000	10.972000	0.749000
H	18.092000	6.739000	0.232000
H	16.462000	6.210000	1.960000
Pd	18.505000	8.543000	-2.770000
C	14.937000	6.735000	4.090000
C	16.152000	6.158000	4.490000
C	16.175000	4.927000	5.140000
C	14.980000	4.247000	5.413000
C	13.761000	4.867000	5.108000
C	13.741000	6.091000	4.452000
H	17.105000	6.676000	4.305000
H	17.146000	4.509000	5.442000
H	12.804000	4.409000	5.391000
H	12.771000	6.555000	4.222000
C	14.990000	-0.952000	6.880000
C	15.529000	-1.504000	8.053000
C	16.124000	-0.640000	8.984000
C	16.191000	0.744000	8.770000
C	15.642000	1.264000	7.586000
N	15.071000	0.398000	6.702000
C	15.596000	2.664000	7.118000
N	14.990000	2.903000	5.971000
C	14.335000	-1.633000	5.745000
N	13.913000	-0.880000	4.747000
H	15.488000	-2.590000	8.239000
H	16.552000	-1.062000	9.912000
H	16.665000	1.406000	9.513000
H	16.084000	3.438000	7.741000
H	14.243000	-2.735000	5.779000
C	12.139000	-2.518000	1.212000
C	11.535000	-2.710000	2.468000
C	12.111000	-2.205000	3.628000
C	13.314000	-1.486000	3.568000
C	13.949000	-1.333000	2.329000
C	13.367000	-1.830000	1.173000
H	10.593000	-3.273000	2.547000
H	11.613000	-2.390000	4.589000
H	14.926000	-0.836000	2.251000
H	13.893000	-1.688000	0.219000
Pd	14.281000	1.134000	5.107000
N	11.491000	-2.908000	-0.010000
N	15.790000	4.672000	-8.011000
N	14.856000	7.936000	3.279000
Cl	4.980000	-1.413000	-0.960000
Cl	9.820000	7.105000	-10.007000
Cl	8.787000	10.821000	2.704000
C	6.693000	1.930000	1.164000
C	5.380000	2.402000	0.929000
C	7.673000	2.790000	1.606000
C	7.360000	4.152000	1.887000
C	6.055000	4.627000	1.640000
C	5.072000	3.728000	1.133000
C	8.337000	5.045000	2.414000
C	8.000000	6.345000	2.716000
C	6.696000	6.824000	2.455000
C	5.747000	5.993000	1.905000
C	9.064000	2.301000	1.764000
N	10.049000	3.217000	2.281000
C	9.729000	4.580000	2.624000
O	10.643000	5.268000	3.044000
O	9.454000	1.186000	1.464000
C	11.457000	2.819000	2.259000
C	12.064000	2.292000	3.408000
N	13.379000	1.923000	3.409000
C	14.106000	2.074000	2.263000
C	13.543000	2.593000	1.098000
C	12.206000	2.972000	1.088000
C	3.714000	4.225000	0.805000
N	3.431000	5.623000	1.021000
C	4.408000	6.532000	1.565000
O	4.068000	7.697000	1.681000
C	2.185000	6.171000	0.487000
C	1.056000	6.302000	1.309000

N	-0.118000	6.807000	0.826000
C	-0.180000	7.188000	-0.484000
C	0.916000	7.074000	-1.337000
C	2.115000	6.563000	-0.854000
O	2.812000	3.552000	0.339000
H	6.912000	0.868000	0.972000
H	4.622000	1.689000	0.568000
H	8.739000	7.035000	3.152000
H	6.463000	7.875000	2.690000
H	11.492000	2.168000	4.344000
H	15.164000	1.767000	2.278000
H	14.157000	2.699000	0.197000
H	11.756000	3.380000	0.175000
H	1.088000	5.997000	2.369000
H	-1.133000	7.598000	-0.858000
H	0.827000	7.388000	-2.383000
H	2.981000	6.469000	-1.519000
C	10.188000	10.199000	-1.315000
C	8.884000	10.690000	-1.562000
C	10.927000	9.645000	-2.336000
C	10.410000	9.615000	-3.663000
C	9.105000	10.091000	-3.908000
C	8.339000	10.610000	-2.824000
C	11.183000	9.115000	-4.750000
C	10.678000	9.136000	-6.031000
C	9.365000	9.600000	-6.273000
C	8.582000	10.045000	-5.232000
C	12.255000	9.050000	-2.043000
N	13.020000	8.526000	-3.146000
C	12.533000	8.552000	-4.504000
O	13.263000	8.080000	-5.356000
O	12.745000	8.940000	-0.934000
C	14.228000	7.753000	-2.859000
C	15.491000	8.361000	-2.922000
N	16.631000	7.653000	-2.666000
C	16.525000	6.330000	-2.343000
C	15.291000	5.686000	-2.271000
C	14.126000	6.398000	-2.530000
C	6.941000	11.049000	-3.049000
N	6.402000	10.944000	-4.383000
C	7.180000	10.454000	-5.493000
O	6.615000	10.383000	-6.570000
C	4.966000	11.146000	-4.570000
C	4.471000	12.393000	-4.980000
N	3.133000	12.601000	-5.156000
C	2.270000	11.569000	-4.923000
C	2.718000	10.313000	-4.516000
C	4.078000	10.091000	-4.336000
O	6.190000	11.472000	-2.189000
H	10.587000	10.260000	-0.290000
H	8.317000	11.119000	-0.721000
H	11.279000	8.780000	-6.883000
H	8.982000	9.585000	-7.305000
H	15.594000	9.427000	-3.185000
H	17.454000	5.774000	-2.134000
H	15.247000	4.623000	-2.010000
H	13.152000	5.899000	-2.475000
H	5.154000	13.238000	-5.170000
H	1.193000	11.752000	-5.072000
H	1.995000	9.509000	-4.340000
H	4.438000	9.107000	-4.016000
C	8.971000	3.616000	-7.626000
C	7.665000	4.090000	-7.887000
C	9.175000	2.606000	-6.713000
C	8.066000	1.986000	-6.068000
C	6.763000	2.469000	-6.317000
C	6.584000	3.552000	-7.225000
C	8.243000	0.888000	-5.178000
C	7.153000	0.280000	-4.597000
C	5.849000	0.773000	-4.834000
C	5.656000	1.860000	-5.657000
C	10.557000	2.181000	-6.382000
N	10.727000	1.080000	-5.468000
C	9.607000	0.402000	-4.862000
O	9.868000	-0.516000	-4.105000
O	11.572000	2.708000	-6.801000
C	12.071000	0.771000	-4.981000
C	12.819000	-0.260000	-5.569000
N	14.072000	-0.570000	-5.121000
C	14.595000	0.146000	-4.081000
C	13.886000	1.176000	-3.467000
C	12.610000	1.498000	-3.915000
C	5.230000	4.114000	-7.448000
N	4.125000	3.530000	-6.729000
C	4.291000	2.412000	-5.835000
O	3.291000	2.014000	-5.263000
C	2.833000	4.213000	-6.763000
C	1.838000	3.807000	-7.665000
N	0.625000	4.435000	-7.712000
C	0.391000	5.479000	-6.863000
C	1.351000	5.915000	-5.951000
C	2.586000	5.280000	-5.893000
O	4.972000	5.056000	-8.175000
H	9.816000	4.082000	-8.158000
H	7.538000	4.904000	-8.619000
H	7.276000	-0.588000	-3.932000
H	4.999000	0.279000	-4.339000
H	12.411000	-0.850000	-6.407000
H	15.609000	-0.112000	-3.736000
H	14.337000	1.727000	-2.634000
H	12.046000	2.307000	-3.437000
H	2.011000	2.969000	-8.360000
H	-0.592000	5.973000	-6.911000
H	1.127000	6.756000	-5.284000
H	3.347000	5.618000	-5.180000

9. References

[1] Yuan, J.; Fang, X.; Zhang, L.; Hong, G.; Lin, Y.; Zheng, Q.; Xu, Y.; Ruan, Y.; Weng, W.; Xia, H.; Chen, G. Multi-responsive self-healing metallo-supramolecular gels based on "click" ligand. *J. Mat. Chem.* **2012**, *22*, 11515–11522.

[2] Koshkakaryan, G.; Klivansky, L. M.; Cao, D.; Snauko, M.; Teat, S. J.; Struppe, J. O.; Liu, Y. Alternative Donor−Acceptor Stacks from Crown Ethers and Naphthalene Diimide Derivatives: Rapid, Selective Formation from Solution and Solid State Grinding. *J. Am. Chem. Soc.* **2009**, *131*, 2078–2079.

[3] Pun, A.; Hanifi, D. A.; Kiel, G.; O'Brien, E.; Liu, Y. Facile Route to an All-Organic, Triply Threaded, Interlocked Structure by Templated Dynamic Clipping. *Angew. Chem., Int. Ed.* **2012**, *51*, 13119–13122.

[4] Harris, R. K. *Nuclear Magnetic Resonance Spectroscopy—A Physicochemical Approach*; Pitman: London, 1983.

[5] Poveda, A.; Alonso, I.; Fernández-Ibáñez, M. Á. Experimental and computational studies on the mechanism of the Pd-catalyzed C(sp^3)–H γ-arylation of amino acid derivatives assisted by the 2-pyridylsulfonyl group. *Chem. Sci.* **2014**, *5*, 3873–3882.

[6] a) Drain, C. M.; Nifiatis, F.; Vasenko, A.; Batteas, J. D. Porphyrin Tessellation by Design: Metal-Mediated Self-Assembly of Large Arrays and Tapes. *Angew. Chem., Int. Ed.* **1998**, *37*, 2344–2347. b) Iengo, E.; Minatel, R.; Milani, B.; Marzilli, L. G.; Alessio, E. Metal-Mediated Self-Assembly of Molecular Squares of Porphyrins Rimmed with Coordination Compounds. *Eur. J. Inorg. Chem.* **2001**, 609–612.

[7] Allan, D.; Nowell, H.; Barnett, S.; Warren, M.; Wilcox, A.; Christensen, J.; Saunders, L.; Peach, A.; Hooper, M.; Zaja, L.; Patel, S.; Cahill, L.; Marshall, R.; Trimnell, S.; Foster, A.; Bates, T.; Lay, S.; Williams, M.; Hathaway, P.; Winter, G.; Gerstel, M.; Wooley, R. A Novel Dual Air-Bearing Fixed-χ Diffractometer for Small-Molecule Single-Crystal X-ray Diffraction on Beamline I19 at Diamond Light Source. *Crystals* **2017**, *7*, 336.

[8] a) Collaborative Computational Project, Number 4. The CCP4 suite: programs for protein crystallography. *Acta Cryst.* **1994**, *D50*, 760–763. b) Evans, P. Scaling and assessment of data quality. *Acta Cryst.* **2006**, *D62*, 72–82. c) Winter, G. xia2: an expert system for macromolecular crystallography data reduction. *J. Appl. Crystallogr.* **2010**, *43*, 186–190.

[9] Farrugia, L. WinGX and ORTEP for Windows: an update. *J. Appl. Crystallogr.* **2012**, *45*, 849–854.

[10] Evans, P. R.; Murshudov, G. N. How good are my data and what is the resolution? *Acta Cryst.* **2013**, *D69*, 1204–1214.

[11] Winn, M. D.; Ballard, C. C.; Cowtan, K. D.; Dodson, E. J.; Emsley, P.; Evans, P. R.; Keegan, R. M.; Krissinel, E. B.; Leslie, A. G. W.; McCoy, A.; McNicholas, S. J.; Murshudov, G. N.; Pannu, N. S.; Potterton, E. A.; Powell, H. R.; Read, R. J.; Vagin, A.; Wilson, K. S. Overview of the CCP4 suite and current developments. *Acta Cryst.* **2011**, *D67*, 235–242.

[12] Sheldrick, G. M. SHELXT – Integrated space-group and crystal-structure determination. *Acta Cryst.* **2015**, *A71*, 3–8.

[13] Sheldrick, G. M. Crystal structure refinement with SHELXL. *Acta Cryst.* **2015**, *C71*, 3–8.

[14] van der Sluis, P.; Spek, A. L. BYPASS: an effective method for the refinement of crystal structures containing disordered solvent regions. *Acta Cryst.* **1990**, *A46*, 194–201.

[15] Spek, A. L. *PLATON: A Multipurpose Crystallographic Tool*; Utrecht University: Utrecht, The Netherlands, 2008.

[16] Bricogne, G.; Blanc, E.; Brandle, M.; Flensburg, C.; Keller, P.; Paciorek, W.; Roversi, P.; Sharff, A.; Smart, O. S.; Vonrhein, C.; Womack, T. O. *BUSTER* 2.11.2 ed.; Global Phasing Ltd.: Cambridge, United Kingdom, 2011.

[17] Smart, O. S.; Womack, T. O. *Grade Web Server*; Global Phasing Ltd.: Cambridge, United Kingdom, 2014.